DOCKET NO.: 48378-0003-00-US
Application No.: 10/621,711
Office Action Dated: August 4, 2006

IN THE UNITED STATES PATENT AND TRADEMARK OFFICE

In re Application of:
Chien, Te-Yen

Application No.: **10/621,711**

Filing Date: **July 17, 2003**

Confirmation No.: **1537**

Group Art Unit: **1615**

Examiner: **Ghali, Isis A.D.**

For: **Transdermal Hormone Delivery System: Compositions and Methods**

DECLARATION OF AGIS KYDONIEUS PURSUANT TO 37 C.F.R. §1.132

I, Agis Kydonieus, declare as follows.

1. I am a United States citizen residing at 17 Savage Road, Kendall Park, New Jersey.

2. I received a Bachelor's degree *summa cum laude* in Chemical Engineering in 1959 and a Ph.D. in Chemical Engineering in 1964 from the University of Florida, as set forth in my professional resume attached hereto.

3. From 1960-1962, I was a chemical engineer at Union Carbide Corporation. From 1964-1968, I was a process scientist at Union Camp Corporation. I served as an Assistant Professor of Chemical Engineering at the Cooper Union Polytechnic Institute (New York, NY) from 1968-1970. During that time and until 1971 I was President and Principal of Chemtech Inc., Boston, MA. I served as Director of Research and Development at Baxter Laboratories from 1973-1974. From 1971-1973 and 1974-1988, I was employed with Health-Chem Corporation, where I served in several roles at Hercon Laboratories

Corporation in the area of transdermal and controlled release technology, including Director of R&D, Vice President, and finally President. I was Vice President of Corporate R&D for the ConvaTec Division of Bristol-Myers Squibb Corporation from 1988-1998. Additional details of my professional history are set forth in my professional resume.

4. From 1998 to the present I have served as President of Samos Pharmaceuticals, LLC, a pharmaceutical consulting company specializing in drug delivery, including oral, transdermal, implantable, injectable, buccal and vaginal delivery. I am currently a consultant in the role of Chief Scientific Officer of Agile Therapeutics, Inc., an early stage pharmaceutical company developing transdermal hormone delivery devices.

5. I have had over forty-five years of scientific training and business experience in the chemical and pharmaceutical industry, including over thirty years in the fields of controlled release and transdermal drug delivery. I am the editor, co-editor or presenter of numerous books, book chapters, publications, invited reviews and invited lectures in these fields, as set forth in my professional resume. I hold thirty-five United States Patents, several of which are in the fields of controlled release or transdermal drug delivery. I am or have been a member of several scientific or business associations, including the Controlled Release Society, the American Institute of Chemical Engineers, the American Association of Pharmaceutical Sciences, Krikos, Inc., Society of Biomaterials, Society of Investigative Dermatology, and the New York Academy of Sciences. I am one of the founders, past president and trustee of the Controlled Release Society, the premier International Society of drug delivery. I serve, or have served, as Director of the New Jersey Center for Biomaterials & Medical Devices-Member Industrial Advisory Board, MIT Biomaterials Consortium-Member Industrial Advisory Board, Health Chem Corp, Hercon Laboratories, Controlled Release Society, Krikos, Inc, Chemtech, Inc, and Exicon Import-Export Company and on the Scientific Advisory Boards of Valera Pharmaceuticals, Inc, Kytogenics Pharmaceuticals, Inc, TyRx Pharma and Transave Pharmaceuticals.

6. As mentioned, I serve as Chief Scientific Officer of Agile Therapeutics, Inc., licensee and developer of the technology disclosed and claimed the above-referenced U.S.

Patent Application Serial No. 10/621,711, entitled "Transdermal Hormone Delivery System: Compositions and Methods" (referred to hereinafter as "the present application"), the claims of which are currently under rejection in the U.S. Patent and Trademark Office.

7. I have read and am familiar with the Official Action dated August 4, 2006 in the present application. I understand the nature of the rejections made by the examiner concerning alleged obviousness of the claimed invention over the teachings of U.S. Patent 5,876,746 ("the 746 patent") in view of U.S. Patent 5,023,084 ("the 084 patent") and, for some claims, additionally in view of U.S. Patent 5, 876,746 ("the 746 patent"). According to the examiner, it would have been obvious to provide a transdermal delivery device to deliver combined estrogen and progestin in a matrix comprising a combination of enhancers as disclosed by the 956 patent, and to add capric acid as disclosed by the 084 patent for a different type of transdermal device, motivated by the teaching of the 084 patent that capric acid provides satisfactory skin absorption enhancement in that different system; therefore a four-component enhancer combination comprising DMSO, lauryl lactate, ethyl lactate and capric acid would be expected to deliver the hormonal combination to the skin of the user at a satisfactory enhanced rate.

8. I strongly disagree that the teachings of the aforementioned patents would have rendered obvious the transdermal delivery system claimed in the present application. The three bases for my opinion in this regard are (1) that the general unpredictability of controlled release and transdermal drug delivery make it impossible to predict the outcome of changing a transdermal formulation, absent empirical experimentation and, more particularly, (2) that one seeking to improve the transdermal system of the 956 patent would not find sufficient information in the 084 patent, directed to a different type of transdermal system, to make the types of modifications that are claimed in the present application; and (3) that the significant improvement in clinical results achieved by a simple re-formulation of the skin permeation enhancer cocktail of the 956 patent, i.e., by adding capric acid , could not have been predicted from the information imparted by the cited patents. These bases for my opinion are expanded upon in the following paragraphs.

The Field of Transdermal Drug Delivery is Not Predictable

9. After over 35 years in the field of controlled release and transdermal drug delivery, it has become my view that the transdermal delivery of drugs has been easy to define and scientifically present, but it has been extremely difficult to accomplish in actual practice. Permeation of drugs through skin has been extensively studied, but the mechanism of action is not completely understood and the permeation *in vivo* difficult to predict.

10. Scientifically speaking, the permeation of a drug through skin is a function of that drug's physicochemical properties, such as molecular weight, melting point and hydrophilicity. However, the drug has to be delivered from an appropriate vehicle from which the drug can then partition into the skin. That partitioning is dependent on the relative solubility of the drug into the two environments, that of the vehicle and that of the skin. Transdermal vehicles or formulations are usually very complex because they have to perform other functions in addition to allowing maximum permeation of the drug through the skin. For example the formulations should allow adhesion to the skin for extended periods of time, prevent irritation of the skin, and be cosmetically acceptable. Therefore the formulations usually contain pressure sensitive adhesives, plastisizers, humectants, emollients, anti-irritants and other modifiers. Thus the vehicle composition greatly affects the rate and extent to which the drug permeates the dermal barrier (1, 2). Science again tells us (Fick's law of diffusion) that the permeation should be maximum when the drug is at maximum thermodynamic activity or chemical potential of unity. In an ideal system, this means that the drug should be in a saturated solution (supersaturated solutions, which would give higher permeation rates, are to be avoided because they provide unstable systems) in the vehicle. Davis and Hadgraft state that postulating the effect that a particular topical delivery vehicle will have on the permeation process is not a simple matter because the dosage form in contact with the skin is seldom a simple solution; more often it is a complex mixture of several chemicals that may interact in several (often opposing) ways as far as permeation enhancement is concerned. The "leaving potential", or thermodynamic activity of the drug in the vehicle is therefore a major factor in the delivery process (3).

11. What makes the process even more unpredictable is the fact that each of the components of the formulation has its own "leaving potential", so during the permeation process the driving forces within the transdermal formulation continuously change. Therefore, consideration of these changes as well is needed to provide a formulation with appropriate penetration rate.[1]

12. The complexity reaches even a higher level when the formulation is applied to the outside of the skin (asymmetric configuration), duplicating clinical use conditions. The reason for this additional complexity is the fact that water moves from the body or receptor phase in to the transdermal formulation thus altering the thermodynamic activity of the drug as well as all of the other components in the patch.[2]

13. The complexities mentioned above that are associated with the development and optimization of a transdermal formulation are further compounded when one considers that the drug after "leaving" the formulation will have to encounter the complexities of the biochemical environment that constitutes the dermal barrier to the ingress of chemicals. It is well understood that the lipid bilayers of the intercellular lipids within the stratum corneum with its highly oriented hydrophilic and lipophilic regions, together with the keratinized intracellular flattened corneocytes, form an excellent permeation barrier to permeation of any chemical substance (5).

14. Enhancers, and more specifically chemical enhancers, can influence permeation by increasing the solubility of the drug in the stratum corneum. This can be accomplished if

---

[1] As one illustration of this, Kurihara-Bergstrom, et al., studying the effect of DMSO on the in vitro permeability of methanol, butanol and octanol (using DMSO solutions on both sides of the skin/balanced configuration) observed that the rate of octanol absorption is reduced at intermediate DMSO concentrations. They concluded that permeability may be different for hydrophilic and hydrophobic compounds, and simple measurements of net effects do not accurately reflect underlying events where competing factors are moving in opposite directions (4).

[2] As another illustrative example, Kurihara-Bergstrom, et al, studying the effect of DMSO on permeation of the alcohols mentioned above in an asymmetric configuration (DMSO solution in donor, saline solution in receptor), concluded that the rate of absorption for methanol was not affected by the application regiment and the absorption was increased 50-fold as DMSO increased to 100%. Conversely, the absorption of octanol was decreased as DMSO increased to 100%. It was postulated that competing solvent flows, DMSO moving toward the receptor phase and water moving in the donor phase introduced significant variables that accounted for this phenomenon.

the drug has good solubility in the chemical enhancer and the chemical enhancer has good solubility in the stratum corneum lipids. In most cases however, the chemical enhancer, once it has penetrated into the dermal bioenvironment, disrupts the tight structure of the intercellular lipid bilayers thus increasing the fluidity of the lipids and increasing permeation (6,7). This disruption can take different forms such as the incorporation of medium chain length (e.g., 12 to 14 carbon atoms) fatty acids into the long chains of the stratum corneum fatty acids (8), the incorporation of kinked (e.g., oleic acid with a cis-double bond) fatty acids (9), formation of pool of enhancer liquid within the bilayer (10), or the extraction of lipids from the bilayer, thus forming a void volume through which permeation can be facilitated (4, 11).

15. It is therefore not surprising that enhancers behave substantially differently when they are co-delivered with other enhancers and vehicles to enhance the permeation of drugs. In the enhanced delivery of naloxone (8) for example, as well as other drugs (12, 13) with fatty acids, it was found that the best results were obtained when the enhancer propylene glycol was used as the vehicle, with a 150 enhancement ratio over the non-fatty acid containing control. The enhancement ratio was dropped to 10 and 2 when the co-delivered enhancers/vehicles were isopropanol and isopropyl myristate respectively.

16. In the case of DMSO, I mentioned above (4) that when it is delivered from water it did not increase the permeation of alcohols (decreased permeation of octanol) until the concentration of DMSO increased above 60%. In a companion study by the same authors, using the same experimental design, the permeation of the antiviral agent vidarabine was studied (14). Similar results were obtained as with the alcohol study, with the permeation decreasing up to 50% DMSO concentration and then rising rapidly as DMSO concentration increased to 100%. Similar results were obtained by others (15,16) when DMSO was delivered from water. In all cases, a 50 to 60 % concentration of DMSO was needed to increase the permeation of such agents as picric acid, tetrachlorosalicylanilide and radiolabelled water. In contrast, when DMSO was delivered from alcoholic solutions, a dose response was obtained for DMSO concentrations from 10% to 50% (17).

17. It is clear from the above observations that the effect of enhancers on the permeation of drugs through skin is unpredictable and dependent on many variables whose effect can only be determined by experiment. When skin permeation enhancers are used in combination, or in different solvent systems as in the case of DMSO discussed above, this unpredictability is compounded greatly.

The Modifications of the 956 Patent's System Made in the Present Application Could not be Gleaned from Information Presented in the 084 Patent

18. The transdermal hormone delivery system of the 956 patent is similar to that of the present application – it was designed to deliver estrogen and progestin hormone from a single layer of adhesive polymer matrix, and utilizes a skin permeation enhancer combination containing a specified ratio of enhancers. However, the system of the 956 patent is deficient in part because it is not able to deliver sufficient amounts of progestin hormone to a woman's bloodstream to ensure contraception. The system of the present application overcomes this deficiency by making a modification to the enhancer system, namely, by adding a small amount of capric acid (about 1-12% by weight of the adhesive polymer matrix[3]). The examiner has stated that a person of skill in the art would have found all information needed to make this modification within the 084 patent. In view of the general unpredictability in the art of transdermal delivery as elaborated above, I believe this would be impossible to do.

19. It must be kept in mind that the 084 patent discloses a very different transdermal delivery system from that of the 956 patent. Instead of delivering progestin and estrogen hormones from a single adhesive polymer matrix, it utilizes a bilayer or trilayer system in which (1) the estrogen is separated into a different layer from the progestin, (2) there may be membranes between the layers, and (3) only a single enhancer is utilized, and only in the progestin-containing layer. Granted, the 084 patent presents *in vitro* skin flux data that capric acid, as a *sole* enhancer, works well in that system, but capric acid was already known generally as a good skin permeation enhancer for steroid hormones (18), so even this was not

---

[3] In certain exemplary embodiments, the adhesive polymer matrix is formulated with about 2.5-5% capric acid and after drying the adhesive polymer matrix contains less than about 9% by weight capric acid (about 6% in one exemplary embodiment).

new information. Moreover, the 084 patent was not particularly instructive in suggesting what range of capric acid would be "suitable," suggesting as broad a range as 10-40% of the polymer material, 15-30% preferred. Given that the bilayer/trilayer system is quite different from the single layer adhesive polymer matrix system of the 956 patent, a skilled person would have to question what to do with this information. If capric acid works well in the bilayer/trilayer system, would it offer any improvement to the enhancer combination of the 956 patent? If so, how much capric acid should be added to the 956 patent's enhancer formulation? If 15-30% yields "highly satisfactory skin absorption enhancement and satisfactory adhesion" (084 Col. 17, lines 54-56), should 15-30% be added to the enhancer combination of the 956 patent? Should other enhancer components be reduced? If so, by how much? Should all other components be altered or only some of them? Indeed, the *in vitro* skin flux data shown in the 084 patent suggest that capric acid *alone* might function *better* than the 956 patent's combination: compare 0.49 - 1.84 $\mu g/cm^2/hr$ progestin (Tables 3 and 10) at 45-50% capric acid in the 084 patent's example patches with about 0.26 $\mu g/cm^2/hr$ progestin (calculated from Fig. 2) for 45% total enhancers in the 956 patent's example patch, using the same *in vitro* skin flux test. In view of this information, should capric acid completely replace the other enhancers of the 956 patent? In my opinion, there would be no possible way to even begin to answer these questions without significant experimentation.

20. As mentioned, the system of the present application modifies the system of the 956 patent by adding a small amount of capric acid (about 1-12% as stated above) to the enhancer combination – much less than the preferred or even broader ranges taught by the 084 patent. Again I submit that these specifically claimed modifications to the 956 patent's transdermal system could not have been imparted in any way to the skilled person by the 084 patent. It is doubtless that significant trial-and-error experimentation was conducted by the inventor before these modifications were settled upon.

The Significant Improvement in Clinical Results Achieved with the System of the Present Invention Could Not Have Been Predicted by Anything in the Cited Prior Art

21. Finally, and perhaps most noteworthy, are the *in vitro* skin flux and *in vivo* clinical results obtained in the 956 patent system as compared with the system of the present

application or its parent, which is incorporated by reference. These are summarized in the table below.

	956 Patent	**Present Application or its parent**
In vitro skin flux model used	Human cadaver skin on the Valia-Chien side-by-side type skin permeation cell system (Crown Glass Co., Branchburg, NJ) [Example 2 of 956 patent]	Human cadaver skin on the Valia-Chien side-by-side type skin permeation cell system (Crown Glass Co., Branchburg, NJ) [Example 2 of parent of present application]
In vitro skin flux rate for progestin	Transdermal patch containing 45% total combined enhancers, 1.10 % progestin: about **0.26 μg/cm^2/hr** as calculated from Fig. 2	Transdermal patch containing 43% total combined enhancers, 1.16% progestin: about **0.16 μg/cm^2/hr** as calculated from Fig. 2 of parent of present application
Clinical model	Fertile Chinese women, test period one menstrual cycle [Example 4 of 956 patent]	1. Fertile Chinese women, test period three menstrual cycles [Example 4 of parent of present application] 2. Fertile women, test period four menstrual cycles [Example 4 of present application]
Serum concentration progestin delivered from 10 cm^2 patch	Serum concentration ranged from about 100-280 pg/ml, but generally was 200 pg/ml or lower [Fig 4, circles]	Serum concentration ranged from about 600-2700 pg/ml but generally was in the 1000-2200 pg/ml range [Fig. 7 of parent of present application]
Serum concentration progestin delivered from two 10 cm^2 patches or one 20 cm^2 patch	Serum concentration ranged from about 250-700 pg/ml, but generally was 500 pg/ml or lower [Fig 4, squares]	Serum concentration ranged from about 900-3900 pg/ml but generally was in the 1500-3000 pg/ml range [Table 2 of present application]

22. As can be seen, the *in vitro* skin flux rate for progestin from a transdermal patch containing capric acid (data shown in parent of the present application) was actually poorer than that seen for the 956 patent's system. That is, from those data, it appears that the addition of capric acid actually decreased the effectiveness of the system for delivering progestin. Yet in the clinical studies, the steady state serum concentration of progestin delivered by a 10 or 20 cm^2 patch of the present invention was three- to eight-fold better than that of the 956 patent's formulation – about 1000-2200 pg/ml for a 10 cm^2 patch (as shown in the parent of the present application) and about 1500-3000 pg/ml for a 20 cm^2 patch (as shown in the present application.), versus only about 100-280 pg/ml on average for a 10 cm^2 patch of the 956 patent's formulation (Fig. 4 of 956 patent, see "Group A") and about 250-700 pg/ml for a 20 cm^2 patch of that formulation (Fig. 4 of 956 patent, see "Group B"). It is

my considered opinion that this many-fold improvement in *in vivo* progestin delivery by re-formulating the matrix to include capric acid could not have been predicted from the information presented in the 956 patent or the 084 patent. Indeed, I do not believe that these results could have been predicted from any literature.

23. In conclusion, I wish to emphasize again that transdermal drug delivery is an unpredictable and inexact science in which empirical observation and significant trial-and-error experimentation can and must play a critical role. It is for this reason, as elaborated above, that I do not believe the transdermal delivery system of the present application is in any way obvious in view of the references cited by the examiner.

I further declare that all statements made herein of my own knowledge are true and that all statements made on information and belief are believed to be true; and further that these statements are made with the knowledge that willful false statements and the like so made are punishable by fine or imprisonment, or both, under Section 1001 of Title 18 of the United States Code, and that such willful false statements may jeopardize the validity of the above-referenced application or any patent issued thereon.

November 1, 2006
DATE

AGIS KYDONIEUS, PH.D.

CONFIDENTIAL RESUME OF
AGIS KYDONIEUS

EDUCATION

University of Florida,
BSChE Summa Cum Laude 1959
Ph.D. Chem. Eng. 1964

17 Savage Road
Kendall Park, NJ 08824
Phone:732-4224600
Fax:732-4227088
e-mail: akydonieus@comcast.net

W O R K E X P E R I E N C E

SAMOS PHARMACEUTICALS, LLC — April 1998 - Present

President

Consultant/Scientific Advisory Board Member/Executive for several companies in the fields of drug delivery, including oral(peptides), transdermal, implantable, injectable, buccal and vaginal delivery, DNA vaccine delivery, and biopolymers, resorbable and non-resorbable for medical devices and tissue engineering, including devices for orthopedics, adhesion prevention, ophthalmics, wound care, cardiovascular applications, as well as for cosmetics and skin care. Experience in preclinical as well as Phase I through III clinical development.
Aids clients in Business Plan preparation and in venture financing, through venture groups and through strategic alliances and joint ventures.

BRISTOL-MYERS SQUIBB CORPORATION — June 1988 - April 1998

Vice President, Corporate R&D - ConvaTec

Responsible for polymer and process research, drug delivery, skin biology, analytical chemistry, clinical supply and preclinical testing groups. In charge of a group of 30 developing polymers, products, and processes for medical devices and pharmaceuticals. Development of devices for the wound care, ostomy and incontinence markets, and transdermal and buccal pharmaceutical systems for BMS support and diversification. Basic research in polymer and adhesive synthesis including urethane adhesives and thermoplastic hydrogels, polymer surface modification, and biodegradable/bioabsorbable polymer modifications including PHB, caprolactone, chitosan, hyaluronic acid and collagen. Application of natural and synthetic polymers as templates for tissue engineering. Fundamental studies in skin adhesion, skin permeation, skin irritation and sensitization, antimicrobial skin lipids, and preparation of living skin equivalents. Responsible for identification, evaluation and project coordination of external Industrial and Academic programs.

HEALTH-CHEM CORP. — June 1971 - August 1973/September 1974 - April 1988

President, Hercon Laboratories Corporation

Responsible for P & L for the company reporting directly to the President of Health-Chem. In charge of 110 employees in R & D, government regulations, quality control and production. Introduced to the marketplace a patch containing nitroglycerine and a novel wound dressing containing chlorhexidine. A clonidine patch for hypertension

was submitted to FDA for approval and a dozen other products were in human clinical trials. The sales of the company had shown at least a 50% increase per year over the last four years.

Made over 50 presentations to stock exchange groups, pharmaceutical analysts and institutional groups worldwide. Instrumental in obtaining a 20 million convertible debenture for Health Chem.

Vice President

Responsible for R & D, government affairs, new product promotions and marketing, patent development and licensing for the newly formed Hercon Division. Introduced multimillion dollar products based on the Hercon controlled release technology, such as the S. C. Johnson Raid Roachtape and the Union Carbide Glad Air Freshener Scentstrips.

Engaged company in transdermal delivery of pharmaceutical products and negotiated 45 agreements including those with Ortho Pharmaceutical, Lederle Labs, Smith Kline, Warner Lambert, Squibb, Schering Plough, Hoffman LaRoche, and others for the development of transdermal therapeutic systems.

Director R & D

Developed processes (Hercon) for controlling the release of chemicals such as drugs, insecticides, repellents and pheromones from polymer membranes. Nineteen U.S.A. patents have issued and two more are pending in the U.S.A. and several foreign countries.

BAXTER LABORATORIES August 1973 - September 1974

Director of Corporate Biomedical Engineering

Responsible for the Corporate R & D for this half billion dollar medical device company. In change of 85 engineers and scientists in the departments of polymer development, container processing, packaging, humidification, special projects, and pilot plant facilities. Major emphasis was in the development of polymers and polymer processes for the manufacturing of new containers for intravenous solutions, blood bags, freezer bags, humidification containers and unit dose vials.

CHEMTECH, INC., BOSTON, MASSACHUSETTS May 1968 - June 1971

President and Principal

Responsible for financial and chemical engineering functions of the company. Supervised development work on urethane elastomers, moisture cured urethanes and two part system urethanes. Designed and installed pilot plant facilities and supervised the manufacture of several urethane products. Arranged financing for the company since its inception and negotiated the merger of Chemtech, Inc., with Ornsteen Chemical Co. (Seabrook, NH). Designed and installed the company's plant facilities for the production of urethane elastomers. Responsible for P & L until company acquired by Morton Thiokol (Chicago, IL).

COOPER UNION (POLYTECHNIC INSTITUTE), New York, NY May 1968 - January 1970

Assistant Professor of Chemical Engineering

Responsibilities involved teaching of graduate and undergraduate courses in chemical engineering. Taught courses in Mass Transfer Operations, Physical Chemistry, Plant Design, Chemical Engineering Economics and Air Pollution. Research interests were in the areas of minimization of intersolubilizing effects in solvent crystallization processes, and simulation of chemical plants by digital computer. Faculty adviser to student chapter of AIChE.

UNION CAMP CORPORATION December 1964 - May 1968

Process Scientist

Responsibilities included project planning and coordination, and economic evaluation and profitability studies of chemical plants. Development studies on processes to separate fatty acids from rosin acids and monounsaturated acids from polyunsaturated fatty acids.

UNION CARBIDE CORPORATION June 1960 - September 1962

Chemical Engineer

Responsibilities included the development of equipment for plastics processing; developed and designed pilot plant equipment used for the elimination of contamination from thermoplastic materials. U.S. Patent #3197533 was issued on the equipment and product obtained. Studied the pyrolysis of thermoplastic materials using pilot plant equipment; investigated the effect of branching and molecular weight distributions on the mechanical and rheological properties of polymers; above investigation allowed the tailor-making of products for specific uses such as blow molding, extrusion, injection molding, coating and wire and cable.

HOBBIES AND OUTSIDE INTERESTS

Photography, Sports, Oil Painting
American Men of Science
Recognition Award by the Controlled Release Society, 1990
BMS Outstanding Corporate Contribution Award, 1992

Adjunct Professor: Cooper Union 1970 - 1971
1975 - 1976

Director to: New Jersey Center for Biomaterials & Medical Devices-Member Industrial Advisory Board/1997
MIT Biomaterials Consortium-Member Industrial Advisory Board/1997
Health Chem Corp./1984
Hercon Labs/1984-1988
Controlled Release Society, Inc./1974-1984
Krikos, Inc./1973-1980
Chemtech, Inc. (Chairman)/1968-1971
Exicon Import-Export Co./1972-1981

Member: Controlled Release Society, Inc./1973-Present
(Cofounder, President, Vice President, Board Member,

Trustee)
American Institute of Chemical Engineers/1962-Present
American Association of Pharmaceutical Scientists
Krikos, Inc./1973-Present (Cofounder, Board Member, Treasurer)
Society of Biomaterials
Society of Investigative Dermatology
New York Academy of Sciences

BOOKS

Kydonieus, A.F., Controlled Release Technologies: Methods, Theory, and Applications, Vol. I, CRC Press, Florida, 1979.

Kydonieus, A.F., Controlled Release Technologies: Methods, Theory, and Applications, Vol. II, CRC Press, Florida, 1979.

Kydonieus, A.F., and Beroza, M., Insect Suppression with Controlled Release Pheromone Systems, Vol. I, CRC Press, Florida, 1982.

Kydonieus, A.F., and Beroza, M., Insect Suppression with Controlled Release Pheromone Systems, Vol. II, CRC Press, Florida, 1982.

Kydonieus, A.F., and Langer, R., Controlled Release of Bioactive Materials, 9th International Symposium Proceedings (Eds.), July 1982.

Kydonieus, A.F., and Berner, B., Transdermal Delivery of Drugs, Vol. I, CRC Press, Florida, December 1986.

Kydonieus, A.F., and Berner, B., Transdermal Delivery of Drugs, Vol. II, CRC Press, Florida, May 1987.

Kydonieus, A.F., and Berner, B., Transdermal Delivery of Drugs, Vol. III, CRC Press, Florida, May 1987.

Kydonieus, A.F., Treatise on Controlled Drug Delivery, Marcel Dekker, New York, September 1991.

Kydonieus, A. F., and Wille, J., Biochemical Modulation of Skin Reactions: Transdermals, Topicals, Cosmetics; CRC Press, Florida, January 2000.

PATENTS

1. U.S. Patent #3,197,533; Gel and Fisheye Reduction in Thermoplastics (July 1965).

2. U.S. Patent #3,961,117; Antistatic Carpet and Method for Manufacturing Same (June 1976).

3. U.S. Patent #4,102,991; Process for Controlling Cockroaches and Other Crawling Insects (July 1978).

4.U.S. Patent #4,119,267; Blood and Intravenous Solution Bags (October 1978).

5.U.S. Patent #4,160,335; Dispensers for the Controlled Release of Pest Controlling Agents (July 1979).

6.U.S. Patent #4,193,984; Method and Composition for Controlling Flying Insects (March 1980).

7.U.S. Patent #4,198,782; Control of Agricultural Pests by Controlled Release Particles (April 1980).

8.U.S. Patent #4,212,153; Time Color Indicator (July 1980).

9.U.S. Patent #4,272,520; Compositions Comprising N-tetradecyl Formate and Their Use in Controlling Insects (June 1981).

10.U.S. Patent #4,320,113; Process for Controlling Cockroaches (March 1982).

11.EP-177329-A; Transdermal Delivery of Nitroglycerin, April 1986.

12.U.S. Patent #4,639,393; Dispensers for the Controlled Release of Pest Controlling Agents (January 1987).

13.U.S. Patent 4,666,767; Dispensers for the Controlled Release of Pest Controlling Agents and Method for Combating Pest Therewith (May 1987).

14.U.S. Patent #4,792,450; Device for Controlled Release Drug Delivery (December 1988).

15.U.S. Patent #4,764,382; Device for Controlled Release Drug Delivery; Gelled Systems (August 1988).

16.U.S. Serial #06/875824; Device for Controlled Release Drug Delivery; System Methods.

17.U.S. Patent #4,767,808; Article Useful for Administration of Pharmacologically Active Substances Transdermally, Orally, or by Means of an Implant (August 1988).

18.U.S. Patent #5468501 Divisional of #17; Broad Polymer (November 1995).

19.U.S. Patent #4,758,434; Divisional of #16; Specific Plasticizers (July 1988).

20.U.S. Patent #5310559; Copolymer Control Membranes (May 1994).

21.U.S. Patent #5322695; Moisture Vapor Permeable Transdermal Dressing (June 1994).

22. U.S. Patent #5028431; Article for the Controlled Release and Delivery to Animal Tissue of a Pharmacologically Active Agent Which is a Causative Factor in the Occurrence of Non-Allergic or Allergic Contact Dermatitis Comprising an Anti-Dermatitic Substance, (July 1991).

23.U.S. Patent #5580573; Temperature Activated Controlled Release Device,(December 1996).

24.U.S. Patent #5591820; Polyurethane Hydrophilic Pressure Sensitive Adhesives, (January 1997).

25. U.S. Patent #5843979; Transdermal Treatment with Mast Cell Degranulating Agents for Drug Induced Hypersensitivity (November 1998).

26.U.S. Patent #5527271; Thermoplastic Hydrogel Impregnated Composite Material, (June 1996).

27.U.S. Patent #6179818; Ostomy Bags and Vessels for Biological Materials, (January 2001).

28.U. S. Patent #5686100; Prophylactic and Therapeutic Treatment of Allergic Contact Dermatitis, (November 1997).

29.U. S. Patent #5618557; Prophylactic Treatment of Allergic Contact Dermatitis, (April 1997).

30.U.S.Patent #5827525; Buccal Delivery System for Therapeutic Agents,(October 1998).

31 U.S. Serial #0845244; Divisional; Contact Irritation Treatment (November 1995).

32.U.S. Patent #5912010; Prophylactic Treatment with Calcium Channel Blocking Agents for Drug Induced Hypersensitivity, (June 1999).

33.U.S. Patent #5910536; Hydrophobic Urethane Adhesives (June 1999).

34.U.S. Patent #5952422; Photopolymerizable Medical Pressure Sensitive Adhesives (September 1999).

35.U.S. Patent #5714543; Water Soluble Polymer Additives for Polyurethane Based Pressure Sensitive Adhesives, (February 1998).

36.W.O. #9816104; Skin Lipid Antibacterial Agents (April 1998).

37.W.O. #0064516; Controlled Release from Bisphosphonate Implants, (November 2000).

38.U.S. Patent #6809085; Adherent N,O-carboxymethylchitosan drug delivery devices for mucosal tissue (October, 2004).

39.EP 1534261; Oral Delivery of Peptides and Proteins (June, 2002)

40.U.S. Patent Application; Implantable Delivery of Antihypertensive Drugs (2005)

41.U.S. Patent Application; Transdermal Delivery of Cardiovascular Drugs (2005)

42.U.S. Patent Appl; Oral Delivery of Peptides and Proteins using Supergels (2004)

43.U.S. Patent Application, Serial # 11/059943; Treatment of Interstitial Cystitis (2005)

BOOK CHAPTER CONTRIBUTIONS

1. Controlled Release of Pheromones Through Multilayered Polymeric Dispensers; ACS Symposium Series #33, pps. 283-294, April 1976.

2. Application of a New Controlled Release Concept in Household Products; ACS Symposium Series #33, pps. 295-303, April 1976.

3. The Effect of Some Variables on the Controlled Release of Chemicals From Polymeric Membranes; ACS Symposium Series #53, April 1977.

4. Fundamental Concepts of Controlled Release; in book Controlled Release Technology, A.F. Kydonieus, ed., Vol. I, p. 1 (1979).

5. Multilayered Laminated Structures; Ibid., p. 183 (1979).

6. Other Controlled Release Technologies and Applications; Ibid., p. 235 (1979).

7. The Hercon Dispenser Formulation and Recent Test Results; in book Management of Insect Pests with Semiochemicals, E.R. Mitchell, ed., pps. 445-454; Plenum Press, (1981).

8. Pink Bollworm and Tobacco Budworm Mating Disruption Studies on Cotton; Ibid., pps. 367-284.

9. Pheromones and Their Use; in book Insect Suppression with Controlled Release Pheromone Systems; A.F. Kydonieus and M. Beroza, Eds., Vol. I, p. 3 (1982).

10. Controlled Release Technologies; in book Insect Suppression with Controlled Release Pheromone Systems; A.F. Kydonieus and M. Beroza, Eds., Vol. I, p. 131 (1982).

11. Laminated Structure Dispensers; in book Insect Suppression with Controlled Release Pheromone Systems; A.F. Kydonieus and M. Beroza, Eds., Vol. I, p. 213 (1982).

12. Mating Disruption as a Method of Suppressing Pink Bollworm and Tobacco Budworm Populations in Cotton; in book Insect Suppression with Controlled Release Pheromone Systems; A.F. Kydonieus and M. Beroza, Eds., Vol. I, p. 75 (1982).

13. Marketing and Economics in Use of Pheromones for Suppression of Insect Populations; in book Insect Suppression with Controlled Release Pheromone Systems; A.F. Kydonieus and M. Beroza, Eds., Vol. II, p. 187 (1982).

14. Formulations and Equipment for Large Volume Pheromone Application by Air; ACS Symposium Series #190, p. 175 (1982).

15. Physical Methods of Controlled Release; in book Controlled Release Technology; G. Das, ed., pps. 61-120, John Wiley & Sons (1983).

16. Controlled Release for Suppression of Rice Storage Pests; in book Controlled Release for Delivery Systems; T. Roseman and Z. Mansdorf, Eds., pp. 301-313, Marcel Dekker (1983).

17. Plastic Laminate Dispensers; in book Insect Pheromones in Plant Protection; A. Jutsum and R. Gordon, Eds., pp. 149-171, J. Wiley & Sons Ltd. (1989).

18. Transdermal Delivery From Solid Multilayered to Polymeric Reservoir Systems; in book Transdermal Delivery of Drugs; A.F. Kydonieus and B. Berner, Eds., pps. 145-156, CRC Press (December 1986).

19. Fundamentals of Transdermal Drug Delivery; in book Transdermal Delivery of Drugs; A.F. Kydonieus and B. Berner, Eds., pps. 3-16, CRC Press (May 1987).

20. Controlled Release Technologies for Pest Management; in book Delivery of Crop- Protection Agents; R. M. Wilkins, Ed., pp. 43-58 (1990).

21. Transdermal Delivery; in book Treatise in Controlled Drug Delivery; A.F. Kydonieus, ed., pps. 341-421, Marcel Dekker (September 1991).

22. Novel Drug Delivery Systems in the book The Drug Development Process: Increasing Efficiency and Cost Effectiveness; P. G. Welling,Ed., pps 169-201, Marcel Dekker, (July 1996).

23. Dermal and Transdermal Delivery of Drugs; in book Biochemical Modulation of Skin Reactions in Dermal and Transdermal Delivery of Drugs; A. F. Kydonieus and J. Wille, Eds., pps 1-15, CRC Press, (January 2000).

24. Modulation of Skin Irritation and Sensitization Reactions: A General Overview; in book Biochemical Modulation of Skin Reactions in Dermal and Transdermal Delivery of Drugs; A. F. Kydonieus and J. Wille, Eds., pps 205-223, CRC Press (January 2000)

25. Ion Channel Modulation of Contact Irritant and Contact Allergic Dermatitis; in book Biochemical Modulation of Skin Reactions in Dermal and Transdermal Delivery of Drugs; A. F. Kydonieus and J. Wille, Eds., pps 233-245, CRC Press (January 2000).

26. Mast Cell Degranulating Agents in Contact Allergic Dermatitis; in book Biochemical Modulation of Skin Reactions in Dermal and Transdermal Delivery of Drugs; A. F. Kydonieus and J. Wille, Eds., pps 245-261, CRC Press (January 2000).

27.Novel Topical Agents for Prevention and Treatment of Allergic and Irritant Contact Dermatitis; in book Advances in Toxicology; H. Maibach, ed.,pp 235-262 Tailor & Francis, Philadelphia (May 2001).

28. Transdermal Delivery Systems; in book Novel Topical Actives and Delivery Systems; J. Wille, ed., Submitted.

29. Abrogation Of Skin Reaction: Agents and Methods; in book Novel Topical Actives and Delivery Systems; J. Wille, ed., Submitted.

30. Fundamental Mechanisms of Skin Reactivity; in book Novel Topical Actives and Delivery Systems; J. Wille, ed., Submitted.

PUBLICATIONS & PRESENTATIONS

1. A Multi-State Aerosol Sampler for Extended Sampling Intervals; American Industrial Hygiene Association Journal 31, November 1970.

2. A Polymeric Delivery System for the Controlled Release of Pesticides; 45th Annual Meeting, Eastern Branch of the Entomological Society of America, New York, N.Y., November 1,1973.

3. HERCON* ROACH-TAPE; Proceedings - 1975 International Controlled Release Pesticides Symposium, pps. 60-75, September 1975.

4. Field Studies on the Control of the German Cockroach using HERCON* ROACH-TAPE and Standard Sprays; Proceedings - 1975 International Controlled Release Pesticides Symposium, pps. 247-257, September 1975.

5. Marketing and Economic Considerations for HERCON* Consumer and Industrial Controlled Release Products; Part I, UNIT p.10 - July/August 1976.

6. Ibid, Part II, UNIT p. 6 - September 1976.

7. HERCON* LURE 'N KILL* FLYTAPE: A Non-Fumigant Insecticidal Strip Containing Attractants; Proceedings - 1976 International Controlled Release Pesticides Symposium, pps. 3.40-3.51, September 1976.

8. HERCON* Granules and Powders for Agricultural Applications; Proceedings - 1976 International Controlled Release Pesticides Symposium, pps. 4.23-4.35, September 1976.

9. HERCON* INSECTAPE: The PCO's New Weapon for the Ancient War on Roaches; Pest Control Magazine, October 1976.

10. INSECTAPE is Working; Pest Control Technology, February 1977.

11. Advantages of Using Controlled Release Formulations for Insect Control in Commercial Food-Handling Establishments, Proceedings - 1977 International Controlled Release Pesticide Symposium, pps. 216-225, August 1977.

12. Insect Control with the Multilayered Luretape* Dispenser, Proceedings - 1977 International Controlled Release Pesticides Symposium, pps. 78-89, August 1977.

13. A Novel Way to Dispense Fragrances and Room Deodorizers; Soap Cosmetics and Chemical Specialties, p. 53, May 1978.

14. Use of Laminated Controlled Release Contact-Action Insecticidal Strips for Cluster Fly Control; Entomological Society of America, 1978 National Meeting Presentation, Houston, Texas, November 26, 1978.

15. Controlled Release Air Fresheners; Maintenance Supplies, July 1978.

16. Controlled Release Modes and Methods; International Controlled Release of Bioactive Materials Symposium, p. 2.56, August 1978.

17. Hercon Luretape Disparture Dispensers for Mating Suppression of Gypsy Moth; Eastern Branch Entomological Society of America, New York, September 27, 1978.

18. Use of Multilayered Pheromone Dispensers for Control of Cotton Insects; Biologically Active Chemicals in Air Symposium of ACS, (Hawaii) April 1, 1978.

19. Hercon Commercial Pheromone Products - 7th International Controlled Release Symposium Proceedings, p. 27, July 1980.

20. Cotton Insects: Dispenser Development and Disruption of Mating Trials; 6th International Controlled Release of Bioactive Materials Proceedings, p. IV-13, July 1979.

21. Diffusion through Laminated Polymeric Films: Theoretical Considerations and Applications to Agriculture. American Institute of Chemical Engineers; National Meeting, Philadelphia, June 10, 1980.

22. Recent Progress with Gossyplure for Pink Bollworm Mating Disruption; 8th Desert Cotton Insect Symposium, March 12, 1980.

23. Mating Disruption and Mass Trapping of Insects with Hercon Flake; Colloquium on Management of Insects with Semiochemicals, Gainesville, Florida, March 24, 1980.

24. Convention Agrichemical Controlled Release Formulations for Agriculture, Forestry, and Food Protection; 8th International Controlled Release of Bioactive Materials Symposium Proceedings, p. 66, July 26, 1981.

25. Controlled Release Insecticide Formulations for Long-Term Fire Ant Control in Nursery and Sod Industry; Imported Fire Ant Workshop, Biloxi, Miss., March 24, 1981.

26. Gossyplure in Laminated Plastic Formulations for Mating Disruption and Pink Bollworm Control; Journal of Economic Entomology, p. 376, August 1981.

27. Lawn and Garden Insect Suppression with Pheromone Baited Traps; 9th International Controlled Release of Bioactive Materials Symposium Proceedings, p. 76, July 25, 1982.

28. Potential of Periplanone B: Enhancement of Cockroach Control Treatments; Pest Control Magazine; in press.

29. Transdermal Delivery of Medication Through Polymeric Laminated Structures; 9th International Controlled Release Symposium of Bioactive Materials Proceedings, p. 128, July 25, 1982.

30. Development of the Hercon Plastic Laminate System for Control of the Artichoke Plume Moth, Joint Meeting ESA-ESC; Toronto, Canada, November 29, 1982.

31. Controlled Release Formulations of Periplanone B Sex Pheromone for American Cockroach Control; 10th International Symposium on Controlled Release of Bioactive Materials Proceedings, pps. 223-230, July 1983.

32. Attraction of American Cockroaches to Traps Containing Periplaone B: Journal

of Economic Entomology, Vol. 3, No. , p. 448, 1984.

33 Transdermal Delivery of Nitroglycerin from a Laminated Reservoir System; 11th International Symposium of Controlled Release of Bioactive Materials Proceedings, p. 2, July 1984.

34. Controlled Release Technology and its Applications to Pharmaceuticals and Agriculture, Presentation to the North Jersey Section of the American Institute of Chemical Engineers; February 26, 1985.

35. Pink Bollworm Management Program Using a Heat Unit-Based Model and Controlled Release Pheromone Systems; 12th International Symposium on Controlled Release of Bioactive Materials Proceedings, p. 62, 1985.

36. Transdermal Delivery of ISDN from Hercon Patches Containing Azone; 12th International Symposium on Controlled Release of Bioactive Materials Proceedings, p. 322, 1985.

37. Applications of Controlled Release to Pharmaceuticals; Presentation at the Annual Technical Conference of the Society of Plastics Engineers, April 1985.

38. Transdermal Delivery of a Prostaglandin from Hercon Polymer Matrix System; 13th International Symposium on Controlled Release of Bioactive Materials, p. 09, 1986.

39. Luretape with Grandlure; 13th International Symposium on Controlled Release of Bioactive Materials, p. 162, 1986.

40. Drug Delivery Systems, 2nd Annual Drug and Health Care Seminar; Plaza Hotel, New York City, October 28, 1986.

41. New Sex Weapon for American Cockroach Control; Pest Control Magazine; p. 40, November 1986.

42. Hercon Technology for Transdermal Delivery of Drugs; Journal of Biomaterials Applications, Vol. 1, p. 239, October 1986.

43. Controlled Release of Propoxur from the Hercon Flea and Tick Collar; 14th International Symposium on Controlled Release of Bioactive Materials, p. 48, 1987.

44. Effect of Bait Color and Placement on Boll Weevil Trap Capture; Entomological Society of America Annual Meeting; Boston, December 1987.

45. Hercon Transdermal Technologies; Presented at Biomedical Business International Conference; Philadelphia, Pa; November 1987.

46. Transdermal Delivery of Prostaglandin R022; AAPS Meeting, Orlando, FL, p. S-128, June 1988.

47. Development and Optimization of a Clonidine Transdermal Patch; 15th International Symposium on Controlled Release of Bioactive Materials, p. 114, 1988.

48. Novel Transdermal Drug Delivery System; 15th International Symposium on

Controlled Release of Bioactive Materials, p. 87, 1988.

49. Patent Watch-Transdermal Update, in Controlled Research Newsletter, T. Roseman, Ed. - 7 (Issue 2):5 (1989).

50. Patent Watch-Transdermal Update, in Controlled Release Newsletter, T. Roseman, Ed. - 7 (Issue 3):8 (1989).

51. Hydrophilic Polyurethane Adhesives and Elastomers for Bioapplications; Bristol-Myers Squibb Product Development Seminar, Hyatt Regency Hotel, Buffalo, NY, July 16, 1990.

52. Patent Watch-Transdermal Update, in Controlled Release Newsletter, T. Roseman, Ed. - 8 (Issue 1):11 (1990).

53. Patent Watch-Transdermal Update, in Controlled Release Newsletter, T. Roseman, Ed. - 8 (Issue 2):10 (1990).

54. Bioadhesive Mechanisms: FTIR Studies on Hydration Induced Hydrocolloid/ Rubber Phase Reversal; 18th International Symposium of Controlled Release of Bioactive Materials, p. 113, 1991.

55. Temperature Activated Controlled Release; 18th International Symposium of Controlled Release of Bioactive Materials, p. 417, 1991.

56. Patent Watch-Transdermal Update, in Controlled Release Newsletter, T. Roseman, Ed. - 9 (Issue 1):16 (1992).

57. Patent Watch-Transdermal Update, in Controlled Release Newsletter, T. Roseman, Ed. - 9 (Issue 2):18 (1992).

58. Patent Watch-Transdermal Update, in Controlled Release Newsletter, T. Roseman, Ed. - 9 (Issue 3):16 (1992).

59. Chemical Stability of Polyurethane Foam Covered Breast Implants; The Toxicologist, Vol. 12, No. 1, p. 133 (1992).

60. Thermoplastic Adhesive Hydrogels; BMS Product Development Seminar, Princeton, NJ; 5/27/92.

61. Development of Mucoadhesives: Physicochemical Studies; BMS Product Development Seminar, Princeton, NJ; 5/27/92.

62. Patent Watch-Transdermal Update, in Controlled Release Newsletter, T. Roseman, Ed. - 10 (Issue 2):12 (1993).

63. Patent Watch-Transdermal Update, in Controlled Release Newsletter, T. Roseman, Ed. - 10 (Issue 3):16 (1993).

64. Analysis of the Extractive and Hydrolytic Behavior of Micro thane poly (ester-urethane) Foam by High Pressure Liquid Chromatography; J. of Biomedical Materials Research, Vol. 27, 655 (1993).

65. Patent Watch-Transdermal Update, in Controlled Release Newsletter, T. Roseman, Ed. - 11 (Issue 1):20 (1994).

66. Patent Watch-Transdermal Update, in Controlled Release Newsletter, T. Roseman, Ed. - 11 (Issue 2):16 (1994).

67. Skin Compatible Polyurethane Pressure Sensitive Adhesives for Ostomy, Wound and Skin Care Applications; BMS Product Development Seminar, New Brunswick, NJ; June 9, 1994.

68. Sensitization of Mice to Topically Applied Drugs: Albuterol, Chlorpheniramine, Clonidine, and Nadolol; J. Investigative Dermatology, 104, No. 4, P. 680 (April 1995).

69. Abrogation of Contact Hypersensitivity in Mice by Topically Applied Mast Cell Degranulating Agents; J. Investigative Dermatology, 104, No. 4, P. 679 (April 1995).

70. Evidence for the Anti-Inflammatory Activity of the Topical Immunosuppressive Agent, Ethacrynic Acid; 6th BMS Pharmaceutical Research Institute Symposium, Wallingford, CT (March 1995).

71. Topical Delivery of Mast Cell Degranulating Agents for Treatment of Transdermal Drug-Induced Hypersensitivity; 22nd International Symposium on Controlled Release of Bioactive Materials; p. 194, (1995).

72. Sensitization of Mice to Topically Applied Drugs: Albuterol, Chlorpheniramine, Clonidine, Nadolol; *Contact Dermatitis*, 35 p. 76, (September 1996).

73. Patent Watch-Transdermal Update, in Controlled Release Newsletter, T. Roseman, Ed., 12 (Issue 1):18 (1995).

74. Patent Watch-Transdermal Update, in Controlled Release Newsletter, T. Roseman, Ed., 12 (Issue 3):16 (1995).

75. Topical Antiirritant Activity of Ethacrynic Acid; First International Symposium on Cosmetic Efficacy, New York,(April 1996).

76. Prevention of Contact Hypersensitivity to Topically Applied Drugs by Ethacrynic Acid: Potential Application to Transdermal Drug Delivery; *Journal of Controlled Release*, 48 pp. 79-87 (1997).

77. Novel Polymeric Gels for Biomedical Applications; Third New Jersey Symposium of Biomaterials and Medical Devices, New Brunswick, NJ (November 1996).

78. Photopolymerizable Urethane-Methacrylate Pressure Sensitive Adhesives; 7th BMS Pharmaceutical Research Institute Symposium; Princeton, NJ (November 1996).

79. Topical Countersensitizer Activity of Ethacrynic Acid, *J. Investigative Dermatology*, 108, No. 4, p. 663 (April 1997).

80. Topical Delivery of Ion Channel-Modulating Agents Prevents Contact Hypersensitivity to Sensitizing Drugs; *J. Investigative Dermatology*, 108, No. 4, p. 662 (April 1997).

81. Patent Watch-Transdermal Update; *Controlled Release Newsletter*, T. Roseman, Ed., 14 (Issue 1), p. 21 (1997).

82. Elimination of Transdermal Drug-Induced Hypersensitivity by Topical Delivery of Ion Channel Modulating Agents; *24th International Symposium on Controlled Release of Bioactive Materials*; p. 211 (1997).

83. Prevention of Contact Hypersensitivity to Topically Applied Drugs by Ethacrynic Acid: Potential Application to Transdermal Drug Delivery; *J of Controlled Release*, Vol. 10, No. 1, p. 79 (1997).

84. Abrogation of Sensitization in Transdermal Delivery; IBC: International Conference on Transdermal Drug Delivery, San Diego, CA. (December 1997).

85. Phenoxyacetic Acid Methyl Ester Inhibits Irritant and Allergic Contact Dermatitis; *J. Of Investigative Dermatology* (Abstract); 110 No. 4, p. 637 (1998).

87. Fundamental Concepts in Skin Irritation and Sensitization; CRS Symposium on Recent Developments in Controlled Release Science and Technology, Athens, Greece (April 1998).

88. Patent Watch - Transdermal Update; in *Controlled Release Newsletter*, T.Roseman,Ed., 15 (Issue 1), p. 13 (1998)

89. Inhibition of Irritation and Contact Hypersensitivity by Ethacrynic Acid; *Skin Pharmacol. Applied Physiol.*, 11, 279 (1998).

90. Several Different Ion Channel Modulators Abrogate Contact Hypersensitivity in Mice; *Skin Pharmacol. Applied* Physiol., 12, 12, (1999).

91. Cis-Urocanic Acid Induces Mast Cell Degranulation and Release of Preformed TNF-∀ : A Possible Mechanism Linking UVB and Cis-Urocanic Acid to Inhibition of Contact Hypersensitivity; *Skin Pharmacol. Applied Physiol.*, 12, 18 (1999).

92. Inhibition of Transdermally Induced Irritation by the Loop Diuretic Ethacrynic Acid and Some Analogues; 26th International Symposium on Controlled Release of Bioactive Materials, p. 5316 (1999).

93. Patent Watch - Transdermal Update; in *Controlled Release Newsletter*, D. Friend, Ed., 16 (Issue 2), p. 24 (1999).

94. Inhibition of Irritation and Contact Hypersensitivity by Phenoxyacetic Acid Methyl Ester (PAME) in Mice; *Skin Pharmacol. Applied Physiol., 13, 65 (2000).*

95. N,O-Carboxymethylchitosan as a Mucoadhesive for Vaginal Delivery of Levonorgestrel; 27th International Symposium on Controlled Release of Bioactive Materials; p. 781 (July 2000).

96. Patent Watch - Transdermal Update; in *Controlled Release Newsletter*, D.Friend, Ed., 17 (Issue 3), p. 25 (2000)

97. N,O-Carboxymethylchitosan as a Viscoelastic Agent in Ophthalmic Surgery; 28th International Symposium on Controlled Release of Bioactive Materials; p. 255 (June 2001).

98. Patent Watch - Transdermal Update: in *Controlled Release Newsletter,* D. Friend, Ed., 18 (issue 3), p. 15 (2001)

99. Transdermal Delivery of Drugs: Promise/Innovation/Challenge; in *Controlled Release Newsletter,* D. Friend, Ed., 19 (issue 2), p.3 (2002).

100. Patent Watch - Transdermal Update: in *Controlled Release Newsletter,* B. Michniak, Ed., 19 (issue 3) p.9 (November 2002).

101. N,O-Carboxymethylchitosan as Permeation Enhancer for the Oral Delivery of Peptides; The 6th NJ Symposium on Biomaterials Science/Design Strategies for the Future; p. 87 (October 2002).

102. In Vitro Enhancement of Oral Delivery of Peptides by Chitinous Derivatives; 30th International Symposium on Controlled Release of Bioactive Materials; p. 694 (July 2003).

103. In Vivo Enhancement of Oral Delivery of Peptides by Chitinous Derivatives; 30th International Symposium on Controlled Release of Bioactive Materials; p. 704 (July 2003).

104. Patent Watch - Transdermal Update: In *Controlled Release Newsletter,* B. Michniac, Ed., 20 (issue 2) p.13 (May 2003)

105. Palmitoleic Acid Isomer, C16:1D6), in Human Skin Sebum Is Effective Against Gram-Positive Bacteria; *Skin Pharmacol Appl Skin Physiol 2003;16:176-187 (2003).*

106. Effect of Chitinous Derivatives on the Permeability of Intestinal Epithelia; 6th International Symposium on Polymer Therapeutics (January 2004)

107. Patent Watch- Transdermal Update: *In Controlled Release Society Newsletter,* B. Michniac, Ed., p. 17 (May 2004).

108. Patent Watch-Transdermal Update: IN Controlled Release Society Newsletter, B. Michniac, Ed., (January 2005).

REFERENCES CITED (Attached):

1. Bonina, F. P., et al., Vehicle effects of in vitro skin penetration of and SC affinity for model drugs caffeine and testosterone, Int. J. Pharm., 100, p. 41 (1993).

2. Smith, E. W., et al., Blanching activities of betamethasone formulations. The effect of dosage form on topical drug delivery, Drug Res., 40, p. 618 (1990).

3. Davis, A. F. and Hadgraft, J., Effect of supersaturation on membrane transport. I. Hydrocortisone acetate, Int. J. Pharm., 76, p. 1 (1991).

4. Kurihara-Bergstrom, T., et al., Physicochemical study of percutaneous absorption enhancement by DMSO, J. Pharm. Sci., 75, p. 479 (1986).

5. Harada, K., et al., Role of intercellular lipids in the stratum corneum in the percutaneous permeation of drugs, J. Invest. Dermatol., 99, p. 278 (1992).

6. Bouwstra, J. A., et al., The influence of alkyl-azones on the ordering of lamellae in human stratum corneum, Int. J. Pharm., 79, p. 141 (1992).

7. Golden, G. M., et al., Role of stratum corneum lipid fluidity in transdermal drug flux, J. Pharm. Sci., 76, p. 25 (1987).

8. Aungst, B. J., et al., Enhancement of naloxone penetration through humal skin in vitro using fatty acids, fatty alcohols, surfactants, sulfoxides and amides, Int. J. Pharm., 33, p. 225 (1986).

9. Barry, B. W., Mode of action of permeation enhancers in human skin, J. Contol. Rel., 6, p. 85 (1987).

10. Ongpipattanakul, B., et al., Evidence that oleic acid exists in a separate phase within the SC lipids, Pharm. Res., 8, p. 350 (1991).

11. Takeuchi, Y., et al., Effects of oleic acid/propylene glycol on rat abdominal SC: lipid extraction and appearance of propylene glycol in the dermis, Chem. Pharm. Bull., 41, p. 1434 (1993).

12. Aungst, B. J., et al., Transdermal oxymorphone formulation development and methods for evaluating flux and lag times for two skin permeation enhancing vehicles, J. Pharm. Sci., 79, p. 1072 (1990).

13. Cooper, E. R., Increased skin permeability for lipophilic drugs, J. Pharm. Sci., 73, p. 1153 (1984).

14. Kurihara-Bergstrom, T., et al., Physicochemical study of percutaneous absorption enhancement by DMSO: DMSO mediation of vidarabine permeation, J. Invest. Dermatol., 89, p. 274 (1987).

15. Sweeney, T. M., et al., The effect of DMSO on the epidermal water barrier, J. Invest. Dermatol., 46, p. 300 (1966).

16. Elfbaum, S. G., et al., The effect of DMSO on percutaneous absorption: a mechanistic study. I., J. Soc. Cosmet. Chem., 19, p. 19 (1968).

17. Stoughton, R. B. and Fritsch, W., Influence of DMSO on percutaneous absorption, Arch. Dermatol. 90, p. 512 (1964).

18. Aungst, B. J., Blake, J. A. and Hussain, M. A., Contributions of drug solubilization, partitioning, barrier disruption, and solvent permeation to the enhancement of skin permeation of various compounds with fatty acids and amines, Pharm Res. 7, p. 712 (1990).

REFERENCE 1

International Journal of Pharmaceutics, 100 (1993) 41–47

IJP 03276

Vehicle effects on in vitro skin permeation of and stratum corneum affinity for model drugs caffeine and testosterone

F.P. Bonina [a], V. Carelli [b], G. Di Colo [b], L. Montenegro [a] and E. Nannipieri [b]

[a] *Institute of Pharmaceutical Chemistry, University of Catania, Catania (Italy) and* [b] *Pharmaceutical Technology Laboratory, Institute of Pharmaceutical Chemistry, University of Pisa, Pisa (Italy)*

(Received 17 February 1993)
(Accepted 6 April 1993)

Key words: Percutaneous absorption; Partition coefficient; Enhancer evaluation; Transcutol; DPPG; Labrasol; Labrafil; Caffeine; Testosterone

Summary

The effects of Labrasol (LBS) (glycolysed ethoxylated C_8/C_{10} glycerides), Labrafil (LBF) (glycolysed ethoxylated glycerides), Transcutol (TSC) (diethylene glycol monoethyl ether) and DPPG (propylene glycol dipelargonate) on the flux across excised human skin of the lipophilic testosterone (TST) and the hydrophilic caffeine (CAF) and on the affinity of the human stratum corneum for these drugs are compared taking propylene glycol (PG) and liquid petrolatum (LP) as reference vehicles. DPPG and LBF enhance CAF flux relative to PG while LBS and TSC increase the stratum corneum affinity for TST relative to LP. However, the materials tested enhance neither the flux of nor the stratum corneum affinity for both drugs with respect to either reference. On the other hand, a saturated solution of DPPG in PG enhances both properties for both drugs relative to PG. Such effects are ascribed to the ability of DPPG to interact with the lipid bilayers and to that of PG to promote DPPG penetration into stratum corneum and to create interaction sites in such a tissue.

Introduction

Low systemic and cutaneous toxicity are prerequisites of the materials used to enhance the percutaneous penetration of drugs. The low toxicity of Labrasol (LBS) (glycolysed ethoxylated C_8/C_{10} glycerides), Labrafil (LBF) (glycolysed ethoxylated glycerides), Transcutol (TSC) (diethylene glycol monoethyl ether) and DPPG (propylene glycol dipelargonate) has recently prompted investigation of the ability of these materials to promote the percutaneous penetration of drugs. According to literature data, TSC can promote the percutaneous penetration of the lipophilic prostaglandin (Watkinson et al., 1991) and the hydrophilic theophylline (Touitou et al., 1991). In particular, the effect on prostaglandin percutaneous absorption was found to be 3–4-fold as strong as that of Azone. However, TSC is unable to exert any such effect on the lipophilic morphine (Rojas et al., 1991) or the hydrophilic peptide vasopressin (Banerjee and Ritschel, 1989). On the other hand, the flux through skin of

Correspondence to: E. Nannipieri, Pharmaceutical Technology Laboratory, Institute of Pharmaceutical Chemistry, University of Pisa, Via Bonanno 6, 56126 Pisa, Italy.

morphine and vasopressin can be accelerated by DPPG (Rojas et al., 1991) and LBF (Banerjee and Ritschel, 1989), respectively.

Consideration of the above results convinced us of the utility of further evaluating the ability of the above materials to influence the skin characteristics relevant to the therapeutic effect of drugs. These are the skin permeability by the drug and its retention capacity of the drug, which are related to the systemic and/or topical action of the drug. The latter is particularly important in cases where the skin is the target organ (Shah et al., 1992). To this aim we studied the effects of LBS, LBF, TSC and DPPG on the flux across excised human skin of testosterone (TST) and caffeine (CAF), chosen as models of lipophilic and hydrophilic drugs, respectively, and on the affinity of the human stratum corneum for these drugs.

Materials and Methods

Materials

Caffeine (CAF), liquid petrolatum (LP) and propylene glycol (PG) were bought from Farmitalia Carlo Erba (Milano, Italy). Testosterone (TST) was purchased from Fluka Chemie AG (Switzerland). DPPG, Labrafil M 1944 (LBF), Labrasol (LBS) and Transcutol (TSC) were a gift from Gattefosse (Saint-Priest Cedex, France).

Strips of human callus were removed from the plantar surface of volunteers with a scalpel, and stored in a desiccator over $CaCl_2$.

Samples of whole adult human skin (mean age 15–45 years) were obtained from breast reduction operations. Subcutaneous fat was carefully trimmed and the skin was immersed in distilled water at 60 ± 1°C for 2 min (Kligman and Christophers, 1963), after which the stratum corneum plus attached viable epidermis (SCE) was peeled off. The SCE samples were dried at room temperature in a desiccator maintained at approx. 25% RH. The dried samples were wrapped in aluminium foil and stored at 4 ± 1°C.

In vitro skin permeation

Skin permeation of CAF and TST was measured using Franz cells (Franz, 1975). Samples of dried SCE were rehydrated by immersion in distilled water at room temperature for 1 h before being mounted in diffusion cells. The receiving chamber had a volume of 4.5 ml and was filled with saline. The receptor phase was stirred and kept at 30 ± 1°C during the experiment. The surface area for permeation was 0.75 cm^2. Suspensions (100 μl) of CAF or TST in PG, PG saturated with DPPG, LP, LBS, LBF, DPPG and TSC were applied to the skin and the experiment was run for 24 h. Samples of the receiving solution were withdrawn at intervals, analysed for drug concentration and replaced with fresh solution.

The flux, J, through the skin was obtained, using linear regression analysis, by plotting the cumulative amount of drug permeated against time and dividing the slopes of the steady-state portion of the graph by the area of the diffusion cell. Each measurement was made in triplicate.

Solubility determination

An excess of drug was added to 4 ml of the appropriate solvent in a glass-stoppered test tube. This was stirred for 48–72 h in a thermostated (30°C) water bath, then the excess solid was removed by filtering through a 0.2 μm pore size polytetrafluoroethylene filter (SM11807 Sartorius GmbH, Gottingen, Germany) in an atmosphere thermostated at 30°C. The clear filtrate was diluted with ethanol and analysed for drug concentration. The assay of TST concentration in LP needed the following procedure. A 50 ml sample of clear LP solution was added with 10 μl of ethanol and the resulting mixture was vigorously shaken for 5 min; the ethanolic phase was assayed for TST concentration after centrifugation at 4000 rpm for 20 min..

Partition coefficient determination

n-Octanol / water. *n*-Octanol and water were presaturated with each other. 1.5 ml of TST solution in *n*-octanol was added with 14.0 ml of water and the mixture was tumble-mixed for 24 h in an atmosphere thermostated at 30°C. After separating the phases by centrifugation, both the alcoholic and the aqueous solution were diluted and analysed for drug concentration.

Human callus / vehicle. Solutions of CAF or TST in the vehicles under study were prepared so that the drug concentration was about 50% of the saturation concentration. Fragments of dry callus (0.5–1.0 g) were hydrated by exposure to water vapour in a closed system at 37°C until the water content was about 30% (w/w) of the hydrated tissue. The hydrated callus fragments were placed in a screw-cap glass vial, stored overnight at 4°C, then added with a drug solution (5.0 ml) in the proper vehicle. The vial was placed in a thermostated (30°C) shaker water bath, and the equilibrium concentration of the fluid phase was determined after 60 h (30 h for water); missing drug was assumed to have entered the tissue. The assay of TST concentration in LP needed the special procedure described under Solubility determination. The fragments of callus were gently sandwiched between filter paper to remove clinging vehicle and then weighed; this weight was used for calculating the partition coefficient, which was expressed as the ratio of molal to molar concentrations.

For the purposes of the present study, human callus was considered representative of epidermal stratum corneum. Our choice was validated by comparing literature data on CAF and TST partitioning into stratum corneum with some of our data obtained using callus (see Table 1).

Assay methods

The drugs were assayed by high-performance liquid chromatography. An isocratic pump (Perkin Elmer, model 250) equipped with UV/Vis spectrophotometric detector (Perkin Elmer, model 290) was used. A 250 × 4.6 mm Partisil ODS-3 (5 μm) column (Whatman Chemical Separation Inc., U.S.A.) was used for both TST and CAF. The mobile phase was a methanol/water mixture at 7:3 and 3.5:6.5 volume ratio for TST and CAF, respectively. TST and CAF were detected at 250 and 273 nm, respectively.

TABLE 1

CAF and TST partitioning data [a]

System	CAF	TST
Human callus/water [b]	1.56 ± 0.50	44.0 ± 3.5
Human callus/LP [b]		4.9 ± 2.8
Horny layer/water [c]	3.50 ± 0.40	47.4 ± 1.7
Horny layer/petrolatum [c]		5.3 ± 0.7
n-Octanol/water [b]	0.70 ± 0.02 [d]	1679 ± 44

[a] Values are the mean ± SD ($n \geq 3$).
[b] The experiments were carried out at 30°C.
[c] Data from Bronaugh and Franz (1986). The experiments were carried out at room temperature.
[d] Datum from Carelli et al. (1990).

Results and Discussion

Under the conditions of our permeation experiments, if the stratum corneum is the only rate-determining barrier, then the drug flux, J, is expressed by the well known equation:

$$J = (D/h) \cdot S_m \qquad (1)$$

where D is the apparent diffusivity of the drug in the barrier, h denotes the effective barrier thickness, and S_m is the drug solubility in the stratum corneum at equilibrium with the vehicle.

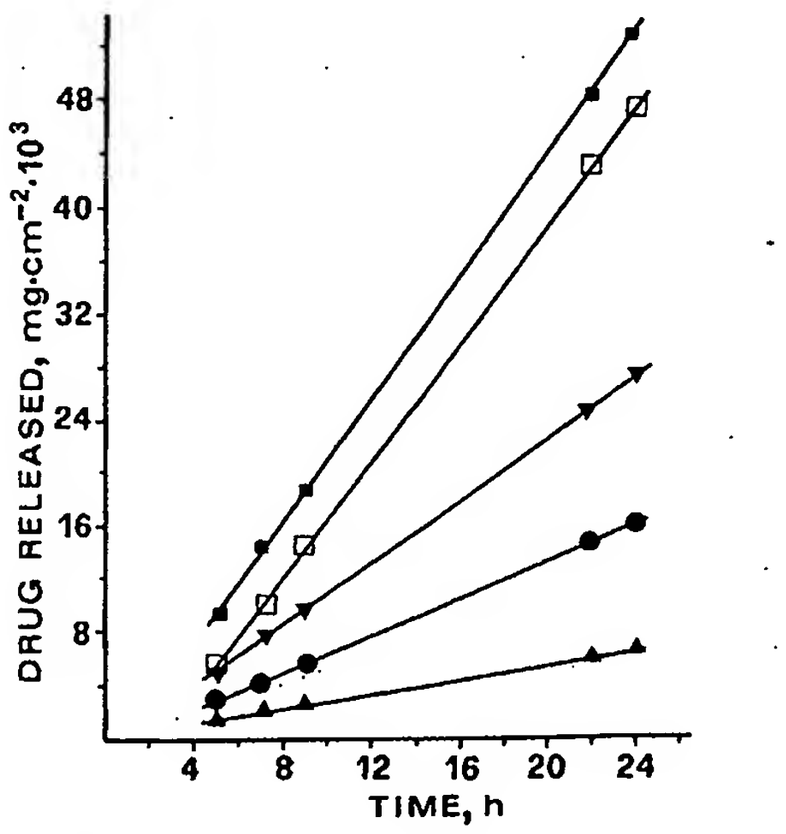

Fig. 1. Typical skin permeation curves of CAF from a drug suspension in LBS (▲), PG (●), LBF (▼), PG-DPPG (□) or DPPG (■). The permeation curve relative to TSC could not be represented because it was superimposed on the PG curve.

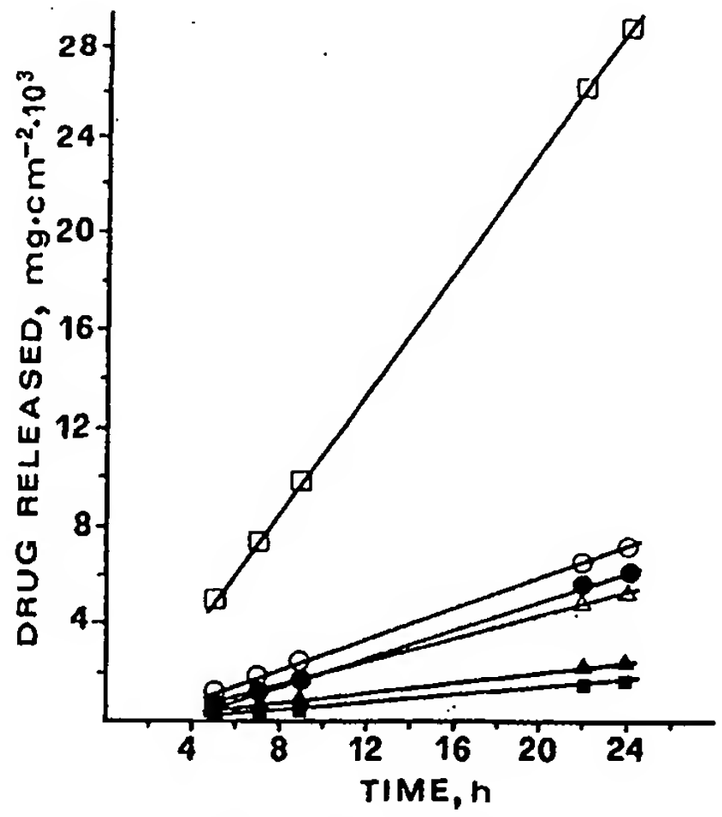

Fig. 2. Typical skin permeation curves of TST from a drug suspension in DPPG (■), LBS (▲), TSC (△), PG (●), LP (○) or PG-DPPG (□). The permeation curve relative to LBF could not be represented because it was superimposed on the PG curve.

Compliance with Eqn 1 implies that the plot of the drug amount permeated vs time should be linear, after a lag time required for attainment of the stationary state. Figs 1 and 2 show that this was in fact the case with all of the drugs and vehicles tested. The J and S_m values for the vehicles under study were expressed in terms of the corresponding values for a reference vehicle. LP and PG were chosen as reference vehicles for their frequent use in topical formulations. For a given vehicle, the relative values, J^* and S_m^*, gauged the modifications by the vehicle of the skin properties relevant to drug flux and of the stratum corneum affinity for the drug, with respect to the reference vehicle. An approximate estimation of S_m^* for each vehicle was achieved from the relevant values of callus/vehicle partition coefficient, K, and drug solubility in vehicle, S_v, listed in Tables 2 and 3, according to the following equation:

$$S_m^* = (K/K_r) \cdot (S_v/S_{vr}) \cdot (d_m/d_{mr}) \qquad (2)$$

where d_m is the density of callus at equilibrium

TABLE 2

Solubility (S_v), partitioning (K) and flux (J) data for CAF [a]

Vehicle	S_v (mg ml^{-1})	K [b] (ml g^{-1})	J (μg cm^{-2} h^{-1})
PG	13.9 ± 1.2	2.87 ± 0.5	0.698 ± 0.099
Water	27.9 ± 1.7	1.56 ± 0.5	0.724 ± 0.041
TSC	14.1 ± 0.9	0.44 ± 0.2	0.635 ± 0.197
LBS	12.0 ± 0.8	0.53 ± 0.2	0.277 ± 0.057
LBF	3.3 ± 0.4	1.64 ± 0.4	1.162 ± 0.085
DPPG	1.9 ± 0.05	2.28 ± 0.1	2.278 ± 0.353
PG-DPPG	13.9 ± 0.9	3.27 ± 0.2	2.193 ± 0.174

[a] Values are mean ± SD ($n \geq 3$).
[b] Human callus/vehicle partition coefficient.

with vehicle and the subscript r identifies the factors for the reference vehicle.

The ratio of densities in Eqn 2 was taken as equal to unity, since in no case did the equilibration with vehicle cause any important weight increase of callus nor was the vehicle density markedly different from that of callus. Determination of S_m^* by Eqn 2 involves the assumptions that callus is representative of epidermal stratum corneum and that Henry's law holds in the phases at equilibrium up to saturation.

Semiquantitative information on the vehicle effect on the kinetic factor, D/h, in Eqn 1 could be obtained, once J^* and S_m^* were assessed, by applying the following equation:

$$J^* = (D/h)^* \cdot S_m^* \qquad (3)$$

TABLE 3

Solubility (S_v), partitioning (K) and flux (J) data for TST [a]

Vehicle	S_v (mg ml^{-1})	K [b] (ml g^{-1})	J (μg cm^{-2} h^{-1})
PG	75.90 ± 0.04	5.20 ± 2.50	0.291 ± 0.054
LP	0.43 ± 0.04	4.90 ± 2.50	0.319 ± 0.084
Water	0.03 ± 0.008	44.00 ± 3.50	0.263 ± 0.040
TSC	104.00 ± 5.00	0.38 ± 0.05	0.231 ± 0.036
LBS	46.10 ± 0.90	0.72 ± 0.04	0.102 ± 0.070
LBF	20.90 ± 1.00	0.05 ± 0.01	0.283 ± 0.029
DPPG	13.20 ± 0.50	0.16 ± 0.06	0.079 ± 0.080
PG-DPPG	74.10 ± 1.10	11.00 ± 2.50	1.226 ± 0.121

[a] Values are mean ± SD ($n \geq 3$).
[b] Human callus/vehicle partition coefficient.

The J^* and S_m^* values for CAF and TST in the different vehicles are listed in Table 4. For CAF only values relative to PG are reported, since we were unable to obtain reproducible values of the callus/LP partition coefficient, perhaps due to excessive sensitivity of this system to the degree of hydration of callus, which could not be controlled with the accuracy needed in this particular case.

Comprehensive consideration of the data in Table 4 shows that in all cases, except that of PG-DPPG, an effect on the affinity parameter, S_m^*, is coupled with an opposite effect on the kinetic parameter, $(D/h)^*$, as calculated from Eqn 3. Nevertheless, it should be recognized that the estimated $(D/h)^*$ values may reflect apparent changes of the kinetic factor instead of real changes. In fact, Eqn 1, from which Eqn 3 was derived, is strictly applicable to the diffusion across a homogeneous plane sheet, therefore, such an equation describes an oversimplified model of the skin barrier, which, in contrast, is a very complex polyphasic membrane. The drug may partly accumulate in zones of the stratum corneum which are excluded from the diffusive pathway (Shah et al., 1992), and the vehicle may influence the drug distribution between the different zones of the tissue. Therefore, variations of drug solubility in the horny layer, ensuing from changes in vehicle composition, may not be reflected by steady-state flux data.

As appears from the relevant J^*(PG) and J^*(LP) values in Table 4, TSC produced no significant change of skin flux of either CAF or TST with respect to PG or of TST with respect to LP. However, the corresponding S_m^* values, S_m^*(PG) and S_m^*(LP), are significantly different from 1, so that a balance between opposite effects on the kinetic factor, $(D/h)^*$, and the thermodynamic factor, S_m^*, in Eqn 3 can be argued. It is worth noting that the TSC effects on S_m^*(PG) were roughly similar for CAF and TST, despite the marked difference in polarity between the two drugs apparent in Table 1 from the respective values of the octanol/water partition coefficient.

Similar considerations can be made for the effects of LBS, except that with this vehicle the J^* values are lower than with TSC.

On the other hand, the effects of DPPG and LBF concerning CAF are not quite similar to those for TST. Indeed, for the former drug, the S_m^*(PG) values are much the same as those obtained with TSC or LBS as the vehicle, so the enhancement of flux by LBF and, especially, DPPG with respect to PG, as quantitated by the relevant J^*(PG) values, was mainly determined by a strong enhancement of the $(D/h)^*$ parameter. With TST as the drug, the two vehicles were unable to increase the drug flux with respect to PG, due to exceedingly low S_m^*(PG) values.

Taken together, the results discussed so far have demonstrated the ability of LBF and DPPG

TABLE 4

Relative values of flux (J^*) and drug solubility in stratum corneum (S_m^*)

Vehicle	CAF		TST			
	J^* (PG) [a]	S_m^* (PG) [a]	J^* (PG) [a]	S_m^* (PG) [a]	J^* (LP) [b]	S_m^* (LP) [b]
PG	1	1	1	1	0.91	187.0
LP	–	–	1.10	0.0054	1	1
Water	1.04	1.10	0.90	0.0033	0.82	0.6
TSC	0.91	0.15	0.79	0.100	0.72	18.7
LBS	0.40	0.16	0.35	0.084	0.32	15.7
LBF	1.66	0.14	0.98	0.0027	0.89	0.5
DPPG	3.26	0.11	0.27	0.0054	0.25	1.0
PG-DPPG	3.14	1.14	4.22	2.091	3.84	391.0

[a] Values relative to PG.
[b] Values relative to LP.

to facilitate the flux and the diffusivity of CAF across the stratum corneum with respect to PG, and the inability of any of the materials tested to increase the stratum corneum affinity for either drug over that produced by PG. Also, PG exerted a strong enhancing effect on the affinity of the stratum corneum for TST with respect to LP, as shown by the relevant S_m^*(LP) value in Table 4. These considerations motivated us to examine a saturated solution of DPPG in PG, where the two components could exert their maximum effects on skin. The J^* and S_m^* values in Table 4 for PG-DPPG as the vehicle are indeed the highest of all vehicles. However, even though the affinity parameter was equal or doubled with respect to PG alone, the effect on the kinetic parameter, as extimated through Eqn 3, was much weaker than that assessed for DPPG alone with either drug and reference vehicle. If the effect of PG-DPPG on S_m were assumed to consist in creating sites or zones in the skin interacting with the drug, without varying the thermodynamic activity in its actual diffusive pathway, then the steady-state flux might remain unaltered, while the apparent diffusivity would undergo a change opposite to that of S_m, even though the true diffusivity in such a pathway would be left unchanged. If the data in Table 4 are viewed in the light of the above hypothesis, an enhancement of the true kinetic factor can only taken for certain where both the experimental J^* value and the $(D/h)^*$ value estimated through Eqn 3 are greater than 1. Inspection of Table 4 leads one to conclude that the certainty of an enhancement of the true kinetic factor for both drugs can only be stated for DPPG in the PG-DPPG mixture, with reference to PG. This property of DPPG may be linked to the comparatively low polarity of this material enabling it to penetrate into the stratum corneum and interact with the lipid bilayers, thus increasing their fluidity or forming, as proposed by Walker and Hadgraft (1991) for oleic acid, fluid-like channels. When DPPG is used in combination with PG, the latter appears to promote DPPG penetration into stratum corneum and to create interaction sites in such a tissue. The fact that both CAF and TST fluxes were apparently affected by such an action of DPPG is in accord with the view that the lipid bilayers are an important rate-determining factor for the transcutaneous penetration of polar as well as nonpolar drugs (Barry, 1991). With LP as the reference, no vehicle can be assumed to increase the kinetic factor for TST penetration. Indeed, LP is so highly occlusive as to result in extensive hydration of the stratum corneum, which is known to increase drug diffusivity in the lipid pathway (Barry, 1987).

Conclusions

The potential of a vehicle to increase the affinity between stratum corneum and drug should be considered with regard not only to transdermal but also to topical drug delivery. Indeed, where drug delivery to the skin as target organ is concerned, drug retention in the skin is the main consideration as opposed to drug flux across the skin (Shah et al., 1992). In this respect, the PG-DPPG mixture may be regarded as an interesting vehicle for nonpolar drugs. The present results have shown that the enhancing effects of the materials studied on the flux of either the polar CAF or the nonpolar TST across excised human skin were determined by the kinetic factor, D/h, rather than the thermodynamic factor, S_m, in Eqn 1, even in those cases where the latter factor was increased to a substantial degree.

Acknowledgement

This work was supported by a grant of Ministero della Universita' e della Ricerca Scientifica e Tecnologica.

References

Banerjee, P.S. and Ritschell, W.A., Transdermal permeation of vasopressin: II. Influence of azone on in vivo and in vitro permeation. *Int. J. Pharm.*, 49 (1989) 199–204.

Barry, B.W., Lipid-protein-partitioning theory of skin penetration enhancement. *J. Controlled Release*, 15 (1991) 237–248.

Bronaugh, R.L. and Franz, T.J., Vehicle effects on percutaneous absorption in vivo and in vitro comparisons with human skin. *Br. J. Dermatol.*, 115 (1986) 1–11.

Carelli, V., Di Colo, G., Nannipieri, E. and Serafini, M.F., Effect of some animal oils of cosmetic use on in vitro skin permeation of model drugs caffeine, salicylamide and 2-hydroxy-4-methoxybenzophenone. *Acta Technol. Legis Medicamenti*, 1 (1990) 173–185.

Franz, T.J., Percutaneous absorption on the relevance of the in vitro data. *J. Invest. Dermatol.*, 64 (1975) 10–195.

Kligman, A.M. and Christophers, E., Preparation of isolated sheets of human stratum corneum. *Arch. Dermatol.*, 88 (1963) 702–705.

Rojas, J., Falson, F., Courraze, G., Francis, A. and Puisieux, F., Optimization of binary and ternary solvent systems in the percutaneous absorption of morphine base. *STP Pharm. Sci.*, 1 (1991) 70–75.

Shah, V.P., Behl, C.R., Flynn, G.L., Higuchi, W.I. and Schaefer, H., Principles and criteria in the development and optimization of topical therapeutic products. *Int. J. Pharm.*, 82 (1992) 21–28.

Touitou, E., Levi-Schaffer, F., Shaco-Ezra, N., Ben-Yiossef, R. and Fabin, B., Enhanced permeation of theophylline through the skin and its effect on fibroplast proliferation. *Int. J. Pharm.*, 70 (1991) 159–166.

Walker, M. and Hadgraft, J., Oleic acid – a membrane fluidiser or fluid within the membrane? *Int. J. Pharm.*, 71 (1991) R1-R4.

Watkinson, A.C., Hadgraft, J. and Bye, A., Aspects of the transdermal delivery of prostaglandins. *Int. J. Pharm.*, 74 (1991) 229–236.

Dermatika
Dermatics

Blanching Activities of Betamethasone Formulations

The effect of dosage form on topical drug availability

E. W. Smith, E. Meyer, and J. M. Haigh

Summary

The blanching activities of Betnovate® cream, lotion, ointment and scalp application (each containing 0.1 % betamethasone (as the 17-valerate)) were determined using healthy human subjects over a 32 h period in both the occluded and unoccluded modes. Considering that all four formulation types contained the same label concentration of corticosteroid, it may be presumed that the formulations would show similar topical drug availability: this was, however, not found to be the case. The scalp application demonstrated the highest topical availability in both the occluded and unoccluded modes. The lotion formulation showed the greatest increase in topical availability on occlusion and the ointment formulation was the least sensitive to the effects of occlusion. These differences, due solely to the effects of the vehicle, may have important clinical implications.

Zusammenfassung

Bleichwirkung von Betamethason-Zubereitungen / Einfluß der Formulierung auf die topische Arzneimittelverfügbarkeit

Die Abblassung der Haut durch Betnovate® Creme, Lotion, Salbe und Skalpanwendung (jeweils 0,1 % Betamethason als 17-Valerat) wurden über 32 h an gesunden Probanden im verschlossenen und nicht-verschlossenen Modus untersucht. Da alle vier Arzneiformen die gleiche Konzentration des Kortikosteroids enthielten, war anzunehmen, daß die vier verschiedenen Arzneiformen ähnliche topische Wirkung zeigen würden. Dies war jedoch nicht der Fall. Die Skalpanwendung ließ die höchste topische Wirkung im verschlossenen und nicht-verschlossenen Modus erkennen. Die Lotion zeigte die größte topische Verfügbarkeit unter Okklusion, während die Salbe gegenüber der Okklusionswirkung am wenigsten sensitiv war. Diese Unterschiede, die ausschließlich auf den Einfluß der Trägersubstanzen zurückzuführen sind, könnten klinisch relevant sein.

Key words: *Betamethasone 17-valerate, clinical studies · Betnovate® · Corticosteroids, topical · Skin, blanching*

1. Introduction

The human skin blanching assay has been shown to be a reliable method of assessing topical corticosteroid potency and availability [1]. This bioassay was used to compare the blanching activities of four commercially available topical formulations from the same manufacturer, each containing a label concentration of 0.1 % betamethasone (as the 17-valerate ester). The corticosteroid formulations tested were a cream, lotion, ointment and scalp application, the objective of the research being to determine the effect that the different delivery vehicles would have on the corticosteroid availability. Appropriate application regimens for the clinical usage of the different products could therefore be suggested.

2. Subjects and methods

The methodology for this trial varied from the general scheme normally used in our laboratories [1—3] in that each forearm application site was exposed to an equivalent mass of corticoste-

School of Pharmaceutical Sciences, Rhodes University, Grahamstown (South Africa)

roid, contained within different aliquots of each formulation type. In normal assay protocol equal masses or volumes of each formulation are applied to each site. This may result in different masses of the active ingredient being exposed to the skin as a result of varying drug concentrations within these formulations. It was believed that these small, interformulation concentration differences may influence the magnitude of blanching elicited. In this study it was important that only the formulation vehicle influences on drug release and subsequent blanching be manifest, without the additional influences of variable drug masses.

All the formulations (Betnovate®[1]) were purchased from a local pharmacy shortly before use and were within their shelf expiration period. Twelve healthy male and female volunteers were selected for the trial from a panel of subjects known to show a skin blanching response to a standard screening preparation (Betnovate cream). All subjects had previously taken part in similar experiments and written informed consent was obtained from each subject. The volunteers had not received topical or systemic corticosteroids for at least six weeks prior to the investigation.

The four products were each assayed by a high-performance liquid chromatographic method described previously [4] which yielded the exact drug concentration in each formulation. Serial weighings were conducted to establish the mass of each stripe of cream or ointment extruded from the 1 ml-tuberculin syringes normally employed in the blanching assay application procedure [1]. Weighings were also conducted to establish the mass per µl of lotion or scalp application that would be delivered to the skin from a transfer pipette (Brand, Wertheim, FR Germany). From this data the mass or volume of each formulation to be applied could be calculated so that an equivalent mass of betamethasone 17-valerate would be deposited on each application site.

Table 1 lists the assay values for each product and the mass of betamethasone (as the 17-valerate) applied to each forearm site. This list indicates that the masses of drug applied for each of the formulations were not identical. This was mainly due to the difficulty in precisely extruding a fraction of a stripe of the semi-solid formulations from the application syringes. Whole-stripe values were therefore adopted for the cream and ointment and the volumes of the lotion and scalp application were adjusted to yield an average applied drug mass of 3.62 µg. The drug dose was, therefore, as uniform as possible given the limitations of the application technique. Adhesive labels from which two 7 × 7 mm squares had been punched were applied to the flexor aspect of both forearms of each volunteer, producing 12 discrete application sites per arm. Since only four formulations were tested, each formulation occupied three sites per arm. The formulations were applied in four different arrangements, each application pattern being chosen randomly to avoid any bias during application and observation.

Table 1: Formulation assay values and mass of betamethasone (as the 17-valerate) applied to each site.

Formulation	Percentage purity	Mass (µg)
Cream	99.02	3.42
Lotion	91.54	3.56
Ointment	104.50	3.87
Scalp application	121.61	3.64

The sites on one forearm of each volunteer were occluded with aporous plastic tape, and the sites on the other arm were left unoccluded. The residual formulations were removed from the sites of both forearms 6 h after application. Thereafter, assessment of the blanching response was made independently by three experienced observers at 7, 8, 9, 10, 12, 14, 16, 18, 28 and 32 h after initial application and the results of the three observers were pooled for statistical analysis. The intensity of blanching was visually graded on a 0—4 scale where 0 represents normal skin and 4 represents intense blanching over the whole application site, with the values of 1, 2 and 3 representing the respective grades of blanching between the two extremes [5]. Four formulations applied to 12 sites on each forearm of twelve volunteers resulted in the blanching produced by each formulation being observed 108 times at each observation interval in both the occluded and unoccluded application modes.

[1] Manufacturer: Glaxo (Pty.) Ltd., Johannesburg (South Africa).

The percentage of the total possible score (% TPS) was calculated [1] and plotted against time in hours after preparation application, to generate blanching profiles for each application mode. The trapezoidal rule was used to calculate the area under the blanching curve (AUC). Statistical analyses (χ^2) at the 95 % level of significance were performed on the graded responses of the formulations being compared, and on direct comparisons between application sites [6].

3. Results and discussion

The blanching profiles of the four formulation types are plotted in Fig. 1 and 2 for the unoccluded and occluded application modes, respectively. Having applied approximately the same mass of betamethasone 17-valerate to

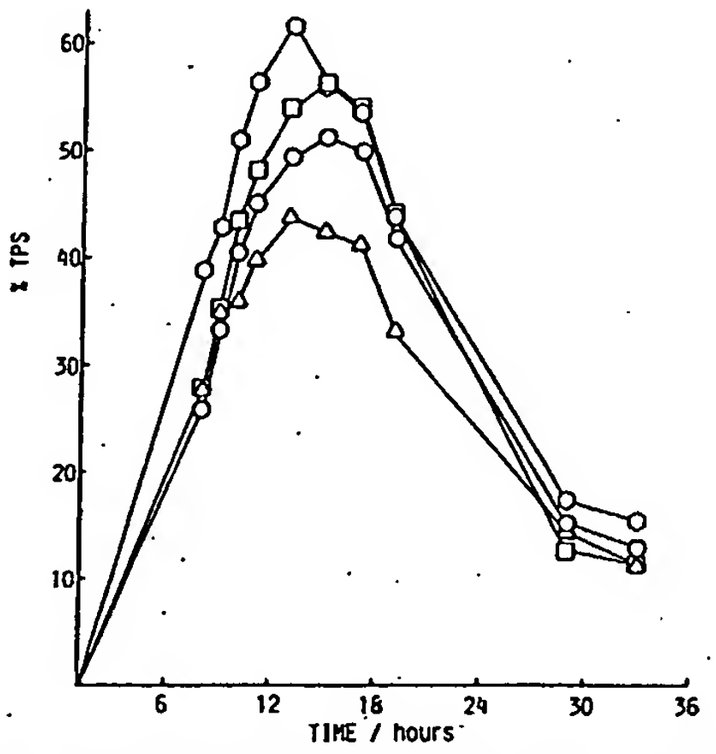

Fig. 1: Blanching profiles of commercial betamethasone 17-valerate formulations assessed in the unoccluded application mode (○ = cream, △ = lotion, □ = ointment, ○ = scalp application). %TPS = percentage of the total possible score.

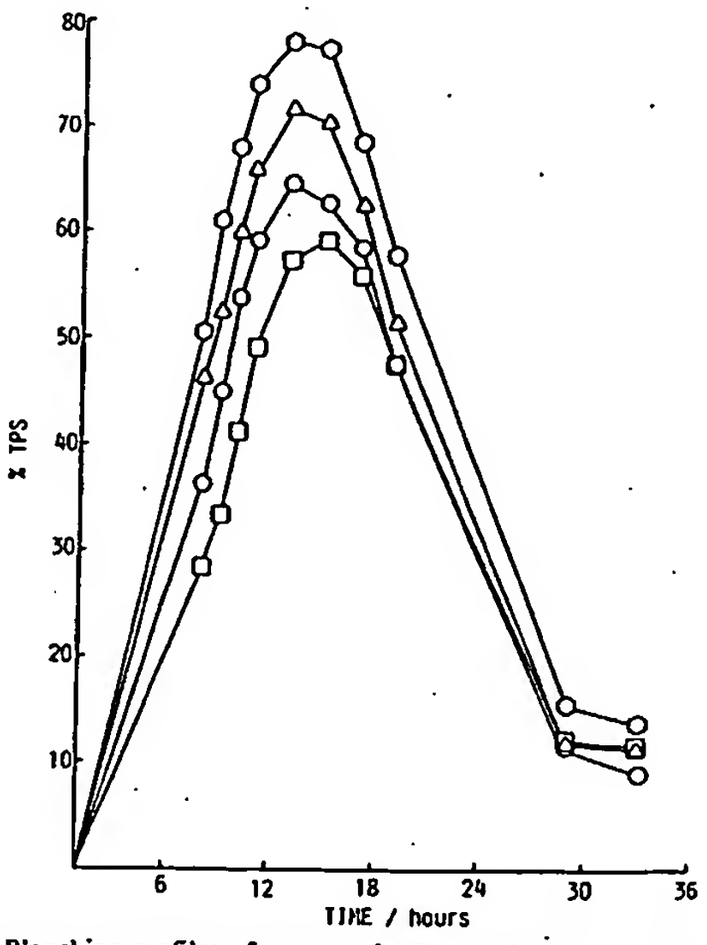

Fig. 2: Blanching profiles of commercial betamethasone 17-valerate formulations assessed in the occluded application mode (○ = cream, △ = lotion, □ = ointment, ○ = scalp application). %TPS = percentage of the total possible score.

each forearm site, it is interesting to note the markedly different blanching profiles elicited by the different formulations and to speculate on reasons for relatively greater drug movement from one formulation compared to that from another.

3.1. Unoccluded application mode

The decreasing rank order of blanching observed in the unoccluded application mode, as indicated by the AUC values (Table 2), is scalp application, ointment, cream and lotion. It was anticipated that drug release would be greatest from the alcoholic solution of the scalp application. Facile partitioning of the corticosteroid obviously occurs from this simple formulation to the stratum corneum. Furthermore, movement of the alcohol molecules into the skin may assist in transporting the drug or in modifying the environment of the horny layer so that the affinity of the drug molecules for this medium is enhanced. The inherently occlusive nature of the lipophilic ointment formulation tends to hydrate the stratum corneum, even in the unoccluded application mode, and this trapped moisture enhances corticosteroid movement through the tissue. The relatively high degree of drug permeation observed from this dosage form is also, therefore, not unexpected. The blanching generated by the cream formulation occupies an intermediate position between that of the ointment and lotion dosage forms. The creams are generally less occlusive to endogenous water loss and, thus, less extensive blanching profiles are normally observed for creams than for ointments in the unoccluded mode. The low degree of blanching elicited by the lotion formulation was unexpected in that it was assumed the drug would be solubilized in this relatively nonviscous formulation in the presence of cosolvents that may enhance partitioning or drug movement through the stratum corneum. In comparison to the other products it appears that, in the unoccluded mode, the affinity of the drug for the lotion vehicle is greater than its affinity for the skin.

Table 2: Area under the curve values for betamethasone 17-valerate formulations in the occluded and unoccluded modes.

Formulation	Occluded	Unoccluded
Cream	1085	929
Lotion	1215	818
Ointment	998	965
Scalp application	1369	1089

In summary, the blanching profile of the scalp application attains its peak value approximately 2 h earlier than the profiles of the other formulations. The ointment, cream and lotion produce similarly-shaped profiles that peak at approximately 14 h.

Statistically, there are significant differences between the degree of blanching elicited by the scalp application and that produced by the cream and ointment formulations at the early and peak observation times (7—12 h), whereas differences are not significant at later periods. The blanching produced by the scalp application is significantly superior to that of the lotion at all observation times between 7 and 18 h at adjacent sites.

There is no statistically significant difference between the blanching produced by the ointment and by the cream at any observation time, even though there is an obvious rank order difference between these two profiles. However, the ointment and lotion blanching profiles demonstrate significant differences between the 9- and 18-h observations and the cream and lotion blanching profiles demonstrate significant differences between the 14- and 18-h observation times, inclusive.

Hence, the majority of statistically significant differences occur over the period of peak blanching, with statistical equivalence observed at early and late reading times.

3.2. Occluded application mode

The use of occlusive dressings in the blanching assay increases the degree of drug permeation from all four dosage forms and causes peak blanching to be elicited 2—4 h earlier, when compared to the unoccluded data. The most marked difference is observed for the lotion formulation which increases its peak %TPS value from 40 % in the unoccluded mode to approximately 70 % in the occluded mode. The additional horny layer moisture that is present in this case may interact with the cosolubilizer ingredients of the lotion formulation to produce a highly favourable partitioning environment for the corticosteroid.

The peak blanching produced under occlusion by the scalp application and cream formulations each increase by approximately 15 % compared to the unoccluded results. Again the additional moisture in the skin must improve partitioning or facilitate drug diffusion through the skin strata that have swollen as a result of the higher water content.

It is possible that not only does the occlusion trap transpirational moisture in the skin, but that the aqueous dosage forms may supply some of the water that is participating in the hydrating process. Another possibility is that water (or other volatile components) may evaporate from the aqueous dosage forms (cream and lotion) during the unoccluded exposure period, thereby altering the micro-environment of the drug within the delivery vehicle. Partitioning of the corticosteroid, although now in greater concentration, from this modified environment into the stratum corneum may be unfavourable and may, therefore, be retarded in the unoccluded mode, producing the relatively low blanching profiles.

On the other hand, the increase in blanching observed for the ointment in the occluded mode is a relatively small 3 %. The inherently occlusive nature of the ointment may induce near-maximal endogeneous hydration of the stratum corneum when this product is applied without further occlusive wrapping. The subsequent use of occlusive tape, as practised in the occluded assay mode, therefore adds little to the occlusion already afforded by the lipophilic ointment and, hence, the relative increase in drug permeation observed in the occluded mode is minimal. A greater relative percentage increase in the blanching elicited by cream formulations in comparison to ointment formulations, in the two application modes, has been reported previously [5].

Statistically, the drug release from the scalp application is significantly superior to that from every other formulation at all observations times up to the 18-h period. In congruency, the blanching produced by the lotion formulation is significantly greater than that produced by either the ointment or cream at all observation times between 7 and 14—16 h, and the degrees of blanching produced by the cream and ointment formulations are significantly different at all observation times between 7 and 12 h.

In summary, the hydration of the stratum corneum induced by the occlusive covering significantly influences the drug partitioning between applied product and skin, and the diffusion of the drug through the skin strata. This is especially apparent for the alcoholic solution and aqueous dosage forms but does not seem instrumental in improving drug permeation from the ointment environment. The blanching profiles elicited by all four preparations in the occluded mode are similar in shape and in the time-to-peak values. In contrast to the unoccluded

mode, the lotion and cream formulations demonstrate superior blanching to the ointment, while permeation from the scalp application is maximal in both modes. There are significant differences between all four profiles indicating statistically real superiority in the drug release potential of certain formulations over that of others. In every comparison the significant differences in the blanching produced are apparent at the first observation time (7 h), and these disparities remain statistically significant until well after the period of maximum blanching. These blanching differences have been ascribed to drug partitioning factors and the augmentation of diffusion through the stratum corneum by partitioned formulation ingredients.

4. Conclusions

In both application modes the blanching generated by the scalp application, and by inference the drug availability from this vehicle, is clearly superior to that of the other three formulation types. This poses interesting clinical questions as the formulation will normally be applied to scalp skin that is reportedly more permeable than skin of many other anatomical sites [7]. It is possible that significant localized, and possibly systemic, concentrations of the drug may develop after repeated, widespread use of this dosage form. This is especially apparent if one examines the assay value for this formulation which was measured to be approximately 20 % overstrength, presumably because of loss of the volatile alcoholic component on storage. Patients would apply this concentrated product, that has inherently high bioavailability potential, to diseased skin of an anatomical region that is inherently more permeable than skin of other anatomical areas. This scenario poses a clear case for concern by the clinician.

The aqueous dosage forms appear to benefit most by additional occlusion of the application sites. The exact reason for the large disparity in the blanching elicited by the aqueous formulations, especially the lotion, in the two application modes is unknown. Either the enhanced hydration of the application site skin under occlusion, or the loss of volatile components from the unoccluded formulations, and resultant alteration of the partitioning potential, may be involved. A combination of these mechanisms may also be operative. Drug availability is especially enhanced from the lotion under occlusion and one should remain aware of this enhancement in the counselling of patients into the correct usage of the products. This is especially important in view of the increasing number of occlusive dressings that are becoming commercially available for occluding corticosteroid application sites. The ointment formulation appears the least affected, relatively, by additional external occlusion, probably because the nonaqueous vehicle cannot deliver additional moisture to hydrate the skin, or the drug partitioning environment is little affected by the evaporation of formulation components. The clinical appearance of the diseased skin and patient preference should advocate the prescription of an ointment vehicle in the normal manner, however, the benefits of applying additional occlusion over these anhydrous formulations to enhance availability appears questionable.

5. References

[1] Haigh, J. M., Kanfer, I., Int. J. Pharm. 19, 245 (1984) — [2] Meyer, E., Magnus, A. D., Haigh, J. M., Kanfer, I., Int. J. Pharm. 41, 63 (1988) — [3] Smith, E. W., Meyer, E., Haigh, J. M., Maibach, H. I., Percutaneous Absorption, Vol. 2, R. L. Bronaugh, H. I. Maibach (eds.), p. 443, Marcel Dekker, New York (1989) — [4] Smith, E. W., Haigh, J. M., Kanfer, I., Int. J. Pharm. 27, 185 (1985) — [5] Meyer, E., Kanfer, I., Haigh, J. M., S. Afr. Pharm. J. 48, 551 (1981) — [6] Poulsen, B. J., Burdick, K., Bessler, S., Arch. Dermatol. 109, 367 (1974) — [7] Scheuplein, R. J., Blank, I. H., Physiol. Rev. 51, 702 (1971)

Acknowledgements

The authors gratefully acknowledge financial assistance from the Rhodes University Council, the South African Council for Scientific and Industrial Research and the H. Bradlow Scholarship for postgraduate study.

Correspondence: Prof. J. M. Haigh, School of Pharmaceutical Sciences, Rhodes University, Grahamstown, 6140 (South Africa)

REFERENCE 3

International Journal of Pharmaceutics, 76 (1991) 1–8

ADONIS 0378517391003264

IJP 02517

Research Papers

Effect of supersaturation on membrane transport: 1. Hydrocortisone acetate

A.F. Davis [1] and J. Hadgraft [2]

[1] *SmithKline Beecham Consumer Brands, OTC Medicines Applied Research Group, Weybridge, Surrey KT13 0DE (U.K.) and* [2] *The Welsh School of Pharmacy, University of Wales, Cardiff CF1 3XF (U.K.)*

(Received 6 March 1991)
(Accepted 10 May 1991)

Key words: Supersaturation; Hydrocortisone acetate; In vitro membrane transport; Solubility; Cosolvent; Topical drug delivery

Summary

In vitro, the transport of hydrocortisone acetate across a model synthetic membrane has been investigated. Subsaturated, saturated and supersaturated solutions of hydrocortisone acetate, formed by mixing appropriate propylene glycol/water cosolvent systems, were studied. Transport was linearly proportional to the degree of saturation over the wide range studied. Supersaturated systems have potential application in topical drug delivery especially when release from saturated solutions is limiting.

Introduction

The importance of the degree, or fraction, of saturated solubility of a drug in a topical formulation on percutaneous absorption was first predicted by Higuchi (1960). Since then, many studies using subsaturated through to saturated systems have demonstrated a correlation between the degree of saturation and in vitro membrane transport, using both synthetic membranes (Poulsen et al., 1968; Flynn and Smith, 1972) and human skin (Ostrenga et al., 1971; Dugard and Scott, 1986), in vivo percutaneous absorption in man (Hadgraft et al., 1973; Woodford and Barry, 1982; Lippold and Schneeman, 1984) and clinical efficacy in man (Malzfeldt et al., 1989).

According to Higuchi (1960), supersaturated and other metastable states will increase transport beyond the limiting value achieved with saturated solutions. Despite early experimental evidence to support this hypothesis (Coldmann et al., 1969) there has, until recently, been little work on supersaturated systems presumably because of concern for their unstable nature.

Recently, however, the remarkable effects of antinucleant polymers in stabilising supersaturated solutions have been utilised to demonstrate marked improvement in percutaneous absorption from supersaturated systems (Kondo et al., 1987; Nitto Electric, 1987). Most previous work has used the effects of volatile additives to produce increasing, thus varying, degrees of supersaturation upon loss of additive.

Correspondence: A.F. Davis, SmithKline Beecham Consumer Brands, OTC Medicines Applied Research Group, Weybridge, Surrey KT13 0DE, U.K.

In this study hydrocortisone acetate in the mixed cosolvent system propylene glycol/water has been used to generate subsaturated, saturated and physically stable supersaturated solutions to allow comparison of their transport across a model membrane.

Materials and Methods

Materials

Hydrocortisone acetate was purchased from Roussel (U.K.). Polydimethylsiloxane membrane was purchased from Dow Corning (U.K.). All other chemicals used were of at least reagent grade and used without further purification.

Methods

Solubility of hydrocortisone acetate in water-propylene glycol cosolvent system

A series of water-propylene glycol mixtures were prepared from 100% water to 100% propylene glycol in 5% w/w increments. To each was added excess solid hydrocortisone acetate (HA) and the suspensions shaken for 24 h at controlled room temperature (23 ± 1°C). Room temperature was used for convenience, especially as previous work had shown little effect of temperature on saturated solubility of HA in the range 20–30°C. The suspensions were centrifuged and the supernatant solutions carefully sampled. The saturated solutions were assayed, diluted as required, by direct injection onto a suitable high-pressure liquid chromatographic system. Experimental conditions used were: ODS 250 mm × 4.6 mm i.d. column; ultraviolet detection at $\lambda = 240$ nm with methanol/water (65:35% v/v) as the mobile phase at a flow rate of 1.5 ml/min. Quantification was by external standard.

Mixing of cosolvent systems to produce subsaturated, saturated and supersaturated solutions

Depending upon the relative polarities of the solute and the binary cosolvent system, saturated solubility plots will often show an exponential increase with solvent composition as shown in Fig. 1 (curve B′B). A basic property of these systems is that by mixing suitable solute-cosolvent solutions, subsaturated, saturated and supersaturated solutions can be formed. Fig. 1 shows schematically that mixing system A (no solute in 100% solvent a) with system B (saturated solute in 100% solvent b) will result in systems C (subsaturated), D (saturated) and E and F (both supersaturated) depending upon the ratio of A to B used. In practice, systems A and B may themselves be mixed cosolvents and system B need not necessarily be saturated with solute. Thus, for example, in all experiments conducted a common donor solution, as represented by B, 0.08% saturated w/w hydrocortisone acetate in 88% propylene glycol/12% water, has been used with cosolvent systems as represented by A, G and H, to form the required degrees of saturation. Given the composition of B and the final composition required, the compositions of systems represented by G and H were calculated using a simple simultaneous equation. All systems represented by A, G and H contained 0.5% hydroxypropylmethyl cellulose as antinucleant polymer to stabilise the supersaturated solutions.

The degree of saturation of experimental solutions of varied composition was calculated by dividing the resulting concentration after mixing with the experimentally determined value of the saturated solubility at that resulting composition.

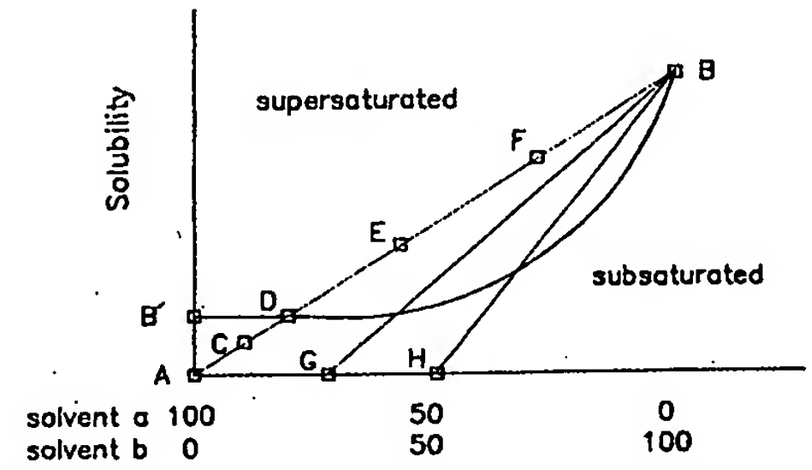

Fig. 1. Saturated solubility of a solute in a binary cosolvent system. Effects of mixing: B′B is the saturated solubility curve of solute in binary cosolvent system ab. System B (saturated solute in solvent b) is mixed with system A (no solute in solvent a) or systems G or H (no solute in cosolvent ab) to produce subsaturated, saturated or supersaturated solutions exemplified by C, D and E, F, respectively.

In vitro membrane transport cell methodology

A simple cylindrical glass cell was used. The receptor compartment (approx. 100 ml) and the donor compartment were clamped together with the membrane between flat flanges. The membrane surface area was approx. 20 cm^2. A port in the receptor compartment was used for sampling. Polydimethylsiloxane membrane (0.005 inch) was washed in water, dried, and then soaked in isopropyl myristate for 1 h and wiped with tissue to remove surface liquid. The receptor fluid used was propylene glycol/water (25:75% v/v) which was stirred at 100 rpm using a magnetic flea. The studies were conducted at controlled room temperature (23 ± 1°C). In previous experiments it was demonstrated that the addition of antinucleant polymer to supersaturated systems produced a (pseudo) stable state showing no measurable changes in transport when studied over several days after mixing. However, all solutions were studied within 1 h after mixing. 10 g samples of the solutions under study, an infinite dose, were placed on the donor side of the membrane. 100 μl of receptor was sampled at appropriate times. Analysis was as described under Solubility studies.

In vitro membrane transport studies

Three series of experiments were conducted (a–c).

(a) Transport from 0.02% w/w saturated hydrocortisone acetate: In order to confirm that the cell and membrane system chosen could be described by Fick's First Law of diffusion, transport of hydrocortisone acetate was studied from a 0.02% w/w saturated solution (propylene glycol/water, 56:44% w/w) over 8 h.

(b) Transport from subsaturated and saturated solutions: Poulsen (1972) has analysed several models of percutaneous absorption. In the simplest case, where the vehicle has no effect on the rate-limiting membrane, the partition coefficient between the vehicle and the membrane (P_c) is a reciprocal function of drug saturated solubility in the vehicle (C_v).

$$P_c = \text{constant} \frac{1}{C_v(\text{saturated})} \qquad (1)$$

In these studies, P_c was not determined experimentally but was expressed as $1/C_v$(saturated) from Eqn 1.

In three experiments, the effects of concentration and partition coefficient (expressed as reciprocal saturated solubility in the vehicle) were studied. (1) A classical concentration response was studied from 0.005, 0.0067, 0.008, 0.10, 0.013 and 0.02% w/w hydrocortisone acetate all in a fixed vehicle of propylene glycol/water (56:44% w/w). These correspond to the following fractional degrees of saturation, 0.25, 0.33, 0.40, 0.50, 0.67 and 1. (2) A response to the partition coefficient was studied using 0.02% w/w hydrocortisone acetate in a range of vehicles chosen to correspond to the following fractional degrees of saturation, 0.25, 0.33, 0.40, 0.50, 0.67 and 1. (3) In Expts 1 and 2, either partition coefficient (expressed as reciprocal saturated solubility in the vehicle) or concentration was fixed with the other being varied. In this study, saturated solutions of 0.005–0.08% w/w were investigated in which both concentration and partition coefficient vary but in relation to each other so that their product is a constant. As transport is proportional to P_cC_v transport from these saturated systems was expected to be similar (Poulsen, 1972). Experiments were conducted over a 3 h period and reported as amount transported per h.

TABLE 1

Composition of supersaturated solutions produced by mixing B:A in various proportions

Vehicle No.	Ratio of B:A B	A	Concentration (% w/w)	Degree of saturation
1	1	0	0.08	1
2	1	1	0.04	4
3	1	2	0.027	6.9
4	1	3	0.02	8.33
5	1	7	0.07	6.67
6	1	15	0.005	3.84

B: 0.08% w/w saturated hydrocortisone acetate (vehicle propylene glycol/water, 88:12 w/w); C: 100% water containing 0.5% antinucleant polymer. Degree of saturation was calculated by reference to Fig. 1.

(c) Transport from supersaturated solutions: Two experiments were conducted. (1) At a fixed concentration of 0.02% w/w hydrocortisone acetate, transport from times 1, 2, 4, 5, 6 and 8 degrees of saturation were studied. Vehicle compositions were calculated by reference to Fig. 1. (2) The effect of mixing systems equivalent to A and B in Fig. 1 in varied ratios was investigated. In this experiment, concentration, degree of saturation and their product was varied. Table 1 lists the ratios used and the resulting concentrations and degrees of saturation. Experiments were run over 1 h and reported as amount transported per h.

Results

Fig. 2 shows the saturated solubility of hydrocortisone acetate in propylene glycol/water cosolvent system. As the percent propylene glycol increases, the saturated solubility of hydrocortisone acetate also increases but in an approx. exponential manner. This exponential increase has been observed with other solutes in propylene glycol/water cosolvent systems and these results are very similar to values reported previously (Yalkowsky and Roseman, 1981).

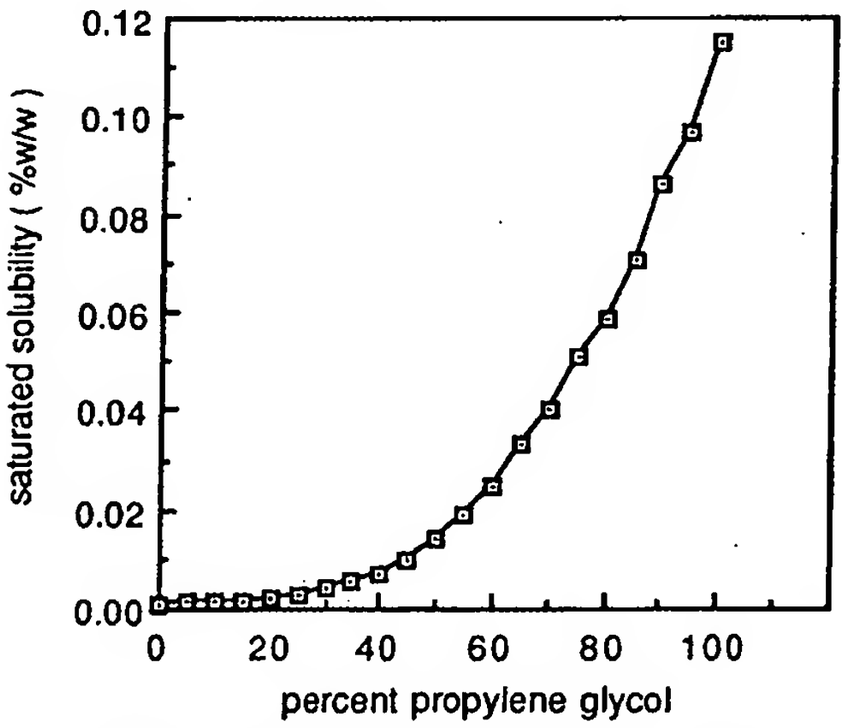

Fig. 2. Saturated solubility of hydrocortisone acetate in water-propylene glycol cosolvent system at 23°C. Mean, $n = 3$.

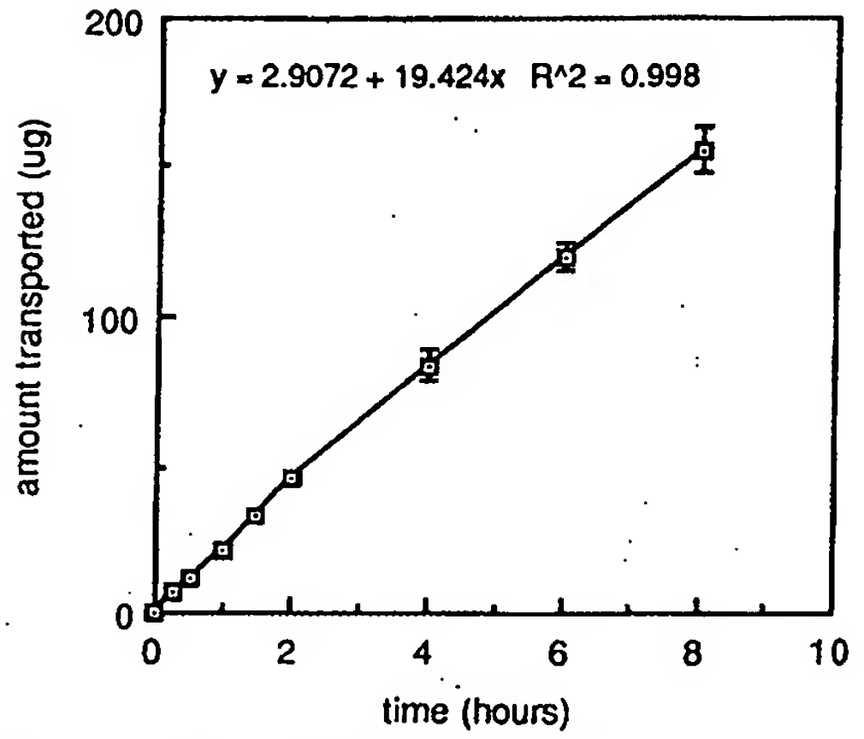

Fig. 3. Transport of hydrocortisone acetate from a saturated 0.02% w/w solution over 8 h (vehicle propylene glycol/water, 56:44% w/w). Demonstration of Fickian diffusion. Mean, $n = 3$, ± S.E.

This plot was used as shown in Fig. 1 to design formulations of varying concentration and degree of saturation produced by mixing appropriate cosolvent-solute systems. Degree of saturation was determined by dividing actual concentration achieved after mixing by the value for saturated solubility, from Fig. 2, for the vehicle composition after mixing.

Fig. 3 shows transport from a 0.02% w/w saturated hydrocortisone acetate formulation over 8 h. Transport is almost linear up to 8 h with approx. 160 μg total release. Slight deviation at later times is probably due to depletion effects from the total loading of 2000 μg per cell. Linearity of transport demonstrates that the membrane is rate limiting.

Fig. 4a–d shows transport from subsaturated to saturated solutions. Fig. 4a shows the classical linear response between transport and concentration for a single vehicle and thus fixed partition coefficient. Less well recognised, Fig. 4b shows the linear response between transport and partition coefficient for a fixed concentration of 0.02% w/w. Fig. 4c redraws these data using degree of saturation as the common abscissa.

Fig. 4d shows transport from saturated solutions from 0.005 to 0.08% w/w hydrocortisone

998

8 10

a saturated
lycol/water,
sion. Mean,

to design
id degree
priate co-
ition was
entration
saturated
position

% w/w
ion over
h with
ation at
effects
Linear-
mbrane

turated
lassical
centra-
artition
shows
l parti-
0.02%
ree of

solu-
tisone

acetate in which both concentration and partition coefficient vary but such that the product of these two parameters is a constant. Release is similar from all saturated solutions studied.

Fig. 5 shows transport from 0.02% w/w hydrocortisone acetate at times 1 to times 8 degrees of saturation. A clear linear response between transport and degree of saturation is seen.

Fig. 6 shows transport from solutions of different concentrations and degrees of saturation in the supersaturated range as formed from mixed type A and B cosolvent systems in varying ratios,

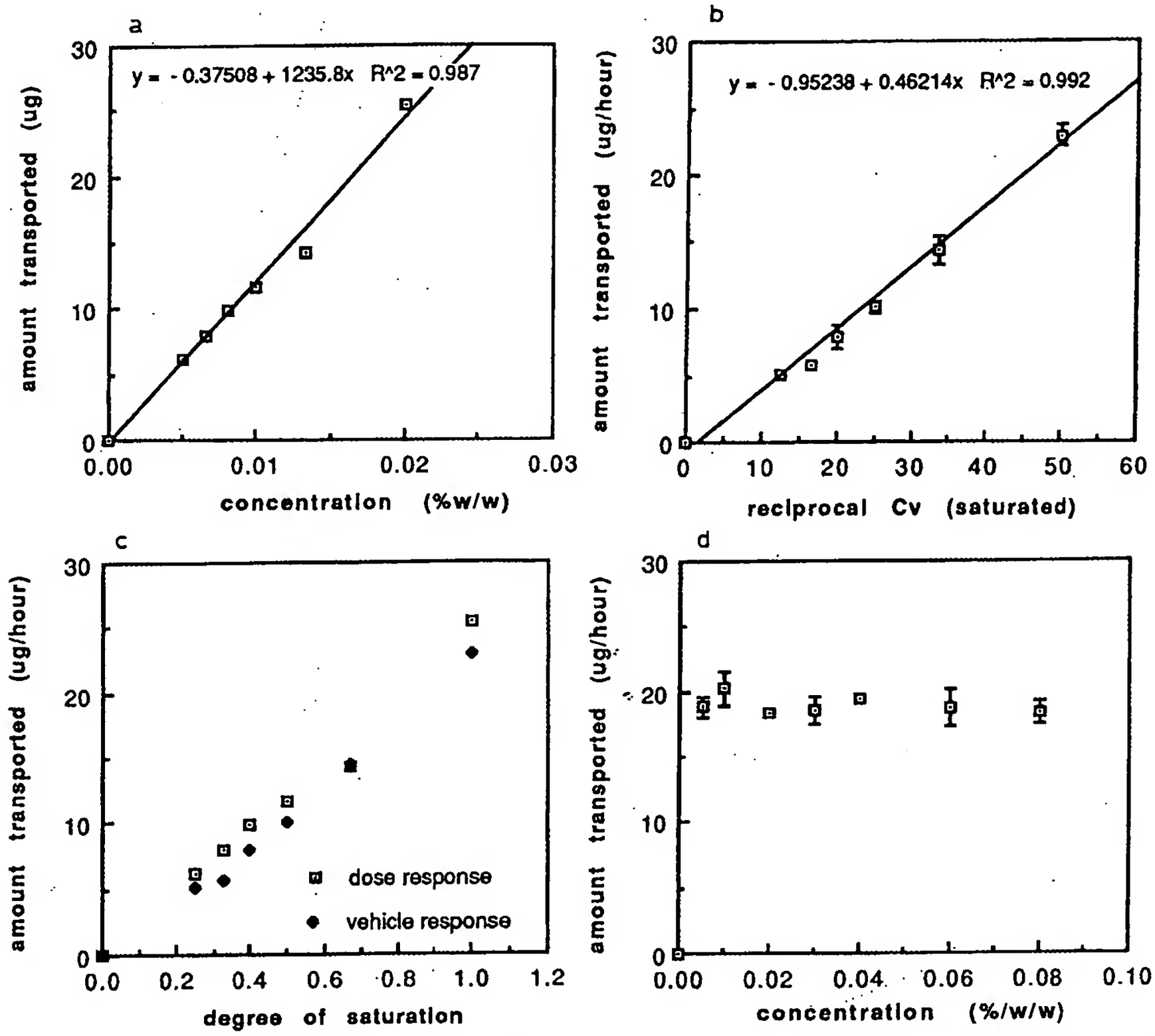

Fig. 4 (a). Transport of hydrocortisone acetate from 0.005 to 0.02% w/w in a single vehicle (propylene glycol/water, 56:44% w/w). Demonstration of response to dose. Mean, $n = 3$, ±S.E. (b) Transport of hydrocortisone acetate, 0.02% w/w from different propylene glycol/water vehicles. Demonstration of response to partition coefficient expressed as reciprocal saturated solubility. Mean, $n = 3$, ±S.E. (c) Comparison of response of concentration and vehicle partition coefficient, expressed as degree of saturation, to transport of hydrocortisone acetate (data as in Panels a and b). (d) Transport of hydrocortisone acetate from 0.005 to 0.08% w/w saturated solution. Increase in concentration is offset by decrease in partition coefficient. Mean, $n = 3$, ±S.E.

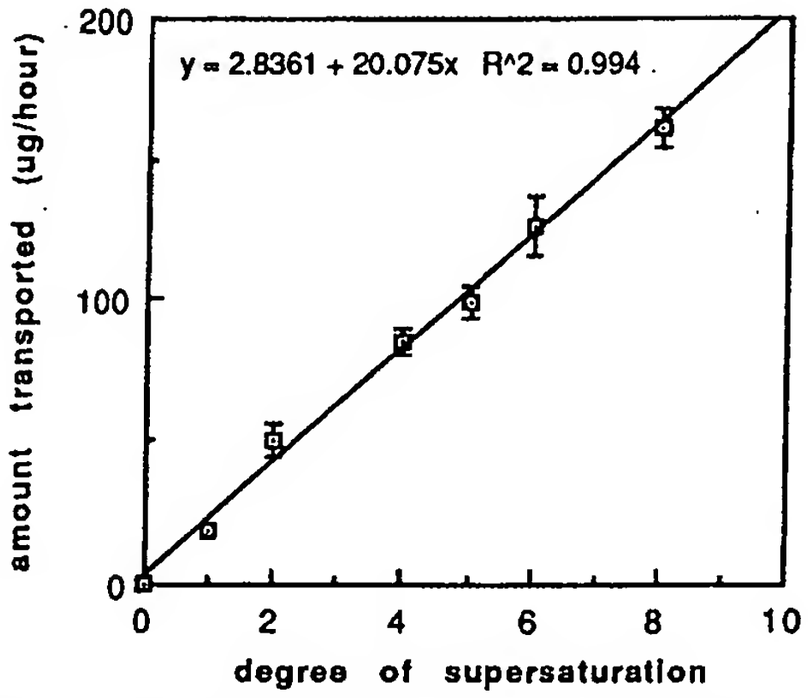

Fig. 5. Transport of hydrocortisone acetate, 0.02% w/w from supersaturated vehicles. Demonstration of response to degree of supersaturation. Mean, $n = 6 \pm$ S.E.

as shown schematically in Fig. 1. Transport again is proportional to degree of saturation. An interesting property of this system is the maximum value of release corresponding to a ratio of A : B = 3 : 1 at approx. 0.02% w/w times 8.3 degrees of saturation.

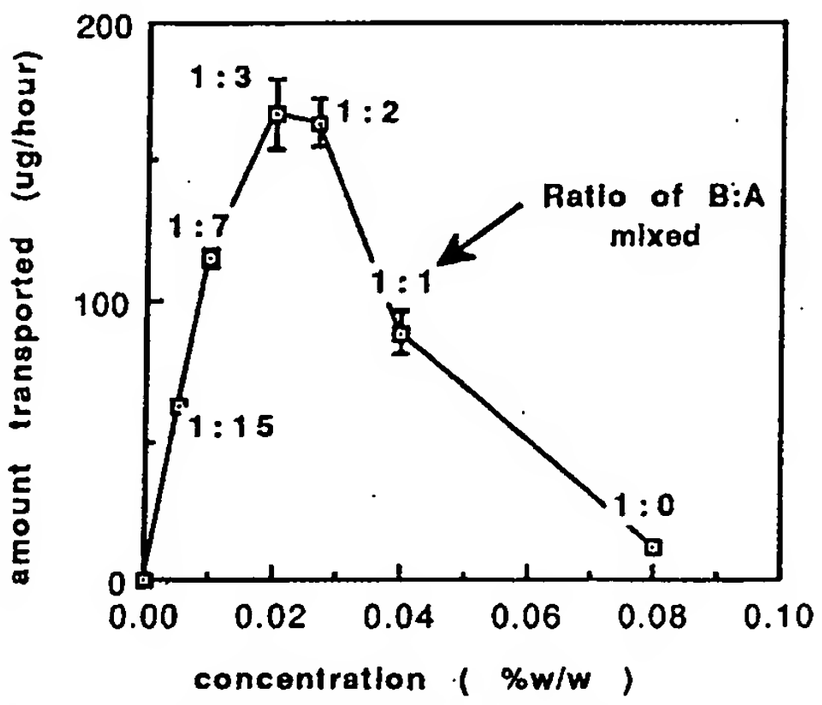

Fig. 6. Transport of hydrocortisone acetate from supersaturated solutions produced by mixing various ratios of B:A (as in Fig. 1). A plateau of transport is seen at around 0.02% w/w times 8 degrees of saturation. See Table 1 for details of compositions.

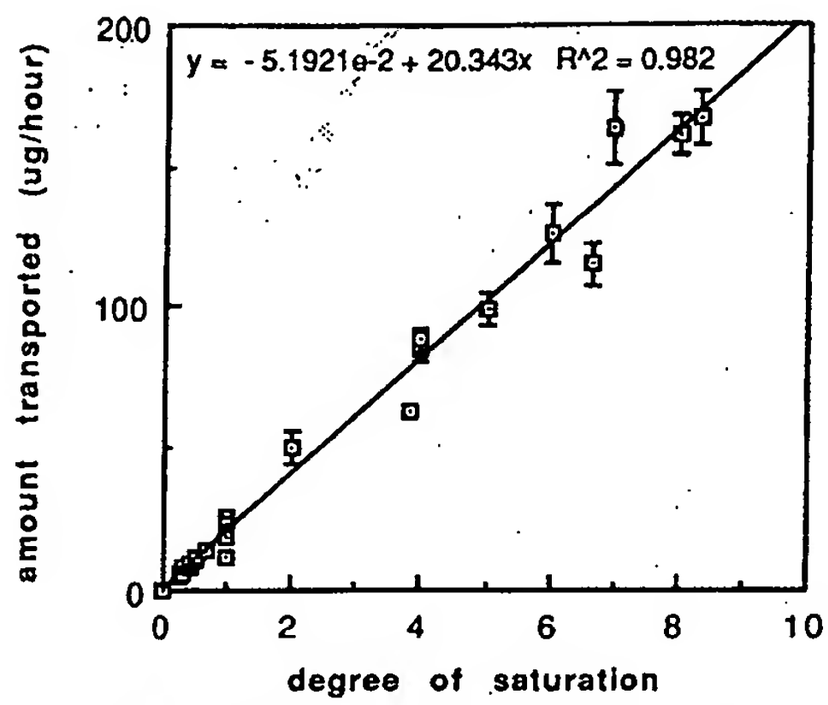

Fig. 7. Linear relationship between transport of hydrocortisone acetate and degree of saturation over the range of subsaturated to supersaturated systems. Combined data from Figs. 4–6. Mean ($n = 3$ or 6) $\pm$ S.E.

Finally, Fig. 7 shows the linear relationship between transport and degree of saturation over the range from subsaturated to supersaturated for all data shown in Figs 4–6.

Discussion

The in vitro transport of hydrocortisone acetate from solutions of varying concentration and partition coefficient as expressed by reciprocal saturated solubility has been shown to be proportional to degree of saturation. Transport is linear from subsaturated through to saturated solutions, as would be anticipated from the literature, (Poulsen et al., 1968; Flynn and Smith, 1972) but this work confirms the observations of Theeuwes et al. (1976), that supersaturated systems result in linear transport proportional to their degree of saturation and beyond the limiting transport value from saturated systems.

The driving force for diffusion across the stratum corneum is the concentration of diffusant within the outermost layer of the skin. This concentration is a mathematical product of the concentration within the vehicle times the partition

coefficient between the vehicle and the stratum corneum (Higuchi, 1960; Poulsen, 1972).

The effects of concentration on response are clearly established, for example, dose responses are the basis of pharmacological and toxicological investigations. The response, of transport, shown in Fig. 4a is a further example of this. Less well established is the linear response to vehicle partition coefficient as depicted in Fig. 4b. Fig. 4c shows that both parameters can be expressed as degree of saturation which, as a single variable, is proportional to transport. Fig. 4d shows that transport from all saturated systems is within experimental limits, as found previously (Hadgraft et al., 1973; Theeuwes et al., 1976; Woodford and Barry, 1982; Dugard and Scott, 1986).

Thus, Fig. 4 shows the response of the in vitro model to both concentration and partition coefficient. Synthetic membrane systems such as used here are often criticised as not being representative of human skin. Mainly this is due to vehicle/membrane interactions which are specific to the skin or membrane being studied and are not easily simulated one by the other. Fig. 4d demonstrates that as release from all saturated systems is similar, vehicle/membrane interactions in the present study are likely to be insignificant. Thus, models similar to that used here may be useful in predicting the drug/vehicle interaction component only of transport across human skin.

Fig. 5 shows that transport from supersaturated systems is linearly proportional to degree of supersaturation at a fixed concentration and Fig. 7 demonstrates that all data reported here from 0.25 times subsaturated to 8 times supersaturated fit a single linear relationship between transport and degree of saturation.

The ability of supersaturated systems to increase transport beyond the limiting value imposed by saturated systems is clearly of interest in topical drug delivery. Fig. 6 shows data to evaluate the potential of mixed cosolvent systems in topical drug delivery. By suitable selection of the ratio and design of the cosolvent system, large increases in degree of saturation can be achieved. Fig. 6 shows that by suitable selection of ratios of B : A, a plateau response can be achieved whereby slight variation in change of ratio as might occur for various reasons in practical pharmaceutical products will not significantly alter degree of saturation or transport.

Further work is currently in progress to evaluate the drug delivery potential of these systems.

Acknowledgement

The authors thank Mr G. James for his contribution to this work.

References

Coldmann, M.F., Poulsen, B.J. and Higuchi, T., Enhancement of percutaneous absorption by the use of volatile:nonvolatile systems as vehicles. *J. Pharm. Sci.*, 58 (1969) 1098–1102.

Dugard, P.H. and Scott, R.C. A method of predicting percutaneous absorption rates from vehicle to vehicle: an experimental assessment. *Int. J. Pharm.*, 28 (1986) 219–227..

Flynn, G.L. and Smith, R.W. Membrane diffusion. III: Influence of solvent composition and permeant solubility on membrane transport. *J. Pharm. Sci.*, 61 (1972) 61–66.

Hadgraft, J., Hadgraft, J.W. and Sarkany, I. The effect of thermodynamic activity on the percutaneous absorption of methyl nicotinate from water glycerol mixtures. *J. Pharm. Pharmacol.*, 25 (1973) Suppl. 123P.

Higuchi, T. Physical chemical analysis of percutaneous absorption process from creams and ointments. *J. Soc. Cosm. Chem.*, 11 (1960) 85–97.

Kondo, S., Yamanaka, C. and Sugimoto, I. Enhancement of transdermal delivery by superfluous thermodynamic potential. III: Percutaneous absorption of nifedipine in rats. *J. Pharmacobio-Dyn.*, 10 (1987) 743–749.

Lippold, B.C. and Schneeman, H. The influence of vehicles on the local bioavailability of betamethasone 17-benzoate from solution and suspension-type ointments. *Int. J. Pharm.*, 22 (1984) 31–43.

Nitto Electric Industries, *Japanese Patent* J6 3297-320-A, 1987.

Malzfeldt, E., Lehmann, P., Goerz, G. and Lippold, B.C. Influence of drug solubility in the vehicle on clinical efficacy of ointments. *Arch. Dermatol. Res.*, 281 (1989) 193–197.

Ostrenga, J., Steinmetz, C., Poulsen, B.J. and Yett, S. Significance of vehicle composition: II: Prediction of optimal composition. *J. Pharm. Sci.*, 60 (1971) 1180–1183.

Poulsen, B.J., Young, E., Coquilla, V. and Katz, M. The effect of topical vehicle composition on the in vitro release of fluocinolone acetonide and its acetate ester. *J. Pharm. Sci.*, 57 (1968) 928–933.

Poulsen, B.J. Diffusion of drugs from topical vehicles: An

analysis of vehicle effects. *Adv. Biol. Skin*, 12 (1972) 495–500.

Theeuwes, F., Gale, R.M. and Baker, R.W. Transference: A comprehensive parameter governing permeation of solutes through membranes. *J. Membr. Sci.*, 1 (1976) 3–16.

Woodford, R. and Barry, B.W. Optimisation of Bioavailability of Topical Steroids: Thermodynamic control. *J. Invest. Dermatol.*, 79 (1982) 388–391.

Yalkowsky, S.H. and Roseman, T.J. Solubilization of drugs by cosolvents. In Yalkowsky, S.H. (Ed.), *Techniques of Solubilization of Drugs*, Dekker, New York, 1981, pp. 81–134.

Intern
© 199
ADO

IJP (

Physicochemical Study of Percutaneous Absorption Enhancement by Dimethyl Sulfoxide: Kinetic and Thermodynamic Determinants of Dimethyl Sulfoxide Mediated Mass Transfer of Alkanols

TAMIE KURIHARA-BERGSTROM*, GORDON L. FLYNN×, AND WILLIAM I. HIGUCHI‡

Received May 20, 1985, from the *College of Pharmacy, The University of Michigan, Ann Arbor, MI 48109–1065.* Accepted for publication February 19, 1986. Present addresses: *Basic Pharmaceutics Research, Ciba-Geigy Corporation, Ardsley, NY 10502, and the ‡Department of Pharmaceutics, College of Pharmacy, The University of Utah, Salt Lake City, Utah 84112.

Abstract □ By first determining the thermodynamic activities and activity coefficients of methanol, 1-butanol and 1-octanol in binary dimethyl sulfoxide:water media, it has been possible to separate solubilizing (thermodynamic) effects of dimethyl sulfoxide from its kinetic (diffusive) influence as they relate to the skin permeation of these small, nonelectrolyte alkanols. This was done by normalizing the experimental permeability coefficients found with full-thickness hairless mouse skin membranes to unit activity in the vehicle. When the dimethyl sulfoxide media were placed on both sides of the skin sections in a two compartment diffusion cell, activity-adjusted permeability coefficients of the permeants were invariant to dimethyl sulfoxide concentrations of 50% strength. Thus, up to this concentration and in the absence of net solvent crosscurrents, the permeabilities of methanol, 1-butanol, and 1-octanol appear to be strictly determined by partitioning into the stratum corneum. However, when the dimethyl sulfoxide percentage strength was raised to ≥75%, activity-adjusted permeability increased systematically and profoundly, indicating severe barrier impairment with increased diffusion across the horny layer (kinetic effect). When neat dimethyl sulfoxide was placed on both sides of the skin, the experimental permeability coefficients of the three alcohols were maximal and equal in magnitude, suggesting total functional impairment of the stratum corneum. When the dimethyl sulfoxide media were placed in contact with the stratum corneum surface of the skin membranes only, accelerating effects were noted at dimethyl sulfoxide concentrations <50%, further supporting the idea that solvent cross flows themselves disrupt the horny structure. The degree of impairment was quantified under all experimental circumstances. Analysis of extracts of the stratum corneum indicated that barrier impairment is due in part to elution of dimethyl sulfoxide soluble components from the horny structure. Delamination of the horny layer and denaturation of its proteins also appeared to play roles in enhancement of diffusion.

Methanol, 1-butanol and 1-octanol possess widely different lipophilic properties. In studies of the effect of polarity (hydrophobicity) on a specific phenomenon or process, they make a useful set of prototype compounds because of their predictable and systematically varying physicochemical properties. They have been useful in studying mass transfer mechanisms through skin and have helped define the reliance of skin permeation on lipophilic character.[1–6] Extensive studies from these labs[1–4] suggest that methanol, 1-butanol, and 1-octanol pass through hairless mouse skin by different pathways and with different rate-controlling mechanisms. These three alcohols were therefore chosen for the present study involving assessment of dimethyl sulfoxide mediation of permeation because their permeabilities through this skin from strictly aqueous solution are known and because they provided a unique opportunity to study solvent influences as a function of permeant lipophilicity.

Theoretical Section

For the simplest possible membrane situation in which a resistant, isotropic membrane separates well-stirred external phases, the permeability coefficient, P, is expressed by:

$$P = \frac{DK_{m/v}}{h} \tag{1}$$

where D, $K_{m/v}$, and h are the diffusivity (diffusion coefficient), partition coefficient between the membrane (m) and medium (v, vehicle), and membrane thickness, respectively.

Normally in studies involving the use of diffusion cells, the membrane thickness is fixed and is little affected by medium changes. Even when this is not so as, for example, when solvents such as water and dimethyl sulfoxide act on the stratum corneum, rarely is the thickness of a membrane expanded by more than a factor of two or three. It appears, then, that varying the solvent composition of the external (vehicle) phases primarily influences the permeability coefficient by altering diffusivity, the kinetic aspect of mass transfer, and by altering partitioning, the thermodynamic determinant, and only marginally by changing the thickness. The permeability coefficient will vary as the product of the proportional changes in each varies. In order to determine kinetic and thermodynamic influences on mass transfer associated with systematic changes in the composition of phases applied to the membrane, an independent determination of the changes taking place in either the diffusion. The unexplained change in permeability which remains can then be assigned to the alternative factor.

In principle, one should be able to separate vehicle driven thermodynamic influences from other mass transfer influences, including vehicle mediated changes in the membrane solvency, by independent assessment. It is reasonable to assume that equilibrium exists across the molecular interface between the membrane and the medium, so that:

$$\begin{aligned} \mu_{2,\text{ medium}} &= \mu_{2,\text{ membrane}} \\ &= \mu_2^0 + RT \ln a_{2,v} \\ &= \mu_2^0 + RT \ln a_{2,m} \end{aligned} \tag{2}$$

where μ_2^0 is the chemical potential of the standard state, a is the activity, and the subscripts m and v refer to the membrane and the vehicle, respectively. It thus follows that the thermodynamic activity of the permeant is, for all practical purposes, the same on either side of the interface; that is:

$$a_{2,v} = a_{2,m} \tag{3}$$

The activity on either side of the membrane interface with the medium can be expressed in a general form as:

$$a_2 = \gamma_2 C_2 \tag{4}$$

where γ_2 is an "activity coefficient," a factor which normalizes a prevailing concentration, C, to the respective activity.

0022-3549/86/0500-0479$01.00/0

It follows that:

$$\gamma_{2,v}C_{2,v} = \gamma_{2,m}C_{2,m} \quad (5)$$

At the medium–membrane interface:

$$K_{m/v} = \frac{C_{2,m}}{C_{2,v}} = \frac{\gamma_{2,v}}{\gamma_{2,m}} \quad (6)$$

Combining eqs. 1 and 6 gives the following form of the mass transfer coefficient:

$$P = \frac{D}{h}\frac{\gamma_{2,v}}{\gamma_{2,m}} \quad (7)$$

Once the flux of a permeant has attained a steady or quasi-steady state, the mass current can be expressed generally as:

$$\left(\frac{dm}{dt}\right)_{ss} = AP(\Delta C) \quad (8)$$

where $(dm/dt)_{ss}$ is the steady or quasi-steady state flux taken directly from the slope of the mass penetrated (m) versus time (t) profile, A is the area of permeation (cm^2), and ΔC is the difference in concentration across the membrane as measured in the phases external to the membrane. When diffusion is into a sink (zero concentration at all times on the downstream side of the membrane), ΔC is the applied concentration. It follows from eqs. 7 and 8 that:

$$\left(\frac{dm}{dt}\right)_{ss} = A\frac{D}{h}\frac{\gamma_{2,v}}{\gamma_{2,m}}\Delta C \quad (9)$$

Equation 9[7] indicates that the toal flux through an isotropic, resistant barrier is proportional to the activiy coefficient in the external medium and inversely proportional to the activity coefficient in the membrane, in addition to its other well established dependencies.

When the medium external to a membrane is varied by systematically varying the proportions of two miscible solvents, three variables in eq. 9 are subject to change, i.e., D, $\gamma_{2,m}$, and especially $\gamma_{2,v}$. For present purposes, h is presumed constant. There is no way to predict in advance how D and $\gamma_{2,m}$ will be affected, but a systematic change in the magnitude of $\gamma_{2,v}$, which relates to the different solvencies of the two solvents for a given solute, is anticipated. Therefore, the sensitivity of $\gamma_{2,v}$ is subject to independent assessment. Changes in D and $\gamma_{2,m}$, on the other hand, are only expected if at some point the binary solvents alter the physicochemical properties of the membrane. Changes in D and $\gamma_{2,m}$ appear as a composite change and are not readily separable. Of considerable importance is the case where D and $\gamma_{2,m}$ remain unchanged as the vehicle composition is varied. For this situation, the product of P times $1/\gamma_{2,v}$ is predicted to be constant, i.e.:

$$P\frac{1}{\gamma_{2,v}} = \frac{D}{h}\frac{1}{\gamma_{2,m}} \quad (10)$$

Thus, if $\gamma_{2,v}$ is independently known, one has a stringent test to determine whether membrane properties are changing with the change in the composition of the applied phase. For solutes like the volatile alkanols, $\gamma_{2,v}$ can be independently assessed from vapor pressure measurements. The concept of activity coefficient determined flux is developed above for the simple isotropic membranes; the underlying principles are general, however, and can be applied to complex membranes such as the skin.

Experimental Section

Materials—[^{14}C]Methanol (30 mCi/mmol), [^{14}C]1-butanol (10 mCi/mmol), [^{14}C]1-octanol (5 mCi/mmol) (ICN Chemical and Radioisotope Division, Irvine, CA) were used as supplied. These were diluted into neat, high purity methanol (Baker Chemical Co., Phillipsberg, NJ), 1-butanol (Matheson, Coleman and Bell Manufacturing Chemists, Norwood, OH), and 1-octanol (Fisher Scientific Co., Fairlawn, NJ), respectively, for the vapor pressure measurements. Dimethyl sulfoxide (Fisher Scientific Co., Fairlawn, NJ) was used as received, and the water used in the studies was double distilled.

Permeation Procedure—Membranes for the study were abdominal sections obtained from the hairless mouse (Skin Cancer Hospital, Temple University, Philadelphia, PA) SKH-hr(−1) strain. In all instances the skin was taken from freshly sacrificed animals (spinal cord dislocation) and immediately mounted in the diffusion cell housing. The full-thickness skin was used.

The general assembly and operation of the diffusion cells have been detailed previously.[1–4,8] Briefly, small glass diffusion cells with ~0.6 cm^2 of diffusional area and with half cell volumes of ~1.5 mL were used. These parameters were determined accurately for each cell. The cells were assembled with a fresh section of skin between the chambers. After rinsing, a permeant containing solution was placed on the stratum corneum side of the skin section, and a collecting medium was placed on the dermal side. Then, the media were stirred (150 rpm). Tests were begun as soon as the cell assembly was complete.

Initial and final samples were taken from the donor (permeant-containing) compartment. Aliquots of 100 μL were taken from the receiver chamber at 1000-s intervals for up to 10,000 s (usually 7,000 s), providing 8–11 data points including one for time zero. Fresh solvent was added to the compartment following sampling to maintain constant volume in the receiver chamber. Corrections were made for the dilutions involved. The 100-μL aliquots were placed directly into 10 mL of scintillation cocktail (Aquasol, New England Nuclear, Boston, MA). Experiments at each set of conditions were done three or more times and the results were averaged.

An aspect of experimental design unique to these studies was that the permeation was followed in media ranging from dimethyl sulfoxide:water (0, 30, 50, 70, 90, and 100% dimethyl sulfoxide with normal saline) to normal saline in one set of experiments and to dimethyl sulfoxide of the same strength in a second set. In the following discussion the first of these solvent configurations is referred to as asymmetric and the second as balanced. In the asymmetric modality the alkanols permeated in the presence of a net flux of dimethyl sulfoxide in the same direction as that of the permeant and against a net flux of water. In the balanced configuration there is no net diffusive exchange of solvent between the compartments. The dimethyl sulfoxide and water fluxes involved in the asymmetric situation were measured and are being reported separately.[8]

Analysis of Permeation Data—As in previous work[1–4,8] counts of the radiolabeled alkanols reaching the receiver chamber (corrected for dilution) were plotted against time. When the permeation process attained a quasi-steady state, as determined graphically, the permeability coefficient for the test was calculated from:

$$P = \frac{V_r\frac{dC}{dt}}{A\Delta C} \quad (11)$$

where P is the permeability coefficient (cm/h), V_r is the receiver volume (1.4 mL), dC/dt is the quasi-steady state rate of change in radiochemical concentration in the receiver chamber (counts per 100-μL sample per 10-min counting time), ΔC is the initial radiochemical concentration in the donor chamber (counts per 100-μL sample per 10-min counting time), and A is the diffusional area (cm^2). The experiments were carried out in a manner which allowed use of the donor concentration for the concentration differential, ΔC. The lag time tended to be too short to be estimated with any accuracy using 1000-s sampling intervals.

Vapor Pressure Measurement—A measured flow of nitrogen gas was passed through the system depicted in Fig. 1. The nitrogen gas stream was warmed to 37°C in a coil and then bubbled through a 37°C solution of the alkanol dissolved in one of the binary dimethyl sulfoxide:water media (0, 30, 50, 70, 90, or 100% dimethyl sulfoxide). The bubble size (frit size), gas flow rate, and solvent column height

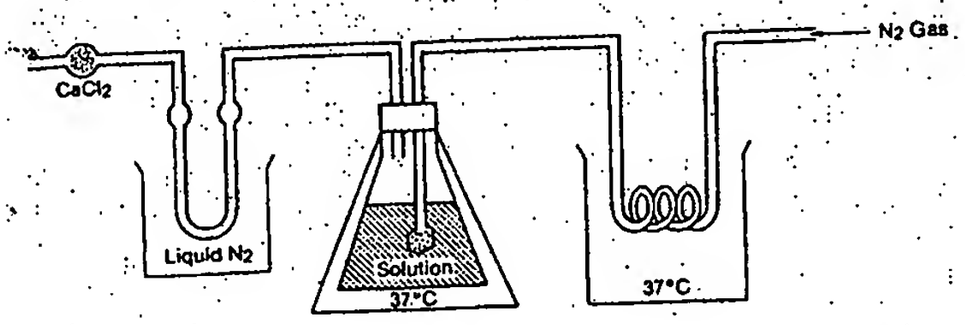

Figure 1—*Measurement of vapor pressure in the gas-saturation method.*

required for solution–vapor equilibrium were determined by trial and error. Conditions were selected which afforded gas saturation with the vapors of the alkanol and its solvent(s) during the passage of the gas through the liquid phase. The vapor saturated gas stream from the solution was passed into a liquid nitrogen chilled cold trap (U-tube) where the solvent vapors were quantitatively removed by condensation. The contents of the cold trap were rinsed directly into scintillation cocktail for counting.

Analysis of Vapor Pressure Data—The partial vapor pressures of the alkanols in solution in the dimethyl sulfoxide:water media were determined from their equilibrium vapor phase concentrations in the gaseous phase passed through the media. If V_n, the volume of gas bubbled through a solution of one of the alkanols, is found to contain g grams of the vaporized alkanol solute (with a molecular weight, M_r) the partial vapor pressure of the alkanol, $P_{i,gas}$, can be calculated approximately using the following equation based on the ideal gas law:

$$P_{i,gas} = \frac{gRT}{M_r V_n} \tag{12}$$

Assuming ideal gas behavior is appropriate at the concentrations of solute vapors obtained. The approximate nature of this method of vapor pressure estimation is due to the fact that the volume, V_n, occupied by the vapor is taken as the volume of the dry nitrogen gas measured before it is saturated with solution component vapor.

For more accurate estimations of partial pressure, the equation can be modified to allow for the increased volume of the gas due to the introduction of solvent vapor. The volume, V_t, of both nitrogen and the vapor through which the vapor molecules are distributed is: $V_b P_b/(P_b - P_{i,gas})$, where V_b is the volume of the pure, dry nitrogen gas before saturation, P_b is the barometric pressure, and $P_{i,gas}$ is the total vapor pressure of the alkanol. It follows that:

$$P_{i,gas} = \frac{g}{M_r}\frac{RT}{V_t} = \frac{g}{M_r}\frac{RT(P_b - P_{i,gas})}{V_b P_b} \tag{13}$$

which, upon solving for $P_{i,gas}$, yields:

$$P_{i,gas} = \frac{gRTP_b}{[M_r V_b P_b] + [gRT]} \tag{14}$$

The vapor pressure of each alkanol in each medium was calculated from eq. 14. The dimethyl sulfoxide:water media was assumed to form an ideal solution, allowing estimation of the partial pressures of each via mole fraction compositions. The partial pressures of dimethyl sulfoxide, water, and alkanol were added to get the system vapor pressure. As a critical test of the gas saturation cell, the 37°C vapor pressures of the pure liquid alkanols were determined and compared with their established vapor pressures.[9]

It was found that 1-octanol was not fully miscible in water nor with dimethyl sulfoxide:water mixtures containing 30 and 50% dimethyl sulfoxide at the 1% total concentration used. This created no difficulty as the actual concentrations of 1-octanol in the water-rich phases were experimentally determined and used to calculate activity coefficients. The measured solubilities were 0.479 mg/mL in water, 1.14 mg/mL in 30% dimethyl sulfoxide, and 2.98 mg/mL in 50% dimethyl sulfoxide.

The vapor pressures of methanol and 1-butanol were measured five times at each condition. The low vapor pressure of 1-octanol proved difficult to measure, and a longer period of gas collection was used. Experiments on neat 1-octanol were only run in triplicate.

The activity of an alkanol in a given medium was calculated from:

$$a_{2,i} = \frac{P_{i,gas}}{P^0_{i,gas}} \tag{15}$$

where $P^0_{i,gas}$ was the experimentally determined vapor pressure of the pure alcohol. Activity coefficients were in turn calculated from the activities by:

$$\gamma_{2,i} = \frac{a_{2,i}}{X_{2,i}} \tag{16}$$

where $X_{2,i}$ is the computed mole fraction alkanol concentration at a given solvent composition. Mole fraction was chosen as the unit of concentration because of its fundamental place in solubility theory. The different molecular weights of water and dimethyl sulfoxide caused the mole fraction composition to be curvilinear with increasing dimethyl sulfoxide concentrations.

Extraction of Lipids and Other Dimethyl Sulfoxide Soluble Materials from the Stratum Corneum—The stratum corneum was isolated by immersing sections of excised skin in 0.25% w/v trypsin (Aldrich Chemical Co., Milwaukee, WI) in saline for 22 h at 37°C and then lifting off the horny layer with a spatula. Samples were rinsed, placed on a piece of aluminum foil, and dried for 1 d in a desiccator under reduced pressure. These were stored over calcium chloride in a desiccator.

Each stratum corneum sample (~ 100 mg) was placed in a petri dish and weighed accurately. Two milliliters of dimethyl sulfoxide:water media at one of the aforementioned percentage compositions was slowly added to the petri dish. The entire chamber was kept in a water bath at 37°C for 2 h, about the length of the permeation experiments. The tissue was then gently lifted from the petri dish with the suction of a pipette and again dried, this time for 7 d in a desiccator under reduced pressure. The sample was again weighed and the percentage change in weight was recorded.

Results

Permeability coefficients for methanol, 1-butanol, and 1-octanol as a function of dimethyl sulfoxide concentration and

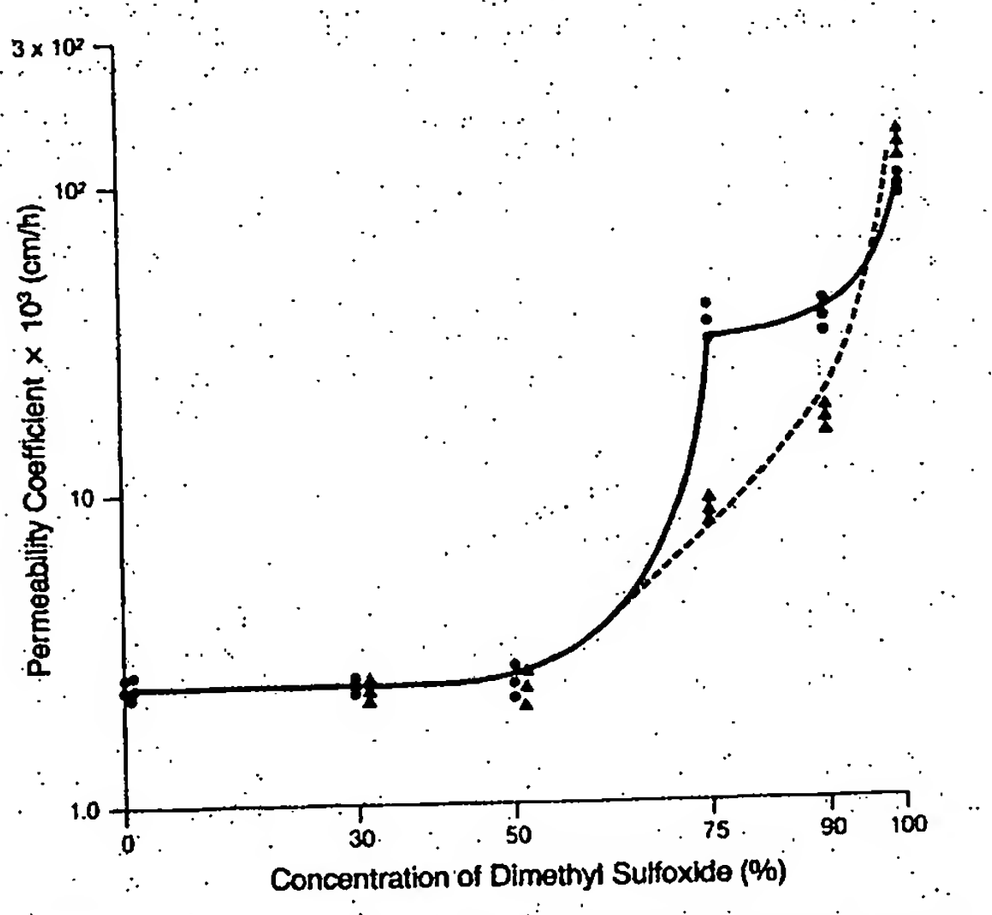

Figure 2—*Permeability coefficients of methanol through fresh hairless mouse skin in dimethyl sulfoxide–water mixture. Key: (●) dimethyl sulfoxide (donor)/saline (receiver); (▲) dimethyl sulfoxide (donor)/dimethyl sulfoxide (receiver).*

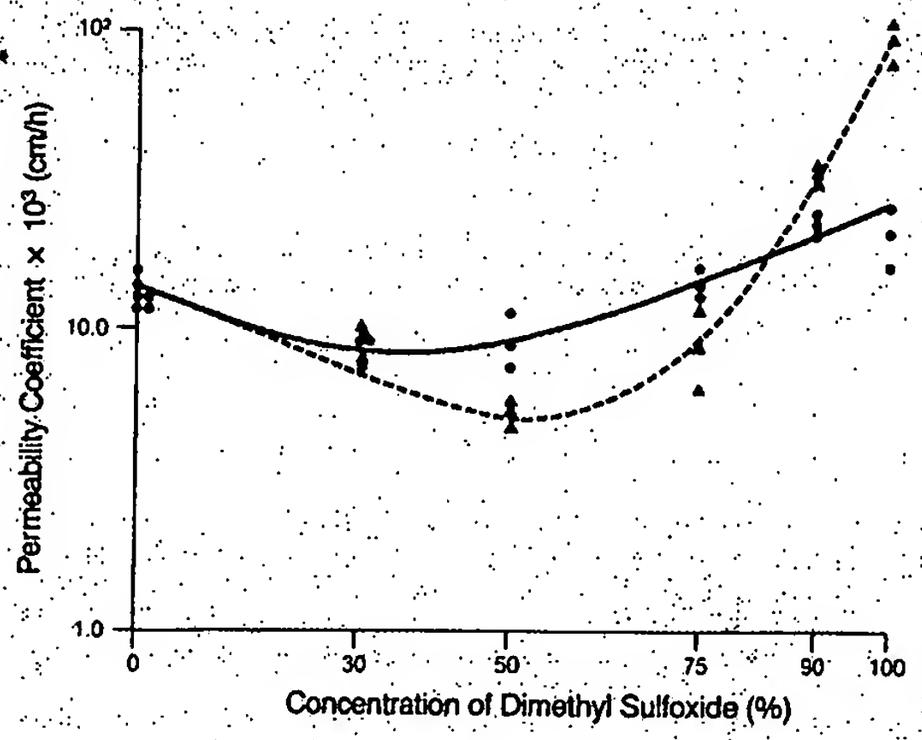

Figure 3—*Permeability coefficients of 1-butanol through fresh hairless mouse skin in dimethyl sulfoxide–water mixture. Key: (●) dimethyl sulfoxide (donor)/saline (receiver); (▲) dimethyl sulfoxide (donor)/dimethyl sulfoxide (receiver).*

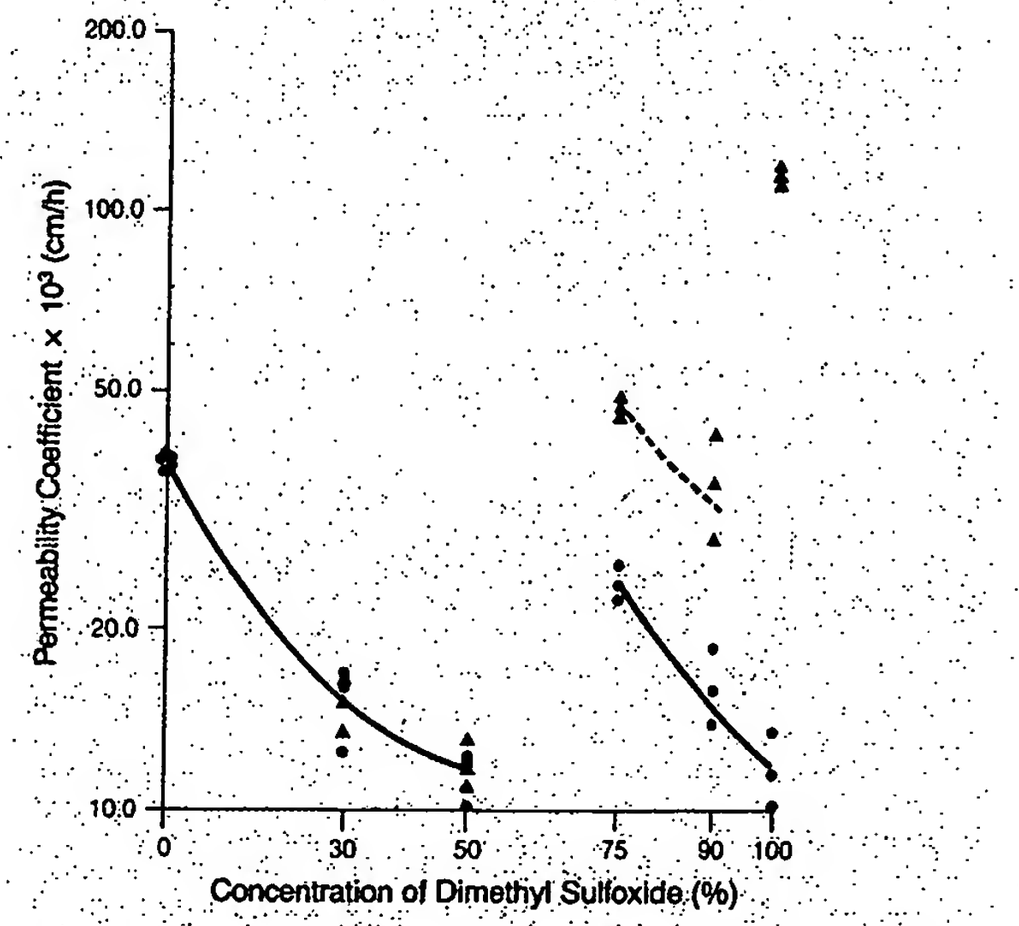

Figure 4—*Permeability coefficients of 1-octanol through fresh hairless mouse skin in dimethyl sulfoxide–water mixture. Key (●) dimethyl sulfoxide (donor)/saline (receiver); (▲) dimethyl sulfoxide (donor)/dimethyl sulfoxide (receiver).*

cell configuration, asymmetric or balanced, are given in Figs. 2, 3, and 4. A high level of reproducibility of results at a given condition is seen.

The partial vapor pressures of these alkanols above the dimethyl sulfoxide:water mixtures are given in Table I, along with computed activities and activity coefficients. The activity coefficient profiles are important and therefore are pictorially illustrated in Figs. 5, 6, and 7 for methanol, 1-butanol, and 1-octanol, respectively. The experimentally determined vapor pressures of the neat liquid alkanols are given in Table II, where they are compared with established literature values.[9]

Figure 8 shows the loss in stratum corneum weight, due to extraction of soluble materials, as a function of dimethyl sulfoxide concentration.

Discussion

The permeability coefficients of the alkanols displayed in Figs. 2, 3, and 4 clearly are affected by dimethyl sulfoxide and the manner in which it is administered to the skin. In the profiles for all three alkanols there are notable differences in

Table I—Partial Vapor Pressures, Activities, and Activity Coefficients of Methanol, 1-Butanol, and 1-Octanol in Binary Dimethyl Sulfoxide:Water Media When Incorporated at 1% Concentration in the Pure and Mixed Solvents

Compound	Conc. of Dimethyl Sulfoxide	Partial Vapor Pressure, mmHg[a]	Activity (P_i/P_i^0)	Activity Coefficient ($\gamma_{2,v}$)
Methanol	0%	$2.10 (\pm 0.17) \times 10^{-1}$	$1.00 (\pm 0.08) \times 10^{-3}$	$2.26 (\pm 0.19) \times 10^{-1}$
1-Butanol		1.71 (± 0.04)	$1.13 (\pm 0.03) \times 10^{-1}$	$5.74 (\pm 0.14) \times 10$
1-Octanol		$7.74 (\pm 2.01) \times 10^{-2}$[b]	$7.76 (\pm 2.00) \times 10^{-1}$	$2.56 (\pm 0.67) \times 10^{3}$
Methanol	30%	$2.61 (\pm 0.21) \times 10^{-1}$	$1.25 (\pm 0.10) \times 10^{-3}$	$2.19 (\pm 0.17) \times 10^{-1}$
1-Butanol		1.51 (± 0.17)	$1.00 (\pm 1.14) \times 10^{-1}$	$3.94 (\pm 0.45) \times 10$
1-Octanol		$6.00 (\pm 1.06) \times 10^{-2}$[b]	$5.94 (\pm 1.04) \times 10^{-1}$	$1.16 (\pm 0.20) \times 10^{3}$
Methanol	50%	$3.35 (\pm 0.51) \times 10^{-1}$	$1.60 (\pm 0.24) \times 10^{-3}$	$2.27 (\pm 0.36) \times 10^{-1}$
1-Butanol		1.10 (± 0.03)	$7.31 (\pm 0.20) \times 10^{-2}$	$2.34 (\pm 0.06) \times 10$
1-Octanol		$4.85 (\pm 0.22) \times 10^{-2}$[b]	$4.80 (\pm 0.22) \times 10^{-1}$	$7.30 (\pm 0.33) \times 10^{2}$
Methanol	75%	$3.62 (\pm 0.26) \times 10^{-1}$	$1.73 (\pm 0.12) \times 10^{-3}$	$1.73 (\pm 0.12) \times 10^{-1}$
1-Butanol		$5.40 (\pm 0.88) \times 10^{-1}$	$3.58 (\pm 0.58) \times 10^{-2}$	8.04 (± 1.31)
1-Octanol		$2.69 (\pm 0.53) \times 10^{-2}$	$2.66 (\pm 0.53) \times 10^{-1}$	$1.03 (\pm 0.53) \times 10^{2}$
Methanol	90%	$4.62 (\pm 0.43) \times 10^{-1}$	$2.20 (\pm 0.20) \times 10^{-3}$	$1.66 (\pm 0.15) \times 10^{-1}$
1-Butanol		$1.20 (\pm 0.21) \times 10^{-1}$	$7.94 (\pm 1.45) \times 10^{-3}$	1.33 (± 0.24)
1-Octanol		$8.10 (\pm 1.81) \times 10^{-3}$	$8.02 (\pm 1.82) \times 10^{-2}$	$2.32 (\pm 0.53) \times 10^{1}$
Methanol	100%	1.13 (± 0.31)	$5.38 (\pm 1.50) \times 10^{-3}$	$3.13 (\pm 0.88) \times 10^{-1}$
1-Butanol		$2.81 (\pm 0.23) \times 10^{-2}$	$1.86 (\pm 0.15) \times 10^{-3}$	$2.42 (\pm 0.19) \times 10^{-1}$
1-Octanol		$1.60 (\pm 0.37) \times 10^{-4}$	$1.59 (\pm 0.37) \times 10^{-3}$	$3.56 (\pm 0.83) \times 10^{-1}$

[a] The values represent averages of five results for methanol and 1-butanol and averages of three results for 1-octanol. Standard deviations are given in brackets. [b] These data were obtained in saturated (two phase) solutions. See text for experimental concentrations in the aqueous phase.

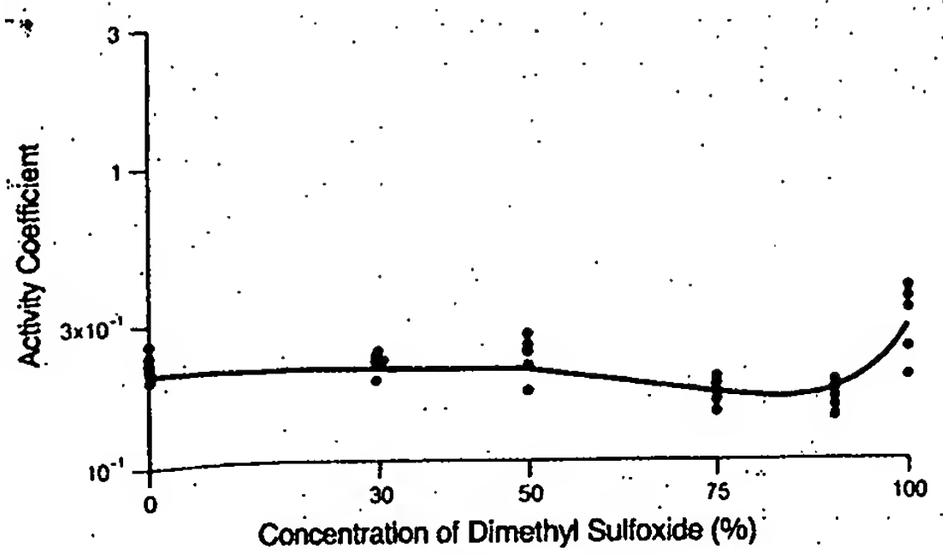

Figure 5—*Activity coefficients of methanol in dimethyl sulfoxide–water mixture at 37°C.*

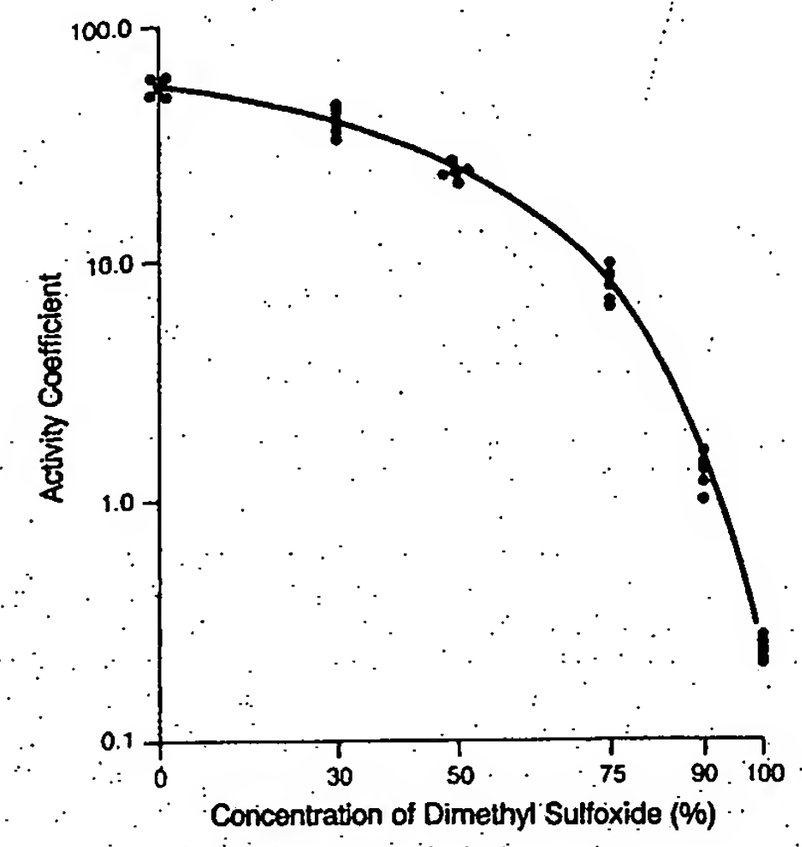

Figure 6—*Activity coefficients of 1-butanol in dimethyl sulfoxide–water mixture at 37°C.*

the patterns of behavior for the asymmetric and balanced solvent configurations. For methanol, the skin is more permeable in the asymmetric mode at 70 and 90% dimethyl sulfoxide concentrations but, if anything, there is a crossover in the curves at or before 100% dimethyl sulfoxide. With 1-butanol, the trends are clearly separated at 50% dimethyl sulfoxide and the crossover comes between 75 and 90% dimethyl sulfoxide. Both asymmetric and balanced configuration patterns for 1-octanol are extraordinary and break abruptly between 50 and 75% dimethyl sulfoxide. It is obvious that the permeation of 1-octanol is favored in the balanced configuration above 50% dimethyl sulfoxide. With the exception of 1-butanol, the permeability profiles for the alkanols in the two solvent configurations are identical for up to 50% dimethyl sulfoxide. Based on simple *t* tests of averages at individual dimethyl sulfoxide concentrations, the differences in values for 1-butanol apparent at 50 and 75% are not statistically significant at an acceptable level of confidence. Overall, the solvent configuration does not appear to make much difference with 0–50% dimethyl sulfoxide concentrations. At the higher dimethyl sulfoxide concentrations, however, profound differences in behavior between the two solvent configurations are noted.

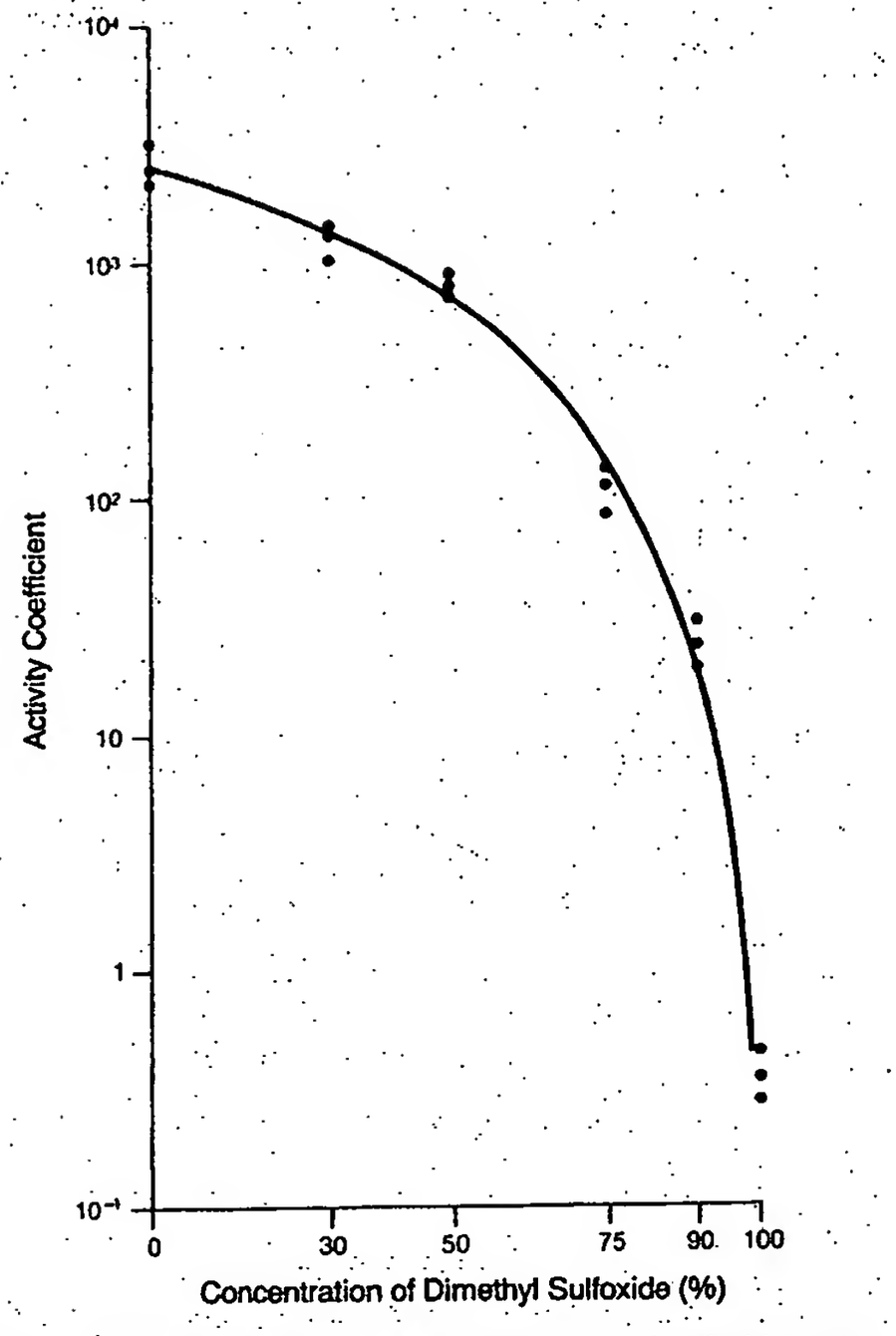

Figure 7—*Activity coefficients of 1-octanol in dimethyl sulfoxide–water mixture at 37°C.*

Table II—Vapor Pressures of Pure Alkanols at 37°C

Compound	Vapor Pressure, mmHg[a]	
	Exp. values	Lit. values[b]
Methanol	209 (± 8.66)	211
1-Butanol	15.1 (± 0.88)	15
1-Octanol	0.101 (± 0.016)	0.37[c]

[a] These values are the average of three results. The standard deviation is in brackets. [b] These data are taken from ref. 9. [c] This value involves extrapolation of data obtained from >100 to 37°C. Apparently, no 37°C estimate exists in the literature. Under these circumstances, the agreement is considered satisfactory.

In an attempt to factor out the causes of the overall permeability behavior, thermodynamic activities and mole fraction based activity coefficients of the respective alkanols were determined as a function of solvent composition. It can be seen from the data in Table I that the activities of each of the alkanols were affected differently as dimethyl sulfoxide was titrated into the solvent medium. For methanol, the activity was systematically increased and, in pure dimethyl sulfoxide, was 5.4 times greater than in water. This simply means water is the better solvent for methanol. In contrast, activities of both 1-butanol and 1-octanol decreased as the dimethyl sulfoxide percentage was raised. Over the solvent range the thermodynamic activity of 1-butanol dropped over 60-fold, while that of 1-octanol dropped almost 500-fold. Thus, as hydrophobicity is increased, solvation of the higher alkanols in dimethyl sulfoxide is markedly favored.

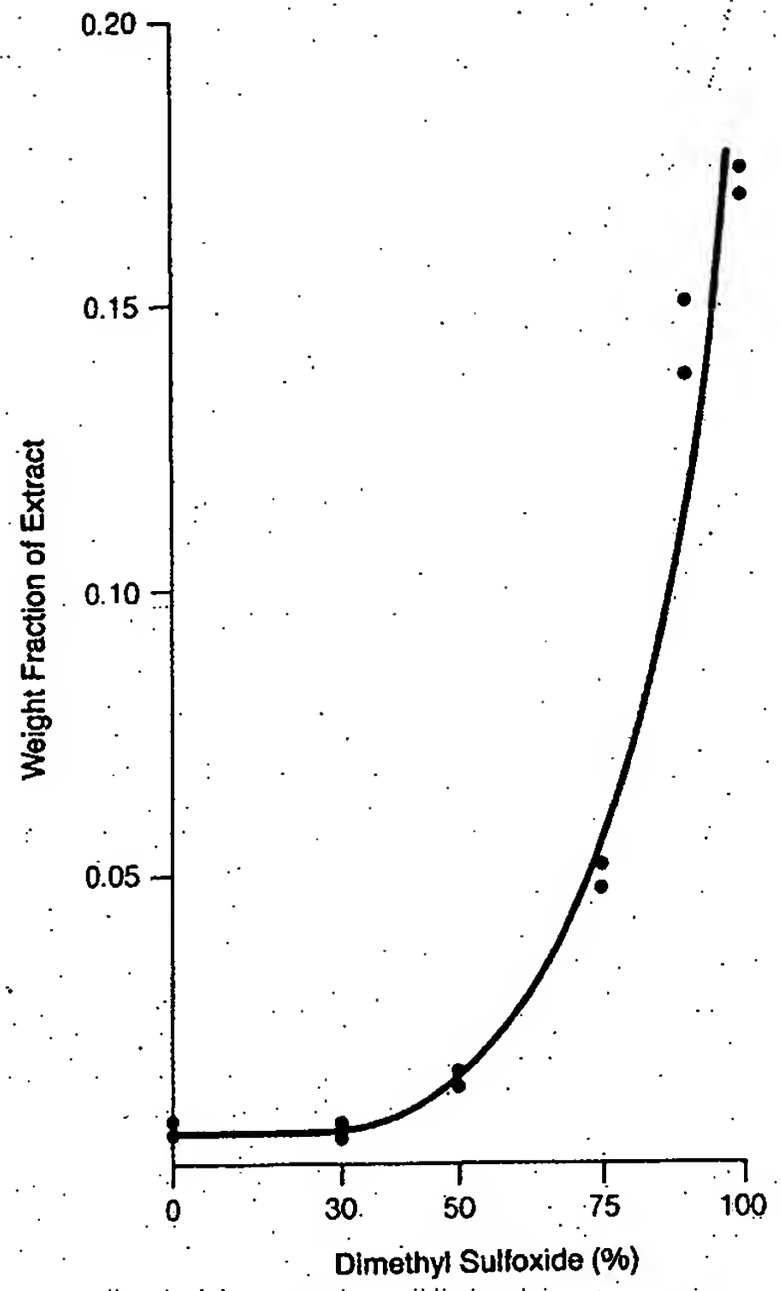

Figure 8—*Solvent extraction from stratum corneum in the presence of dimethyl sulfoxide.*

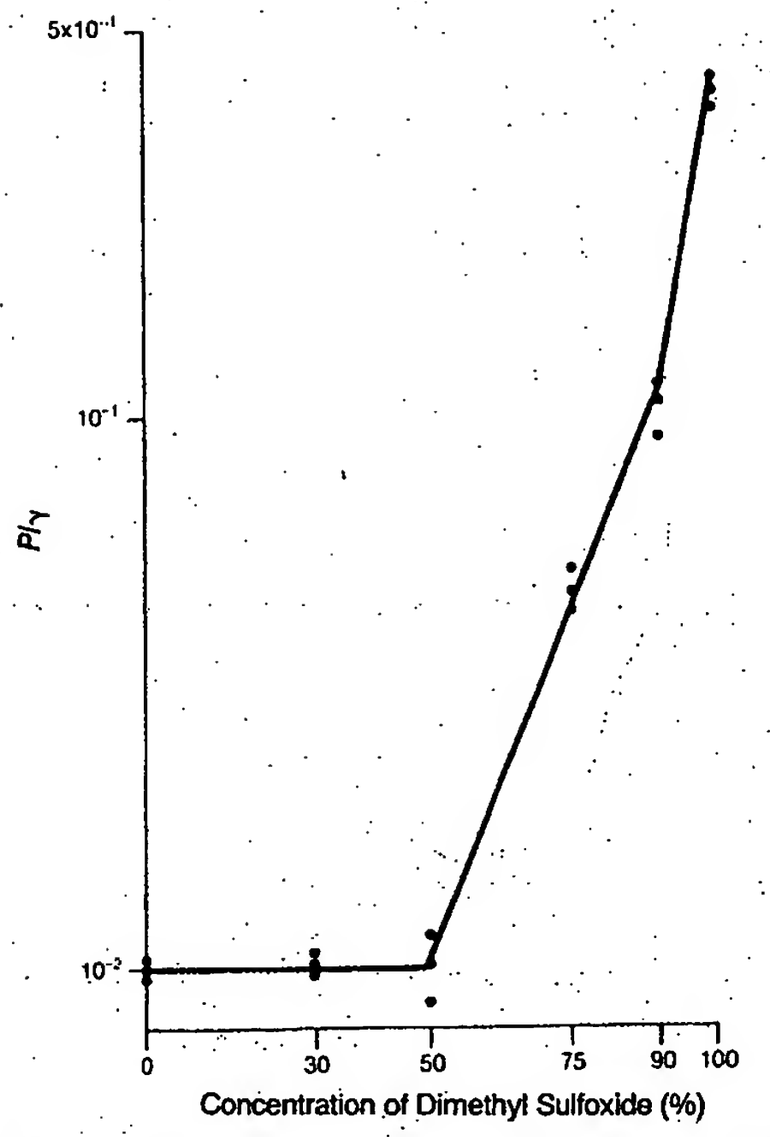

Figure 9—*The ratio of permeability coefficient and activity coefficient of methanol in the presence of dimethyl sulfoxide.*

Patterns in mole fraction based activity coefficients are displayed in Figs. 5, 6, and 7 for methanol, 1-butanol, and 1-octanol, respectively. The choice of mole fraction as the unit of solute concentration results in a surprisingly flat curve for methanol. The trend for 1-butanol from pure water to pure dimethyl sulfoxide is continuously downward. The sensitivity of 1-butanol to increasing dimethyl sulfoxide composition lies between that of methanol and 1-octanol. The activity coefficient of 1-octanol dropped precipitously. Its activity coefficient of 0.34 in pure dimethyl sulfoxide was 7500 times less than that found in pure water (2.56×10^3). In part, the choice of mole fraction concentration to compute activity coefficients magnifies the difference in the activity coefficients seen across the solvent composition span due to the difference in molecular weights and liquid densities of water and dimethyl sulfoxide. The choice of mole fraction itself leads to a fourfold change in the activity coefficient in pure water compared with that in pure dimethyl sulfoxide. Another factor in the case of 1-octanol is that the octanol added was not completely solubilized in the 0, 30, and 50% dimethyl sulfoxide. Therefore, the measured concentrations of 1-octanol in the aqueous phases of these mixtures (0.479, 1.14, and 2.98 mg/mL, respectively) were used in the calculations. Because the 1-octanol was not completely solubilized in this range, the thermodynamic activity itself varied only slightly, as expected.

According to eq. 10, when changes in the thermodynamic activity of a permeant in the vehicle alone decide the relative rate of the permeation process, permeability coefficients can be normalized to a constant value by dividing the experimental values by the respective activity coefficients in the solvents of application. When applied to the data for methanol, 1-butanol, and 1-octanol permeating the skin, this normalizing procedure produces the interesting results seen in Figs. 9, 10, and 11. These figures are produced from data for the alkanols administered in the balanced solvent configuration. For all three alkanols, the permeability is invariant within the boundaries of expected experimental variability up to and including the 50% strength of dimethyl sulfoxide. Considering that this is true for three permeants of wide ranging polarity, these results prove unequivocally that partitioning changes due to altered solvency in the vehicle phase are the overwhelmingly important factor in the data trends. It might be noted that D and $\gamma_{2,m}$, which relate here to the stratum corneum, are both expected to vary in the same upward direction and, therefore, should not offset each other. At dimethyl sulfoxide concentrations up to 50%, normalized permeability coefficients obtained in the asymmetric solvent configuration exhibit essentially identical features.

Concentrations of dimethyl sulfoxide above 50% show an absolute departure in the permeability patterns for the two methods used to configure the donor and receiver media. As seen in the activity coefficient normalized data, there is also a departure from the simple partitioning-determined trend. In either configuration, the $P/\gamma_{2,v}$ values for each of the alkanols takes a dramatic upward turn. This indicates general and profound changes in membrane permeability, which in this study means substantial impairment of the stratum corneum. Imbibition of dimethyl sulfoxide and altered solvency in the critical horny phase of the skin membrane (change in $\gamma_{2,m}$) is one possible general cause. Increasing diffusivity due to solvent alteration of the molecular structure or organization of the stratum corneum (i.e., a change in D) is the second possibility. Both might be associated with the opening of new pathways through the horny layer and a change in the permeation mechanism. The increases at high dimethyl sulfoxide concentrations are so large that a change in mechanism is highly probable. In this regard, the nearly

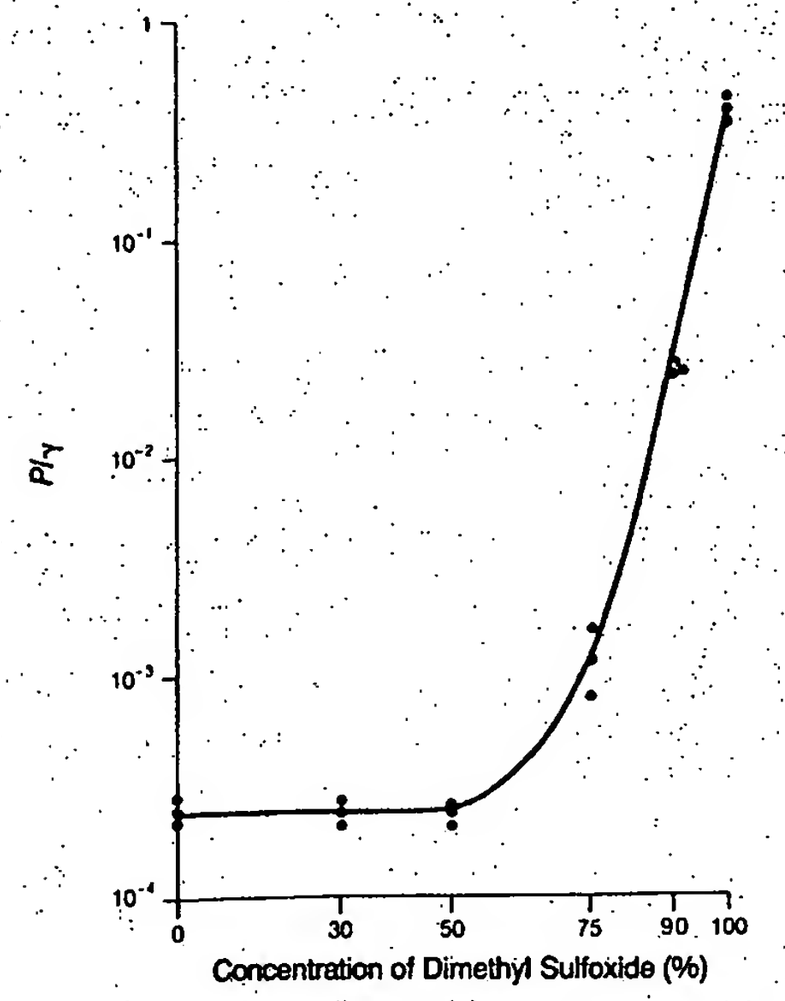

Figure 10—*The ratio of permeability coefficient and activity coefficient of 1-butanol in the presence of dimethyl sulfoxide.*

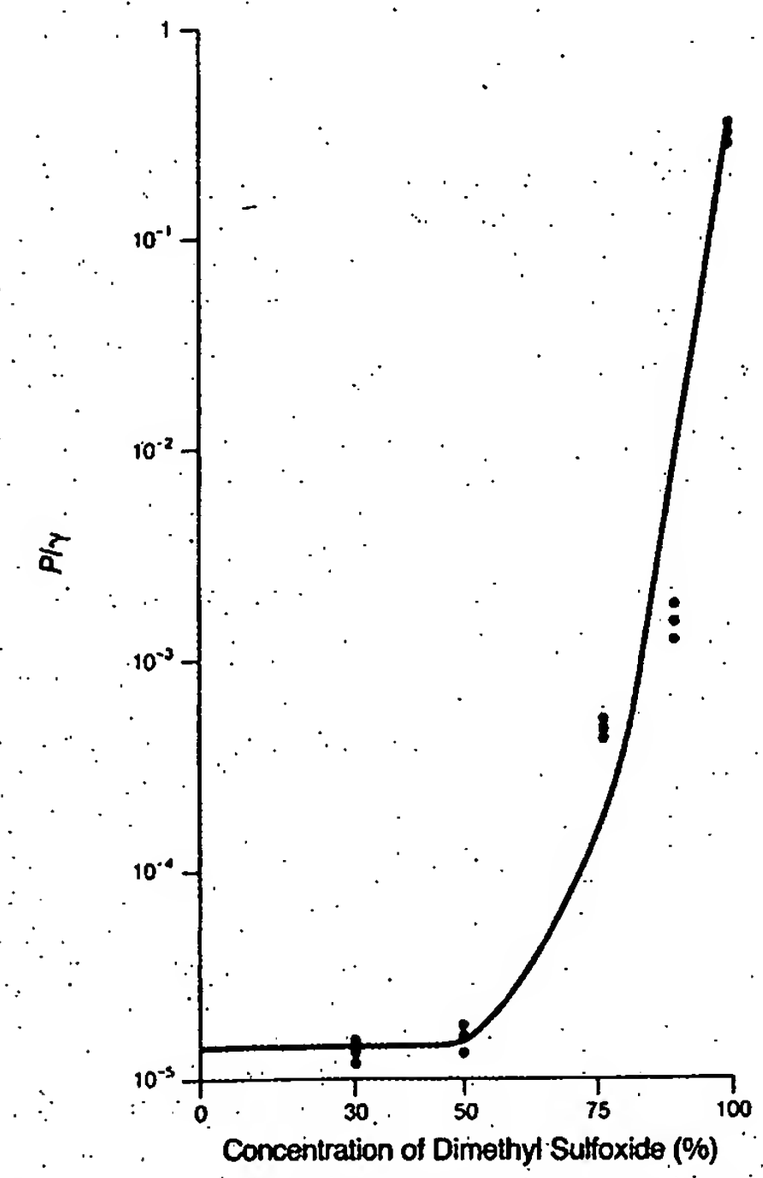

Figure 11—*The ratio of permeability coefficient and activity coefficient of 1-octanol in the presence of dimethyl sulfoxide.*

identical permeability coefficients (absolute values) for methanol, 1-butanol, and 1-octanol in neat dimethyl sulfoxide in the balanced solvent configuration is an indicating factor. Such behavior would only be seen under circumstances where diffusion is structurally insensitive, as would occur through a continuous solvent medium. This suggests that a dimethyl sulfoxide rich pathway is established through the stratum corneum and other skin structures. The average of all permeability coefficients of these alkanols is $\sim 3 \times 10^{-5}$ cm/s (0.11 cm/h). Assuming a partition coefficient of unity for the presumed dimethyl sulfoxide regime in the skin structure, and taking into account the 400-μm thickness of the full-skin sections, a diffusion coefficient estimate of 1.2×10^{-6} cm^2/s is produced. This is in good agreement with a previous estimate of the diffusivity of vidarabine in the water-filled dermal matrix of 1.3×10^{-6} cm^2/s.[10] The slightly lower magnitude for the smaller alkanols is reasonable in this instance because the viscosity and density of dimethyl sulfoxide are larger than those found for water.

Several mechanisms have been advanced for the enhancement of dimethyl sulfoxide on skin permeability, including elution of stratum corneum lipids,[11,12] denaturation of stratum corneum structural proteins (keratin),[13-15] and delamination of the horny layer by stress resulting from crosscurrents of highly water interactive dimethyl sulfoxide and water.[16] We believe the data patterns in these studies support all three mechanisms; the effect which dominates in a particular situation seems to be a result of the concentration of dimethyl sulfoxide and its method and duration of application to the skin. First, Fig. 8 shows that neither water nor binary dimethyl sulfoxide:water mixtures with up to 50% dimethyl sulfoxide have much ability to elute material from the stratum corneum. This ability increases dramatically as the dimethyl sulfoxide concentration is further increased, resulting in an 18% weight loss in the stratum corneum mass in neat dimethyl sulfoxide. These studies were done with a ratio of dimethyl sulfoxide to stratum corneum that was virtually the same as the ratio in the permeability experiments; the contact time was also similar. The striking parallel in tissue weight loss and in lost barrier integrity for three compounds as physicochemically different as methanol, 1-butanol, and 1-octanol (as seen in Figs. 9, 10, and 11) can hardly be an accident. Second, the higher permeability of methanol (and possibly 1-butanol) from binary dimethyl sulfoxide:water solutions of high dimethyl sulfoxide concentration and into water (asymmetric solvent configuration) and similar, even more profound effects seen with vidarabine[8] add to the already convincing evidence of Chandrasekaran et al.[16] which supports the idea that the horny structure is physically disrupted by the cross flows of the two solvents in question. Finally, the permeation of these model permeants out of a pure phase of dimethyl sulfoxide and into a pure dimethyl sulfoxide phase (balanced configuration) has an irregularity most notable in the profile for 1-octanol (Fig. 4). Here, the permeability is high. As mentioned, the barrier property left is about that expected if the solvent (dimethyl sulfoxide) itself were the conducting medium in the membrane. We suspect this exaggeratedly impaired state of the membrane is in part caused by denaturation of the keratin structure, a phenomenon which can be demonstrated in dimethyl sulfoxide soaked pieces of stratum corneum by several techniques, including X-ray diffraction.[13-16] Taking all data into account it appears that maximum impairment of the stratum corneum may be approached in the 100% dimethyl sulfoxide balanced configuration and possibly even in the 100% dimethyl sulfoxide to saline system. Transport would then be solely controlled by the cellular epidermis and the dermis, much as it is when the skin is stripped. With 100% dimethyl sulfoxide:saline, it is likely the epidermis/dermis is relatively water rich. This would not greatly affect the P value for methanol because it is so evenly soluble in water and dimethyl sulfoxide, as reflected in its activity coefficients. Thus, the values for the balanced and asymmetric configurations are similar at 118×10^{-3} cm/h versus 91.8

$\times 10^{-3}$ cm/h, respectively. However, the permeability coefficient for octanol should be influenced by media configuration and it was, as seen in the 113×10^{-3} cm/h value for the balanced configuration and the 11×10^{-3} cm/h value for the 100% dimethyl sulfoxide to saline case. Alternatively, the exaggerated degree of denaturation seen when pure dimethyl sulfoxide was placed on both sides of the skin may not occur in the asymmetric solvent situation due to a relatively rapid flow of water out of the horny surface, a factor which we believe could keep the dimethyl sulfoxide concentration in the horny layer below the critical level for full denaturation of its protein mass.

References and Notes

1. Durrheim, H. H.; Flynn, G. L.; Higuchi, W. I.; Behl, C. R. *J. Pharm. Sci.* 1980, *69*, 781–786.
2. Flynn, G. L.; Durrheim, H. H.; Higuchi, W. I. *J. Pharm. Sci.* 1981, *70*, 52–65.
3. Behl, C. R.; Flynn, G. L.; Kurihara, T.; Harper, N.; Smith, W.; Higuchi, W. I.; Ho, N. F. H.; Pierson, C. L. *J. Invest. Dermatol.* 1980, *75*, 346–352.
4. Behl, C. R.; Flynn, G. L.; Kurihara, T.; Smith, W.; Gatmaitan, O.; Higuchi, W. I.; Ho, N. F. H.; Pierson, C. L. *J. Invest. Dermatol.* 1980, *75*, 340–345.
5. Scheuplein, R. J. *J. Invest. Dermatol.* 1967, *48*, 79–88.
6. Scheuplein, R. J.; Blank, I. H. *J. Invest. Dermatol.* 1973, *60*, 286–296.
7. Higuchi, T. *J. Soc. Cosmet. Chem.* 1960, *11*, 85–97.
8. Kurihara, T., Ph.D. Thesis; University of Michigan, Ann Arbor, MI, 1983.
9. Jordan, T. E. "Vapor Pressure of Organic Compounds"; Interscience: New York, 1954; pp 65, 69, and 76.
10. Yu, C. D.; Higuchi, W. I.; Ho, N. F. H.; Fox, J. L.; Flynn, G. L. *J. Pharm. Sci.* 1980, *69*, 770–772.
11. Allenby, A. C.; Creasey, N. H.; Edington, J. A. G.; Fletcher, J. A.; Schock, C. *Br. J. Dermatol.* 1969, *81*, 47–55.
12. Embery, G.; Dugard, P. H. *J. Invest. Dermatol.* 1971, *57*, 308–31.
13. Elfbaum, S. E.; Laden, K. *J. Soc. Cosmet. Chem.* March 1968, *19*, 163–172.
14. Montes, L. F.; Day, J. L.; Wand, C. J.; Kennedy, L. *J. Invest. Dermatol.* 1967, *48*, 184–196.
15. Scheuplein, R. J.; Ross, L. *J. Soc. Cosmet. Chem.* 1970, *21*, 853–873.
16. Chandrasekaran, S. K.; Campbell, P. S.; Michaels, A. S. *AIChE J.* 1977, *23*, 810–815.

Role of Intercellular Lipids in Stratum Corneum in the Percutaneous Permeation of Drugs

Kayo Harada, Teruo Murakami, Noboru Yata, and Shoso Yamamoto

Department of Dermatology, Hiroshima University School of Medicine (KH, SY); and Department of Biopharmaceutics (KH, TM, NY), Institute of Pharmaceutical Sciences, Hiroshima University School of Medicine, Hiroshima, Japan

The effect of the depletion of intercellular lipids from human stratum corneum and shed snake skin on the permeability to salicylic acid (SA) was investigated in vitro. Shed snake skin was used as a model membrane for human stratum corneum. Lipid depletion with a mixture of chloroform and methanol increased the permeability of those skins to the ionized form but not to the unionized form of SA. Moreover, lipid depletion increased dramatically the permeability of shed snake skin to compounds with low lipophilicity, although it did not have a significant effect on the more lipophilic compounds. As a hypothesis to explain the marked increase of skin permeability to compounds of low lipophilicity, including the ionized form of SA, we suggest increased water transport. *J Invest Dermatol 99:278–282, 1992*

The skin, particularly the stratum corneum, protects the vital organs from chemical and biologically harmful influences and controls transepidermal water loss to regulate body temperature. Current investigations regarding the barrier function of the stratum corneum have focused on intercellular lipids with respect to their composition [1–6] and structure [7–10]. Intercellular lipids in human stratum corneum principally consist of fatty acid, cholesterol, cholesteryl sulfate, and sphingolipids such as ceramides. These lipids form broad, multilamellar sheets in intercellular spaces and are important in regulating the barrier function of the skin [11,12]. However, the role of intercellular lipids in percutaneous permeation of various compounds is not well characterized.

Studies on human percutaneous absorption have been conducted by employing various model membranes such as animal skin [13,14], artificial membrane [15] and human cadaver skin. The usefulness of shed snake skin as a model membrane has also been reported; Itoh et al [16] showed the similarities between human stratum corneum and shed snake skin in terms of thickness, lipid content, and skin permeability to various compounds such as phenol, methylparaben, corticosterone, and so on. In a recent study, we also compared the skin permeability to salicylic acid (SA) using human skin excised from various anatomic sites and shed snake skin in vitro.* In this analysis, the permeability of shed snake skin was shown to be almost the same as that of the human back and mamma.

Shed snake skin is pure, non-vital stratum corneum containing multilamellar lipid sheets that exist in intermediate mesolayers between cornified cells [8,17]. The total lipid content in shed snake skin is similar to that of human stratum corneum [4,16], although the components are markedly different. The main polar lipids in human stratum corneum are ceramides [5] whereas those in shed snake skin are phospholipids [18]. Elias et al [19] reported that total lipid content, rather than lipid composition, is more important in barrier function. Thus, shed snake skin was thought to be a suitable model membrane for human stratum corneum for a study of the role of intercellular lipids in stratum corneum in drug permeation.

In the present study, we first evaluated the effect of lipid depletion on the permeability to SA from different pH buffer solutions, using human skin and shed snake skin. The effect of lipid depletion on the permeability through shed snake skin was then examined by using various compounds with differing lipophilicities.

MATERIALS AND METHODS

Chemicals Salicylic acid (SA) and phenol were purchased from Wako Pure Chemicals (Osaka, Japan). Dinitrochlorobenzene (DNCB) and propyl p-aminobenzoate (propyl-PABA) were obtained from Tokyo Kasei (Tokyo, Japan). Acetaminophen (AAP), p-aminobenzoic acid (PABA), salicylamide (SAA), methyl p-aminobenzoate (methyl-PABA), ethyl p-aminobenzoate (ethyl-PABA), butyl p-aminobenzoate (butyl-PABA), butyl p-hydroxybenzoate (butyl-paraben), and Clea-sol I as a scintillation cocktail were from Nacalai Tesqu Ltd. (Kyoto, Japan). Tritium-labeled water (100 mCi/ml) was purchased from ICN Biomedicals Inc (CA, U.S.A.). All other chemicals and solvents were of reagent grade and used without further purification.

Skin Sources and Preparation Shed snake skin of *Python reticulatus*, a gift from Dainihon Pharmaceutical Co., Ltd., was stored at 70% relative humidity at room temperature. One scale of the ventral skin (thickness, 50 μm) was used for each permeation study after overnight hydration in pH 7.4 Tris-HCl buffer solution prior to experiments.

Human mamma skin was obtained at surgery from five women between the ages of 38 and 72 years. Immediately after excision, subcutaneous fat was removed with surgical scissors and forceps. The skin was kept at 4°C and used within 24 h after excision. The thickness of the mounted skin specimens was approximately 0.18 cm.

Manuscript received June 4, 1991; accepted for publication April 15, 1992.

Reprint requests to: Dr. Noboru Yata, Department of Biopharmaceutics, Institute of Pharmaceutical Sciences, Hiroshima University School of Medicine, 1-2-3 Kasumi, Minami-ku, Hiroshima 734, Japan.

Abbreviations:
AAP: acetaminophen
DNCB: dinitrochlorobenzene
PABA: methyl-p-aminobenzoate
PABA: p-aminobenzoic acid
paraben: p-hydroxybenzoate
SA: salicylic acid
SAA: salicylamide

* Harada K, Murakami T, Kawasaki E, Higashi Y, Yamamoto S, Yata N: Comparison of skin permeability to salicylic acid among human, rodent and shed snake skin in vitro. J Pharm Pharmacol (submitted for publication).

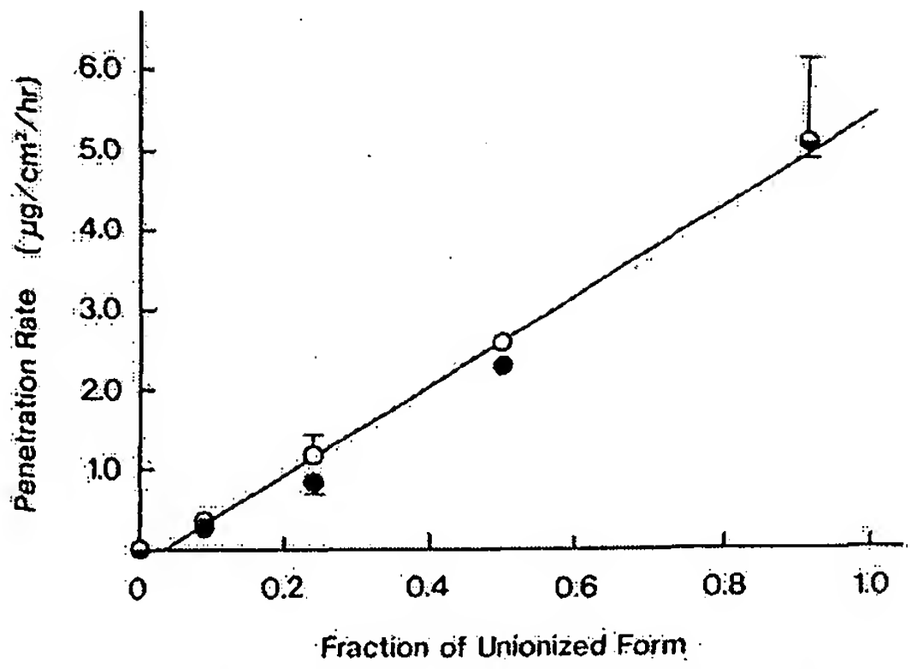

Figure 1. Relationship between penetration rate and fraction of unionized form of SA (pKa = 3.0) through human skin *(open circle)* and shed snake skin *(closed circle)*. One milliliter of SA buffer solution (500 μg/ml) was applied to donor cell at 25°C. *Bar*, SEM of 3–11 trials. *Line*, the regression analysis curve.

Lipid Depletion The ventral scale of shed snake skin (13.22 ± 0.70 mg) was placed in 10 ml of chloroform and methanol mixture (2:1 v/v) overnight at ambient temperature for extraction of intercellular lipids. The skin was then washed with methanol (10 ml) to remove chloroform and dried in a vacuum at room temperature. To estimate the extracted lipid contents of the shed snake skin, we evaporated the solvent extract under nitrogen gas and then dried the residue under reduced pressure until the weight became constant. The lipids of excised human skin were extracted according to the following procedure. After setting a circular piece of human skin between two halves of a diffusion cell, 1 ml of chloroform and methanol mixture (2:1 v/v) was placed on the skin surface. The organic solvent was discarded after 30 min, and the skin surface was rinsed three times with 1 ml of methanol, followed by distilled water [20].

Permeation Study All permeation experiments were performed by using a diffusion cell (Franz-type) in a room with constant temperature maintained at 25°C. A circular piece of skin (untreated or lipid-depleted) was held securely between the two halves of the cell. The area of skin exposed to the test solution or drug particles was 0.785 cm^2 (1 cm diameter). The lower receiver cell was filled with isotonic pH 7.4 Tris-HCl buffer solution. The volume of each receiver cell was accurately determined in advance. The solution in the receiver cell was stirred vigorously with a magnetic bar during the experiments to minimize the diffusion boundary layer at the membrane interface. Aliquots of the solution in the receiver cell were withdrawn at designated time intervals, and then the same volume of the above buffer solution was resupplied to the cell. Samples were stored at −30°C until analysis. The permeation rate of a test compound was determined from a slope of a regression line obtained by plotting the cumulative amount penetrated against the time.

A compound was applied to the skin surface in two different states—solution and solvent-deposited.

Solution: Dosing solutions of various compounds were prepared as follows. SA (pKa = 3.0) was dissolved in isotonic pH 2.0 phosphate buffer, pH 3.0, pH 3.5, pH 4.0 citric acid-phosphate buffer, or pH 7.4 Tris-HCl buffer at a concentration of 500 μg/ml. AAP (pKa = 9.5), phenol (pKa = 10.0), SAA, DNCB, methyl-PABA, ethyl-PABA, propyl-PABA, butyl-PABA, and butyl-paraben were each dissolved at a concentration of 5 μmol/ml in a mixture of ethanol and pH 4.0 citric acid–phosphate buffer solution (1:5 v/v) so that more than 99% of each compound existed in the unionized form in the dosing solution. For PABA (pKa = 4.65, 4.80), the pH 3.0 buffer solution was used. ^3H-water was mixed with saline at a radioactive concentration of 20 μCi/ml. One milliliter of each test solution was placed on the stratum corneum side (beta-layer side in shed snake skin) and the upper donor cell was sealed with parafilm.

Solvent-Deposited: Application of a compound in a solid form was carried out according to the method of Scheuplein and Ross [21]. AAP, SAA, DNCB, and butyl-PABA were dissolved in acetone at a concentration of 500 μmol/ml. After shed snake skin (untreated and lipid-depleted) had been set on a diffusion cell and pH 7.4 buffer solution added to the receiver cell, a sheet of wet filter paper (15 × 25 mm) was coiled around the inside of the cylindrical part of the donor cell and the opening of the cylindrical part was sealed with parafilm. Thus, the skin surface was hydrated for 24 h prior to the experiments. Ten microliters of an acetone solution of a compound (5 μmol) was placed on the skin surface. Acetone was completely evaporated by aeration on the skin. This was followed by a permeation study during which the opening of the cylindrical part of the donor cell was sealed with parafilm to keep the atmosphere above the skin surface hydrated at about 100% relative humidity.

Determination of Lipophilicity As a lipophilic index, the log k value of each compound was determined by high-performance liquid chromatography, according to the method of Yamana et al [22]. Briefly, a methanol solution of a compound was injected on a TSK gel–reverse-phase column (ODS-80TM, Toyo Soda, Tokyo, Japan) and the compound was eluted with a mixture of methanol and water at a flow rate of 1 ml/min. The composition of methanol in the mobile phase was changed from 20% to 70% according to the retention time of the compound. Detection of the compound was done at UV 254 nm. From the retention time of the compound (retained) and mobile phase (unretained), log k′ is defined as log $k' = \log[(Tr/T0) - 1]$, where Tr and T0 denote the retention time of the retained and unretained peaks, respectively. The calculated log k′ values were plotted against the concentration of methanol (v/v%) in the mobile phase and the resultant line was extrapolated to 0% methanol to obtain the log k value.

Analysis The concentration of SA, SAA, and phenol in the aqueous samples was determined by fluorescence spectroscopy (F-3000 Fluorescence Spectrophotometer, Hitachi, Japan) at wave-

Table I. Effect of Lipid Depletion with Chloroform/Methanol Mixture on Penetration Rate of SA Through Shed Snake Skin and Human Skin[a]

	Penetration Rate (μg/cm^2/h)					
	Shed Snake Skin			Human Mamma Skin		
	pH 2.0	pH 4.0	pH 7.4	pH 2.0	pH 4.0	pH 7.4
Untreated	5.09 ± 0.18[b]	0.29 ± 0.05	ND[c]	5.09 ± 1.03	0.37 ± 0.09	ND
Lipid depleted	14.92 ± 0.78	7.37 ± 0.32	0.54 ± 0.12	16.10	6.40	0.21

[a] One milliliter of SA buffer solution (500 μg/ml) was applied to donor cells at 25°C.
[b] Each value represents the mean ± SEM of 5–8 trials. Values without SEM were one trial.
[c] ND, not detected.

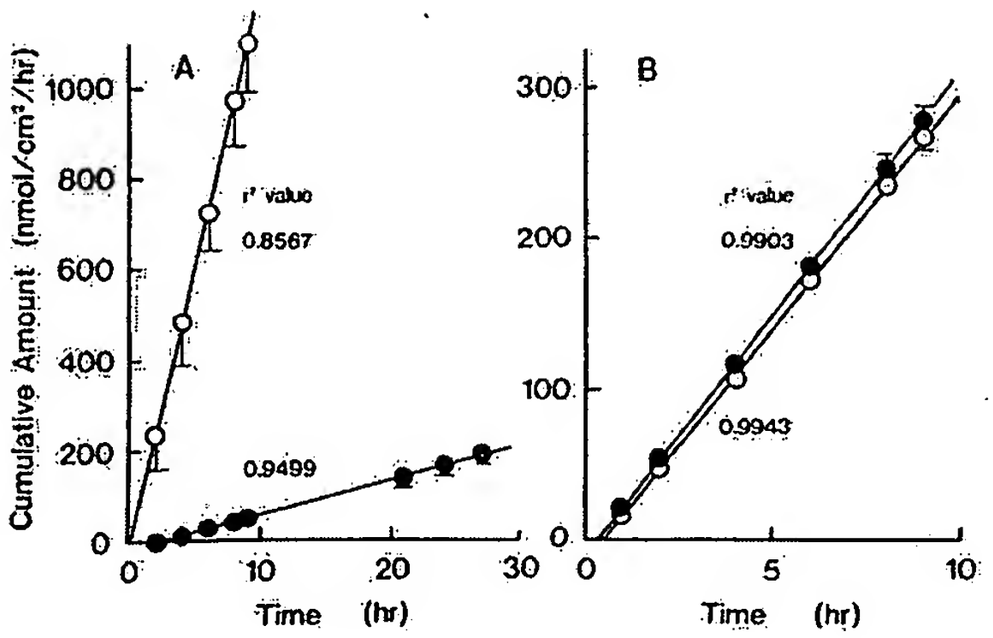

Figure 2. Time course of cumulative amount of SAA *(A)* and DNCB *(B)* penetrated through untreated *(closed circle)* and lipid-depleted *(open circle)* shed snake skin. One milliliter of SAA and DNCB buffer solution (pH 4.0) was applied to donor cell at 25°C. *Bar*, SEM of three trials. *Line*, the regression analysis curve. The number beside the line represents the r^2 value.

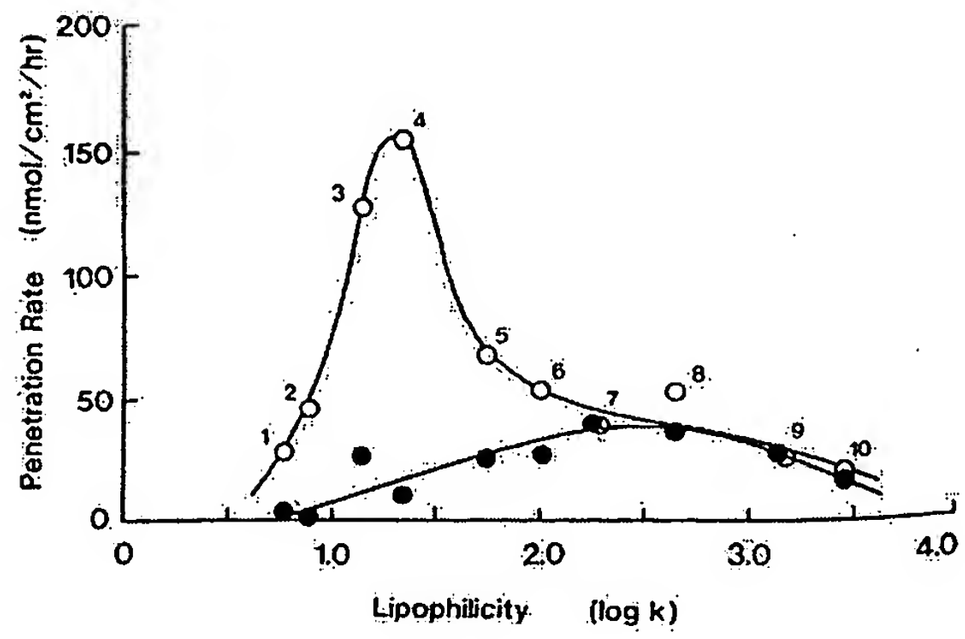

Figure 3. Relationship between penetration rate and lipophilicity (log k) of various compounds as unionized form through untreated *(closed circle)* and lipid-depleted *(open circle)* shed snake skin. One milliliter of a compound buffer solution (5 μmol/ml) was applied to donor cell at 25°C. 1, AAP; 2, PABA; 3, phenol; 4, SAA; 5, methyl-PABA; 6, ethyl-PABA; 7, DNCB; 8, propyl-PABA; 9, butyl-PABA; 10, butyl-paraben. Each value represents the mean of three trials. The standard errors were within the diameter of the symbols.

lengths of 298 nm (excitation) and 407 nm (emission) for SA; 333 nm and 415 nm for SAA; and 273 nm and 300 nm for phenol. Other compounds were assayed with a spectrophotometer (UV-160A, Simadzu, Kyoto, Japan) at 241 nm for AAP, 251 nm for DNCB, 257 nm for butyl-paraben, 266 nm for PABA, 285 nm for PABA-esters, and 550 nm for phenol red. Detection limits for these compounds were 2 μM or less, with the exception of phenol red, which had a detection limit of 0.5 μM. No substances interfering with ultraviolet and fluorescence spectroscopic analysis of these drugs were released from either human skin or shed snake skin. For the ^{3}H-water samples (100 μl each), 3 ml of scintillation cocktail was added and the radioactivity was determined by a liquid scintillation counter (LSL-903, Aloka, Tokyo, Japan) with an external standard.

RESULTS

Effect of Lipid Depletion on Permeability to SA of Human Skin and Shed Snake Skin The extent of skin permeability to weak organic acids such as SA is known to depend on the mole fraction of unionized compound [23,24]. The penetration rate of SA through untreated human skin and shed snake skin also increased linearly with an increase of unionized fraction, consistent with the pH-partition theory (Fig 1). No permeation of SA was observed at pH 7.4. The effect of lipid depletion on SA permeation was examined by using different pH solutions. Depletion of lipids resulted in a significantly increased permeation of SA at all pH values in both skins (Table I). The enhancement ratios (treated/untreated) were calculated to be 3.2 at pH 2.0 and 17.3 at pH 4.0 in human mamma skin, and 2.9 at pH 2.0 and 24.5 at pH 4.0 in shed snake skin, respectively. Interestingly, SA penetrated the lipid-depleted human skin and shed snake skin even at pH 7.4. The extent of increased penetration rate of SA at any pH tested was found to be comparable in human skin and shed snake skin. Also, greater effects were observed on the ionized form rather than the unionized form of SA.

Effect of Lipid Depletion on the Permeability of Shed Snake Skin to Compounds with Different Lipophilicities In this study, compounds were applied to the skin surface as both an aqueous solution and a solvent-deposited solid. In Fig 2 are typical examples of the application of an aqueous solution, the permeation time profiles of SAA and DNCB in the lipid-depleted and untreated shed snake skin. These compounds were selected as examples of relatively less lipophilic (SAA, log k = 1.34) and more lipophilic (DNCB, log k = 2.24) compounds. No effect of lipid depletion on the permeability of DNCB was observed, whereas the permeability of SAA increased 10 times in the lipid-depleted skin. This finding indicates that shed snake skin was more permeable to the relatively less lipophilic compound when lipids were depleted.

The effect of lipid depletion on the penetration rate of several compounds having different lipophilicities was examined. In Fig 3, the penetration rate of these compounds from an aqueous solution is plotted against the lipophilic index, log k. In untreated skin, a parabolic relationship with a peak at the log k value of 2.5 was obtained. The effect of lipid depletion on the penetration rate varied markedly depending on the lipophilicities of the permeants. A plotting of the increased ratio of the penetration rate against the lipophilic index, log k, revealed the greater effects on compounds with lower lipophilicities having log k values of less than 2 (Fig 4). On the other hand, little effect was observed on compounds with higher lipophilicities (log k > 2).

The contrasting effects of lipid depletion on the permeability of more and less lipophilic compounds was further examined by a solid application method. In this case, the influence of unstirred aqueous boundary layers on the skin surface should be negligible. AAP, SAA,

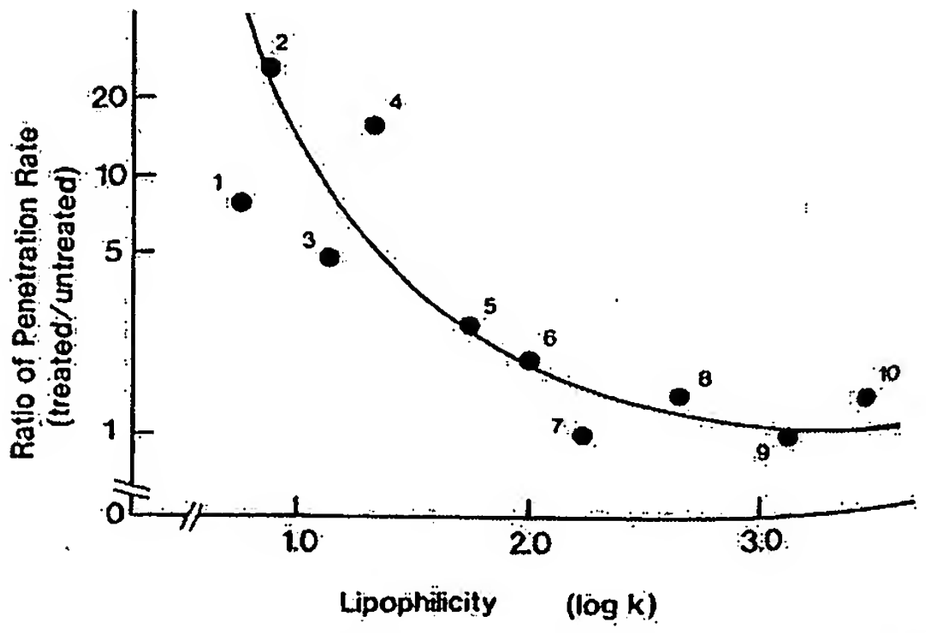

Figure 4. Enhanced penetration rates of various compounds by lipid depletion in shed snake skin. 1, AAP; 2, PABA; 3, phenol; 4, SAA; 5, methyl-PABA; 6, ethyl-PABA; 7, DNCB; 8, propyl-PABA; 9, butyl-PABA; 10, butyl-paraben.

Table II. Effect of Lipid Depletion with Chloroform/Methanol Mixture on Penetration Rate of Compounds Applied in a Solid Form Through Shed Snake Skin[a]

	Penetration Rate (nmol/cm²/h)			
	AAP (log k = 0.76)	SAA (log k = 1.34)	DNCB (log k = 2.24)	Butyl-PABA (log k = 3.16)
Untreated	12.1 ± 0.7[b]	44.5 ± 1.3	71.5 ± 5.3	29.6 ± 2.0
Lipid depleted	973.3 ± 51.6	457.0 ± 20.9	87.9 ± 3.8	36.8 ± 1.4
Ratio (treated/untreated)	80.44	10.27	1.23	1.24

[a] Five micromoles of each compound was applied to donor cells at 25°C.
[b] Each value represents the mean ± SEM of three trials.

DNCB, and butyl-PABA were used as model permeants, and the results are summarized in Table II. The increased permeation by lipid depletion was again observed in the less lipophilic compounds, which is seen in the solution application.

Effect of Lipid Depletion on Water Transport The effect of lipid depletion on water transport was examined by using ^{3}H-water. As summarized in Table III, water permeation increased in the lipid-depleted skin (both human and shed snake skin).

DISCUSSION

To clarify the role of intercellular stratum corneum lipids in drug permeation, we investigated the effect of lipid depletion of the stratum corneum on skin permeability to various compounds. In untreated skin, SA penetrated the skin following pH-partition theory (Fig 1). This finding shows that the barrier properties of the stratum corneum for SA permeation are predominantly caused by the lipids.

Lipid depletion of both human and shed snake skin facilitated the permeation of completely ionized SA (at pH 7.4), which is usually impermeable through untreated skin (see Table I). In addition, the permeation of relatively hydrophilic compounds (log k < 2) increased markedly (Fig 3). However, in a separate experiment with phenol red, which is extremely water soluble and impermeable through untreated skin, the depletion of lipids did not measurably affect its permeation through shed snake skin. This shows that lipid-depleted skin still retains some of its barrier function against certain water-soluble compounds, depending on the molecular size.

On the other hand, permeability of the lipid-depleted skin to more lipophilic compounds (log k > 2) was almost the same as that of untreated skin (Fig 3). In the study employing aqueous solutions of a compound, the solution in the donor cell was not stirred during the permeation experiment. This experimental condition raises the possibility that the maximal flux of a compound, especially a highly lipophilic compound, could be limited by the unstirred boundary layer on the skin surface. To examine this possibility, the application of a compound in a solid form in which the existence of the unstirred boundary layer on the skin surface was eliminated, was also studied. Similar results to that of the solution application were observed (see Table II). These findings indicate that the possible existence of an unstirred boundary layer in the donor solution does not affect the skin permeation of the rather lipophilic compounds used in the present study.

The possible presence of another unstirred boundary layer in the receptor solution should also be taken into consideration. However, the effects of the unstirred boundary layer in the receptor solution can be set aside in the present study because the receptor solution was vigorously agitated to reduce the thickness of the layer.

Our experiments were conducted with full-thickness human skin and shed snake skin. Full-thickness human skin has an underlying tissue (viable epidermis and dermis), which is predominantly aqueous and has an effective thickness (1 to 3 mm) of aqueous boundary layers. Bronaugh has reported that the thick dermal tissue can present a substantial barrier in an in vitro permeation study, particularly for lipophilic compounds [25]. Estimating the diffusion coefficient (D) in the tissue to be 0.007 for SA in the absence of any stratum corneum barrier would be calculated as follows: $J = (D/h) \cdot C = (0.007\ cm^2/h)(500\ \mu g/ml)/(0.18\ cm) = 19.4\ \mu g/cm^2/h$, where C and h denote the SA concentration in the donor cell and the thickness of the underlying tissue of human mamma skin, respectively. This calculated J value approximates the increased flux value of SA at pH 2.0 (16.1 $\mu g/cm^2/h$) observed in the lipid-depleted human skin (see Table I). Thus, the diffusion process through the underlying tissue can be a rate-determining step in the overall diffusion through the skin, especially when the diffusion resistance of the stratum corneum to permeants is markedly decreased. On the other hand, shed snake skin is much thinner (≈50 μm) than human skin, indicating that the aqueous boundary layer effects in shed snake skin can be discounted. The observed selectivity of the lipid-depletion effect on enhancing the flux of hydrophilic compounds can be attributed to an effect specific to the barrier properties of the stratum corneum alone.

In the present study, 4.92 ± 0.23% (n = 10) of the shed snake skin weight was extracted as lipids. However, Itoh et al [16] reported that lipids comprise about 6% of the shed snake skin weight. Therefore, the fact that the permeation of highly lipophilic compounds was not influenced by lipid depletion also suggests that some amounts of lipid must remain in the stratum corneum even after the extraction by solvent, and provide a route for the permeation of compounds with higher lipid affinity.

The fact that lipid depletion increased the membrane permeability to the less lipophilic compounds may be related only to the marked increase in the water flux (about 40 times as shown in Table III). It has been reported that high relative humidity (75%), which increases the water content in stratum corneum by up to 20 w/w% [26], increases the percutaneous absorption of relatively water-soluble compounds [27]. This finding has been accounted for by the mechanism of increased lipid fluidity, i.e., hydration loosens intermolecular forces both in the polar head and packed hydrophobic groups and extends the hydrophilic domain by allowing insertion of water molecules around polar head groups, resulting in easier migration of compounds [28]. The increased water flux and preferential enhancement of permeability to less lipophilic compounds

Table III. Effect of Lipid Depletion with Chloroform/Methanol Mixture on Penetration Rate of ^{3}H-Water[a]

	Penetration Rate (μl/cm²/h)	
	Shed Snake Skin	Human Mamma Skin
Untreated	0.099 ± 0.005[b]	0.150 ± 0.034
Lipid depleted	4.453 ± 0.142	6.150 ± 0.394

[a] One milliliter of ^{3}H-water (20 μCi/ml) was applied to donor cell at 25°C.
[b] Each value represents the mean ± SEM of 3–4 trials.

caused by lipid depletion may also be explained by the above mechanism.

REFERENCES

1. Werzs PW, Swartzendruber DC, Madison KC, Downing DT: Composition and morphology of epidermal cyst lipids. J Invest Dermatol 89:419–425, 1987
2. Lampe MA, Williams ML, Elias PM: Human epidermal lipids: Characterization and moduations during differentiation. J Lipid Res 24:131–140, 1983
3. Gray GM, White RJ, Williams RH, Yardley HJ: Lipid composition of the superficial stratum corneum cells of pig epidermis. Br J Dermatol 106:59–63, 1982
4. Lampe MA, Burlingame AL, Whitney J, et al: Human stratum corneum lipids: Characterization and regional variation. J Lipid Res 24:120–129, 1983
5. Long SA, Wertz PW, Strauss JS, Downing DT: Human stratum corneum polar lipids and desquamation. Arch Dermatol Res 277:284–287, 1985
6. Gray GM, White RJ: Glycosphingolipids and ceramides in human and pig epidermis. J Invest Dermatol 70:336–341, 1978
7. Madison KC, Swartzendruber DC, Wertz PW, Downing DT: Presence of intact intercellular lipid lamellae in the upper layers of the stratum corneum. J Invest Dermatol 88:714–718, 1978
8. Landmann L: Epidermal permeability barrier: Transformation of lamellar granule-disks into intercellular sheets by a membrane-fusion process, a freeze-fracture study. J Invest Dermatol 87:202–209, 1986
9. Landmann L: The epidermal permeability barrier. Anat Embryol (Berl) 178:1–13, 1988
10. Swartzendruber DC, Wertz PW, Kitko DJ, Madison KC, Downing DT: Molecular model of the intercellular lipid lamellae in mammalian stratum corneum. J Invest Dermatol 92:251–257, 1989
11. Elias PM: Epidermal lipids, barrier function, and desquamation. J Invest Dermatol 80:44S–49S, 1983
12. Imokawa G, Akasaki S, Hattori M, Yoshizuka N: Selective recovery of deranged water-holding properties by stratum corneum lipids. J Invest Dermatol 87:758–761, 1986
13. Hinz RS, Hodson CD, Lorence CR, Guy RH: In vitro penetration: Evaluation of the utility of hairless mouse skin. J Invest Dermatol 93:87–91, 1989
14. Bond JR, Barry BW: Limitations of hairless mouse skin as a model for in vitro permeation studies through human skin: Hydration damage. J Invest Dermatol 90:486–489, 1988
15. Houk J, Guy RH: Membrane model for skin penetration study. Chem Rev 88:455–471, 1988
16. Itoh T, Xia J, Magavi R, Nishihata T, Rytting H: Use of shed snake skin as a model membrane for in vitro percutaneous penetration studies: comparison with human skin. Pharm Res 7:1042–1047, 1990
17. Landmann L, Stolinski C, Martin B: The permeability barrier in the epidermis of the grass snake during the resting stage of the sloughing cycle. Cell Tissue Res 215:369–382, 1981
18. Roberts JB, Lillywhite HB: Lipid barrier to water exchange in reptile epidermis. Science 207:1077–1079, 1980
19. Elias PM, Cooper ER, Korc A, Brown BE: Percutaneous transport in relation to stratum corneum structure and lipid composition. J Invest Dermatol 76:297–301, 1981
20. Sweeney TM, Downing DT: The role of lipids in the epidermal barrier to water diffusion. J Invest Dermatol 55:135–140, 1970
21. Scheuplein RJ, Ross LW: Mechanism of percutaneous absorption: percutaneous absorption of solvent deposited solids. J Invest Dermatol 62:353–360, 1974
22. Yamana T, Tsuji A, Miyamoto E, Kubo O: Novel method for determination of partition coefficients of penicillins and cephalosporins by high-pressure liquid chromatography. J Pharm Sci 66:747–749, 1977
23. Kurosaki Y, Aya N, Okada Y, Nakayama T, Kimura T: Studies on drug absorption from oral cavity: physiocochemical factors affecting absorption from hamster cheek pouch. J Pharmacobiodyn 9:287–296, 1986
24. Flynn GL: Mechanism of percutaneous absorption from physiochemical evidence. In: Bronaugh RL, Maibach HI (eds.). Percutaneous Absorption. New York, Marcel Dekker, 1989, pp 27–51
25. Bronaugh RL: Determination of percutaneous absorption by in vitro techniques. In: Bronaugh RL, Maibach HI (eds.). Percutaneous Absorption. New York, Marcel Dekker, 1989, pp 239–258
26. Potts RO: Stratum corneum hydration: Experimental techniques and interpretations of results. J Soc Cosmet Chem 37:9–33, 1986
27. Reifenrath WG: Evaporation and penetration from skin. In: Bronaugh RL, Maibach HI (eds.). Percutaneous Absorption. New York, Marcel Dekker, 1989, pp 313–334
28. Barry BW: Mode of action of penetration enhancers in human skin. J Controlled Rel 6:85–97, 1987

International Journal of Pharmaceutics, 79 (1992) 141–148
Elsevier Science Publishers B.V.

IJP 02620

The influence of alkyl-azones on the ordering of the lamellae in human stratum corneum

J.A. Bouwstra [1], G.S. Gooris [1], J. Brussee [2], M.A. Salomons-de Vries [1] and W. Bras [3]

[1] *Center for Bio-Pharmaceutical Sciences,* [2] *Organic Chemistry Department, University of Leiden, P.O. Box 9502, 2300 RA Leiden, (The Netherlands) and* [3] *Daresbury Synchrotron Radiation Station / NWO, Warrington WA4 (U.K.)*

(Received 7 May 1991)
(Modified version received 31 July 1991)
(Accepted 23 August 1991)

Key words: Azone; Lamellar structure; Small angle X-ray scattering; Stratum corneum

Summary

The effect of a series of alkyl-azones (*N*-alkylazocycloheptane-2-one) on the structure of human stratum corneum has been studied by small angle X-ray scattering. Treatment with alkyl-azones having alkyl chains greater than six carbons in length resulted in the disordering of the lamellae in the stratum corneum. The results could be correlated with those obtained by thermal analysis. The remaining thermal transition after treatment with longer alkyl chain azones is probably due to the lipids associated with the proteins.

Introduction

The intercellular regions in the stratum corneum consist of lipids that are arranged in a lamellar phase (Elias and Friend, 1975). The lipids which constitute the lamellar phase are, e.g. ceramides, cholesterol, glycerides and alkyl acids. The intercellular route is supposed to be the main pathway by which drugs and other substances diffuse across the stratum corneum. For this reason it is very important to obtain information on the structure of the intercellular lipids and the changes in this structure induced by penetration enhancers. Using small-angle X-ray scattering (SAXS), one of the first studies on the structure of the lipids in human stratum corneum was carried out by Friberg and Osborne (1985). They observed a single broad diffraction peak. Assuming a lamellar phase, a repeat distance of approx. 6.0 nm was calculated. White et al. (1988) studied the structure of the lipids in murine stratum corneum. They observed a series of sharp diffraction peaks which were based on a lamellar phase with a repeat distance of 13.1 nm. Bouwstra et al. (1991a) found a repeat distance of 6.5 nm for human stratum corneum, but could not exclude a distance of approx. 13 nm. Garson et al. (1991) found two repeat distances of 6.5 and 4.4 nm in human stratum corneum. In more recent studies, it appeared that the scattering curve of human stratum corneum could be explained by

Correspondence: J.A. Bouwstra, Center for Bio-Pharmaceutical Sciences, University of Leiden, P.O. Box 9502, 2300 RA Leiden, The Netherlands.

two unit cells with repeat distances of 6.4 and 13.4 nm, respectively (Bouwstra et al., 1991b).

Several techniques were used to investigate the influence of penetration enhancers on the structure of lipids in the stratum corneum. Thermal analysis was used to study the influence of water (Golden et al., 1987), dimethyl sulfoxide (Goodman and Barry, 1986) and oleic surfactants (Golden et al., 1988) on the phase transitions. Fourier transform infrared spectroscopy (FTIR) was used to study the effect of oleic acid and D_2O on the C-H stretching absorbance (Mak et al., 1991).

Several investigations were carried out on the effect of alkyl-azones on the penetration route (Boddé et al., 1989), thermal transitions (Bouwstra et al., 1989) and penetration enhancement. Dodecyl-azone in combination with propylene glycol (PG) favoured the intercellular transport of $HgCl_2$ (Boddé et al., 1989), while hexyl-azone did not change the distribution of $HgCl_2$ between corneocytes and lipid regions. In another study, an increase in penetration enhancement was observed using longer alkyl-azones (Hoogstraate et al., 1991). The increase in penetration enhancement is accompanied by a decrease in the total enthalpy of two lipid phase transitions. The influence of dodecyl-azone on the bilayers was studied using DPPC liposomes (Beastall et al., 1988), which are supposed to be a model system for the bilayers in the stratum corneum. It was concluded that intercalation of dodecyl-azone resulted in a decrease in the diffusional resistance of the bilayers.

This paper describes the influence of alkyl-azones on the lamellar structure in human stratum corneum measured by small-angle X-ray scattering (SAXS).

Materials and Methods

Preparation of the samples

Human mamma or abdomen skin obtained after surgical operation was dermatomed to a thickness of approx. 200 μm. The stratum corneum was separated from the epidermis by digestion with a 0.1% trypsin solution for 14 h.

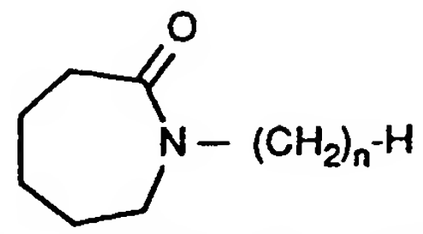

Fig. 1. The structure of alkyl-azones, in which *n* represents the number of C atoms in the alkyl chain.

The stratum corneum was washed and dried over silica gel. Before use it was equilibrated above 27% w/w NaBr solution to achieve a hydration level of 20% w/w.

Synthesis of alkyl-azones

The synthesis of the alkyl-azones was carried out as described before (Bouwstra et al., 1989). The purity of the azones was checked by NMR and appeared to be better than 98%. The structure of alkyl-azones is shown in Fig. 1.

Pretreatment of human stratum corneum with alkyl-azones

Pretreatment was carried out by immersing the stratum corneum in a solution of propylene glycol (PG) or alkyl-azone in PG (0.15 M solution) for a period of 24 h. The alkyl chain length varied between 6 and 16 atoms. In another series of experiments stratum corneum was heated to 90°C and cooled down in order to recrystallize the lipids, after which the stratum corneum was pretreated with alkyl azones in PG as described above.

Small angle X-ray scattering (SAXS)

All measurements were carried out at the Synchrotron Radiation Source at Daresbury's Laboratories using station 8.2. This station has been built as part of an NWO/SERC agreement. The camera produces a highly collimated beam with a cross-section of 0.4×4 mm^2 at the sample position. With the SRS operating at 200 mA and 2 GeV the X-ray intensity is approx. 4×10^{11} photons/s with $\lambda = 0.15$ nm at the sample position. Smearing of the diffraction pattern due to the finite size of the X-ray beam is negligible. The sample-to-detector distance can be set between 0.2 and 4.5 m enabling studies of systems with

repeat distances $0.4 < d < 100$ nm. For data collection a multiwire, position-sensitive quadrant detector was used. This detector can handle count rates up to 250000 s^{-1}. The detector system spatial resolution is 0.5 mm. This detector definitely improves the signal-to-noise ratio at higher diffraction angles compared with a previously used linear detector (Bouwstra et al., 1991a). For all the experiments the sample-to-detector distance was set to 2.0 m. The diffraction patterns were normalized with respect to synchrotron beam decay and absorption of the sample. Background subtractions and corrections for positional inhomogeneity in the detector sensitivity were performed as well. No smoothing algorithms were applied to the data. Calibrations were performed with the help of a wet rat tail collagen sample with a repeat distance of 67 nm.

The stratum corneum, approx. 5 mg in weight, was put in a specially designed temperature-controlled sample cell. Scattering curves were collected for 15 min. The scattering intensities are plotted as a function of the scattering vector Q defined as $Q = (4\pi \sin \theta)/\lambda$, in which θ is the scattering angle and λ the wavelength.

Results and Discussion

After pretreatment of stratum corneum with alkyl-azones in combination with PG a check on the lipid loss was performed. No lipids could be detected in the alkyl-azone/PG solution using thin-layer chromatography (Ponec et al., 1988).

In Fig. 2 the scattering pattern of untreated human stratum corneum hydrated to 20% w/w is shown. The scattering pattern of 40% w/w hydrated stratum corneum has been added to this plot, since at this hydration level the diffraction peaks are more pronounced. The scattering curve is characterized by a high intensity at $Q < 0.8$ nm^{-1} and a broad diffraction peak at $Q = 0.98$ nm^{-1}. The broad diffraction peak clearly exhibits a shoulder on the right-hand side, indicating that it actually consists of two partially unresolved peaks. At $Q = 1.85$ nm^{-1} a weak diffraction peak could be detected. The weak diffraction peak also exhibits a shoulder on the right-hand side.

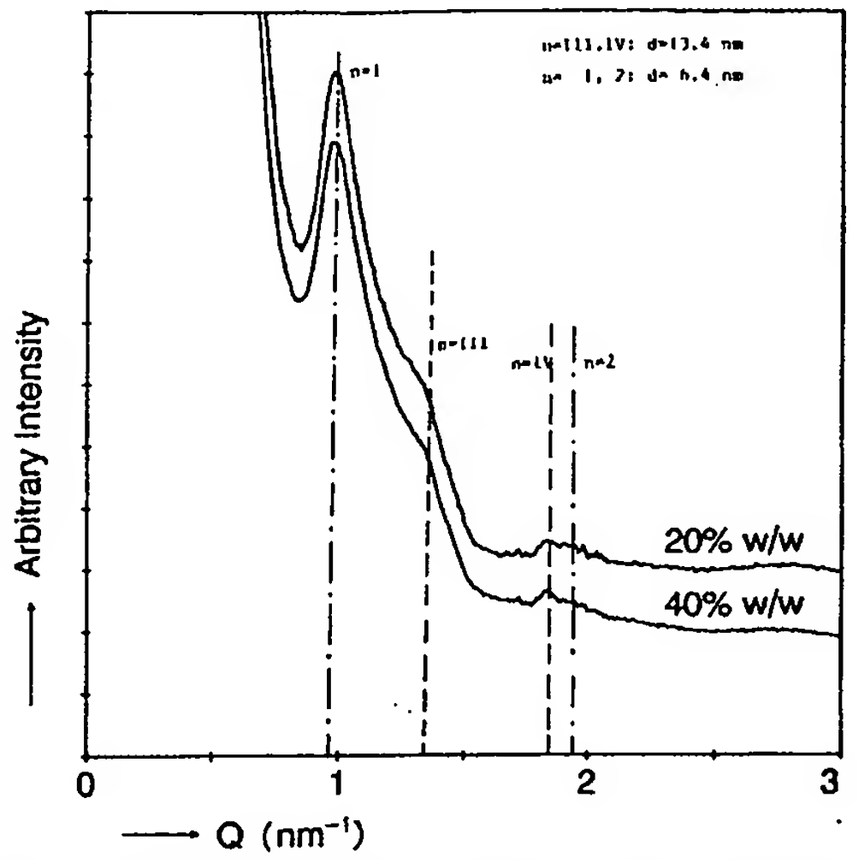

Fig. 2. The scattering curve of untreated stratum corneum hydrated to 20 or 40% w/w.

A lamellar phase results in a scattering curve with Bragg reflections located at equidistant positions in reciprocal space. The position of the n-th order diffraction peak is directly related to the repeat distance d (length of the unit cell) according to the following equation:

$$Q_n = 2n\pi/d$$

In recent studies (Bouwstra et al., 1991b), it has been shown that the presence of the two diffraction peaks can be explained by the existence of two lamellar arrangements with repeat distances of 6.4 and 13.4 nm, respectively. The main peak of the strong diffraction doublet and the shoulder of the weak diffraction peak originate from a unit cell with a repeat distance of 6.4 nm, while the shoulder of the strong diffraction doublet and the main position of the weak diffraction doublet correspond to a unit cell with a repeat distance of 13.4 nm. These conclusions were based on experiments considering recrystallization of the lipids in the stratum corneum which showed a lipid arrangement of only one unit cell with a repeat distance of 13.4 nm.

In Fig. 3a and b, the scattering curves of stratum corneum treated with PG or alkyl-azones in combination with PG are shown. After treatment with PG no significant changes were observed in the scattering curve, even the position of the main diffraction peak showing no shift, which implies that no swelling of the lamellae occurred. A similar behaviour was observed upon hydration (Bouwstra et al., 1991a,b). Changes in hydration level from 6 to 40% w/w did not change the main peak position of the strong diffraction doublet, which is quite remarkable. Treatment with hexyl-azone in combination with PG decreased the intensity of the strong diffraction doublet. The main peak as well as the shoulder decreased in intensity indicating that hexyl-azone interacts with the lipids in both unit cells. Treatment with octyl-azone and longer alkyl chain azones resulted in the almost complete disappearance of the main diffraction doublet. Only a shoulder was observed on the descending scattering curve. Alkyl-azones with 8 or more C atoms in the alkyl chain produced a much stronger disordering of the lamellae than did hexyl-azone. This diference in interaction observed using SAXS can be related with changes observed in the phase transitions after treatment with alkyl-azones (Bouwstra et al., 1991a).

In Fig. 4 the change in the thermal transitions of stratum corneum is shown after treatment with a whole series of alkyl-azones. The thermal behaviour of untreated human stratum corneum exhibits four transitions (Golden et al., 1987, 1988; Bouwstra et al., 1989). The first and second transition appeared at 37 and 70°C, respectively. Both peaks in the DTA curve were ascribed to reversible phase transitions of the lipids in the stratum corneum. The third transition (87°C) is probably due to lipids associated with proteins in the stratum corneum. This transition was only reversible in the cases where heating did not denature the proteins. The fourth irreversible transition located at 120°C is due to denaturation of the proteins in the stratum corneum. Treatment with PG resulted in a shift of the transition temperature of the two lipid transitions originally located at 70 and 87°C to lower temperatures, indicating that PG interacts with the intercellular lipids. No change in the total enthalpy involved in these two transitions was observed. In fact treat-

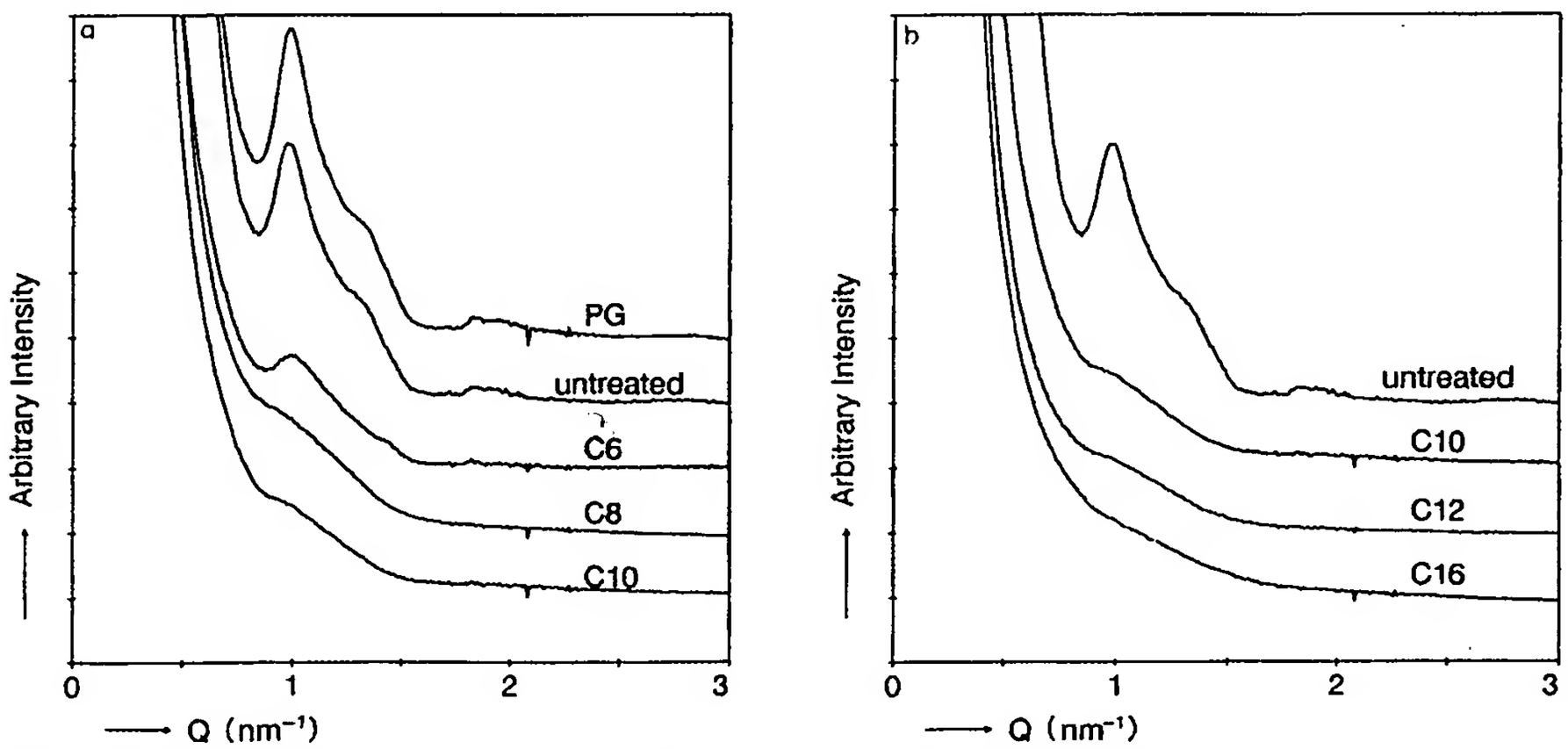

Fig. 3. (a) The scattering curve of human stratum corneum after treatment with hexyl-azone (C_6), oxtyl-azone (C_8) or decyl-azone (C_{10}) in combination with propylene glycol. (b) The scattering curve of human stratum corneum after treatment with decyl-azone (C_{10}), dodecyl-azone (C_{12}) or hexadecyl-azone (C_{16}) in combination with propylene glycol.

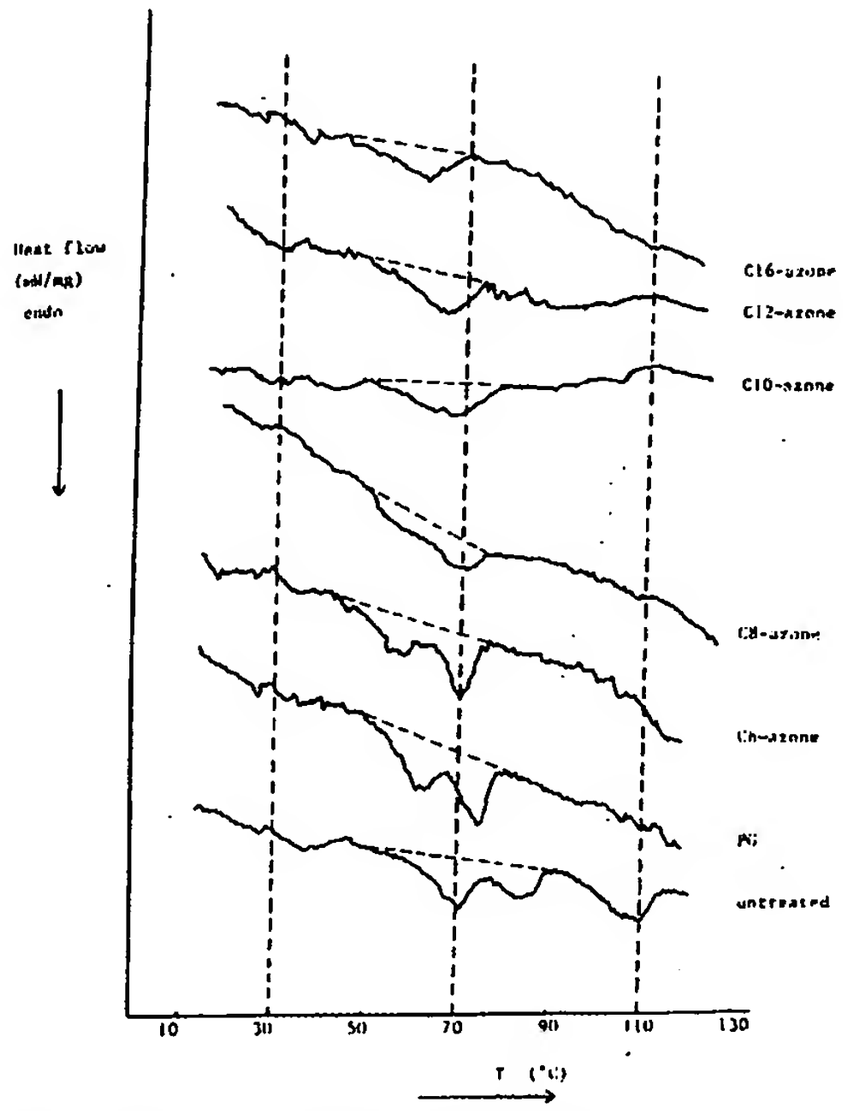

Fig. 4. The thermal behaviour of stratum corneum after treatment with a whole series of alkyl-azones in combination with PG.

ment with PG does not influence the scattering curve, but it does decrease the transition temperature of the lipids. The same behaviour has been found in increasing the hydration level of the stratum corneum. An increase in hydration level to 40% w/w did not result in a swelling of the bilayers, while a decrease in the transition temperatures of the intercellular lipids was observed. Using both techniques a sharpening of the peaks was observed after PG treatment or at increasing hydration level to 40% w/w.

After treatment with octyl-azone in combination with PG the two peaks in the DTA curve were not completely separated. The curve between the two transitions did not return to the baseline. The area under the peak, which is a measure for the enthalpy involved in the transition, decreased significantly (Bouwstra et al., 1989). Treatment with decyl-azone and longer alkyl-azones results in a single peak and in a further shift of the peak to lower temperatures. From the shape of the peak it is not clear whether both transitions still occur and whether the enthalpy involved in these transitions decreased or one of the two transitions disappeared. With respect to the transition originally located at 70°C the temperature of the resulting single peak after decyl-azone treatment was higher than the transition temperature after treatment with octyl-azone. Since an upward jump in temperature is not very likely, it is probable that the lipid transition originally located at 70°C has disappeared, while the lipid transition originally located at 87°C has shifted to lower temperatures. More evidence for the correctness of this hypothesis can be found in the SAXS curves that were obtained at higher temperatures. These scattering curves are shown in Fig. 5. The scattering curve measured at 60°C does not differ significantly from that recorded at 25°C, indicating that no detectable disordering of the lamellae occurred during the lipid transition at 40°C. It appears that this transition is due to a change from crystalline state bilayers to gel state bilayers. At 75°C the main diffraction peak and the weak diffraction peak completely disap-

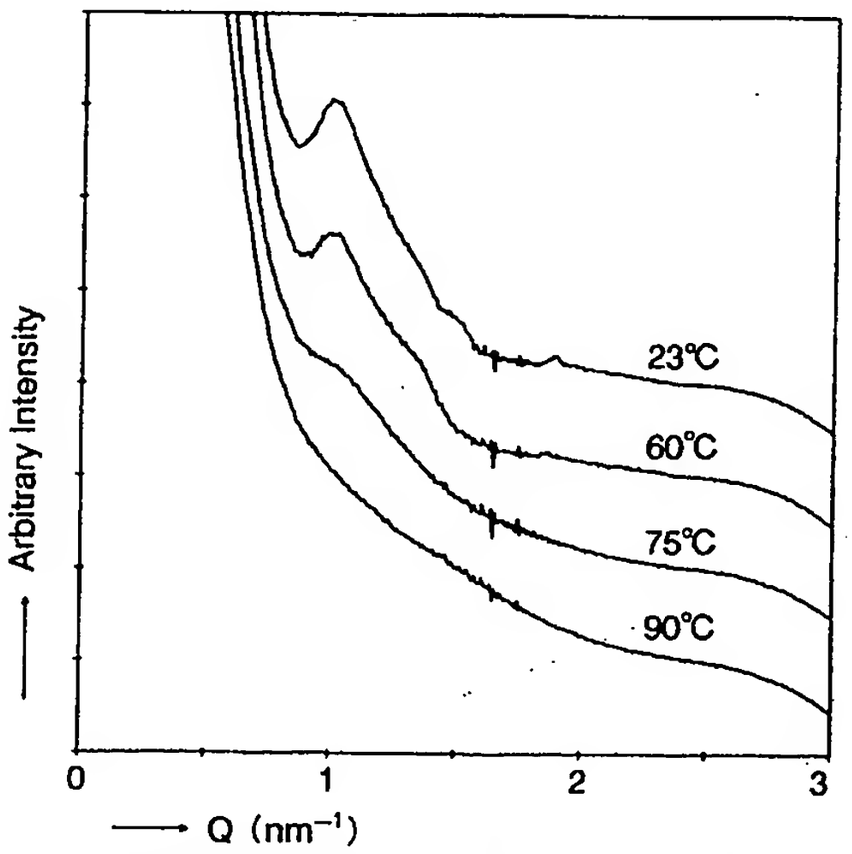

Fig. 5. Scattering curves after heating to various temperatures as indicated. At 75°C only a shoulder on the descending scattering curve is observed.

peared. Only a shoulder on the descending scattering curve remained at $Q = 1$ nm^{-1}. It appears that a phase change took place. Since no new diffraction peaks appeared the most likely explanation is a disordering of the lamellar structure. The origin of the shoulder on the descending curve still present at 75°C is not fully understood, but the thermal analysis results indicate that it is caused by lipids associated with proteins in the stratum corneum. This has been confirmed by SAXS, since after recrystallization of the lipids a reheating of the stratum corneum did not exhibit the shoulder on the scattering curve found in the first heating experiment at 75°C. It appears that the shoulder at the scattering curve is influenced by the denaturation of the protein and is therefore indeed due to the lipids associated with the proteins. The presence of only a residual shoulder on the scattering curve implies that the long-range order completely disappeared. In fact, the shoulder in the scattering curve could possibly be caused by the presence of one well-ordered lipid layer, which might be the corneocyte lipid envelope. At 90°C, which is just above the third thermal transition, the shoulder disappeared confirming the hypothesis that the shoulder is due to lipids linked to the proteins in the stratum corneum. If one now returns to Fig. 3a and b, a similar shoulder at the descending scattering curve is observed after treatment with alkyl-azones with more than six C atoms in their alkyl chain. This strongly indicates that the third thermal transition, which can be related to the shoulder in the descending scattering curve, is still present after treatment with longer alkyl chain azones while the second thermal transition disappeared, indicating that the remaining thermal transition is due to the lipids which are assumed to be associated with proteins. This also implies that the alkyl-azones in combination with PG only influence the lipids which are not associated with the proteins. Hoogstraate et al. (1991) showed that after treatment with dodecyl-azone in PG, a lamellar structure is still present in the intercellular spaces. This apparent discrepancy can be explained in two ways. The first explanation is that after treatment with dodecyl-azone, there are still lamellae present but the long-range order has completely disappeared. The second is based on the difference in treatment. For visualization, the stratum corneum was treated on the apical side, while in the experiments described in this paper the treatment was carried out by soaking the stratum corneum in the alkyl-azone/PG solution. Very recent results obtained using the wide-angle X-ray diffraction (WAXD) technique showed that the two reflections corresponding to distances of 0.415 and 0.378 nm are still present after treatment with dodecyl-azone in PG, although the intensity of the reflections might be decreased. The treatment was carried out by soaking stratum corneum in the solution for 12 h. The two reflections are based on an orthorhombic and/or hexagonal lateral packing of the hydrocarbons in the bilayers. These findings confirm the existence of bilayers after treatment with alkyl-azones in PG.

In a series of experiments the stratum corneum was heated to 90°C, and cooled down to room temperature to recrystallize the lipids. After recrystallization the stratum corneum was pretreated with alkyl-azones in PG. The results are shown in Fig. 6. Bouwstra et al. (1991b) showed

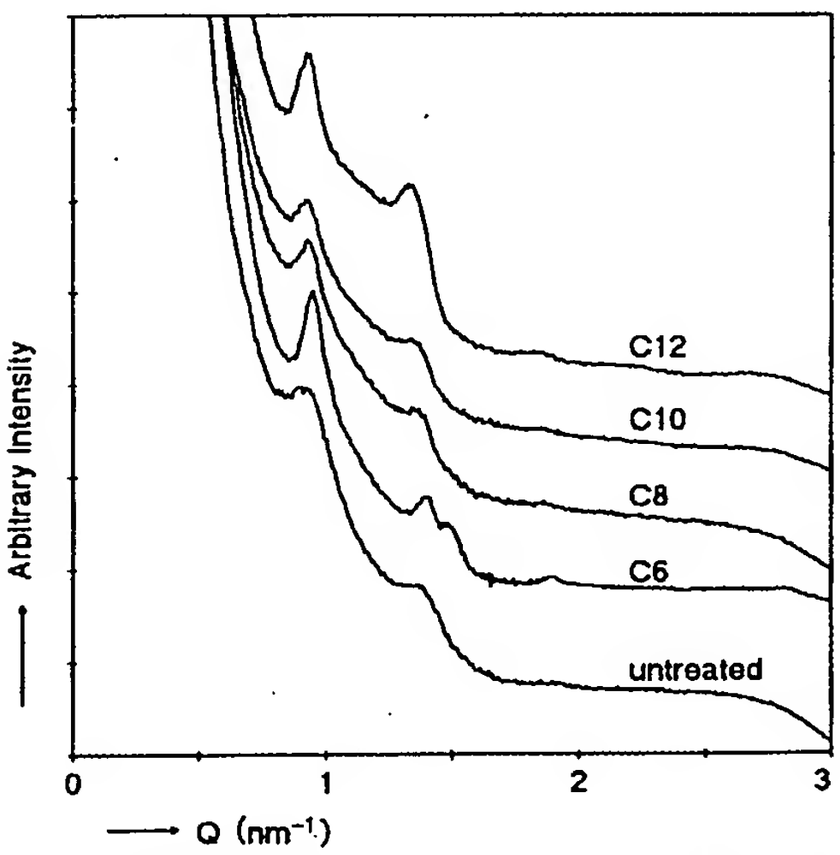

Fig. 6. Scattering curves of human stratum corneum after recrystallization of the lipids and treatment with hexyl-, octyl-, decyl- and dodecyl-azone.

second is
or visual-
d on the
cribed in
by soak-
zone/PG
using the
echnique
onding to
l present
PG, al-
might be
l out by
for 12 h.
thorhom-
f the hy-
ings con-
nent with

corneum
to room
After re-
was pre-
sults are
) showed

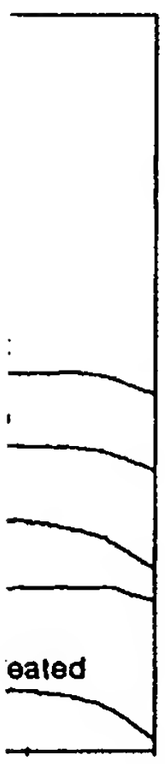

neum after
exyl-, octyl-,

that recrystallization of the lipids revealed one lamellar structure with a repeat distance of 13.4 nm. The diffraction peaks of untreated stratum corneum are broader than found previously (Bouwstra et al., 1991b), indicating that the long-range order of the lipid lamellae is less pronounced. After pretreatment with azones it appeared that no significant disordering occurred, which is quite remarkable. It seems that the interaction between alkyl-azones and the lipid bilayers changed after recrystallization of the lipids, but the origin of the change in interactions is not yet known. A similar change in interaction between pig stratum corneum and detergent after heating was also observed by Wertz et al. (1989). They suggested that it might be caused by a change in the interactions between the protein bound lipid envelopes of different cells. A possibility is the forming of more compact bilayers or larger lipid regions which makes it more difficult for alkyl-azones to intercalate. More experiments must be carried out in order to elucidate this phenomenon.

Conclusions

The influence of alkyl-azones on the long-range ordering of the lamellae in human stratum corneum depends on the length of the alkyl chain. Azones with a hydrocarbon chain length of more than six carbon atoms induce a disordering in the lipid structure of human stratum corneum, whereas after treatment with hexyl-azone no large differences in the structure could be detected. A similar jump in behaviour has also been observed in other studies. From in vitro toxicity studies, it could be concluded that hexyl-azone was less toxic than alkyl-azones (Ponec et al., 1989) with 8 or more C atoms in their hydrocarbon tail. A study in which the the penetration enhancement of alkyl-azones (Hoogstraate et al., 1991) was investigated revealed a significant effect of enhanced penetration of DGAVP after pretreatment of human stratum corneum with decyl-, dodecyl- and tetradecyl-azone, while hexyl- and octyl-azone had only a minor influence on the transport of DGAVP.

The exact mechanism behind the observed difference in behaviour of the alkyl-azones is not yet known, but it appears that it is not caused by a difference in intercalation in the stratum corneum bilayers, since recent experiments using skin lipid liposomes strongly indicate that hexyl-azone (Bouwstra and Salomons-de Vries, unpublished results) is also intercalated in bilayer regions in liposomes. It seems that the way in which the alkyl-azones are intercalated and the resulting distortion also play important roles.

References

Beastall, J.C., Hadgraft, J. and Washington, C., Mechanism of action of Azone as a percutaneous penetration enhancer: lipid bilayer fluidity and transition temperature effects. *Int. J. Pharm.*, 43 (1988) 207–213.

Boddé, H.E., Kruithof, M.A.M., Brussee, J. and Koerten, H.K., Visualisation of normal and enhanced $HgCl_2$ transport through human skin in vitro. *Int. J. Pharm.*, 53 (1989) 13–24.

Bouwstra, J.A., Peschier, L.J.C., Brussee, J. and Boddé, H.E., Effect of *N*-alkylazocycloheptane-2-ones including azone on the thermal behaviour of human stratum corneum. *Int. J. Pharm.*, 52 (1989) 47–54.

Bouwstra, J.A., de Vries, M.A., Gooris, G.S., Bras, W., Brussee, J. and Ponec, M., Thermodynamic and Structural aspects of the skin barrier. *J. Contr. Rel.*, 15 (1991a) 209–220.

Bouwstra, J.A., Gooris, G.S., Van der Spek, J.A. and Bras, W. The structure of human stratum corneum determined with small angle X-ray scattering. *J. Invest. Dermatol.* (1991b) in press.

Elias, P.M. and Friend, D.S., *J. Cell. Biol.*, 65 (1975) 186–191.

Friberg, S.E. and Osborne, D.W., Small-angle X-ray diffraction patterns of stratum corneum and model structure for its lipids. *J. Disp. Sci. Technol.*, 6 (1985) 485–495.

Garson, J.-C., Doucet, J., Leveque, J.-L. and Tsoucaris, G., Oriented structure in human stratum corneum revealed by X-Ray diffraction. *J. Invest. Dermatol.*, 96 (1991) 43–49.

Golden, G.M., McKie, J.E. and Potts, R.O., Stratum corneum lipid phase transitions and water barrier properties. *Biochemistry*, 26 (1987) 2382–2388.

Golden, G.M., McKie, J.E. and Potts, R.O., The role of stratum corneum lipid fluidity in transdermal drug flux. *J. Pharm. Sci.*, 76 (1988) 25–28.

Goodman, M. and Barry, B.W., Differential scanning calorimetry of human stratum corneum: Effect of penetration enhancers azone and dimethyl sulphoxide. *Anal. Proc.*, 23 (1986) 397–398.

Hoogstraate, A.J., Verhoef, J., Brussee, J., IJzerman, A.P. and Spies, F., In vitro transport of 9-desglycinamide, 8-arginine vasopressin (DGAVP) through human stratum

corneum: Kinetics, ultrastructural aspects and molecular modelling of transdermal peptide flux enhancement by *N*-alkylazacycloheptanones. *Int. J. Pharm.*, 76 (1991) 37–47.

Mak, V.H.W., Potts, R.O. and Guy, R.H., Does hydration affect intercellular lipid organization in the stratum corneum? *Pharm. Res.*, 8 (1991) 1064–1065.

Ponec, M., Weerheim, A., Kempenaar, J., Mommaas, A.-M. and Nugteren, D.H., Lipid composition of cultured human keratinocytes in relation to their differentiation. *J. Lipid Res.*, 29 (1988) 949–962.

Ponec, M., Haverkort, M., Soei, Y.L., Kempenaar, J., Brussee, J. and Boddé, H., Toxicity screening of *N*-alkylazacycloheptan-2-one derivatives in cultured human skin cells: Structure-toxicity relationships. *J. Pharm. Sci.*, 78 (1989) 738–741.

Wertz, P.W., Swartzendruber, D.C., Kitko, D.J. and Madison, K.C., The role of corneocyte lipid envelopes in cohesion of stratum corneum. *J. Invest. Dermatol.*, 93 (1989) 169–172.

White, S.H., Mirejovsky, D. and King, G.I., Structure of lamellar lipid domains and corneocytes envelopes of murine stratum corneum. An X-ray diffraction study. *Biochemistry*, 27 (1988) 3725–3732.

Role of Stratum Corneum Lipid Fluidity in Transdermal Drug Flux

GUIA M. GOLDEN, JAMES E. MCKIE, AND RUSSELL O. POTTS[x]

Received August 23, 1985, from *Pfizer Central Research, Groton, CT 06340.* Accepted for publication November 12, 1986.

Abstract □ Fatty acids are effective penetration enhancers for the transdermal delivery of certain co-applied drugs. In order to assess the mechanism of enhancement, spectrometric, calorimetric, and flux techniques were used to study porcine stratum corneum following treatment with a series of cis- and trans-positional isomers of octadecenoic acid. Results obtained from spectrometric and calorimetric measurements show increased lipid fluidity following treatment of the stratum corneum with the cis monoenoic acids which have the site of unsaturation centrally located. Under similar conditions, these same cis monounsaturated acids resulted in enhancement of salicyclic acid flux through porcine skin. The striking parallelism between flux and fluidity measurements suggests that transdermal drug flux may be ultimately related to stratum corneum lipid structure.

The primary barrier to transdermal diffusion is the stratum corneum, the thin outermost layer of the skin which is comprised of a regular array of protein-rich cells that are embedded in a multilamellar lipid domain. Using differential scanning calorimetry (DSC) and infrared (IR) spectrometry, we have previously shown that increasing the temperature of the stratum corneum results in increased fluidity of the intercellular lipids.[1] Furthermore, hydration- and temperature-induced changes in stratum corneum permeability parallel changes in lipid fluidity, suggesting a correlation between transdermal flux and stratum corneum lipid disorder.[2]

Long-chain fatty acids have been shown to be effective penetrant enhancers in vitro for a variety of co-applied drugs.[3-6] In this study we have systematically investigated the effects of treatment with a series of fatty acid isomers of 18-carbon length on the permeability and lipid fluidity of porcine stratum corneum.

Experimental Section

Stratum corneum sheets were prepared from porcine skin by trypsin treatment. In particular, full-thickness skin samples were dermatomed to a thickness of 350 μm and then spread, stratum corneum side up, on filter paper saturated with 0.5% crude trypsin (Type II-Sigma) in phosphate buffered saline at pH 7.4. After several hours of incubation at 37 °C, the stratum corneum was peeled away from underlying layers. This sample was washed in soybean trypsin inhibitor and then several changes of distilled water and spread on wire mesh to dry. Samples were stored desiccated at room temperature until used.

Prior to differential scanning calorimetry (DSC) and IR experiments, dry samples of known mass were incubated for 2 h in a 0.15-M solution of the appropriate fatty acid in ethanol. At the end of the incubation, the samples were washed for 10 s in ethanol, spread on wire mesh, dried for several hours over a desiccant, and reweighed. All samples were then placed for several days in a chamber maintained at 95% relative humidity and 22 °C. Stratum corneum samples equilibrated to a water content of ~30% (w/w) under these conditions.

Infrared Spectroscopic Measurements—Infrared spectra were obtained using a fourier transform IR (FTIR) spectrometer (Analect model FX-6200; Laser Precision Corp., Irvine, CA) equipped with a liquid nitrogen cooled mercury-cadmium-telluride detector. Due to digital signal processing, a sensitive detection system, high throughput, and simultaneous interaction with the sample at all infrared energies, the FTIR system enables rapid acquisition and analysis of IR spectra.

In order to prevent water loss during the experiment, hydrated samples were sealed between zinc sulfide windows while maintained at 95% relative humidity and 22 °C. Sealed samples were then placed in the spectrometer where multiple spectra of duplicate samples were obtained for each fatty acid treatment. All spectra presented here represent an average of 127 scans obtained in ~6 min. The digitized data were transferred to an Apple IIe computer where peak frequency and band width of the C–H antisymmetric stretching absorbance were determined. Due to the digital nature of the FTIR instrument, absorbance and frequency data exist only in discrete increments. With the instrument used in these experiments, the exact value of any frequency point could not be determined from raw data with a precision greater than ~2.7 cm^{-1}. The peak frequency was estimated with much greater precision, however, using a center of gravity algorithm for digitized data.[7]

Differential Scanning Calorimetry Measurements—A Microcal model MC-1 differential scanning calorimeter (Microcal Inc., Amherst, MA) was used at a scan rate of 0.75 °C/min. Duplicate samples from each IR experiment were combined for the differential scanning calorimetry (DSC) measurement. Alternately, stratum corneum samples of known mass (~20 mg) were treated with each fatty acid in an identical manner to that described above. Treated samples were hydrated for several days at 95% relative humidity and 22 °C, and reweighed. Results show an approximate 30% (w/w) water uptake regardless of fatty acid treatment.

Flux Measurements—Sheets of freshly excised porcine skin cut to 350-μm thickness were mounted between two halves of a diffusion cell with the stratum corneum side toward the donor compartment. The donor side contained 1.0 mL of a saturated solution of salicylic acid in ethanol (0.31 g/mL) plus ~100 000 dpm/mL [^{14}C]salicylic acid. The appropriate fatty acid was then added to this solution to yield a final concentration of 0.15 M. The receiver side contained 1.0 mL of phosphate buffered saline at pH 7.4. Both sides were stirred with a magnetic stirrer and maintained at 32 °C.

Samples were removed periodically from the receiver side of the diffusion cell, mixed with a scintillation cocktail (Scintisol; Isolabs, Inc., Akron, OH), and counted for several minutes in a liquid scintillation counter (model Mark III-6881; Tracor Analytical, Elk Grove Village, IL). Following an initial lag time of ~6 h, the amount of salicylic acid appearing in the receiver side was linear with time for the duration of the experiment (routinely 24–48 h). From a linear least squares regression analysis of these data, the rate of appearance of salicylic acid in the receiver (dpm/h) was determined. This value, when divided by the specific activity of salicylic acid in the saturated solution (~300 dpm/mg) and the area of exposed skin (0.2 cm^2), yielded the flux (mg/cm^2/h). Samples removed from the donor side at the beginning and end of the experiment contained, within error, the same amount of salicylic acid. Thus, constant concentration of the permeant was maintained on the donor side throughout the experiment.

Results and Discussion

The results presented in Fig. 1 compare the IR spectrum in the C–H stretching region for an untreated sample (lower trace) to the spectrum of a sample treated with 0.15 M *cis*-11-octadecenoic acid (upper trace), both hydrated to 30% (w/w) water content. Compared with the control, treatment of the stratum corneum with *cis*-11-octadecenoic acid results in a

0022-3549/87/0100-0025$01.00/0

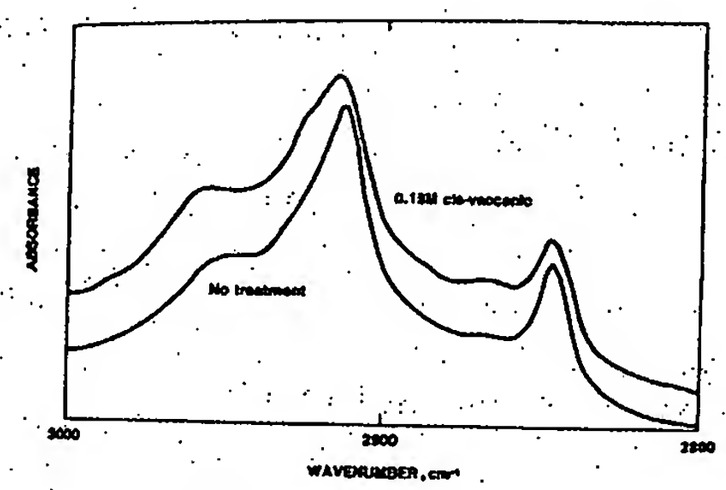

Figure 1—*The IR spectra of porcine stratum corneum in the C–H stretching region. The upper trace is the spectrum obtained following treatment of the sample with 0.15 M cis-11-octadecenoic acid in ethanol, while the lower trace is the spectrum of an untreated sample. Both spectra were obtained at 25 °C with samples hydrated to 30% (w/w) water content.*

Table I—Summary of Spectral, Thermal, and Flux Changes Following Treatment of Porcine Stratum Corneum with Fatty Acids of 18 Carbon Length

Treatment	IR Frequency,[a] cm^{-1}	DSC T_m,[b] °C	Flux of Salicylic Acid, $mg \cdot cm^{-2} \cdot h^{-1}$
Octadecanoic acid	2918.1 ± 0.4	62.5 ± 1.0	1.21
cis-6-Octadecenoic acid	2919.0 ± 0.4	60.5 ± 0.9	0.79
trans-6-Octadecenoic acid	2919.0 ± 0.3	62.0 ± 0.9	0.97
cis-9-Octadecenoic acid	2920.0 ± 0.5	59.0 ± 1.5	3.81
trans-9-Octadecenoic acid	2919.4 ± 0.4	61.5 ± 0.9	2.35
cis-11-Octadecenoic acid	2920.1 ± 0.4	57.0 ± 1.1	5.53
trans-11-Octadecenoic acid	2918.8 ± 0.5	61.0 ± 1.0	1.11
Ethanol	2918.8 ± 0.4	62.0 ± 1.0	1.31
No treatment	2918.8 ± 0.4	62.0 ± 1.0	—

[a] Value represents the average ± SEM of three samples. [b] Differential scanning calorimetry (DSC) determination of the temperature of the transitions maximum (T_m); values represent the average ± SEM of three samples.

shift to higher frequency and absorbance broadening for the C–H antisymmetric stretch peak near 2920 cm^{-1}. Frequency changes following treatment of the stratum corneum with stearic acid and isomers of octadecenoic acid are summarized in Table I. These data show that treatment with either *cis*-9- or *cis*-11-octadecenoic acid results in a significant frequency increase compared with ethanol and untreated controls, while the corresponding trans acids show relatively little effect. Similar results were obtained for band width measurements (data not shown), with only *cis*-9- and *cis*-11-octadecenoic acid treatments resulting in band width increases relative to controls.

The largest frequency changes associated with fatty acid treatment are less than the digital resolution of the instrument (2.7 cm^{-1}). Nevertheless, as shown by Cameron et al.[7] the center-of-gravity technique of peak frequency determination allows sufficient precision to easily estimate differences of <1.0 cm^{-1} from digitized data. Furthermore, as shown in Table I, several conditions were repeated in triplicate, each yielding a standard error of the mean (SEM) of <0.5 cm^{-1}. Thus, while small in magnitude, the frequency changes seen following treatment of the stratum corneum with *cis*-9- and *cis*-11-octadecenoic acid are real.

We have previously shown that temperature-induced increases in band width and frequency of the C–H antisymmetric stretching peak are due to transitions in stratum corneum lipids involving enhanced motional freedom of the hydrocarbon chains (i.e., increased lipid fluidity).[1,2] Briefly, those results showed that the stratum corneum IR spectrum exhibited sharp increases in band width and frequency of the C–H antisymmetric stretching absorbance with increasing temperature, identical to thermally induced changes seen in a variety of synthetic and biological membranes undergoing thermotropic lipid transitions. The results presented here show that treatment with fatty acids can also cause an increase in frequency and band width (data not shown), and thus, an increase in stratum corneum lipid fluidity. The greatest increase in fluidity results from treatment with monounsaturated compounds, with cis isomers resulting in greater changes than corresponding trans fatty acids.

Samples of stratum corneum were also analyzed by the DSC technique. The results shown in Fig. 2 compare the thermal profile of porcine stratum corneum treated with 0.15 M *cis*-11-octadecenoic acid in ethanol (upper trace) with that of an untreated sample (lower trace); again, both hydrated to 30% (w/w) water. The results show decreases in both the temperature of the transitions maximum (T_m) and sharpness (ratio of peak height to width) of transitions near 65 and 75 °C for the treated sample. In contrast, fatty acid treatment results in little if any change in the high temperature peak. Changes in T_m of the peak near 65 °C following treatment of the stratum corneum with the same series of fatty acids as used in the IR experiments are summarized in Table I. Several interesting trends emerge from these data.

1. Treatment with the saturated octadecanoic acid results in no change in T_m relative to the untreated and ethanol-treated controls.
2. Introduction of a trans olefinic bond has little or no effect on T_m relative to controls, regardless of the position of the double bond along the chain.
3. Introduction of a cis olefinic bond both decreases the T_m and broadens the transition (data not shown) relative to controls. Furthermore, for the series of fatty acids studied here, both the decrease in T_m and the transition broadening increase with the distance of the olefinic bond from the carboxyl end of the molecule. Similar results were obtained for the transition occurring near 75 °C (data not shown). In contrast, however, no systematic change was observed for the highest temperature peak, regardless of treatment (data not shown).

We have previously proposed that for both human and porcine stratum corneum,[1,2] the DSC peaks near 65, 75, and 105 °C are due to thermal transitions involving intercellular lipids, lipid–protein complexes, and intracellular keratin,

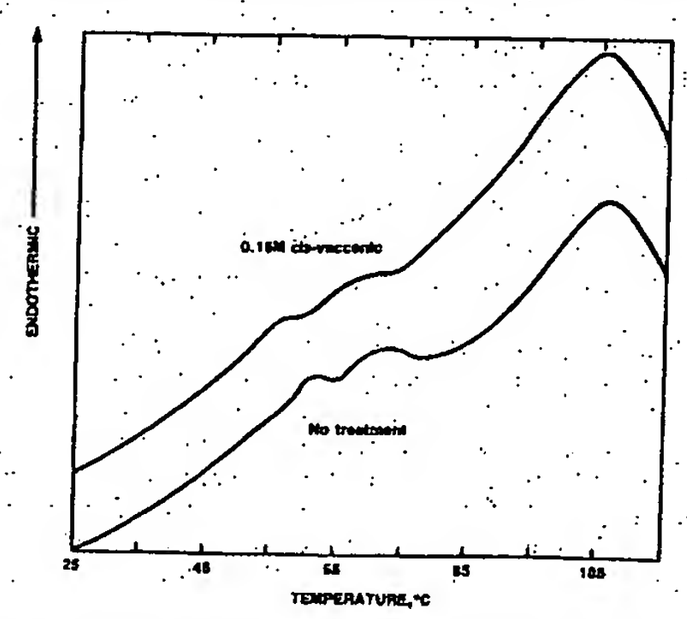

Figure 2—*The differential scanning calorimetry (DSC) thermal profile obtained for porcine stratum corneum hydrated to 30% (w/w) water content. The upper trace is the thermal profile of a sample treated with 0.15 M cis-11-octadecenoic acid, while the lower trace is the profile for the untreated control.*

respectively. The lipid transitions involve decreased packing order relative to the initial state. Furthermore, a decrease in T_m and sharpness reflects a thermal transition starting from a less ordered, more heterogeneous state. In other words, the thermal profile changes seen following treatment with several cis monounsaturated acids suggests that incorporation of these compounds into stratum corneum results in decreased lipid order.

A comparison of the IR and DSC results listed in Table I shows a high degree of correlation between these variables ($r = 0.86$; $p > 0.99$). Thus, spectral and thermal profile changes are each measures of a common physical property of the stratum corneum. In particular, these techniques provide a measure of the fluidity of stratum corneum lipids.

The combined IR and DSC results suggest that certain exogenously applied fatty acids can disrupt stratum corneum lipid structure. It is not clear from these results, however, whether differences seen among the various acids are due to their relative disrupting power or simply reflect varied uptake of these compounds by the stratum corneum. In order to distinguish between these two mechanisms the mass and IR absorbance at 2850 cm^{-1} (C–H symmetric stretching peak) were measured before and after fatty acid treatment. In a positive control experiment, stratum corneum samples were treated with varying concentrations of *cis*-9-octadecenoic and other fatty acids. Results show that both the mass and absorbance (2850 cm^{-1}) of the treated sample increased with increasing fatty acid concentration. In contrast, for all samples treated with 0.15 M fatty acids, both absorbance and mass values remained constant, within error, and greater than the corresponding values obtained with ethanol treatment alone. Thus, these results suggest that differences in fluidity following treatment of the stratum corneum are primarily due to the ability of each acid to disrupt lipid structural domains in this tissue. Since stratum corneum lipids contain a large amount of free and esterified long chain fatty acids,[8] it is not surprising that the fatty acids containing 18 carbon atoms length should partition into this domain.

Similar fluidizing effects have been observed for erythrocyte,[9,10] synaptic,[11] liver,[12] and adipocyte[13] plasma membranes following incubation in ethanol solutions of *cis*-11-octadecenoic acid. For example, results of electron paramagnetic resonance show that while treatment with 1 mM *cis*-octadecenoic acid caused an increase in membrane fluidity of synaptic plasma membranes, the corresponding trans isomer and octadecenoic acid had no effect.[11] In the most comprehensive study,[3] the activity of adenylate cyclase, a membrane-bound enzyme, was measured in erythrocytes following treatment with a series of fatty acids including those tested here. Results showed that enzyme activity increased following treatment with cis monounsaturated acids, but was unaffected by treatment with the corresponding trans isomers or octadecanoic acid. Furthermore, the order of enzyme activation for the cis acids was *cis*-11- ≥ *cis*-9- >> *cis*-6-octadecenoic. Since adenylate cyclase activity increases with decreasing membrane microviscosity, the results show the differential fluidizing effect of these fatty acids.

As reviewed by Small,[14] saturated and cis monounsaturated fatty acids have very different lipid packing properties due to a "kink" in the cis alkenyl chain. In contrast, cis polyunsaturated acids, like *cis*-9,12-octadecadienoic and *cis*-9,12,15-octadecatrienoic, have packing properties similar to those of saturated octadecanoic acid. In agreement with this observation, DSC and IR results (data not shown) show that the membrane fluidizing properties of *cis*-9,12-octadecedinoic and *cis*-9,12,15-octadecetrinoic acids are similar to those of octadecanoic acid. Similarly, octadecanoic and *cis*-9,12-octadecedinoic acids had little fluidizing effect on erythrocyte plasma membranes, in contrast to *cis*-9- and *cis*-11-octadecenoic acids.[9] These results suggest that the incorporation of a cis monounsaturated acid into the primarily saturated-like domain of stratum corneum lipids causes increased fluidity due to differences in lipid packing.

The flux of salicylic acid through porcine stratum corneum was measured from saturated ethanol solutions in the presence of each fatty acid. The results summarized in Table I show that significant enhancement of salicylic acid flux is only achieved with *cis*-9- and *cis*-11-octadecenoic acid. In addition, with the exception of *cis*-6- and *trans*-6-octadecenoic acids, which show no enhancement relative to the ethanol-treated control, greater flux is achieved with the cis versus the corresponding trans isomer. Finally, the flux of salicylic acid increases with increasing distance of the cis olefinic bond from the carboxyl end of the co-applied fatty acid. Cooper and co-workers noted a similar increase in salicylic acid flux with *cis*-9- and *cis*-11-octadecenoic acids under conditions very similar to ours.[3,4] Their results also showed greater enhancement with *cis*-11-octadecenoic than *cis*-9-octadecenoic acid. Similarly, *cis*-9-octadecenoic acid has been shown to be an effective penetration enhancer for flurbiprofen[5] and betamethasone 17-benzoate.[6]

A comparison of the results shown in Table I shows a strong correlation between IR and DSC measurements of lipid order and the flux of salicylic acid under similar experimental conditions. Figs. 3a and 3b show plots of frequency or T_m versus flux, respectively, with the straight line in each plot representing the best linear fit to the data. The correlation coefficient obtained for the linear fit of frequency ($r = 0.87$) or T_m ($r = 0.89$) versus flux are both statistically significant ($p > 0.99$). Thus, these results suggest that the transdermal flux of salicylic acid is ultimately related to packing in the intercellular lipid domains of the stratum corneum. The same hypothesis has been used to explain hydration-induced increases in flux.[2] In addition, a

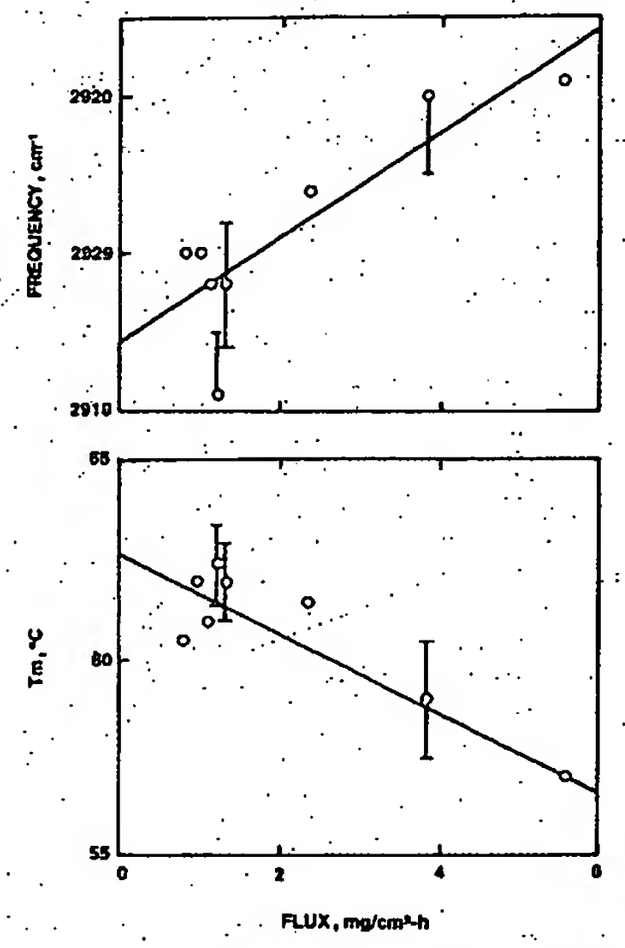

Figure 3—(A) *The data of Table I plotted as the frequency of the C–H antisymmetric stretching peak of stratum corneum versus the transdermal flux of salicylic acid through porcine skin. The straight line represents the best linear fit to the data.* (B) *The data of Table I plotted as the temperature of the transitions maximum (T_m) for the stratum corneum thermal transition near 65 °C versus transdermal flux of salicylic acid. The straight line represents the best linear fit to the data.*

similar correlation between water permeability and lipid order has been noted for a variety of phospholipid vesicles.[15]

While the ability of cis mononunsaturated acids to disrupt stratum corneum lipid structure and enhance transdermal flux can be explained by their "kinked" nature, this hypothesis does not explain increased fluidity and flux with increasing distance of the olefinic bond from the carboxyl group. Insight into this positional variation can be derived from the results of a systematic investigation of the effect of cis-positional isomers of octadecenoic acid on the fluidity of synthetic and biological phospholipid membranes.[16] These results showed that maximum fluidity was achieved for membranes containing fatty acids with the cis olefinic bond in the center of the alkenyl chain. Since lipid packing is very similar between phospholipids and the corresponding fatty acids, it is reasonable to expect that maximum disruption of stratum corneum barrier lipids may similarly result from incorporation of monounsaturated acids with olefinic bonds near the center of the lipid bilayer.

Conclusions

While the use of fatty acids as penetration enhancers has been previously reported, the present investigation is the first to support a molecular mechanism by which these agents might act. In particular, due to the large concentration of free and esterified fatty acids in stratum corneum lipids, exogenous acids of similar length are likely to partition into this barrier domain. Once incorporated, cis octadecenoic acids with the olefinic bond near the center of the alkenyl chain will disrupt stratum corneum lipid packing and, hence, decrease diffusional resistance to permeants. These results suggest that penetrant enhancers should have properties similar enough to stratum corneum lipids to allow significant partitioning into this domain, yet dissimilar enough to maximally disrupt lipid packing.

References and Notes

1. Golden, G. M.; Guzek, D. B.; Harris, R. R.; McKie, J. M.; Potts, R. O. *J. Invest. Dermatol.* 1986, *86*, 255–259.
2. Knutson, K.; Potts, R. O.; Guzek, D. B.; Golden, G. M.; Lambert, W. J.; McKie, J. M.; Higuchi W. I. *J. Controlled Release* 1985, *2*, 67–87.
3. Cooper, E. R. *J. Pharm. Sci.* 1984, *73*, 1153–1156.
4. Wickett, R. R.; Cooper, E. R.; Loomans, M. E. *European Patent* 81303128.3, 1981.
5. Akhter, S. A.; Barry, B. W. *J. Pharm. Pharmacol., Dec. Suppl.*, 1984, *36*, 7P.
6. Bennett, S. L.; Barry, B. W. *J. Pharm. Pharmacol., Dec. Suppl.*, 1984, *36*, 8P.
7. Cameron, D. G.; Kauppinen, J. K.; Moffatt, D. J.; Mantsch, H. H. *Appl. Spectrosc.* 1982, *36*, 245–250.
8. Lampe, M. A.; Williams, M. L.; Elias, P. M. *J. Lipid Res.* 1983, *24*, 131–140.
9. Orly, J.; Schramm, M. *Proc. Nat. Acad. Sci. U.S.A.* 1975, *72*, 3433–3437.
10. Yamamoto, H-A; Harris, R. A. *Biochem. Pharm.* 1983, *32*, 2787–2791.
11. Michaels, M. L.; Michaels, E. K.; Tehan, T. *Pharm. Biochem. Behav. Suppl. 1*, 1983, *18*, 19–23.
12. Riordan, J. R. *Can. J. Biochem.* 1980, *58*, 928–934.
13. Pilch, P. F.; Thompson, P. A.; Czech, M. P. *Proc. Nat. Acad. Sci. U.S.A.* 1980, *77*, 915–918.
14. Small, D. M. *J. Lipid Res.* 1984, *25*, 1490–1500.
15. Fettiplace, R.; Haydon, D. A. *Physiol. Rev.* 1980, *60*, 510–550.
16. Macdonald, P. M.; Sykes, B. D.; McElhaney, R. N.; Gunstone, F. D. *Biochemistry* 1985, *24*, 177–184.

International Journal of Pharmaceutics, 33 (1986) 225–234
Elsevier

IJP 01123

Enhancement of naloxone penetration through human skin in vitro using fatty acids, fatty alcohols, surfactants, sulfoxides and amides

Bruce J. Aungst, Nancy J. Rogers and Eli Shefter

E.I. du Pont de Nemours and Co., Biomedical Products Department, Wilmington, DE 19898, U.S.A.

(Received 25 April 1986)
(Accepted 11 June 1986)

Key words: Percutaneous absorption – Penetration enhancer – Naloxone – Transdermal opioid – Surfactant – Sulfoxide – Amide – Fatty acid

Summary

Human skin permeation of naloxone was examined in vitro using various vehicles and penetration enhancers. To screen various chemicals as penetration enhancers propylene glycol containing 10% adjuvant was used. Fatty acids and fatty alcohols were very effective promoters of naloxone flux. In both the acid and alcohol series, maximum flux was with C_{12} adjuvants, and for C_{18} acids and alcohols unsaturated adjuvants were more effective than saturated ones. Other effective skin penetration enhancers included some non-ionic and cationic surfactants, decylmethylsulfoxide, Azone, and N-alkylpyrrolidones. Lauric acid and lauryl alcohol in isopropanol, polyethylene glycol 400, and mineral oil vehicles were not as effective in promoting naloxone skin penetration as when dissolved in propylene glycol. Sodium lauryl sulfate in propylene glycol slightly increased flux, but a much greater effect was observed using a mineral oil vehicle. Concentration/enhancement profiles were determined for lauric acid and lauryl alcohol. Skin penetration enhancing effects are, to some extent, specific and dependent on the drug, vehicle, enhancer concentration and probably other factors. Possible mechanisms of altering skin permeability are discussed.

Introduction

The major advantages that transdermal drug delivery can offer are: (1) avoidance of first-pass metabolism often associated with oral dosing; and (2) sustained and more constant plasma concentrations of the drug. The 3-hydroxymorphinan and hydroxybenzomorphan opioid analgesics and antagonists as a class have poor oral bioavailability, due to a high first-pass metabolism effect. These drugs also generally have short elimination half-lives and 4–5 h durations of action. Because of these problems, they are logical candidates for transdermal delivery.

Naloxone-HCl (Narcan, DuPont Pharmaceuticals) is a potent opioid antagonist. It is presently available in 0.4 mg unit doses for injection, and is used for reversal of narcosis. The terminal half-life of naloxone after i.v. injection in normal volunteers was reported to be 64 min (Ngai et al., 1976) and 151 min (Aitkenhead et al., 1984) in two separate studies. Because of this short half-life, it has been suggested that infusion may be preferred in some cases of narcosis (Bradberry and Raebel,

Correspondence: B.J. Aungst. E.I. du Pont de Nemours & Co., Biomedical Products Department, Experimental Station, Bldg, 400, Wilmington, DE 19898, U.S.A.

1981; Gourlay and Coulthard, 1983). In addition, recently naloxone has been shown to have other potential applications. Naloxone has shown beneficial effects in treatment of cardiovascular shock (McNicholas and Martin, 1984), chronic idiopathic constipation (Kreek et al., 1983), senile dementia of the Alzheimer's type (Reisberg et al., 1983a and b), and for appetite suppression (Atkinson, 1982). A regimen of frequent injections would not be acceptable for these uses, and transdermal delivery might be more appropriate. In addition, it has been reported that topical naloxone has antipruritic effects (Bernstein et al., 1982).

Human skin permeability of naloxone was examined. In order to maximize naloxone delivery through skin, penetration enhancers were evaluated. The agents studied include various types of chemicals, some of which are known to enhance skin penetration of other drugs. The primary objective of the work presented here was to identify agents which increase naloxone skin permeability. In addition, however, the data that were obtained provide some insight on the selectivity of certain penetration enhancers, and to some extent relationships between structure and penetration enhancing effect were developed. Although there are many papers reporting the effects of one or several penetration enhancers, relative comparisons of various classes of enhancers and within a homologous series, as we have done, are much less frequent. The more practical aspects of developing a transdermal delivery system, including the toxicology of these adjuvants, will be given separate consideration.

Materials and Methods

Skin penetration

Naloxone diffusion rates through human cadaver skin were measured using Franz diffusion cells (Crown Glass). The reservoir volume was 7–9 ml and was maintained at 37°C with a water jacket or dry block heater. The reservoir contained saline (0.9%) and was stirred with a bar magnet. Sink conditions were maintained by removing the entire reservoir volume and replacing with drug-free saline. The skin surface area available for diffusion was 1.8 cm^2. The volume of vehicle applied was generally 0.5 ml, except for semisolid drug donors, for which an unmeasured amount was spread onto the skin. The donor chamber was closed to the atmosphere with parafilm or a rubber stopper.

Human cadaver skin was obtained from a local hospital. The thickness of these specimens was 0.4 mm, which based on average skin layer thickness includes the stratum corneum, the epidermis, and part of the dermis. Skin was stored at −20°C indefinitely. The average age of the donors was 43 years with a standard deviation of 19 years and a range of 16 to 72 years. 18% of the donors were female and 15% were black. Vehicles and skin specimens were randomly matched, with the exception that any vehicle-specimen combination was used only once. Prior to use, each skin specimen was visually inspected for integrity.

Naloxone concentrations in the reservoir were determined by HPLC, using UV detection at 284 nm, and a 25 cm × 4.5 mm octylsilane column (Zorbax C_8, DuPont). The mobile phase was acetonitrile/tetrahydrofuran/0.05 M phosphate buffer (10 : 0.8 : 89.2). The amount of drug penetrating through skin during any time interval was calculated as the sample concentration multiplied by the reservoir volume. Individual plots of cumulative amount penetrating versus time were made, and from the slope of the linear portion of such plots naloxone steady-state flux was calculated. There were at least 3 experiments per group. All data are expressed as mean ± S.E.

Vehicles

In the initial experiments, the effects of various agents on naloxone skin penetration were examined. For these experiments, vehicles were prepared by dissolving the adjuvants in propylene glycol (Fisher Scientific). Propylene glycol was selected so that both hydrophilic and hydrophobic adjuvants could be dissolved. The arbitrary concentration of adjuvant was 10% (w/v or v/v), however, not every adjuvant was completely dissolved at this concentration. The adjuvants and their sources are presented in the Results section. Naloxone base was added to the adjuvant/pro

available for
ıe of vehicle
for semisolid
ured amount
chamber was
m or a rubber

l from a local
mens was 0.4
ıyer thickness
ɔidermis, and
d at −20°C
lonors was 43
9 years and a
donors were
les and skin
with the ex-
combination
:h skin speci-
ity.
eservoir were
ection at 284
ilane column
: phase was
1 phosphate
ınt of drug
time interval
:ration multi-
dual plots of
us time were
ar portion of
x was calcu-
its per group.

:ts of various
were exam-
es were pre-
in propylene
: glycol was
hydrophobic
rbitrary con-
'/v or v/v),
mpletely dis-
djuvants and
sults section.
ıdjuvant/pro

pylene glycol vehicle in amounts in excess of its solubility. This maximized the thermodynamic activity of naloxone in the vehicle, since the objective was to maximize naloxone flux through skin.

Lauric acid, lauryl alcohol, and sodium lauryl sulfate were also tested in isopropanol (Fisher), polyethylene glycol 400 (Fisher), and mineral oil (Nujol, Plough) vehicles. In addition, lauric acid/isopropyl myristate vehicles were examined. The concentration of adjuvant was 10% (w/v) and naloxone was added as a suspension. Propylene glycol vehicles containing various concentrations of lauric acid or lauryl alcohol were also prepared and naloxone added in excess of its solubility.

Solubility determinations

Naloxone base solubility was determined for some of the vehicles tested. Vehicles were prepared and naloxone was added and the suspensions stirred for at least 20 h at room temperature (22–24°). Suspensions were centrifuged and the supernatant removed and filtered through glass wool packed into a transfer pipette. These solutions were diluted with 0.1 N HCl and assayed by HPLC as previously described.

Partition coefficient

Naloxone partitioning between propylene glycol or 10% lauric acid in propylene glycol and isopropyl myristate was determined. Lauric acid was dissolved in propylene glycol and naloxone was added in excess of its solubility. The suspension was then mixed with an equal volume of isopropyl myristate (Eastman Kodak) and tumbled at room temperature for 24 h. After centrifugation both phases were filtered and aliquots diluted with 0.1 N HCl and assayed by HPLC.

Results

Effects of various adjuvants

Naloxone skin penetration rates were determined using propylene glycol vehicles containing various potential absorption promoters at a concentration of 10% (w/v or v/v). An example of the effects of enhanced skin penetration is illustrated in Fig. 1, which shows average data using

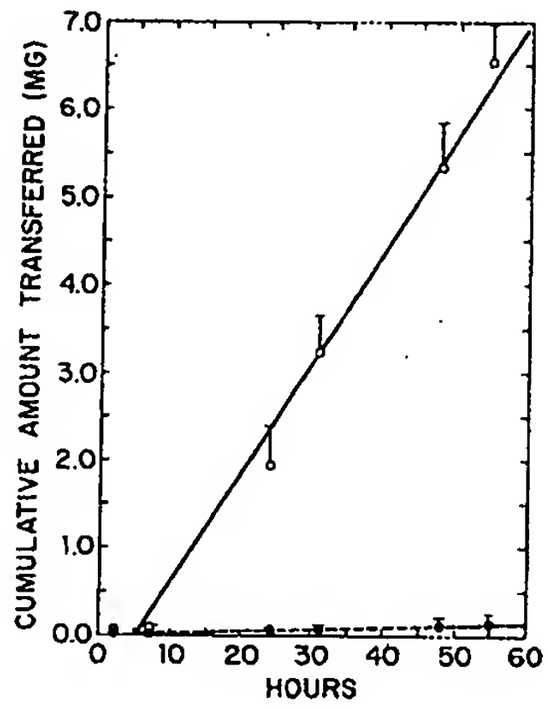

Fig. 1. Representative averaged profiles for naloxone diffusion through human skin using propylene glycol (●) or myristic acid/propylene glycol (○) vehicles.

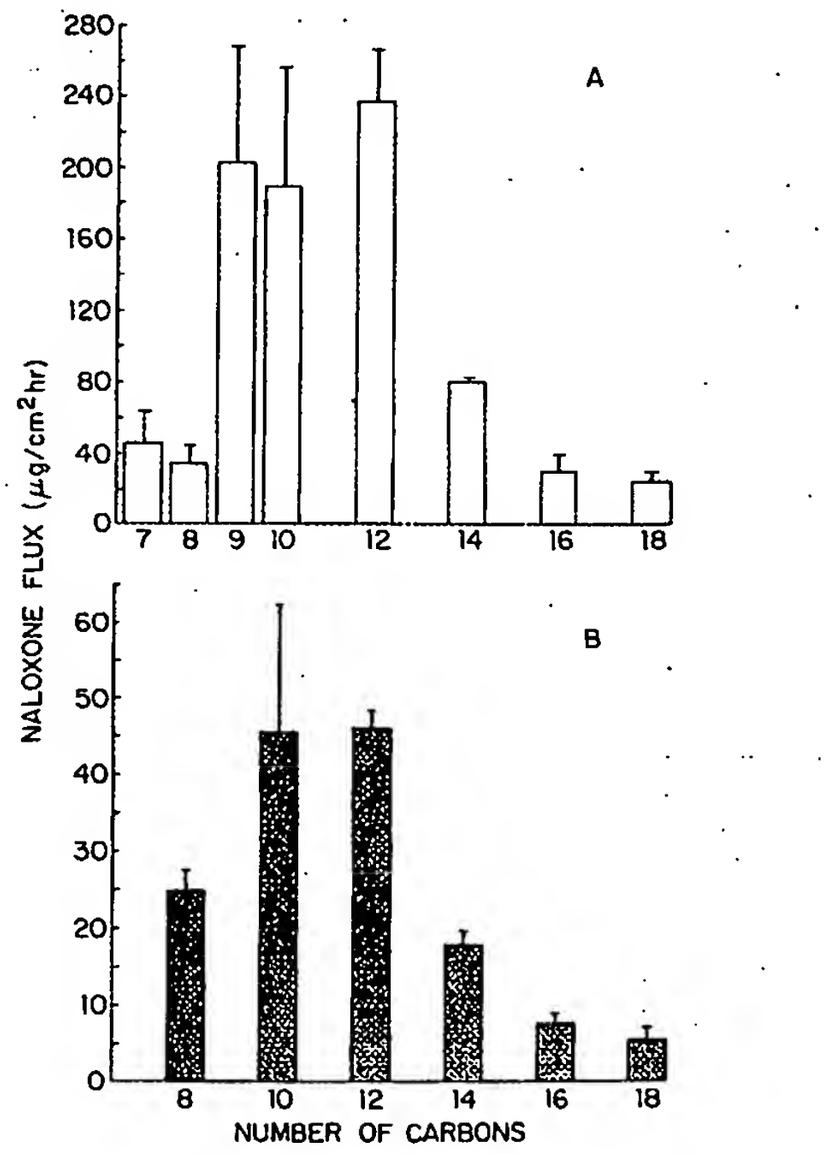

Fig. 2. Dependence of naloxone flux on chain length of fatty acid (A) or fatty alcohol (B) adjuvants (10% in propylene glycol).

TABLE 1

EFFECTS OF VARIOUS ADJUVANTS (10% IN PROPYLENE GLYCOL) ON NALOXONE FLUX THROUGH HUMAN CADAVER SKIN

Adjuvant [a]	Supplier	Naloxone flux [b] ($\mu g/cm^2 \cdot h$)	Number of experiments
None	–	1.6 ± 0.4	10
(A) Non-ionics			
Caprylic alcohol	Fisher	24.8 ± 2.6	3
Decyl alcohol	Sigma	45.3 ± 16.9	3
Lauryl alcohol	Pfaltz and Bauer	45.8 ± 2.4	3
2-Lauryl alcohol	Pfaltz and Bauer	43.9 ± 9.4	3
Myristyl alcohol	Sigma	17.7 ± 1.8	3
Cetyl alcohol [c]	Sigma	7.5 ± 1.2	3
Stearyl alcohol [c]	Sigma	5.2 ± 1.7	3
Oleyl alcohol	Sigma	25.0 ± 8.5	3
Linoleyl alcohol	Sigma	69.9 ± 28.0	4
Linolenyl alcohol	Sigma	116.3 ± 64.2	4
Propylene glycol laurate	Pfaltz and Bauer	43.8 ± 5.5	3
Sorbitan laurate [d]	Span 20, Sigma	27.9 ± 4.6	3
Polysorbate 20	Tween 20, Sigma	1.5 ± 0.4	3
Laureth 4	Brij 30, Sigma	34.5 ± 8.3	3
Laureth 23	Brij 35, Sigma	1.5 ± 0.6	3
PEG-4 laurate [d]	PEG 200 Monolaurate, Emery	11.8 ± 1.8	3
PEG-4 dilaurate [d]	PEG 200 Dilaurate, Emery	11.0 ± 1.2	3
Glyceryl laurate	Sigma	23.4 ± 3.6	3
Glyceryl dilaurate [d]	Stepan	18.7 ± 1.8	3
Dilauroyl lecithin	Avanti	8.2 ± 2.1	3
Sorbitan oleate [d]	Span 80, Sigma	9.9 ± 1.1	3
Sorbitan trioleate [d]	Span 85, Sigma	14.3 ± 4.6	3
Oleth-20	Brij 99, Sigma	1.6 ± 0.7	3
Glyceryl oleate [d]	Stepan	20.7 ± 2.0	3
Dilauroyl lecithin	Avanti	14.1 ± 4.5	3
Poloxamer 188 [c]	Pluronic F68, Ruger	4.2 ± 2.3	4
Poloxamer 401 [c]	Pluronic L121, BASF	5.8 ± 0.9	3
Cocomorpholine	Lonza	32.0 ± 3.9	3
(B) Anionics			
Heptanoic acid (7:0)	Celanese	46.2 ± 17.8	4
Caprylic acid (8:0)	Sigma	34.3 ± 10.0	3
Pelargonic acid (9:0)	Celanese	201.9 ± 65.4	3
Capric acid (10:0)	Sigma	187.9 ± 67.5	4
Undecylenic acid ($11:1^{\Delta 10}$)	Fluka	115.1 ± 4.5	3
Lauric acid (12:0)	Sigma	235.2 ± 29.9	3
Myristic acid (14:0)	Emery	78.1 ± 2.4	3
Palmitic acid (16:0) [c]	Sigma	27.8 ± 9.4	3
Stearic acid (18:0) [c]	Ruger	21.8 ± 5.6	3
Oleic acid ($18:1^{\Delta 9}$)	Emery	35.6 ± 9.8	3
Linolenic acid ($18:2^{\Delta 9,12}$)	Sigma	103.0 ± 14.1	3
Linolenic acid ($18:3^{\Delta 9,12,15}$)	Sigma	93.8 ± 14.7	3
Arachidonic acid ($20:4^{\Delta 5,8,11,14}$)	Sigma	47.8 ± 12.0	3
Sodium laurate	Sigma	7.3 ± 0.8	3
Sodium lauryl sulfate	Sigma	4.6 ± 0.9	3
Sodium oleate	Aldrich	3.8 ± 0.5	3
Dodecanedioic acid [d]	DuPont	2.0 ± 0.4	3
Trans-dodecenedioic acid [d]	Traumatic acid, Sigma	7.4 ± 2.4	3

TABLE 1 (continued)

Adjuvant [a]	Supplier	Naloxone flux [b] ($\mu g/cm^2 \cdot h$)	Number of experiments
Retanoic acid [d]	Sigma	7.4 ± 2.9	4
Lauroyl sarcosine	Hampshire	7.2 ± 3.0	3
(C) Cationics			
Dodecylamine	Fluka	25.1 ± 0.9	3
Stearylamine	Fluka	19.4 ± 7.0	4
(D) Amphoterics			
Lauroamphoglycinate	Mona	5.2 ± 0.2	3
Lauroamidopropylbetaine	Mona	5.8 ± 1.5	3
(E) Sulfoxides			
Dimethylsulfoxide	Sigma	1.7 ± 0.9	3
Decylmethylsulfoxide	Wateree	49.2 ± 19.8	5
(F) Amides			
Urea	Fisher	0.4 ± 0.1	3
Dimethylacetamide	Fisher	2.0 ± 0.3	3
Diethyltoluamide	Sigma	8.6 ± 2.9	3
1-Dodecylazocycloheptan-2-one	Azone, Nelson	25.2 ± 5.4	3
N-Methylpyrrolidone	GAF	1.8 ± 0.3	3
N-Hydroxyethylpyrrolidone	GAF	1.8 ± 0.1	3
N-Cyclohexylpyrrolidone	GAF	3.4 ± 1.4	3
N-Dimethylaminopropylpyrrolidone	GAF	3.9 ± 2.0	3
N-Cocoalkylpyrrolidone	GAF	55.2 ± 12.2	4
N-Tallowalkylpyrrolidone	GAF	38.4 ± 2.9	3

[a] CTFA adopted name if applicable.
[b] Mean ± S.E.
[c] Semisolid vehicle.
[d] Adjuvant not completely soluble/miscible at 10% concentration.

propylene glycol and propylene glycol/myristic acid vehicles. In this example, naloxone flux was increased 48-fold in the presence of myristic acid.

Fatty acids and fatty alcohols were among the most potent agents in increasing naloxone skin penetration. Within both the acid and alcohol series, the magnitude of enhancement was related to the chain length of the hydrophobic group (Fig. 2). The maximum naloxone flux was with the C_{12} acid and alcohol. The enhancing effects of unsaturated C_{18} acids and alcohols were also examined. Increasing the number of double bonds generally resulted in greater enhancement of naloxone skin penetration (Fig. 3). Based on these results, the other adjuvants selected for evaluation were predominantly those containing laurate or oleate hydrophobic groups.

Table 1 summarizes the effects of the various

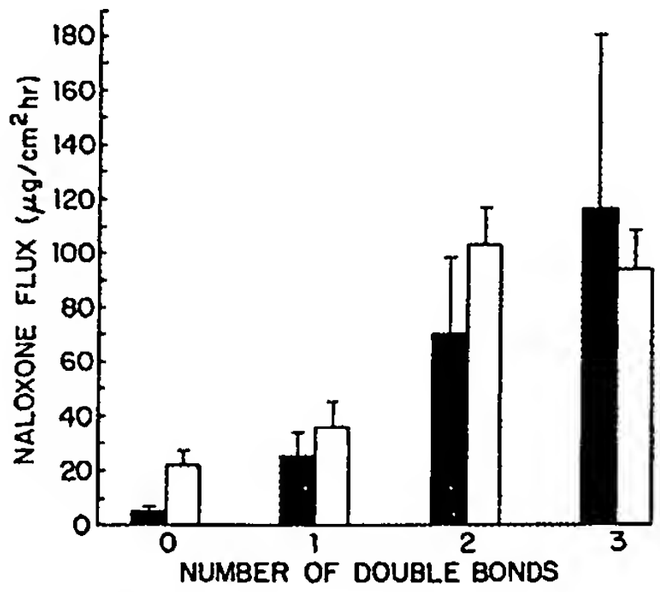

Fig. 3. Effects of saturated and *cis*-unsaturated C_{18} fatty alcohols (closed bars) and fatty acids (open bars) on naloxone skin penetration. The adjuvants were dissolved in propylene glycol at a concentration of 10%.

adjuvants tested. Although fatty acids were very effective penetration enhancers, the sodium salts, sodium laurate, sodium oleate, and sodium lauryl sulfate had minimal effects on naloxone skin penetration. The C_{12} diacids, dodecanedioic acid (saturated) and *trans*-dodecenedioic acid (unsaturated), also did not appreciably increase naloxone flux.

The ester and ether non-ionic surfactants were generally less effective than fatty acids in enhancing naloxone skin penetration. Naloxone flux was plotted versus the hydrophil–lipophil balance (HLB) value for the non-ionic and anionic surfactants with laurate hydrophobic groups (Fig. 4). A trend was clearly apparent for surfactants with low HLB values (e.g. more hydrophobic) to have greater effects on naloxone skin penetration. However, there was not a general relationship for all surfactants between HLB value and naloxone flux. For example, Poloxamer 188 (HLB = 29.0) and Poloxamer 401 (HLB = 0.5) had similar effects on naloxone flux.

The two amphoteric surfactants tested only slightly increased naloxone flux. The two cationic surfactants examined, both of which are known skin irritants, increased flux significantly.

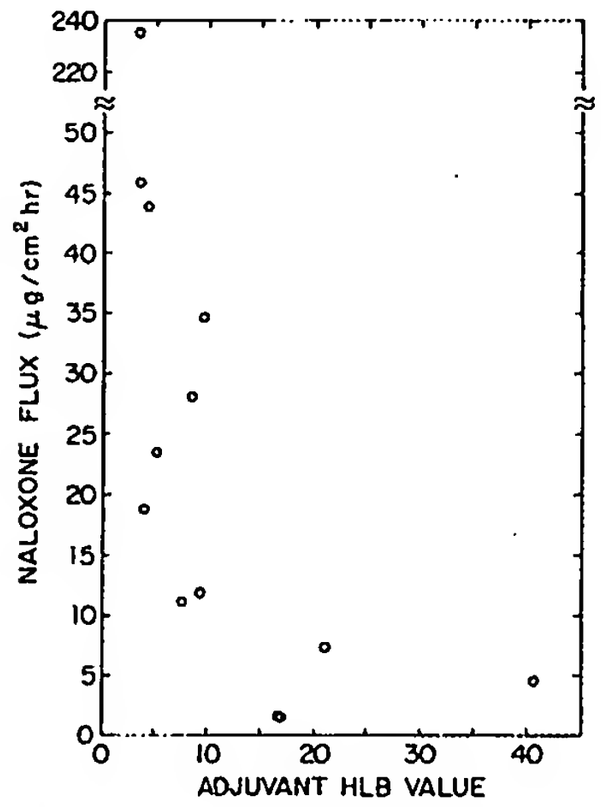

Fig. 4. Naloxone flux as a function of the hydrophil–lipophil balance (HLB) value of the adjuvant, for adjuvants with laurate hydrophobic groups. The adjuvant concentration in propylene glycol was 10%.

A number of sulfoxides and amides known to act as skin penetration enhancers were also evaluated. Decylmethylsulfoxide was a very effective skin penetration enhancer for naloxone, whereas dimethylsulfoxide was not. Urea and dimethylacetamide had no effects on naloxone flux. Diethyltoluamide increased flux slightly. Generally, solvents like DMSO and DMA must be at higher concentrations to influence skin permeability. Azone increased flux approximately 15-fold. The effects of the pyrrolidones were dependent on the substituent group on the nitrogen atom. Although N-methylpyrrolidone (NMP) has been frequently used as a skin penetration enhancer (e.g. Akhter and Barry, 1985), naloxone flux was unaffected by 10% NMP. Higher concentrations of NMP did, however, increase naloxone penetration (data not shown). The most effective pyrrolidone skin penetration enhancers tested had cocoalkyl [1] and tallowalkyl [2] hydrophobic groups. To the best of our knowledge, these agents have not been previously used to promote percutaneous absorption. The relationship between flux and the hydrophobic group of the enhancer is consistent with results for the other classes of compounds. That is that C_{12} and C_{18} unsaturated hydrophobic tails maximize penetration enhancement.

Influence of vehicle

The penetration enhancing effects of lauric acid, lauryl alcohol, and sodium lauryl sulfate were also examined using vehicles other than propylene glycol. Results are summarized in Table 2. In the absence of a penetration enhancer, naloxone flux was similar using propylene glycol, PEG400, or mineral oil as the vehicle. This would be expected when: (1) the thermodynamic activity of the drug is the same in each vehicle (saturated solution); and (2) the vehicles do not alter the barrier properties of skin (Higuchi, 1960). Naloxone flux values from saturated solutions of isopropanol and isopropyl myristate were significantly higher than with the other vehicles. It could thus be inferred

[1] Approximate composition: $C_8 = 5\%$, $C_{10} = 10\%$, $C_{12} = 59\%$, $C_{14} = 17\%$, $C_{16} = 9\%$ (GAF product literature).

[2] Approximate composition: $C_{18\ sat.+unsat.} = 62\%$, $C_{16sat.} = 34\%$, lower alkyl = 4% (GAF product literature).

TABLE 2

EFFECTS OF LAURIC ACID, LAURYL ALCOHOL, AND SODIUM LAURYL SULFATE ON NALOXONE SKIN PENETRATION USING VARIOUS VEHICLES CONTAINING 10% ADJUVANT AND NALOXONE IN EXCESS OF SATURATED SOLUBILITY

Vehicle	Naloxone flux ($\mu g/cm^2 \cdot h$)			
Adjuvant:	None	Lauric acid	Lauryl alcohol	Na lauryl sulfate
Propylene glycol	1.6 ± 0.4	235.2 ± 29.9	45.8 ± 2.4	4.6 ± 0.9
Isopropanol	16.6 ± 4.7	160.6 ± 60.0	28.4 ± 11.8	31.5 ± 19.8
PEG 400	1.8 ± 0.6	46.1 ± 25.3	12.2 ± 5.4	1.6 ± 0.5
Mineral oil	1.3 ± 0.3	18.8 ± 6.4	11.1 ± 2.7	42.4 ± 32.3
Isopropyl myristate	7.7 ± 0.1	20.0 ± 3.0		

that isopropanol and isopropyl myristate increased skin permeability. Isopropanol (Coldman et al., 1969) and isopropyl myristate (Bronaugh et al., 1981) were previously shown to increase skin permeability to other solutes.

The addition of 10% lauric acid or lauryl alcohol to each of the four vehicles increased naloxone flux, but the greatest increases were with propylene glycol. In propylene glycol and isopropanol, sodium lauryl sulfate approximately doubled naloxone flux, and had no effect when dissolved in PEG400. However, in a mineral oil vehicle, sodium lauryl sulfate had a more significant effect on naloxone flux. From these results, it is apparent that the effects of penetration enhancers are dependent on the vehicle.

Concentration / effect relationships

Naloxone skin penetration was evaluated as a function of lauric acid or lauryl alcohol concentration, using various penetration enhancer/propylene glycol concentrations. These results are illustrated in Fig. 5. 1% lauric acid only slightly increased naloxone flux, relative to the propylene glycol control, but with further increases to 2.5% and 5% concentrations, flux increased tremendously. Maximum flux was observed using 20% lauric acid. The most effective lauryl alcohol concentration was 5%. Higher adjuvant concentrations decreased flux, possibly due to a reduction of the skin/vehicle partition coefficient of naloxone.

Partition coefficients

The solubility of naloxone base in lauric acid/

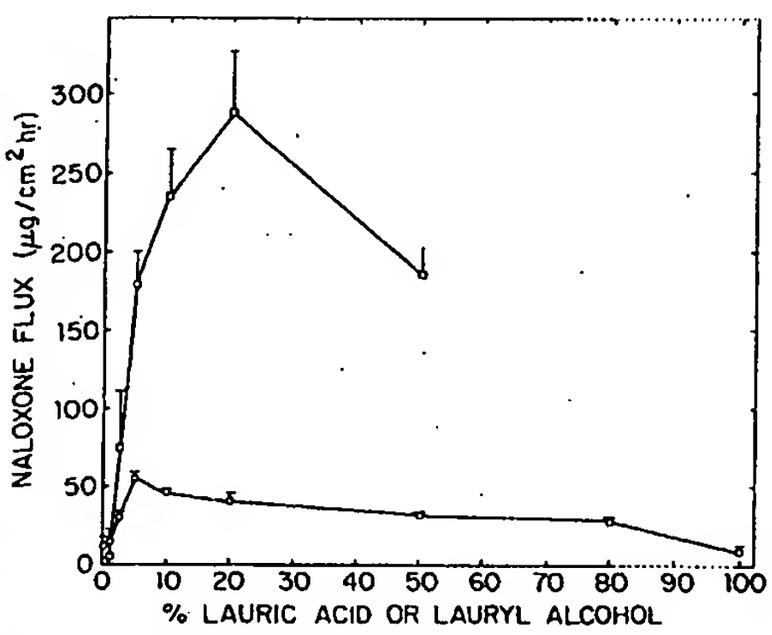

Fig. 5. Concentration dependence of the effects of lauric acid (□) and lauryl alcohol (○) on naloxone skin penetration, using propylene glycol as the solvent.

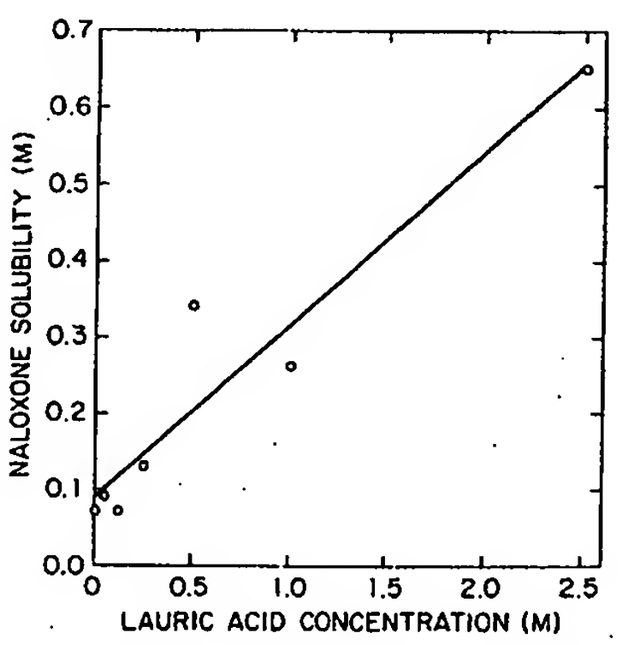

Fig. 6. Effect of lauric acid concentration in propylene glycol on naloxone base solubility.

propylene glycol vehicles was proportional to the concentration of lauric acid (Fig. 6). It seemed possible that naloxone base solubilization by lauric acid could be due to the formation of a charge transfer complex. This could contribute to the increased naloxone skin penetration if the complex had a higher skin/vehicle partition coefficient (K_p) than free naloxone. Increased naloxone solubility could have also been due to micelle formation. Fatty alcohols had only minor effects on naloxone solubility. To examine whether increased naloxone flux might have been due to formation of a complex with a higher K_p, the effect of lauric acid on naloxone K_p was determined. The K_p for isopropyl myristate/propylene glycol was 0.17, and that for isopropyl myristate/10% lauric acid in propylene glycol was 0.15.

Discussion

Naloxone skin penetration rates were determined using various vehicles, and in the presence of numerous adjuvants which were considered potential skin penetration enhancers. Some of these agents markedly increased naloxone flux, while others had little or no effects. This prompts questioning: (a) the mechanisms of enhancement; and (b) whether skin penetration promoting effects are selective for certain drugs.

Specificity can be addressed by examining the literature on these skin penetration enhancers, where different diffusing solutes were studied. Maximum naloxone flux was observed using fatty acid or fatty alcohol/propylene glycol vehicles. In the saturated fatty acid and alcohol series, the most effective penetration enhancers had 12 carbon atoms. Unsaturated C_{18} acids and alcohols were more effective enhancers than the corresponding saturated acid or alcohol. Oleic acid and oleyl alcohol (0.1 M in propylene glycol) have been used previously to increase the human skin penetration of salicylic acid (Cooper, 1984) and acyclovir (Cooper et al., 1985). Similarly, oleic acid (5% in propylene glycol) increased the penetration of both mannitol and hydrocortisone (Bennett and Barry, 1985). However, neither lauric acid or capric acid (0.1 M in propylene glycol) had much effect on salicylic acid skin penetration (Cooper, 1984). Metronidazole and estradiol penetration from vehicles containing equal parts of propylene glycol and a C_{8-18} fatty alcohol was determined in another study (Mollgaard and Hoelgaard, 1983). Metronidazole penetration was not significantly affected by any of the fatty alcohols, but estradiol penetration was promoted by palmityl and stearyl alcohols. C_{8-14} alcohols did not increase estradiol penetration. Collectively, these reports suggest some measure of selectivity for fatty acid and fatty alcohol skin penetration enhancers.

Several agents known to be skin penetration enhancers had minor or no effect on naloxone skin permeability when dissolved in propylene glycol. These include sodium lauryl sulfate, sodium laurate, N-methylpyrrolidone and dimethylacetamide. Cooper (1982) reported that sodium lauryl sulfate increased the skin penetration of urea and pentanol 8300-fold and 7-fold, respectively. The effects of other enhancers, including, for example, PEG10 laurate (Walters et al., 1984) and 2-pyrrolidone (Southwell and Barry, 1983) are also apparently greater for polar solutes than for nonpolar solutes. Additional confounding variables in comparing these studies, however, are differences in the vehicle and adjuvant concentrations, both of which can significantly influence the effectiveness of a skin penetration enhancer, as we have demonstrated.

A number of mechanisms for promotion of skin permeability can be proposed. These include: increasing drug solubility in skin; dissolving skin lipids; altering the conformation or denaturing skin proteins, e.g. keratin; disruption of water structure in skin; and increasing membrane fluidity.

These are not necessarily separate actions, since several of these effects may be operative in concert. For example, Scheuplein (1970) has proposed that organic solvents extract lipids, thus creating holes; but that this also results in a loss of water binding capacity. He further suggested that hydrogen-bonding solvents, like dimethylsulfoxide, displace structured water in the membrane, and that anionic surfactants disrupt protein structure, which

also results in a loss of water binding capacity. Akerman et al. (1979) also proposed that aliphatic and cyclic amides, including dimethylacetamide and N-methylpyrrolidone, displace bound stratum corneum water and thus increased the penetration of lidocaine. Cyclic amides with a hydrophobic tail (e.g. N-alkylpyrrolidones and Azone) probably have additional effects on other membrane components, acting as surfactants as well as solvents. It was recently reported that Azone treatment of human stratum corneum was associated with removal of lipids, as indicated by differential scanning calorimetry (Goodman and Barry, 1985).

Initially we suspected that fatty acids might promote naloxone skin penetration by increasing its solubility in skin (partitioning into skin). Fatty acids increased naloxone solubility in propylene glycol, possibly by complexation. However, the isopropyl myristate/propylene glycol partition coefficient of naloxone was not increased in the presence of lauric acid. Fatty acids and fatty alcohols apparently increase flux by altering the diffusion coefficient rather than K_p. The mechanisms of effect of fatty acids and fatty alcohols on skin permeability is not known.

One intriguing aspect of this study is that maximum skin penetration enhancement was observed with C_{12} saturated hydrophobic groups, and that agents with unsaturated groups were more effective than saturated ones. This relationship had not been previously described for fatty acids and alcohols affecting skin. However, similar phenomena have been described for other enhancers or membranes. In the alkyl methyl sulfoxide series, C_{10}MSO was a more effective enhancer of nicotinic acid skin penetration than DMSO, C_6MSO, C_{12}MSO, or C_{14}MSO (Sekura and Scala, 1972). For a series of polyethylene alkyl ethers, maximum effects were seen with dodecyl hydrophobic groups for hemolysis of red blood cells (Zaslavsky et al., 1978), absorption of paraquat through the gastric mucosal membrane (Walters et al., 1981), and methyl nicotinate flux through hairless mouse skin (Walters and Olejnik, 1983). Oleyl ethers were more effective than stearyl ethers. N-alkylpyrrolidones also appeared to exhibit this relationship in promoting naloxone skin permeation.

At least two hypotheses have been proposed to explain why C_{12} hydrophobic groups have maximum effects on membranes. Florence et al. (1984) suggested that increasing the carbon chain length within a homologous series increases the lipophilicity, but decreases the critical micelle concentration. C_{12} hydrophobic groups have the greatest membrane penetration because of an optimal balance of partition coefficient and monomer concentration. Another theory was proposed by Dominguez et al. (1977). They suggested that surfactants do not necessarily adopt a linear structure in skin, but rather form a coiled, "open-cyclohexane" structure. The molecular size of the surfactants forming these "open-cyclohexane" structures was postulated to be minimum when the hydrophobic chain is C_{12}. Minimizing molecular size favors increased membrane penetration.

It is also known that lipids of like structures pack tightly together, but mixtures of long and short chain lipids, or saturated and unsaturated lipids, form loosely organized structures (Small, 1984). The most abundant stratum corneum lipids are free fatty acids, triglycerides, cholesterol, and ceramides. The majority of these lipids, including the free fatty acids, have 16 or more carbon atom hydrophobic groups (Elias, 1983). One could hypothesize, therefore, that the introduction of shorter fatty acid chains disrupts the crystalline lipid packing and results in a more fluid and permeable membrane.

In conclusion, agents to increase naloxone penetration through human skin have been identified. Generally, penetration enhancing effects are via alteration of the normal skin structure and could be expected to be associated with an inflammatory response. The next step in applying this information to practice, for transdermal or topical naloxone administration, is to optimize the penetration enhancement while minimizing skin irritation.

References

Aitkenhead, A.R., Derbyshire, D.R., Pinnock, C.A., Achola, K. and Smith, G., Pharmacokinetics of intravenous naloxone in healthy volunteers. *Anesthesiology*, 61 (1984) A381.

Akerman, B., Haegerstam, G., Pring, B.G. and Sandberg, R., Penetration enhancers and other factors governing percuta-

neous local anaesthesia with lidocaine, *Acta Pharmacol. Toxicol.*, 45 (1979) 58–65.

Akhter, S.A. and Barry, B.W., Absorption through human skin of ibuprofen and flurbiprofen; effect of dose variation, deposited drug films, occlusion and the penetration enhancer N-methyl-2-pyrrolidone. *J. Pharm. Pharmacol.*, 37 (1985) 27–37.

Atkinson, R.L., Naloxone decreases food intake in obese humans. *J. Clin. Endocrinol. Metab.*, 55 (1982) 196–198.

Bennett, S.L. and Barry, B.W., Effectiveness of skin penetration enhancers propylene glycol, Azone, decylmethylsulphoxide and oleic acid with model polar (mannitol) and nonpolar (hydrocortisone) penetrants. *J. Pharm. Pharmacol.*, 37 Suppl. (1985) 84P.

Bernstein, J.E., Swift, R.M. Soltani, K. and Lorincz, A.L., Antipruritic effect of an opiate antagonist, naloxone hydrochloride. *J. Invest. Dermatol.*, 78 (1982) 82–83.

Bradberry, J.C. and Raebel, M.A., Continuous infusion of naloxone in the treatment of narcotic overdose. *Drug Intell. Clin. Pharm.*, 15 (1981) 945–950.

Bronaugh, R.L., Congdon, E.R. and Scheuplein, R.J., The effect of cosmetic vehicles on the penetration of N-nitrosodiethanolamine through excised human skin. *J. Invest. Dermatol.*, 76 (1981) 94–96.

Coldman, M.F., Poulsen, B.J. and Higuchi, T., Enhancement of percutaneous absorption by the use of volatile: nonvolatile systems as vehicles, *J. Pharm. Sci.*, 58 (1969) 1098–1102.

Cooper, E.R., Effect of decylmethylsulfoxide on skin penetration. In K.L. Mittal and E.J. Fendler (Eds.), *Solution Behavior of Surfactants, Vol. 2*, Plenum Press, New York, 1982.

Cooper, E.R., Increased skin permeability for lipophilic molecules. *J. Pharm. Sci.*, 73 (1984) 1153–1156.

Cooper, E.R., Merritt, E.W. and Smith, R.L., Effect of fatty acids and alcohols on the penetration of acyclovir across human skin in vitro. *J. Pharm. Sci.*., 74 (1985) 688–689.

Dominguez, J., Parra, J.L., Infante, M.R., Pelejero, C.M., Balaguer, F. and Sastre, T., A new approach to the theory of adsorption and permeability of surfactants on keratinic proteins: the specific behaviour of certain hydrophobic chains. *J. Soc. Cosmet. Chem.*, 28 (1977) 165–182.

Elias, P.M., Epidermal lipids, barrier function, and desquamation. *J. Invest. Dermatol.*, 80 (1983) 44S–49S.

Florence, A.T., Tucker, I.G. and Walters, K.A., Interactions of non-ionic polyoxyethylene alkyl and aryl ethers with membranes and other biological systems. In M.J. Rosen (Ed.), *Structure/Performance Relationships in Surfactants*, American Chemical Society, Washington, DC, 1984.

Goodman, M. and Barry, B.W., Differential scanning calorimetry (DSC) of human stratum corneum: Effect of Azone. *J. Pharm. Pharmacol.*, 37 Suppl. (1985) 80P.

Gourlay, G.K. and Coulthard, K., The role of naloxone infusions in the treatment of overdoses of long half-life narcotic agonists: application to non-methadone. *Br. J. Clin. Pharmacol.*, 15 (1983) 269–272.

Higuchi, T., Physical chemical analysis of percutaneous absorption processes from creams and ointments. *J. Soc. Cosmet. Chem.*, 11 (1960) 85–97.

Kreek, M.-J., Schaeffer, R.A., Hahn, E.F. and Fishman, J., Naloxone, a specific opioid antagonist, reverses chronic idiopathic constipation. *Lancet* 1 (1983) 261–262.

McNicholas, L.F. and Martin, W.R., New and experimental therapeutic roles for naloxone and related opioid antagonists. *Drugs*, 27 (1984) 81–93.

Mollgaard, B. and Hoelgaard, A., Vehicle effect on topical drug delivery II. Concurrent skin transport of drugs and vehicle components. *Acta Pharm. Suec.*, 20 (1983) 443–450.

Ngai, S.H., Berkowitz, B.A., Yang, J.C., Hempstead, J. and Spector, S., Pharmacokinetics of naloxone in rats and in man: basis for its potency and short duration of action. *Anesthesiology*, 44 (1976) 398–401.

Reisberg, B., Ferris, S.H., Anand, R., Mir, P., Geibel, V. DeLeon, M.J. and Roberts, E., Effects of naloxone in senile dementia: a double-blind trial. *N. Engl. J. Med.*, 308 (1983a) 721–722.

Reisberg, B., London, E., Ferris, S.H., Anand, R. and DeLeon, M.J., Novel pharmacologic approaches to the treatment of senile dementia of the Alzheimer's type (SDAT). *Psychopharmacol. Bull.*, 19 (1983b) 220–225.

Scheuplein, R. and Ross, L., Effects of surfactants and solvents on the permeability of epidermis. *J. Soc. Cosmet. Chem.*, 21 (1970) 853–873.

Sekura, D.L. and Scala, J., The percutaneous absorption of alkyl methyl sulfoxides. In Montagna, W., Van Scott, E.J. and Stoughton, R.B. (Eds.), *Pharmacology and the Skin*, Appleton-Century-Crofts, New York, 1972.

Small, D.M., Lateral chain packing in lipids and membranes. *J. Lipid Res.*, 25 (1984) 1490–1500.

Southwell, D. and Barry, B.W., Penetration enhancers for human skin: mode of action of 2-pyrrolidone and dimethylformamide on partition and diffusion of model compounds water, *n*-alcohols and caffeine. *J. Invest. Dermatol.*, 80 (1983) 507–514.

Walters, K.A., Dugard, P.H. and Florence, A.T., Non-ionic surfactants and gastric mucosal transport of paraquat. *J. Pharm. Pharmacol.*, 33 (1981) 207–213.

Walters, K.A. and Olejnik, O., Effects of non-ionic surfactants on the hairless mouse skin penetration of methyl nicotinate. *J. Pharm. Pharmacol.*, 35 Suppl. (1983) 79P.

Walters, K.A., Olejnik, O. and Harris, S., Influence of non-ionic surfactant on the permeation of ionized molecules through hairless mouse skin. *J. Pharm. Pharmacol.*, 36 Suppl. (1984) 78P.

Zaslavsky, B.Y., Ossipov, N.N., Krivich, V.S., Baholdina, L.P. and Rogozhin, S.V., Action of surface-active substances on biological membranes II. Hemolytic activity of non-ionic surfactants. *Biochem. Biophys. Acta*, 507 (1978) 1–7.

Journal of Controlled Release, 6 (1987) 85–97
Elsevier Science Publishers B.V., Amsterdam — Printed in The Netherlands

MODE OF ACTION OF PENETRATION ENHANCERS IN HUMAN SKIN

B.W. Barry
Postgraduate School of Studies in Pharmacy, University of Bradford, Bradford, BD7 1DP West Yorkshire (Great Britain)

Skin penetration enhancers are molecules which reversibly remove the barrier resistance of the stratum corneum. They allow drugs to penetrate more readily to the viable tissues and thus enter the systemic circulation. This paper presents a general theory for enhancer activity based on possible alterations at the molecular level of the stratum corneum. Within the intercellular route, accelerants may interact at the polar head groups of the lipids, within aqueous regions between lipid head groups, and between the hydrophobic tails of the bilayer. Within the corneocyte the keratin fibrils and their associated water provide the target. High concentrations of solvents may also alter partitioning phenomena. The theory has been applied specifically to water, Azone, dimethylsulfoxide, dimethylformamide, 2-pyrrolidone, N-methyl-2-pyrrolidone, oleic acid, decylmethylsulfoxide, sodium lauryl sulfate and propylene glycol. The main techniques which supplied experimental support for the theory were permeation studies through human skin, the vasoconstrictor assay and differential scanning calorimetry; the results from DSC are mainly considered here.

INTRODUCTION

In recent years, investigators have intensified their interests in the controlled delivery of drugs through human skin, and transdermal devices have been developed for drugs such as clonidine, estradiol, testosterone, fentanyl, scopolamine and nitroglycerin. A major problem in attempting to control the drug flux arises from the impermeability of human skin and its biological variability. It would be very useful to circumvent these problems by including in the formulation molecules which would reversibly remove the barrier resistance of the stratum corneum and thus allow the drug to penetrate to the viable tissues and enter the systemic circulation [1]. Such entities are known as penetration enhancers and this paper discusses the mechanism of action of many of the most important enhancers used to date and proposes a general theory of skin accelerant activity.

PERMEABILITY BARRIER OF HUMAN SKIN

The importance of the stratum corneum in the barrier function of skin is well established, with the entire horny layer providing the major rate-limiting barrier. There are some exceptions to this – for instance for very lipophilic drugs the aqueous epidermal and dermal layers may provide a significant hindrance because of the clearance effect. Also, the appendage route may be important for ionic molecules or large polar compounds. However for most penetrants, permeation through the bulk of the stratum corneum provides the rate-limiting step at

Paper presented at the Third International Symposium on Recent Advances in Drug Delivery Systems, February 24–27, 1987, Salt Lake City, UT, U.S.A.

0168-3659/87/$03.50

steady state and this region will be considered as the major barrier in the discussion.

The literature view of the route of drug permeation through the stratum corneum has altered somewhat as the tissue structure has become better understood. We may summarise the modern view of the horny layer and represent it as a wall-like structure with protein bricks and lipid mortar. Both the structured lipid environment between the cells and the hydrated protein within the corneocytes play major roles in skin permeability; cell membranes are probably of only minor consequence (Fig. 1). This figure illustrates two potential routes for drug permeation, between the cells (intercellular route) or through the protein-filled cells and across lipid-rich regions in tandem (transcellular route). For each penetrant, the relative importance of these dual routes depends among other things upon its solubility (or chemical potential), its partition coefficients for the various phases and its diffusivities within these phases, be they proteinaceous or lipid [2].

Overall, at least for polar drugs, it is likely that the transcellular route provides the main pathway during percutaneous absorption. As penetrants become more non-polar, the intercellular route probably becomes more significant, although whether it entirely dominates, even for non-polar drugs, is unclear. In any event, the stratum corneum lipids provide a significant part of the barrier function of the stratum corneum and an understanding of their nature and organisation is crucial to a review of penetration enhancer activity. That intercellular lipids can form bilayers at physiological pH has been demonstrated, directly for pig epidermis [3] and at least indirectly for other mammalian species, including man [4].

A previous publication presented a general theory for penetration enhancer activity based on considerations of possible molecular locations for accelerant action [2]. Within the intercellular route, it was proposed that accelerants may interact at the polar head groups of the lipids, within the aqueous region between lipid head groups, and between the hydrophobic tails of the bilayer. Within the corneocyte the major site of action would be the keratin

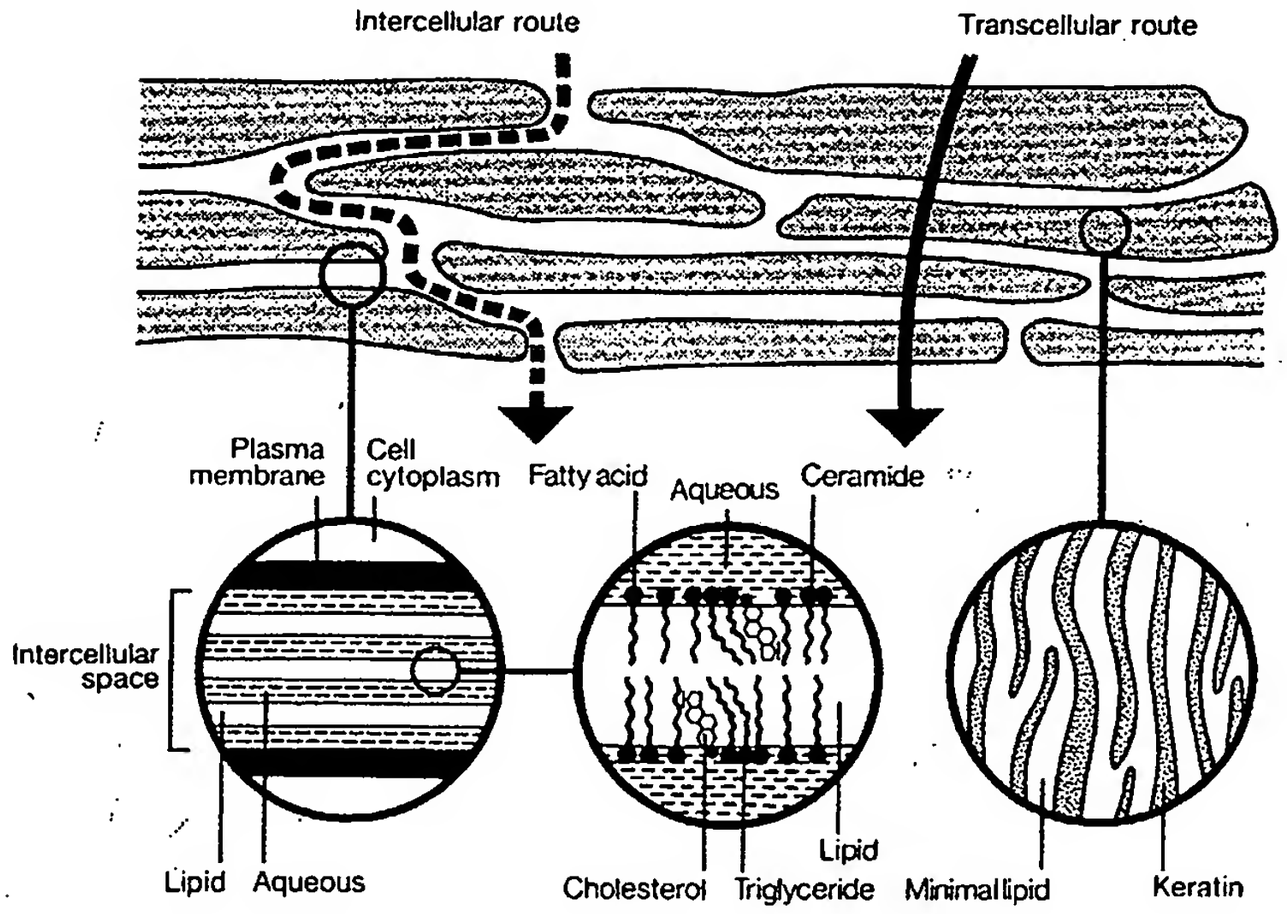

Fig. 1. Suggested routes of drug penetration through human stratum corneum; macroscopic and molecular domains.

fibrils and their associated water molecules. A penetration enhancer may also have a direct action whereby regions of the tissue change their bulk constitution. Thus with high concentrations of solvents such as propylene glycol, ethanol, the pyrrolidones or dimethylsulfoxide, so much solvent may penetrate into the tissue that it changes the partition coefficient (stratum corneum: vehicle) for the drug. This paper extends this theory and applies it to individual penetration enhancers.

We believe that the interactions proposed here are the main ones dominating accelerant activity in human stratum corneum. There may also be minor rearrangements such as those associated with lipid–protein complexes in the corneocyte membrane; however, other workers propose that these complexes provide one of the important thermotropic transitions in stratum corneum [5,6].

EXPERIMENTAL TECHNIQUES

We have used three methods to probe the mechanisms of action of various penetration enhancers.

1. Permeation studies through cadaver skin

We selected a range of penetrant molecules of widely different polarities to assess the effects of diverse enhancers on polar and lipid routes through the stratum corneum e.g. mannitol, 5-fluorouracil, estradiol, hydrocortisone and progesterone. We used both pseudosteady-state techniques and *in vivo* mimic approaches with enhancers such as Azone, dimethylsulfoxide, dimethylformamide, 2-pyrrolidone, *N*-methyl-2-pyrrolidone, oleic acid, decylmethylsulfoxide, sodium laurly sulfate and propylene glycol [7,8].

2. Vasoconstrictor assays with topical steroids

These procedures are valuable means for assessing accelerant activity in volunteers by simply scoring the degree of pallor induced by a test steroid and how an accelerant modifies the response [9,10].

3. Differential scanning calorimetry (DSC) of human stratum corneum

DSC experiments provide evidence regarding the structure of the stratum corneum and how enhancers modify phase transitions within this tissue. In a typical hydrated sample of human stratum corneum we can resolve four main transitions [5,6,11–14] which we identify in ascending order of temperature as follows:

Endotherm T1

Ascribed to lipid melting, possibly arising from sebaceous lipids or cholesterol side-chain motion.

Endotherm T2

Due to melting of the lipid chain portion buried within the bilayer structure, together with some non-polar material.

Endotherm T3

Break-up of associations between lipid polar head groups together with disruption of cholesterol-stiffened regions. Other workers ascribe this transition to protein-lipid associations in cell membranes [5,6].

Endotherm T4

Protein denaturation of intracellular keratin.

Figure 2 illustrates a typical DSC trace of human stratum corneum, together with one modified by Azone treatment.

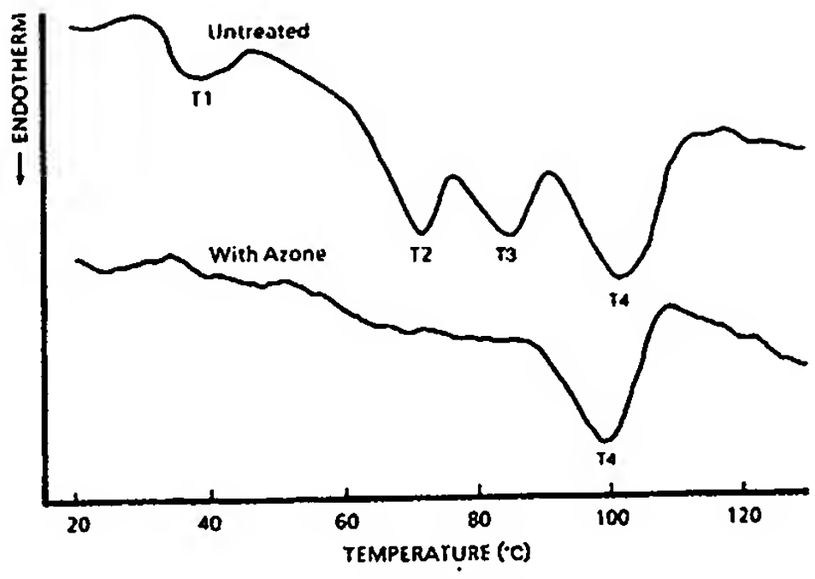

Fig. 2. Differential scanning calorimetry of human stratum corneum, untreated and modified by Azone.

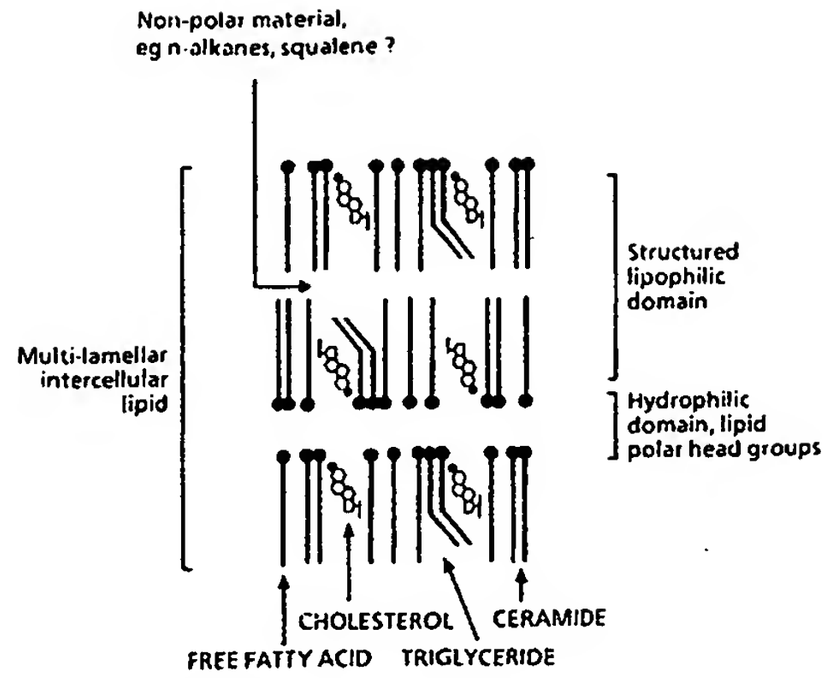

Fig. 3. Suggested model representing the structure of lipid bilayers within the intercellular spaces of human stratum corneum.

MECHANISM OF ACTION OF PENETRATION ENHANCERS

Before we consider the ways in which accelerants modify the horny layer, it is helpful to examine the constituents of the stratum corneum lipid fraction and how these are arranged. During epidermal differentiation, the composition of lipids changes from a polar character to a neutral mixture [15]. For whole stratum corneum, the major fractions are neutral lipids (78%) and sphingolipids (18%) together with a small amount of polar lipid. There is a considerable quantity of non-polar material present such as squalene and n-alkanes, totalling about 11%. Both saturated and unsaturated fatty chains exist in all neutral lipid species, with unsaturated chains predominating except for the free fatty acids fraction. The ceramide (sphingolipid) fraction comprises primarily saturated fatty acid chains. The n-alkanes range in a bell-shaped distribution from C_{19} to C_{34} [15].

Thus many lipid species exist in the horny layer, differing both in type and chain length; this complex lipid mixture forms bilayer structures [3,4,17–19], and Fig. 3 shows our idealised representation. The exact location and role of the nonpolar material (i.e. sterol esters, n-alkanes) is at present unclear. Also, no information if available as to whether or not the lipid structure exists in distinct solid and fluid domains or is totally homogeneous.

The four endothermic transitions T1-T4 which hydrated human stratum corneum typically provides under DSC were briefly interpreted above. T1 was allocated to lipid melting, possibly arising from the sebaceous lipids together with cholesterol side-chain motion. T4 was ascribed to irreversible protein conformational transition, i.e. denaturation. We propose that T2 arises from the melting of the lipid chains deep in the bilayer structure and that T3 develops from complete breakdown of any associations within the lipid polar head region. To aid further discussion we can add additional detail to the interpretation of T2 and T3 by considering lipid fluidity.

If the hydrocarbon tails of lipids in a bilayer structure are long and saturated, they can interact to form a somewhat rigid structure which can alter in two major ways. Firstly, if some hydrocarbon tails are unsaturated then kinks arising from cis double bonds reduce the tendency of the chains to pack closely and the structure increases in fluidity. Secondly, cholesterol is a major determinant of lipid bilayer rheology. Cholesterol molecules orientate themselves within the bilayer with their

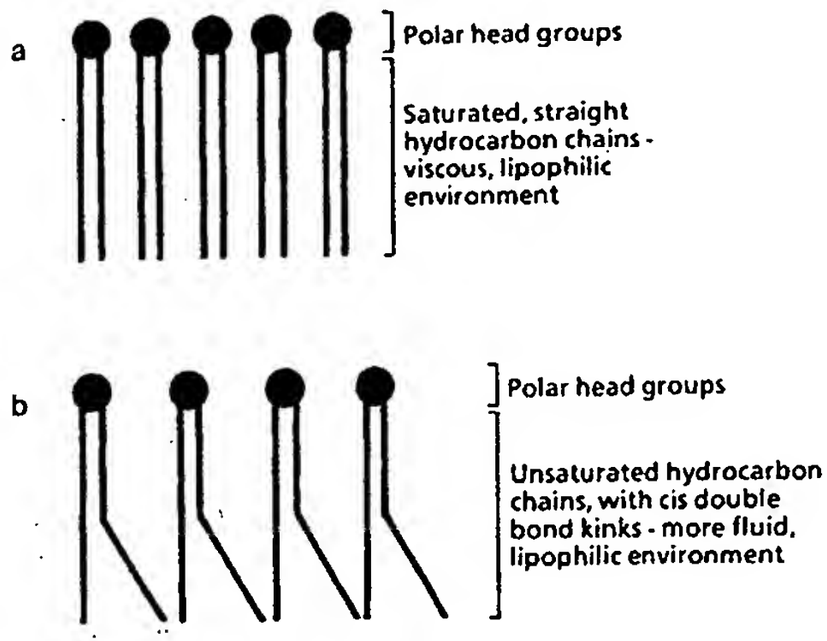

Fig. 4. The effect of composition on fluidity of the lipid bilayer: (a) saturated fatty acid chains packed tightly together; (b) kinks arising from cis double bonds dilate the structure; (c) the saucer-like steroid molecules of cholesterol interact with and partly immobilise the hydrocarbon chain region closest to the polar head groups, leaving the remainder of the chain flexible [22].

hydroxyl groups close to the lipid polar head region. Their saucer-like steroid rings interact with and partly immobilise the hydrocarbon chain region closest to the polar head groups, leaving the remainder of the chain more flexible. Cholesterol sulfate, although present in small amounts in normal stratum corneum, may be critically important for stabilizing lipid bilayers in the absence of phospholipids [4]. The effects of cholesterol and unsaturated chains on a lipid bilayer are illustrated in Fig. 4..

T2 may represent melting of the lower region of the lipid chains arising from increased molecular motion – this domain is the 'more fluid' region shown in Fig. 4. The endotherm may also include melting of some of the non-polar material present in the stratum corneum. T3 then represents the complete breakdown of the bilayer structure, encompassing disassociation of any head groups and the melting of the "cholesterol-stiffened" region.

We can now discuss the mechanism of action of the major penetration enhancers in the light of our understanding of the molecular structure of the stratum corneum. Fig. 5 illustrates the formulae of some common accelerants.

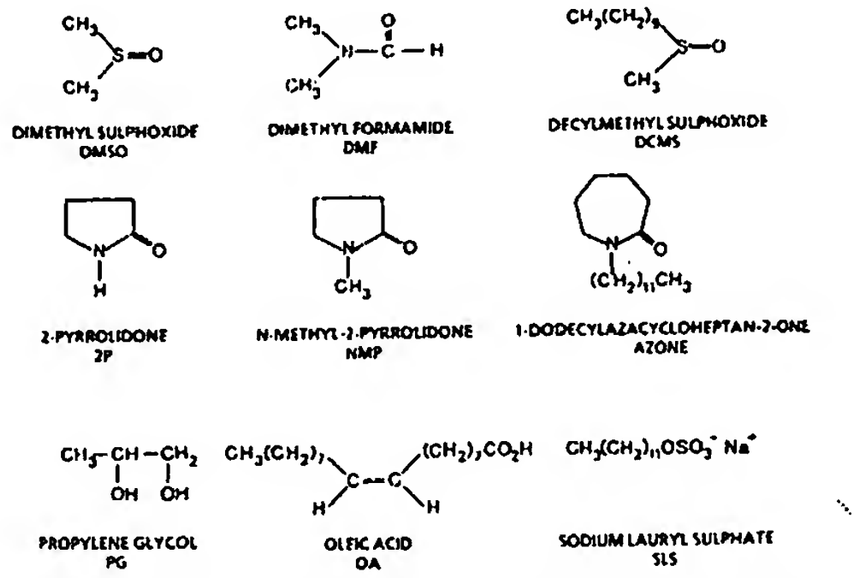

Fig. 5. Formulae of some common penetration enhancers.

Water

Water affected the stratum corneum DSC thermogram as follows. T1 was not greatly modified while T2 and T3 fell slightly in transition temperature as hydration increased up to 60% w/w. T2 was not affected in appearance, but T3 tended to enlarge and became thermally sharper. T4 fell considerably in temperature and also increased in thermal sharpness.

The fact that water lowered both major lipid endotherms demonstrated that the bilayer region had increased in fluidity. As lipids provide a significant part of the skin's barrier function, any reduction in the relevant intermolecular forces will allow drug to migrate more easily. This may help to explain why, for most molecules, hydration increases both polar and non-polar permeant fluxes; all drug chemicals will be more mobile in the less tightly

packed lipophilic region of the bilayer.

Figure 6 includes a schematic representation of how hydration promotes lipid fluidity as shown by reduced T2 and T3. Water molecules associated via hydrogen-bonding with lipid polar head groups forming a small hydration shell. This water insertion loosens the lipid packing, decreases intermolecular forces and hence reduced both T2 and T3. In addition hydrogen-bonding between the polar head groups and water could extend the network between these groups, so explaining why T3 enlarged. Thus water may act on T3 in two ways – it increases fluidity in the cholesterol-stiffened region but also enhances interactions between head groups.

The extended hydrophilic domain between the lipid polar head groups provides additional volume for drug permeation. Also water affects considerably the alphakeratin denaturation temperature. Dry stratum corneum is a dense structure with considerable spacial restriction on the rearrangement and folding of protein molecules i.e. denaturation. As the tissue hydrates it swells as the polar, proteinaceous region takes up most of the water. Thus as the water content rises, restrictions on protein rearrangements lessen and hence T4 falls. Also water competes for hydrogen-bonding sites on the protein chains, thus reducing interactions between them. Hence denaturation would require less energy, as revealed by a lower T4. Thus hydration aids drug mobility within the cell by creating a more fluid character and competing for hydrogen-bonding sites.

Dimethylsulfoxide (DMSO)

Most current theories on DMSO action consider that it displaces bound protein water, thereby substituting a looser structure [1]. It may also interact with the stratum corneum lipids. A major clue to DMSO action arises from the concentration-dependent behavior of this accelerant. It is well known that usually only high concentrations (above 60%) promote steady-state drug permeation through the skin. We have found a similar concentration dependence in terms of DMSO interaction with stratum corneum lipids. Treatment of the horny layer with solutions of 60% and above lowered the lipid transitions T2 and T3 with the effect becoming more pronounced with increased concentration. However DMSO interacted with stratum corneum protein even down to the 20% level.

The accelerant probably partitions preferentially into the polar cell contents of the tissue until it is at a fairly high concentration there. Afterwards it also partitions significantly into the intercellular domain.

These results imply that DMSO interaction

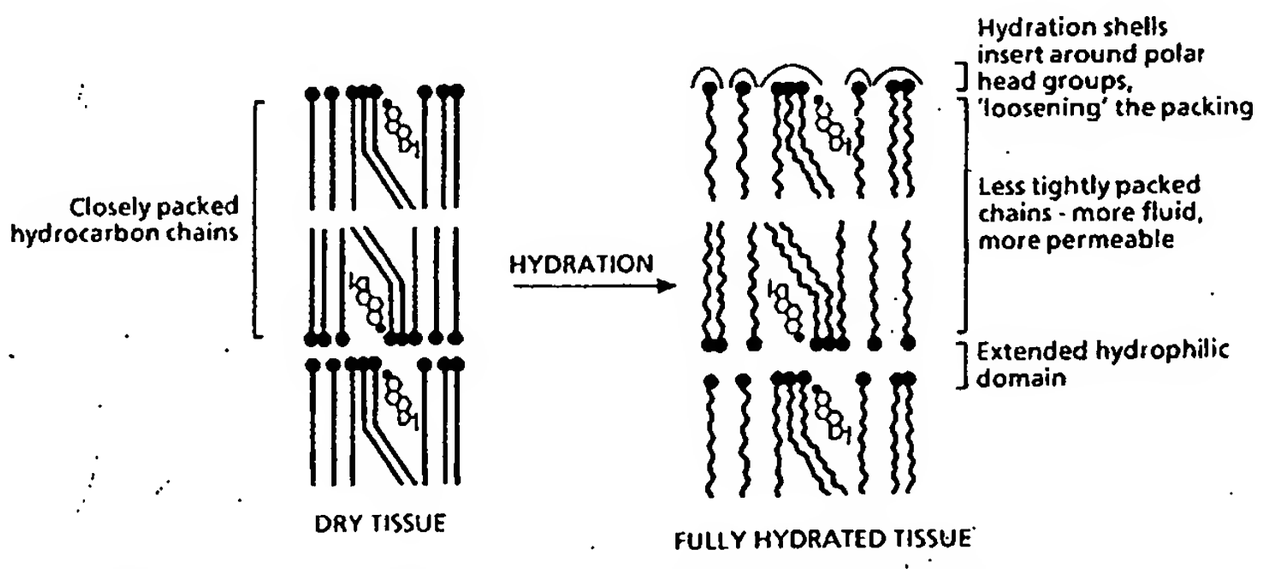

Fig. 6. How hydration increases the fluidity of the stratum corneum lipids by insertion of water molecules between polar head groups.

with stratum corneum lipids is important in its enhancing action. The accelerant lowered T2 and T3 considerably compared with a hydrated control. Thus DMSO increased lipid fluidity significantly more than did water and consequently it should also enhance drug mobility within this region as the lipid chains become less tightly packed. Because of the polar nature of DMSO (log [octanol/water] partition coefficient = −1.35), the accelerant should not partition directly into the lipid chains at least not in great amounts. If it did the lipid transitions should vanish entirely, which they did not. An interaction with the lipid polar head groups via hydrogen-bonding is more likely. DMSO is a powerful aprotic solvent which mixes exothermically with water. The enhancer may displace water from the lipid head groups and create a larger solvation shell around these groups. This larger shell could then loosen the lipid packing more than does water, which explains the lower transition temperatures.

As for water, lipid interaction may not be the only effect of DMSO on skin permeability. The expanded hydrophilic region between the lipid polar head groups may aid drug diffusion, particularly for polar materials. Also treatment of delipidised stratum corneum with increasing concentrations of DMSO made T4 smaller and broader. Thus DMSO may displace bound protein-water, substituting a looser structure in which permeants can move more freely. Additionally the solvent may occupy many hydrogen-bonding sites on the protein, leaving less available to bind and hinder molecular diffusion within the cells. As the lipids usually form the main diffusional barrier, this effect may not be significant until lipid fluidity increases. However, once the resistance of the lipid barrier falls, intracellular transport and its enhancement may become relatively more important.

A further indirect effect of DMSO on skin permeability arises from its solvent power for most drugs. High levels of the sulfoxide within the membrane help drugs to partition into the skin, thus promoting an increased flux. In suitable circumstances DMSO may operate via both mechanisms – reducing the skin's resistance and aiding drug partitioning (see Fig. 7).

Dimethylformamide (DMF), *N*-methyl-2-pyrrolidone (NMP) and 2-pyrrolidone (2P)

Like DMSO, the enhancers DMF, NMP and 2P are relatively polar powerful solvents which mix exothermically with water in all proportions. In our DSC work they exhibited similar properties to DMSO. At low concentrations they appeared to partition preferentially into the keratin regions as shown by them modifying T4. At higher concentrations, they also affected the lipid, as illustrated by reduced T2 and T3 temperatures i.e. these enhancers increased lipid fluidity. Thus it seems likely that DMF, NMP and 2P increase skin permeability in a similar manner to DMSO. At high concentrations their mode of action is to provide a substantial solvation shell around the polar head groups of the lipid and thus loosen lipid packing. Drug mobility within this region would then increase. However, as with DMSO, there may be secondary effects. Once the lipid resistance falls, increased intracellular transport may become more significant. Also these enhancers may promote drug partitioning into the skin, thereby increasing permeant flux. Overall the same mechanism of action as that depicted for DMSO in Fig. 7 probably applies to these enhancers.

Propylene glycol (PG)

The literature contains conflicting reports as to whether this molecule increases skin permeability. To help resolve this argument, and because PG is widely used in dermatological formulations and as a cosolvent for other accelerants, we examined PG-skin interactions by DSC and permeation studies. Overall, our results indicated that PG can act as a penetration enhancer. Its effect is most noticeable when

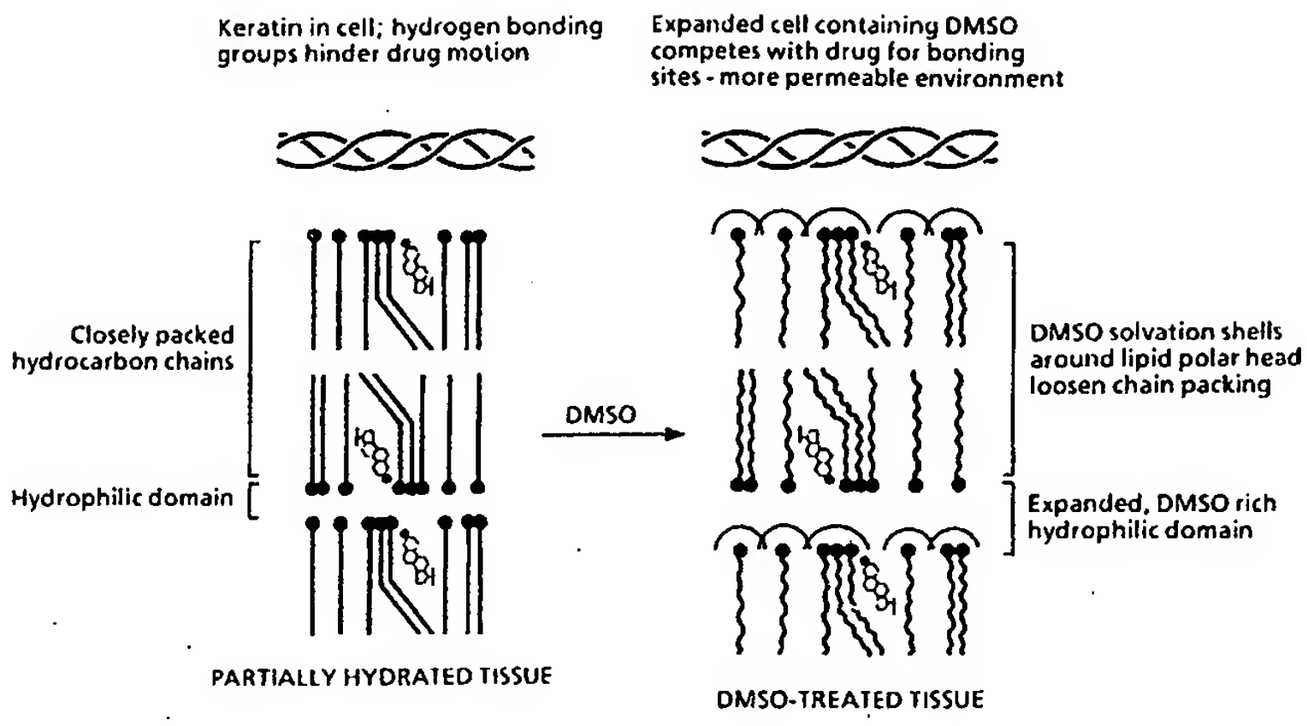

Fig. 7. Effect of dimethylsulfoxide on the permeability of human stratum corneum – interaction with intercellular lipids and cellular keratin.

used in the *in vivo* mimic situation (where the stratum corneum is not fully hydrated) either on its own or when operating synergistically with other accelerants (e.g. Azone and oleic acid). It probably works by solvating alpha-keratin and occupying hydrogen-bonding sites, thus reducing drug/tissue binding. However, it does not appear to influence horny layer lipid structure to any extent above that provided by water. Thus when applied alone to fully hydrated tissue, it does not increase drug permeation – but in this situation we should remember that the excessive amount of water present itself functions as a penetration enhancer. If PG is used combined with an accelerant which acts on the lipid barrier – such as Azone – then much glycol may enter the tissue and enhance intracellular drug diffusion more than water does. Propylene glycol promotes Azone penetration of skin and vice versa. Like the powerful polar solvents previously discussed, PG may also act by promoting drug partitioning into the skin, yielding higher fluxes.

Azone

We have examined in some detail the effects of Azone on the stratum corneum, in terms of DSC thermograms and permeability studies. In most situation, Azone dramatically affected the lipid structure. All three lipid transitions (T1, T2 and T3) disappeared from the resultant thermograms or were reduced markedly in size although not in temperature. This behaviour was quite different to the other enhancers, which did reduce T2 and T3 temperatures. Thus Azone probably increases skin permeability by a different mechanism to that proposed for molecules such as DMSO. In addition, Azone showed no protein interaction, suggesting that it does not enter the cells in significant amounts, at least at the low concentrations we used. This is understandable as Azone is a non-polar material (log [octanol/water] partition coefficient = 6.6).

The DSC data and Azone's non-polar nature suggested that it partitions directly into the lipid bilayer structure, disrupting it as illustrated in Fig. 8. Drug permeation through this less rigid environment would then increase.

Azone was much more effective in both steady-state and in vivo mimic experiments when used in conjunction with PG. An explanation for this behavior is that Azone enhances intercellular drug diffusion only; the intracellular protein contents, which offer considerable

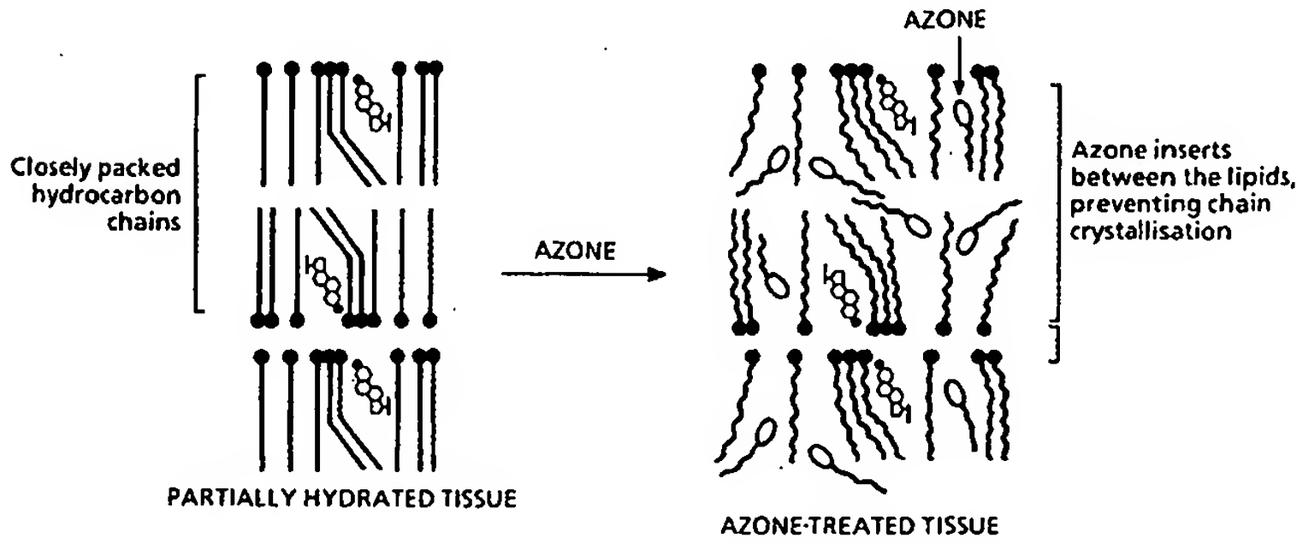

Fig. 8. Azone molecules disrupting the lipid structure of the intercellular region of the stratum corneum.

diffusional resistance, remain unaffected by this accelerant. However PG enhances intracellular transport, so the PG+Azone combination is more effective than Azone alone (see above).

Solvents such as PG and ethanol, once present in the stratum corneum, may help Azone to enter. For instance, PG molecules may occupy some hydrophilic regions between the lipid polar head groups. Azone, being more soluble in PG than in water, may then be able to partition more easily into the intercellular domain.

In the presence of high concentrations of mixtures such as Azone+PG, it is possible that the intercellular leaflet structure breaks down completely and globular micelles form, dispersed in a continuous phase of solvent. The horny layer would then become quite permeable [2].

Oleic acid (OA)

Cooper reported that materials such as OA, when used combined with a polar diol such as PG, promoted the percutaneous absorption of non-polar drugs [20]. However, our past work [7] and current studies demonstrated that OA also enhances polar drug absorption. Treatment of the stratum corneum with 5% OA in PG lowered T2 and T3 transition temperatures and slightly reduced endotherm sizes. T4 was also affected, but further work showed that this was because of the influence of the PG. Thus OA interacts only with the stratum corneum lipids. The behavior of this enhancer is somewhat similar to that of Azone, except that the lipid structure does not appear to be so drastically disrupted. OA possesses a cis double bond halfway along the C_{18} chain, i.e. it is kinked. Saturated fatty acids provide a major component of horny layer lipids. Thus OA probably operates by penetrating into the lipid structure, with its polar end close to the lipid polar heads. Because of its bent structure, it then disrupts and increases the fluidity of the lipid region, as illustrated in Fig. 9. Drug mobility in this less tightly packed arrangement will then increase. Once again, PG probably enhances intracellular drug mobility, and may aid OA to get to its site of action; both aspects make the PG/OA combination an effective accelerant.

Decylmethylsulfoxide (DCMS)

As with Azone, DCMS is effective at low concentrations, even down to 0.1%. As for accelerants in general, it enhances polar drug permeation more dramatically than non-polar penetration [7,21]. This phenomenon was reflected in our current diffusion work; DCMS was a more potent accelerant for 5-fluorouracil than for estradiol in both the steady-state and *in vivo* mimic methods.

In the DSC work, tissue samples treated with 15% DCMS in PG and 4% DCMS in water were

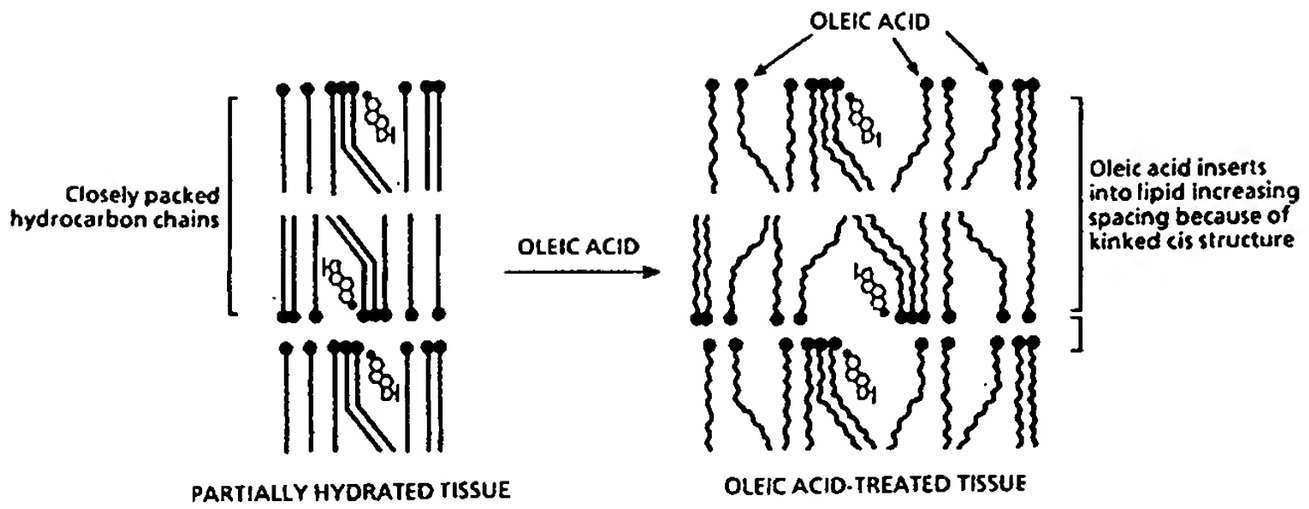

Fig. 9. Oleic acid increases the fluidity of intercellular lipids of the stratum corneum.

examined. The sulfoxide lowered T2, T3 and T4 transition temperatures with the accelerant increasing lipid fluidity more than did water. Cooper considered that the barrier-reducing mechanism of the sulfoxide was via protein/DCMS interaction [21]. He postulated that DCMS acted as a surfactant, changing protein conformations and thus opening up aqueous channels. Both his and our DSC work do suggest that this effect occurs (as seen from the lowered T4 endotherm). However we believe that in common with so many other accelerant studies so far performed, it is probably lipid interaction that is the important step in DCMS action (T2 and T3 were lowered by treatment with either 15% DCMS in PG or 4% DCMS in water). The molecule possesses a polar head and a saturated C_{10} tail; the tail could insert between the structured lipids in a manner similar to OA. However as the tail is not kinked, the lipid structure does not disrupt to the same extent as for OA – indeed T2 and T3 did not reduce in size as they did for OA and Azone. Nevertheless, the insertion of this relatively short chain should increase lipid fluidity; Fig. 10 illustrates a postulated mechanism. Overall, the mode of action of DCMS is similar to that of DMSO i.e. both sulfoxides increase lipid fluidity and interact with stratum corneum proteins, but much smaller concentrations of DCMS are necessary. This illustrates a difference between the two sulfoxides. DMSO may accumulate in quite high concentrations in the horny layer, as demonstrated by its swelling action. However, at the low effective levels of DCMS, this is unlikely to occur. Thus although a part of the action of DMSO may be to increase the partition coefficient of the drug (stratum corneum:vehicle), this will not occur with the usual levels of DCMS employed.

Sodium lauryl sulfate (SLS)

Anionic surfactants such as SLS grossly swell the stratum corneum, uncoiling and extending alpha-keratin helices and thereby opening up the protein-controlled polar pathway. In our work, 0.1–1% SLS solutions markedly affected all the endothermic transitions, reducing them in size and merging T2, T3 and T4. The effect was concentration dependent, with the DSC trace for 1% SLS being almost unrecognisable as a stratum corneum thermogram. Hence SLS disrupted the entire membrane affecting both protein and lipid structure. However, even the drastic effect of 1% SLS was at least partly reversible; thus SLS does not destroy lipid or protein structure entirely. The grossly swollen protein domain probably imbibes much water and thus permits drugs to permeate more freely. The expansion of intercellular spaces and the insertion of SLS molecules into the lipid structure also disrupts this region. Essentially, SLS – treated tissue is considerably more fluid than untreated tissue.

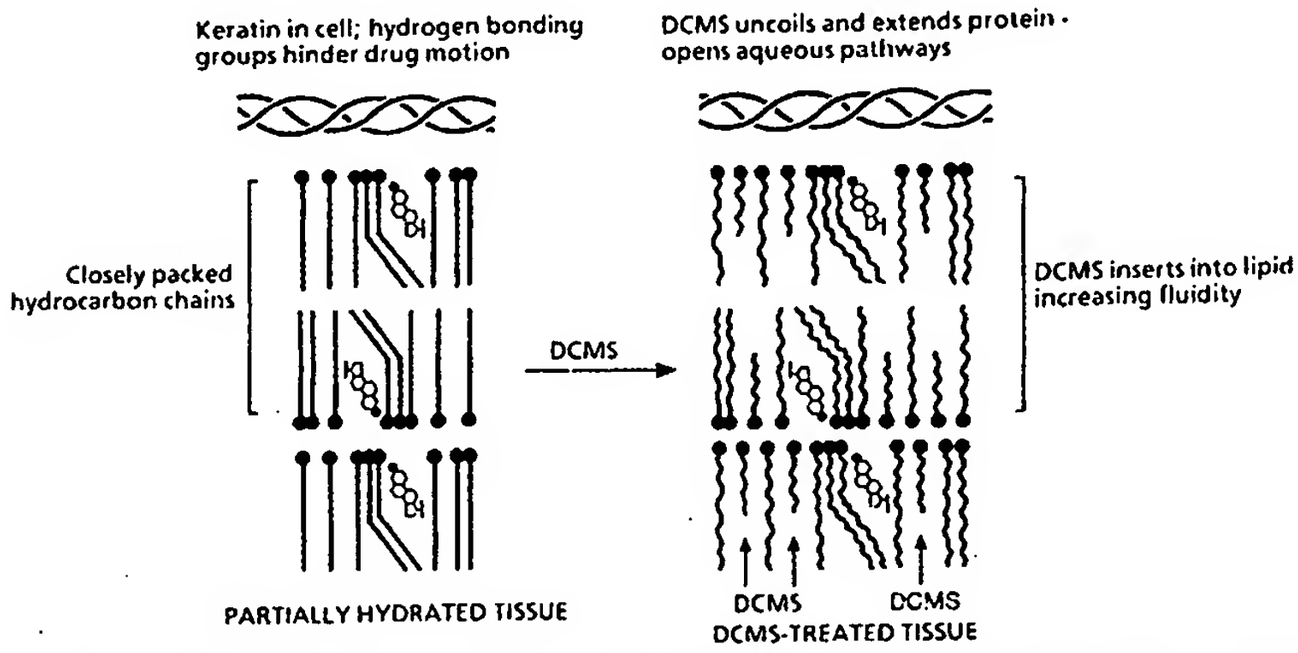

Fig. 10. Decylmethylsulfoxide modifies the permeability of human stratum corneum by interacting with intercellular lipids and cellular keratin.

SUMMARY OF PENETRATION ENHANCER ACTION

This paper has outlined proposed mechanisms of action for a variety of penetration enhancers, based on a reasonable representation of horny layer lipid structure, plus evidence from permeation and DSC studies. Our concepts of the mechanisms by which accelerants reduce the barrier function of the skin are summarised below.

1. The most significant finding from our DSC work is that *all* the penetration enhancers we investigated interacted in some way with the stratum corneum lipid structure, disrupting its organisation and increasing its fluidity. Such effects would permit drugs to permeate more readily through this less rigid environment.
2. Many accelerants also interacted with intracellular protein, as shown by the effect on alpha-keratin denaturation (T4). The exceptions were Azone and OA; however these were most effective when dissolved in a polar co-solvent such as PG, which itself interacted with protein. Although drug flux can increase via lipid interaction alone, once the lipid barrier weakens, the protein-filled cells may still provide a significant diffusional resistance. Thus an enhancer which affects both lipid and protein domains will be more potent. Intracellular drug transport could be increased by the solvating action of enhancers on the protein helices. This mechanism encompasses the displacement of bound protein-water, the expansion of protein structure, and the competition with permeants for hydrogen-bonding sites. These three actions may account for the reduced size and broadening of T4 arising from accelerant treatment.
3. The diffusional resistance of the intracellular contents alters markedly with skin hydration – water itself is quite a potent penetration enhancer. In dry tissue, the intracellular contents will be essentially solid and many hydrogen-bonding groups will be available to interact and hinder drug transport. Hence dry cells provide a significant barrier to diffusion. In the fully hydrated situation, the intracellular regions will be more fluid and water will compete for drug-binding sites, lowering the diffusional barrier. Therefore a material such as PG which exerts its major action on protein alone, will not show a significant additional enhancing effect in fully hydrated tissue. However, in

TABLE 1

Partition coefficients for penetration enhancers (log *P*, octanol/water)

Penetration Enhancer	Log *P*
Dimethylsulfoxide (DMSO)	−1.35
Dimethylformamide (DMF)	−1.01
N-methyl-2-Pyrrolidone (NMP)	−1
2-Pyrrolidone (2P)	−1
Propylene Glycol (PG)	−0.92
Azone	6.60
Oleic Acid (OA)	7.64
Decylmethylsulfoxide (DCMS)	3.42

the dry or partially hydrated situation it may have more impact.

4. Some penetration enhancers may act further on stratum corneum barrier function. Our DSC results demonstrated that small polar accelerants such as DMSO and its analogues, the pyrrolidones and PG may accummulate in both intercellular and protein regions of the tissue. The presence of these powerful solvents may then increase drug partitioning into the skin, yielding increased fluxes.
5. The mechanisms of action of enhancers can be related to their octanol/water partition coefficients (see Table 1). Small polar enhancers (e.g. DMSO, DMF, NMP and 2P) partition preferentially at low concentrations into the protein region of the stratum corneum. At high concentrations they interact with stratum corneum lipid, increasing its fluidity. Such a mechanism underlines the importance of reducing the lipid barrier, as these enhancers are only effective at high concentrations. Non-polar materials such as Azone and OA appear to enter the lipid regions only, where they disrupt the structure. DCMS, with an intermediate polarity, interacts with both protein and lipid. PG, a polar material, preferentially enters the keratin location, but does not exert much effect on lipid fluidity. Perhaps its hydrogen-bonding capacity is insufficient for it to interact significantly with the lipid polar head groups.

REFERENCES

1 B.W. Barry, Dermatological Formulations: Percutaneous Absorption, Marcel Dekker, New York, 1983.
2 B.W. Barry, Penetration enhancers; mode of action in human skin, C.I.R.D. Symposium Advances in Skin Pharmacology - Skin Pharmacokinetics, Nice, 1986.
3 P.W. Wertz, W. Abraham, L. Landmann and D.T. Downing, Preparation of liposomes from stratum corneum lipids, J. Invest. Dermatol., 87 (1986) 582.
4 M.L. Williams and P.M. Elias, The extracellular matrix of stratum corneum: role of lipids in normal and pathological function, CRC Critical Reviews in Therapeutic Drug Carrier Systems, 3 (1987) 95.
5 G.M. Golden, D.B. Guzek, R.R. Harris, J.E. McKie and R.O. Potts, Lipid thermotropic transitions in human stratum corneum, J. Invest. Dermatol., 86 (1986) 255.
6 K. Knutson, R.O. Potts, D.B. Guzek, G.M. Golden, J.E. McKie, W.J. Lambert and W.I. Higuchi, Macro- and molecular physical-chemical considerations in understanding drug transport in the stratum corneum, in: J.M. Anderson and S.W. Kim (Eds.), Advances in Drug Delivery Systems, Elsevier, Amsterdam, 1986, p. 67.
7 B.W. Barry and S.L. Bennett, Effect of penetration enhancers on the permeation of mannitol, hydrocortisone and progesterone through human skin, J. Pharm. Pharmacol., 39 (1987) 535.
8 M. Goodman and B.W. Barry, to be published.
9 B.W. Barry, D. Southwell and R. Woodford, Optimization of bioavailability of topical steroids: penetration enhancers under occlusion, J. Invest. Dermatol., 82 (1984) 49.
10 S.L. Bennett, B.W. Barry and R. Woodford, Optimization of bioavailability of topical steroids: non-occluded penetration enhancers under thermodynamic control. J. Pharm. Pharmacol., 37 (1985) 298.
11 B.F. Van Duzee, Thermal analysis of human stratum corneum, J. Invest. Dermatol., 65 (1975) 404.
12 M. Goodman and B.W. Barry, Differential scanning calorimetry (DSC) of human stratum corneum: effect of Azone, J. Pharm. Pharmacol., 37 (Suppl. (1985) 80P.
13 M. Goodman and B.W. Barry, Differential scanning calorimetry of human stratum corneum: effect of penetration enhancers Azone and DMSO, Analytical Proceedings, 26 (1983) 397.
14 M. Goodman and B.W. Barry, Action of skin penetration enhancers Azone, oleic acid and decylmethylsulphoxide; permeation and differential scanning

calorimetry (DSC) studies, J. Pharm. Pharmacol., 38 (Suppl. (1986) 71P.
15 M.A. Lampe, M.L. Williams and P.M. Elias, Human epidermal lipids: characterization and modulations during differentiation, J. Lipid Res., 24 (1983) 131.
16 M.A. Lampe, A.L. Burlingame, J.A. Whitney, M.L. Williams, B.E. Brown, E. Roitman and P.M. Elias, Human stratum corneum lipids: characterization and regional variations, J. Lipid Res., 24 (1983) 120.
17 P.M. Elias, Epidermal lipids, membranes, and keratinization, Int. J. Dermatol., 20 (1981) 1.
18 G. Imokawa, S. Akasaki, M. Hattori and N. Yoshizuka, Selective recovery of deranged water-holding properties by stratum corneum lipids, J. Invest. Dermatol., 87 (1986) 758.
19 P. Cox and C.A. Squier, Variations in lipids in different layers of porcine epidermis, J. Invest. Dermatol., 87 (1986) 741.
20 E.R. Cooper, Increased skin permeability for lipophilic molecules, J. Pharm. Sci., 73 (1984) 1153.
21 E.R. Cooper, Effect of decylmethyl sulfoxide on skin penetration, in: K.L. Mittal and E.J. Fendler (Eds.), Solution Behavior of Surfactants: Theoretical and Applied Aspects, Plenum Press, New York, 1982, p. 1505.
22 B. Alberts, D. Bray, J. Lewis, M. Raff, K. Roberts and J.D. Watson, Molecular Biology of The Cell, Garland Publishing Inc., New York, 1983, p. 259.

Pharmaceutical Research, Vol. 8, No. 3, 1991

Evidence that Oleic Acid Exists in a Separate Phase Within Stratum Corneum Lipids

Boonsri Ongpipattanakul,[1,2] Ronald R. Burnette,[2] Russell O. Potts,[1] and Michael L. Francoeur[1,3]

Received March 12, 1990; accepted August 29, 1990

Oleic acid is known to be a penetration enhancer for polar to moderately polar molecules. A mechanism related to lipid phase separation has been previously proposed by this laboratory to explain the increases in skin transport. In the studies presented here, Fourier transform infrared spectroscopy (FT-IR) was utilized to investigate whether or not oleic acid exists in a separate phase within stratum corneum (SC) lipids. Per-deuterated oleic acid was employed allowing the conformational phase behavior of the exogenously added fatty acid and the endogenous SC lipids to be monitored independently of each other. The results indicated that oleic acid exerts a significant effect on the SC lipids, lowering the lipid transition temperature (T_m) in addition to increasing the conformational freedom or flexibility of the endogenous lipid alkyl chains above their T_m. At temperatures lower than T_m, however, oleic acid did not significantly change the chain disorder of the SC lipids. Similar results were obtained with lipids isolated from the SC by chloroform:methanol extraction. Oleic acid, itself, was almost fully disordered at temperatures both above and below the endogenous lipid T_m in the intact SC and extracted lipid samples. This finding suggested that oleic acid does exist as a liquid within the SC lipids. The coexistence of fluid oleic acid and ordered SC lipids, at physiological temperatures, is consistent with the previously proposed phase-separation transport mechanism for enhanced diffusion. In this mechanism, the enhanced transport of polar molecules across the SC can be explained by the formation of permeable interfacial defects within the SC lipid bilayers which effectively decrease either the diffusional path length or the resistance, without necessarily invoking the formation of frank pores.

KEY WORDS: oleic acid; penetration enhancer; Fourier Transform Infrared Spectroscopy (FT-IR); lipid phase-separation transport mechanism.

INTRODUCTION

Previous calorimetric studies with porcine stratum corneum (SC) show that the T_m of the two lipid transitions, which occur between 60 and 70°C, are significantly reduced in the presence of oleic acid (1). This decrease in the lipid-associated T_m is correlated with the amount of oleic acid taken up by the SC, and the *in vitro* flux enhancement of ionically charged molecules, stressing the importance of the lipid pathway in skin transport. Further, the extent of enhancement increases with the concentration of the charged permeant within the applied vehicle, suggesting nonadherence to the classical pH-partition hypothesis. These observations, analyzed in the context of a number of phospholipid references (2–8) describing lateral phase separation, fatty acid phase behavior, and increased ion permeability at the gel–liquid crystal phase transition, suggest that the enhancement of transport across the skin may be related to a microperturbation of the SC lipid bilayer structure. Consequently, a mechanism is proposed in which oleic acid exists in a separate phase contained within the endogenous SC lipids, thereby forming a number of permeable defects at liquid–solid interfaces. This mechanism is also tacitly consistent with reports that increased TEWL occurs in a number of skin disorders characterized by lipid abnormalities, which may involve phase separation (9,10). Grubauer *et al.* (11) in fact, experimentally correlate TEWL to the presence of separate polar and nonpolar lipid phases in mouse skin. In the studies described here, Fourier transform infrared (FT-IR) spectroscopy was employed to investigate specifically the possibility of liquid–solid phase separation within the SC lipid domain in conjunction with oleic acid. A salient aspect of these studies is that the C-D stretching band is located at a lower wavenumber region, allowing the conformational behavior of ^{2}H-oleic acid to be differentiated from that of the endogenous SC lipids (12).

MATERIALS AND METHODS

Preparation of Stratum Corneum (SC) and Extracted Lipids

Full-thickness skin was obtained immediately after sacrifice from pigs weighing 15 to 30 kg. Only the thoracic sections were utilized. The hair was first clipped with standard shears and then dermatomed to a thickness of about 500 μm. As described elsewhere (13), skin sections of about 6 cm^2 were incubated with a 0.5% trypsin buffer (pH 7) to separate the SC from the epidermis. The isolated SC was rinsed briefly with cold hexane, then distilled H_2O, and air-dried before storing in a desiccator.

The lipids were isolated from the SC according to the method described by Wertz *et al.* (14). The SC was extracted successively in three different chloroform–methanol mixtures, each for 2 hr. These mixtures were 2:1, 1:1, and 1:2 chloroform–methanol, respectively. This series was then repeated at 1-hr intervals before finally extracting the SC overnight with methanol. All fractions were combined and evaporated to dryness under N_2. The dried lipid residue was placed under vacuum (~25 in. Hg) until a constant weight was achieved. The lipids were then stored under N_2 at −20°C until needed.

Treatment of the SC and Extracted Lipids with Oleic Acid

For these experiments, an ethanol solution of per-deuterated oleic acid (Cambridge Isotope Laboratories, Woburn, MA) was prepared to a final concentration of 300

[1] Dermal Therapeutics Group, Central Research Division, Pfizer Inc., Groton, Connecticut 06340.
[2] University of Wisconsin, School of Pharmacy, Department of Pharmaceutics, Madison, Wisconsin 53706.
[3] To whom correspondence should be addressed.

0724-8741/91/0300-0350$06.50/0

mg/ml. To treat the SC, an aliquot of 30 μl was layered on the apical side of a piece measuring about 4 cm^2. After evaporation of the ethanol, this tissue was carefully placed (same side up) in a 75% RH chamber for at least 24 hr. Subsequently, the SC was rinsed by briefly immersing the sample with forceps into three different solutions of cold ethanol. The excess ethanol was removed by gentle blotting and evaporation before the SC was reequilibrated at 75% RH. Untreated SC samples were also hydrated to 75% RH. In a separate set of experiments, the same treatment process described above was repeated several times using ^{3}H-oleic acid to quantitate the amount taken by the SC. The oleic acid content in SC was then measured by a standard liquid scintillation technique.

The extracted SC lipids were processed by a method similar to that reported by White *et al.* (15). The lipid residue was first dissolved in a small volume of chloroform–methanol (2:1) and dried under N_2 to a thin film. The lipids were dispersed in sufficient quantity of distilled H_2O to give a concentration of 1 mg/ml. This mixture was recycled through several heating/cooling cycles (up to 80°C) to obtain a uniform dispersion. Subsequently, 300 μl of this dispersion was deposited on the FT-IR window and partially dried in a $CaSO_4$ desiccator. The film was rehydrated at 75% RH before use. The treated samples were prepared by dissolving the ^{2}H-oleic acid in the initial chloroform–methanol mixture at a ratio of 1:2 (w/w; oleic acid:SC lipid) to approximate the amount of oleic acid taken up by the intact SC. This approximation assumes that all of the OA was taken up by the SC lipids, which constitute about 15% of the total SC mass (1). The ^{2}H-oleic acid spectrum (Fig. 4) was obtained in a similar manner by placing 20 μl between two FT-IR windows.

FT-IR Spectroscopy

Infrared spectra were recorded with a Nicolet 730 FT-IR spectrophotometer (Nicolet, Madison, WI) equipped with a liquid N_2 cooled MCT detector. To obtain a spectrum at each temperature, three groups of 64 scans were collected at 0.5-cm^{-1} resolution, coadded, and transformed using a Happ-Genzel apodization function. The samples were contained between ZnS (IRTRAN 2, SpectraTech, Stamford, CT) windows mounted in a specially designed heating/cooling cell. The cell was connected to a Lauda low-temperature water circulator (Model RC-6, Brinkman Instruments, Westbury, NY), which was controlled by a separate computer interfaced to the spectrometer workstation. The circulating fluid consisted of a 50% ethylene glycol–H_2O mixture. The ZnS windows were sealed around the edge with electrical tape, and an Alumel–Chromel thermocouple (Omega, Stamford, CT) was inserted through a hole drilled in one sample window to monitor directly the sample temperature to within ±0.2°C. The spectra were collected at 1 to 5°C increments as programmed by the water bath computer. Overall, the rate of temperature increase averaged less than 20°C/hr. To eliminate optical channeling in the frequency domain, the appropriate part of the interferogram was replaced with a straight line before transformation (16). Peak positions were determined using the software supplied by Nicolet, which was based on a polynomial least-squares method (17), or with a center of gravity algorithm (18) allowing frequencies, in all cases, to be determined with an uncertainty of less than 0.1 cm^{-1}.

RESULTS AND DISCUSSION

FT-IR Spectra

An infrared spectrum, spanning from about 3000 to 1900 cm^{-1}, is illustrated in Fig. 1 for a porcine SC sample which had been treated with ^{2}H-oleic acid. Of particular interest for these studies are the C–H and C–D symmetric stretching frequencies found at approximately 2850 and 2090 cm^{-1}, respectively. The significance of these particular bands is that they reflect, on a molecular level, conformational changes of the alkyl lipid chains (19–21). Specifically, as gauche conformers are introduced along the hydrocarbon chain, the stretching frequency shifts to higher values due to steric hindrance of partially eclipsed methylene groups along the lipid molecular axis. The increase in the number of gauche conformers is associated with increased conformational freedom and flexibility of the alkyl chains leading to a reduction in bilayer thickness and segmental order. The inflection midpoint of the temperature-frequency curve, consequently, can be taken as the T_m for the corresponding calorimetric phase transition (22). For these data the inflection point, or T_m, was estimated graphically (12).

Figure 2 illustrates the changes in $\nu_s(CH_2)$ obtained for the oleic acid-treated and the untreated SC as a function of temperature. For these experiments, the average concentration of oleic acid taken up by the SC was determined to be 60 μg/mg SC (SE = 4.0, n = 6). The incorporation of oleic acid did not have a significant effect on the conformational order of the endogenous lipids below the T_m, as there was no statistical difference (α = 0.05) between the $\nu_s(CH_2)$ for the treated and that for the control samples (Table I). Treatment with oleic acid did, however, lower the T_m of the inherent SC lipids by 7.7°C (SE = 1.3, n = 4), in agreement with results obtained by differential scanning calorimetry (1,23). At temperatures above the T_m, higher values ($P < 0.05$) for $\nu_s(CH_2)$ were found in the treated samples, indicating that fluid SC lipids are further disordered in the presence of oleic acid. Similar effects of oleic acid were observed in the extracted SC lipid samples (Fig. 3). There was no difference (α = 0.05) between the conformational order of the treated and that of

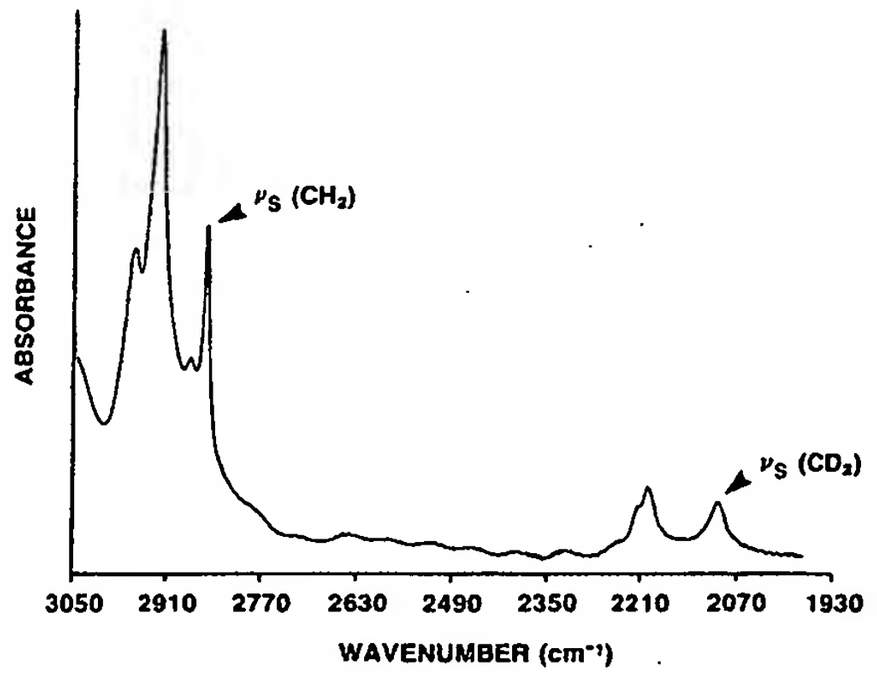

Fig. 1. Partial infrared spectrum of porcine stratum corneum treated with per-deuterated oleic acid. Note the separate C–H and C–D stretching bands at about 2850 and 2096 cm^{-1}.

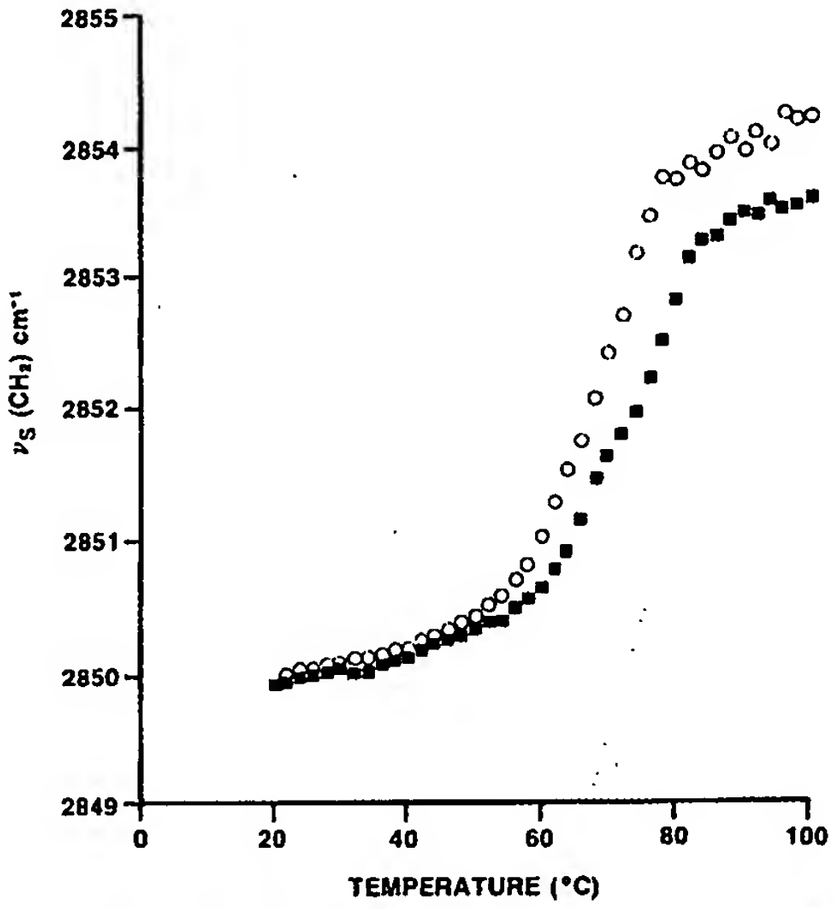

Fig. 2. The change in C–H symmetric stretching frequency, $\nu_s(CH_2)$, for porcine stratum corneum as a function of temperature. Included are the oleic acid-treated and the untreated (control) samples. ■, control; ○, ^{2}H-OA treatment.

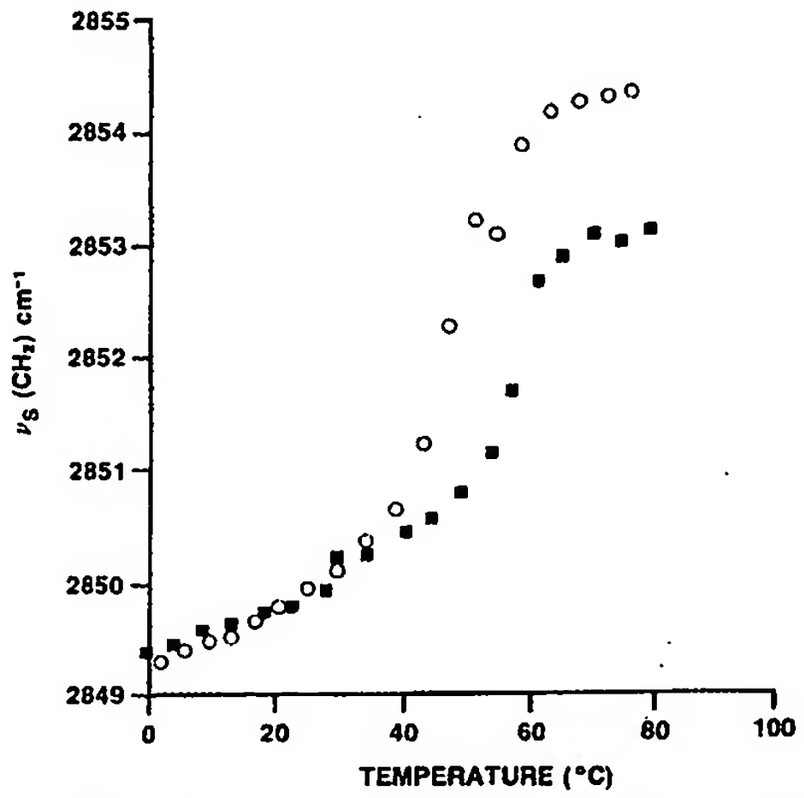

Fig. 3. The change in C–H symmetric stretching frequency, $\nu_s(CH_2)$, for lipids extracted from porcine stratum corneum as a function of temperature. Included are untreated and oleic acid-treated lipid samples. ■, control; ○, ^{2}H-OA treatment.

the control lipids below the T_m, but like the intact SC, the oleic acid-treated extracts showed greater ($P < 0.05$) disorder above the T_m (Table I). The T_m of the extracted lipids was likewise shifted to a lower value ($\Delta T_m = -9.5$°C, SE = 1.25, $n = 3$).

The decrease in T_m for the endogenous SC lipids following treatment with oleic acid can be partially explained on the basis of thermodynamic principles. At the SC lipid phase transition, $\Delta G = 0$ since the respective lipid phases are in equilibrium. Accordingly, T_m will be equal to $\Delta H/\Delta S$, where $\Delta S = S_{final} - S_{initial}$. Previous calorimetric experiments have indicated that the $\Delta H_{SC\ LIPIDS}$ is only slightly altered by oleic acid (1), suggesting that an increase in ΔS may, in part, account for the reduction in T_m. Indeed, the changes in $\nu_s(CH_2)$ above the T_m suggest that oleic acid increases S_{final} with no effect on $S_{initial}$. No change in $S_{initial}$ implies that the mechanism by which the transport of polar molecules, at physiological temperatures, is enhanced must be due to subtle microphysical changes within the lipid bilayers, and cannot be ascribed to macroscopic perturbation or fluidization.

The increase in conformational disorder or entropy of the endogenous fluid SC lipids may reflect at least two effects. Deuterium NMR and FT-IR studies have shown that the greatest conformational disorder exists toward the middle of the bilayer for fluid phospholipids (24,25). The methylene groups closest to the polar head region remain somewhat ordered, even in the liquid-crystalline state. If this analogy holds here for the SC lipids, it can be speculated that oleic acid exerts its primary effect(s) on the first 6 to 10 alkyl carbons proximal to the polar region of the bilayer. The other possible explanation is that oleic acid may increase the fraction of total lipids which have undergone a fluid phase transition. The latter possibility, though, would suggest that there are normally ordered lipids present in the untreated SC above the observed phase transition. While infrared spectroscopic analysis cannot distinguish between the two effects, X-ray diffraction studies suggest that it is unlikely that these ordered lipids exist at 90°C (15). Thus, these results suggest that oleic acid primarily disorders the alkyl chain near the polar region of the bilayers. No effect by oleic acid on the terminal $-CH_3$ (data not shown) stretching above the T_m support this conclusion.

The net frequency changes for the ^{2}H-oleic acid and the SC lipids are compared in Table II. While the C–H stretching frequency for the SC lipids increases by 4 to 5 cm^{-1}, the corresponding change in the C–D value is less than 1 cm^{-1}. Thus, it is apparent that the oleic acid present in the SC or extracted lipids does not undergo a major phase transition. Furthermore, the actual value of $\nu_s(CD_2)$ at 32°C is approximately 2097 cm^{-1}. As shown by Fig. 4, a frequency of 2097 cm^{-1} corresponds to ^{2}H-oleic acid that is almost fully disordered. Therefore, it can be concluded that the alkyl chains of the ^{2}H-oleic acid within the SC are, on average, in the

Table I. The Symmetric Stretching Frequency, $\nu_s(CH_2)$, for Stratum Corneum and Extracted Lipids Treated with ^{2}H-Oleic Acid: The Temperatures Represent Values Above and Below the Transition (see Figs. 2 and 3)

	Stratum corneum		Extracted lipids	
	30°C	90°C	20°C	75°C
Control	2850.1 (0.1)[a] $n = 8$	2853.4 (0.1)[a] $n = 7$	2849.7 (0.0)[a] $n = 2$	2853.2 (0.2)[a] $n = 2$
Oleic acid treated	2850.1 (0.1) $n = 4$	2854.2 (0.2) $n = 4$	2849.7 (0.1) $n = 2$	2854.2 (0.2) $n = 2$

[a] Numbers in parentheses represent SE.

Table II. The Symmetric Stretching Frequency, $\nu_s(CD_2)$, for ^2H-Oleic Acid in Treated Stratum Corneum and Extracted Lipid Samples

Temperature (°C)	Stratum corneum	Extracted lipids
20	2096.9 (0.5)[a]	2097.1 (0.0)
30	2097.2 (0.6)	2097.4 (0.2)
40	2097.5 (0.4)	2097.6 (0.1)
50	2097.8 (0.2)	2098.3 (0.4)
60	2098.3 (0.2)	2098.7 (0.0)
70	2098.0 (0.1)	2098.4 (0.0)
80	2098.0 (0.1)	2098.3 (0.1)
90	2097.6 (0.3)	—
100	2097.8 (0.1)	—

[a] Numbers in parentheses represent SE where $n = 2$.

liquid state. It should be noted that this FT-IR analysis cannot measure the long-range order of the liquid oleic acid molecules to establish whether the fatty acid is dispersed in the same plane as the endogenous lipid bilayer or if it induces the formation of a more exotic domain such as a hexagonal II phase. In either case, the ideas of phase-separated defects and enhanced transport would still apply. At this time, the precise composition of the lipid phase containing the liquid oleic acid is not known. It is likely that the oleic acid exists in a heterogeneous phase containing one or more other SC lipid components (e.g., cholesterol) and, as such, would not

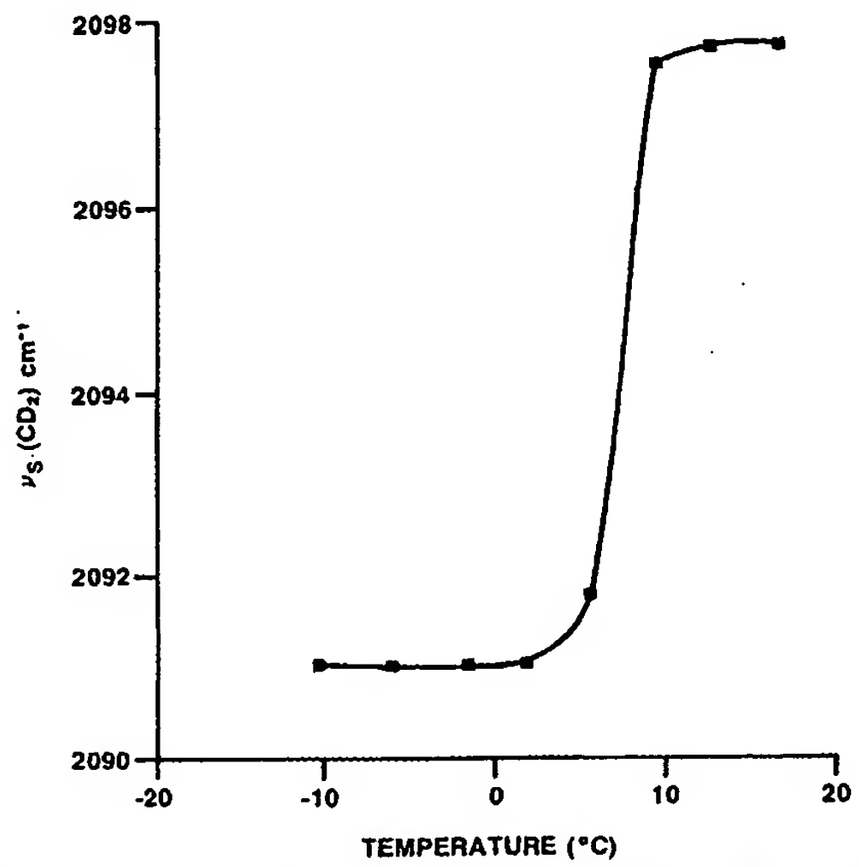

Fig. 4. The change in C–D symmetric stretching frequency, $\nu_s(CD_2)$, for pure ^2H-oleic acid as a function of temperature.

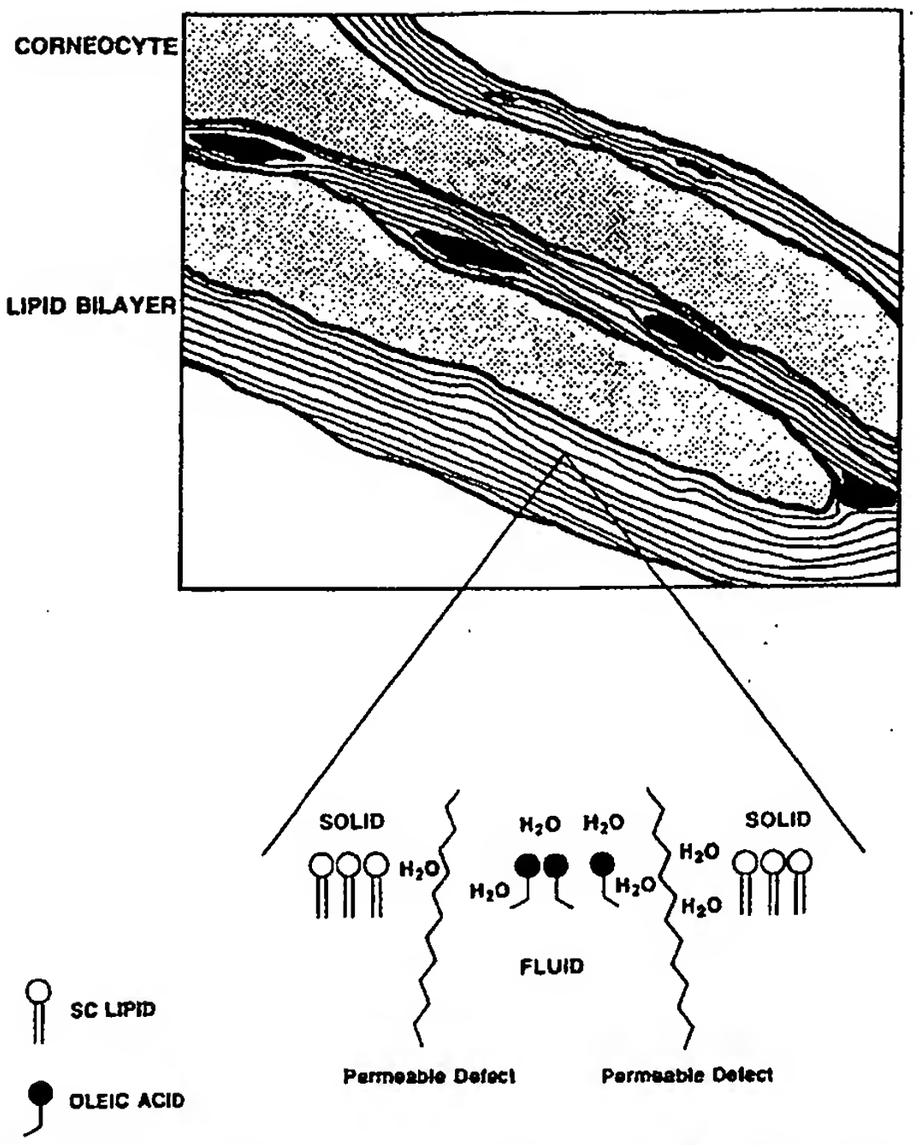

Fig. 5. Simplified schematic representation for one type of permeable defect which could be formed within the lipid bilayers. Stratum corneum illustration is an actual tracing of an electron micrograph (~385,000×), with the dark intercellular patches attributed to desmosomal fragments.

be expected to manifest a separate cooperative phase transition. Nevertheless, it is unequivocal that the oleic acid molecules in the SC at physiological temperatures are in the liquid state and, therefore, are phase-separated from the endogenous solid lipids.

While previous reports have correctly concluded that oleic acid increases the overall alkyl-chain disorder of the SC lipids (23,26), the changes in the $\nu_s(CH_2)$ under those conditions reflect an average contribution from both oleic acid and the endogenous lipids. Hence, the oleic acid must be in the fluid state to account for the overall increase in $\nu_s(CH_2)$ which is observed. The conformational behavior of the SC lipids and the added fatty acid in these FT-IR experiments here was resolved with the use of per-deuterated oleic acid.

Phase Separation Hypothesis for Enhanced Transport

The possible significance of oleic acid, existing as a separate liquid phase in the SC lipids, to increased skin transport can be inferred from the phospholipid literature (2–8). Anomalously high diffusion rates for small ions such as Na^+ and K^+ are reported for various phospholipid systems which are heated to their phase transition temperature (2,5). The enhanced flux of these ions is thought to be related to the formation of permeable defects at the fluid–solid interface of lipids at their T_m. In addition, enhanced ion transport is observed in two component lipid systems which exhibit lateral phase separation (3,4). Given the likely existence of separate liquid and solid phases within oleic acid-treated SC lipids,

and previous results (1) that show a dramatic increase in permeability of charged compounds, it seems reasonable to propose a similar mechanism of enhanced skin transport. For any molecule to diffuse across the SC it must, at some point, encounter the lipid bilayers, as they are the only continuous structure. The formation of some type of permeable interfacial defects (Fig. 5) within the bilayer could explain the enhanced transport by reducing either the diffusional path length or the resistance. Further, the apparent tendency of oleic acid to increase the transport of charged or polar molecules suggests that the defect areas may also be associated with water (1,6). In conclusion, the FT-IR results obtained here with oleic acid are consistent with, but do not prove, this type of mechanism.

ACKNOWLEDGMENTS

The authors would like to acknowledge Ms. Guia Golden, Ms. Julie Humm, and Mr. Bill Peterson for their technical assistance and enthusiasm and Dr. Doug Mann for supplying porcine skin samples. In particular, the comments and thoughts of Drs. Vivien Mak, Richard Guy, and Bill Curatolo are greatly appreciated. This research was funded, in part, through a Pfizer summer extern program sponsored by Pharmaceutical R&D.

REFERENCES

1. M. L. Francoeur, G. M. Golden, and R. O. Potts. Oleic acid: Its effects on stratum corneum in relation to (trans)dermal drug delivery. *Pharm. Res.* 7:621 (1990).
2. M. C. Blok, E. C. M. Van Der Neut-Ko, L. L. M. Van Deenen, and J. DeGier. The effect of chain length and lipid phase transitions on the selective permeability properties of liposomes. *Biochim. Biophys. Acta.* 406:187–196 (1975).
3. S. H. W. Wu and H. M. McConnell. Lateral phase separations and perpendicular transport in membranes. *Biochem. Biophys. Res. Comm.* 55:484 (1973).
4. E. J. Shimshick, W. Kleeman, W. L. Hubbell, and H. M. McConnell. Lateral phase separations in membranes. *J. Supramol. Struct.* 285–295 (1973).
5. D. Papahadjopoulos, K. Jacobson, S. Nir, and T. Isac. Phase transitions in phospholipid vesicles. Fluorescence polarization and permeability measurements concerning the effect of temperature and cholesterol. *Biochim. Biophys. Acta* 311:330–348 (1973).
6. R. Klausner, A. Kleinfeld, R. Hoover, and M. Karnovsky. Lipid domains in membranes. Evidence derived from structural perturbations induced by free fatty acid and lifetime heterogeneity analysis. *J. Biol. Chem.* 255:1286–1295 (1980).
7. A. Ortiz and J. Gomez-Fernandez. A differential scanning calorimetry study of the interaction of free fatty acids with phospholipid membranes. *Chem. Phys. Lipids* 45:75–91 (1987).
8. S. Verma, D. Wallach, and F. Sakura. Raman analysis of the thermotropic behavior of lecithin-fatty acid systems and of their interaction with proteolipid apoprotein. *Biochemistry* 19:574–579 (1980).
9. S. J. Rehfeld, M. L. Williams, and P. M. Elias. Interactions of cholesterol and cholesterol sulfate with free fatty acids. Possible relevance for the pathogenesis of recessive X-linked ichthyosis. *Arch. Dermatol. Res.* 278:259–263 (1986).
10. P. M. Elias and M. L. Williams. Neutral lipid storage disease with ichthyosis. *Arch. Dermatol.* 121:1000–1008 (1985).
11. G. Grubauer, K. R. Feingold, R. M. Harris, and P. M. Elias. Lipid content and lipid type as determinants of the epidermal permeability barrier. *J. Lipid Res.* 30:89–96 (1989).
12. R. A. Dluhy, D. J. Moffatt, D. G. Cameron, R. Mendelsohn, and H. H. Mantsch. Characterization of cooperative conformational transitions by Fourier transform infrared spectroscopy: Application to phospholipid binary mixtures. *Can. J. Chem.* 63:1925–1932 (1985).
13. G. M. Golden, D. L. Guzek, A. H. Kennedy, J. E. McKie, and R. O. Potts. Stratum corneum lipid phase transitions and water barrier properties. *Biochemistry* 26:2382–2388 (1987).
14. P. W. Wertz and D. T. Downing. Covalently bound ω-hydroxyacylsphingosine in the stratum corneum. *Biochim. Biophys. Acta* 917:108–111 (1987).
15. S. H. White, D. Mirejovsky, and G. I. King. Structure of lamellar lipid domains and corneocyte envelopes of murine stratum corneum. *Biochemistry* 27:3725–3732 (1988).
16. D. J. Moffatt and D. G. Cameron. Location of low-frequency fringe signatures in Fourier-transforms of spectra. *Appl. Spectrosc.* 37:566 (1983).
17. R. N. Jones and K. S. Seshadri. The objective evaluation of the position of infrared absorption maxima. *Can. J. Chem.* 40:334 (1962).
18. D. G. Cameron, J. K. Kauppinen, D. J. Moffatt, and H. H. Mantsch. Precision in condensed phase vibrational spectroscopy. *Appl. Spectrosc.* 36:245–250 (1982).
19. R. Mendelsohn, R. A. Dluhy, J. Taraschi, D. G. Cameron, and H. H. Mantsch. Raman and Fourier transform infrared spectroscopic studies of the interaction between glycophorin and dimysteroylphosphatidylcholine. *Biochemistry* 20:6699–6706 (1981).
20. D. G. Cameron and H. H. Mantsch. Metastability and polymorphism in the gel phase of 1,2-dipalmitoyl-3-sn-phosphatidylcholine. A Fourier-transform infrared study of the subtransition. *Biophys. J.* 38:175–184 (1982).
21. C. Huang, J. R. Lapides, and I. W. Levin. Phase transition behavior of saturated, symmetric chain phospholipid bilayer dispersions determined by Raman spectroscopy: Correlation between spectral and thermodynamic parameters. *J. Am. Chem. Soc.* 104:5926–5930 (1982).
22. D. A. Wilkinson and J. F. Nagle. Dilatometry and calorimetry of saturated phosphatidylethanolamine dispersions. *Biochemistry* 20:187–192 (1981).
23. G. M. Golden, J. E. McKie, and R. O. Potts. Role of stratum corneum fluidity in transdermal drug flux. *J. Pharm. Sci.* 76:25–28 (1987).
24. A. Seelig and J. Seelig. The dynamic structure of fatty acyl chains in a phospholipid bilayer measured by deuterium magnetic resonance. *Biochemistry* 13:4839–4845 (1974).
25. R. G. Snyder, M. Maroncelli, H. L. Strauss, C. A. Elliger, D. G. Cameron, H. L. Casal, and H. H. Mantsch. Distribution of gauche bonds in crystalline n-$C_{21}H_{44}$ in phase II. *J. Am. Chem. Soc.* 105:133–134 (1983).
26. V. H. W. Mak, R. O. Potts, and R. H. Guy. Oleic acid concentration and effect on human stratum corneum: Non-invasive determination by attenuated total reflectance infrared spectroscopy in vivo. *J. Control. Release* 12:67–75 (1990).

Chem. Pharm. Bull. 41(8) 1434—1437 (1993) Vol. 41, No. 8

Effects of Oleic Acid/Propylene Glycol on Rat Abdominal Stratum Corneum: Lipid Extraction and Appearance of Propylene Glycol in the Dermis Measured by Fourier Transform Infrared/Attenuated Total Reflectance (FT-IR/ATR) Spectroscopy

Yoshikazu TAKEUCHI,*[,a] Hidehito YASUKAWA,[a] Yumiko YAMAOKA,[a] Naoki TAKAHASHI,[a] Chizu TAMURA,[a] Yasuko MORIMOTO,[a] Shoji FUKUSHIMA,[a] and Ravindra C. VASAVADA[b]

Department of Pharmaceutics, Faculty of Pharmaceutical Sciences, Kobe-Gakuin University,[a] Arise Igawadani-cho, Nishi-ku, Kobe 651–21, Japan and School of Pharmacy, University of The Pacific,[b] 3601 Pacific Avenue, Stockton, California 95211, U.S.A. Received January 11, 1993

Fourie transform infrared/attenuated total reflection analysis demonstrated that the absorbance intensity of C=O stretching bands, which reflect the amounts of lipids in the stratum corneum, decreased with an increase in the duration of skin treatment with 0.15 M oleic acid/propylene glycol (PG) system, suggesting that the oleic acid/PG system induced the lipid extraction, which was followed by a reorganization of the stratum corneum structures. The spectral peaks which originated from the PG molecule were detected in dermal tissues after 30 min of treatment of the stratum corneum with the same system. This observation suggested that the reorganization of the lipid domains due to the lipid extraction by the oleic acid/PG system helped the PG molecules enter the dermal tissues. It was also suggested that an effective volume within the stratum corneum for solutes and/or solvents which could penetrate through the inter-, and/or intracellular routes could be altered in conjunction with the structural changes of the lipids.

Keywords oleic acid; propylene glycol; stratum corneum; delipidization; dermis; FT-IR/ATR spectroscopy

Oleic acid has been studied as a skin penetration enhancer for drugs primarily *via* its action primarily on stratum corneum lipid structures.[1–3] As to the behavior of oleic acid in the skin, Francoeur *et al.* suggested[4,5] that fluid oleic acid and ordered stratum corneum lipids can coexist when the oleic acid is taken into the stratum corneum at a normal physiological temperature. In their experiment, the action of oleic acid on the stratum corneum resulting in the permeability enhancement of drugs was examined in the single component system of oleic acid. One might suggest that the skin penetration enhancing effect of vehicles would be different depending upon the system used. For example, if one used a combined system consisting of two or more materials which affected the membrane structures, the permeant flux might be enhanced by the complex action of coexisting penetration enhancers. It was reported that the penetration of both polar[6] and non-polar[7] drugs through the skin was enhanced by oleic acid when used in combination with propylene glycol (PG). Such an enhancement was considered to be the result of two different mechanisms in which PG enhanced intracellular drug mobility by solvating alphakeratin in corneocytes, allowing oleic acid to act on the lipid barrier.[8] As to the perturbation of the stratum corneum, the lipid extraction from the stratum corneum could also be an important factor for permeants to penetrate the epidermal lipid barrier. Based on these considerations, factors affecting permeant flux and/or stratum corneum structures should be elucidated on an individual basis considering all components that make up the permeant-containing vehicle.

We have examined the spectral behavior of the rat stratum corneum following treatment of the skin surface with fatty acids and fatty amines in PG using Fourier transform infrared/attenuated total reflection (FT-IR/ATR) in relation to the permeant flux of hydrophilic and hydrophobic solutes, 5- and 6-carboxyfluorescein (CF) and indomethacin, respectively.[9,10] In this experiment, it was found that some fatty acids and fatty amines in PG, as well as PG alone, could alter the conformation of stratum corneum keratinized proteins. Such conformational changes were possibly due to the incorporation of the fatty acid and the fatty amine into the lipid domains and corneocytes when used in combination with PG. In this paper, we have investigated the time profiles of structural changes in the stratum corneum lipids by measuring CH_2 asymmetric stretching vibrations resulting primarily from acyl chains of the stratum corneum lipids. We also examined the ability of the oleic acid/PG vehicle to remove lipids from the rat stratum corneum with increasing duration of exposure of the skin to oleic acid in PG. The appearance of PG into the dermal tissues was also pursued following treatment of the skin with oleic acid in PG by measurement of PG spectra using FT-IR/ATR.

Materials and Methods

Materials Oleic acid and propylene glycol, both of reagent grade, were purchased from Nakaloai Tesque. All other chemicals were also of a reagent grade.

Skin Preparation for FT-IR/ATR Spectroscopy Measurement As previously reported,[9,10] the abdominal skin was removed from male Wistar rats (8—9 weeks old) under pentobarbital anesthesia, shaved with an electric clipper and then with an electric razor. The freshly excised full thickness skin with subcutaneous fat removed was weighed. The skin surface area available for FT-IR/ATR measurement was 1.05 cm^2. The skin samples were then mounted between the two compartments of the diffusion cells with the dermis side facing the receiver compartment. The formulations used were PG with or without oleic acid in a concentration of 0.15 M. One gram of the vehicle was applied into the donor compartment. The donor compartment was sealed from the atmosphere with Parafilm®. The receiver compartment was filled with 14.2 ml of a phosphate buffered solution (PBS; 140 mM NaCl, 2.68 mM KCl, 8.10 mM Na_2HPO_4 and 1.47 mM KH_2PO_4, pH 7.4). The assembled diffusion cells were then immediately immersed in a water bath at 37 °C and the buffer solution was stirred with a magnetic stirrer. The receiver compartments were maintained at 37 °C. Each of the skin samples was taken out from the cell at appropriate time

intervals after the incubation. The surface of the stratum corneum was gently wiped with Kimwipes® and then left as it was for 10 min at ambient temperature. For FT-IR/ATR measurement, the skin was placed on the element with the epidermal surface attached to the reflection surface, then the spectra of the epidermal surface was measured. The same procedure was also used in the measurement of PG that appeared in dermis, with the exception of the skin being placed on the element with the dermal surface attached to the reflection surface so that the spectra of the dermal surface were obtained.

FT-IR/ATR Spectroscopy Measurement IR spectra of the surface of either the stratum corneum or the dermal tissues were obtained at an ambient temperature with a JEOL JTR-100 FT-IR spectrometer equipped with a liquid nitrogen-cooled, narrow band mercury-cadmium-telluride detector (MCT detector) with a resolution of 0.45 cm^{-1}. The internal reflection element was KRS-5 (52 × 20 × 2 mm trapezoidal cut at 45°). The CH_2 asymmetric stretching band peak which originated from alkyl chains in the lipids was obtained by the built-in programmed curve fitting method of the FT-IR/ATR instrument.

Results and Discussion

Time Profile of Stratum Corneum Perturbation The time profiles of the FT-IR/ATR spectra of the surface of the rat skins treated with 0.15 M oleic acid in PG for (b) 5 min, (c) 30 min, (d) 2 h, (e) 12 h, and (a) untreated sample are illustrated in Fig. 1A. As is already known, the CH_2 asymmetric and symmetric stretching vibrations absorbing near 2920 and 2850 cm^{-1}, respectively,[3] result primarily from the methylene groups of the stratum corneum lipid hydrocarbon chains. As for the CH_2 asymmetric stretching vibrations, we have already reported that the degree of the frequency shift depended on the concentration of oleic acid which was applied to the skin.[10] As seen in the spectra of (a) to (e) of Fig. 1A and Table I, after treatment of the skin surface with 0.15 M of oleic acid in PG for 5 min, CH_2 asymmetric stretching vibrations at 2920 cm^{-1} showed a slight shift (0.9 cm^{-1}) toward higher wave numbers. By increasing the duration of exposure of the skin to 0.15 M oleic acid in PG, additional shifting towards high wavenumbers, along with a broadening of the spectra was observed. After 30 min, 2 h and 12 h of treatment, there was an average increase of 2.4, 3.4 and 3.9 cm^{-1}, respectively, showing that the degree of the shift was similar between the 2 and 12 h treatment samples. A similar shift was not observed with the samples treated with PG alone for (b) 2 h and (c) 12 h in comparison with the untreated skin sample (a) as shown in Fig. 1B. These results indicated that disordering of the stratum corneum structures could be initiated at least by 5 min of treatment with 0.15 M oleic acid in PG. Such disordering effects were increased by increasing the duration of exposure of the skin to the skin penetration enhancer in PG, and a maximum effect was reached after 2 h of treatment, suggesting that the uptake of oleic acid and PG into the stratum corneum approached saturation after at least 2 h of treatment.

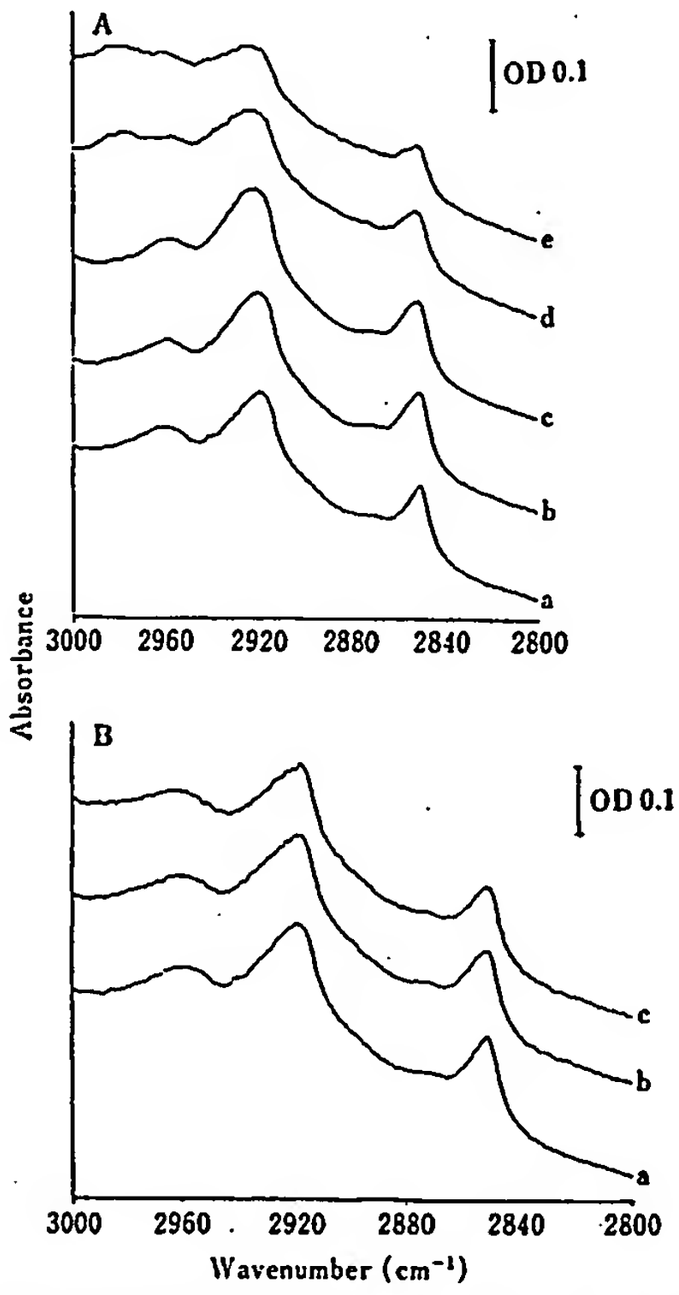

Fig. 1. Representative FT-IR/ART Spectra of Rat Abdominal Stratum Corneum in the CH_2 Asymmetric and Symmetric Stretching Region Resulting Primarily from Stratum Corneum Lipids Following Treatment of the Stratum Corneum with 0.15 M Oleic Acid/PG System and PG Alone

A, the skin was treated with 0.15 M oleic acid in PG for either: a, without treatment; b, 5 min; c, 30 min; d, 2 h; e, 12 h. B, the skin was treated with PG alone either: a, without treatment; b for 2 h; c for 12 h.

Delipidization with Oleic Acid in PG System The peak intensity resulting from CH_2 asymmetric stretching vibrations near 2920 cm^{-1} is known to be affected by stratum corneum proteins.[11] Thus, the peak intensity may not be available for evaluating the amounts of lipids which exist in the stratum corneum. The absorbance at 1741 cm^{-1} in the spectra is assigned to the C=O mode of esterified stratum corneum lipids, and the exogeneously introduced oleic acid produces the characteristic 1710 cm^{-1} absorbance.[3] It is also reported that the absorption band at approximately 1740 cm^{-1}, which originated from the C=O stretching vibrations, is not affected by stratum corneum proteins.[11] Raykar *et al.*[12] took advantage of this observation and evaluated the degree of delipidization of the stratum corneum following treatment of the stratum corneum with a 2:1 chloroform/methanol mixture by measuring changes in absorbance at 1740 cm^{-1}. In our study we also adapted this technique and investigated whether oleic acid extracted lipids from the stratum corneum, when used in combination with PG, by measuring the absorbance intensity at 1740 cm^{-1} as a function of time following

TABLE I. Time Course of Frequency Changes in the CH_2 Asymmetric Stretching Peak Resulting from Rat Abdominal Stratum Corneum Treated with 0.15 M Oleic Acid in PG and/or PG Alone

Treatment time	Frequency (cm^{-1})	
	PG	Oleic acid in PG
0 min	2919.8 ± 0.2 (12)	2919.8 ± 0.2 (12)
5 min	2919.7 ± 0.4 (3)	2920.2 ± 0.1 (3)
30 min	2919.1 ± 0.4 (3)	2922.2 ± 0.1 (3)
2 h	2920.1 ± 0.1 (3)	2923.2 ± 0.3 (3)
12 h	2920.1 ± 0.4 (3)	2923.7 ± 0.5 (3)

The values given are mean ± S.D. Numbers of trials are given in parentheses.

treatment of the skin surface with 0.15 M oleic acid in PG. The results are shown in Fig. 2A. It was apparent that the absorbance intensity at 1740 cm^{-1} decreased with an increase in the skin treatment time with 0.15 M oleic acid in PG. However, no decrease was observed in the samples treated with PG alone for 2 and 12 h, as compared with untreated sample (Fig. 2B). This implied that treatment of the stratum corneum with 0.15 M oleic acid in PG caused the decrease in the amount of the C=O group contributing to the absorbance intensity at 1740 cm^{-1}, suggesting that lipid extraction from the stratum corneum occurred. Another explanation for the decrease in the absorbance intensity was that the spectral characteristic was changed, although no direct evidence was shown at present. However, it was probably reasonable to assume that the structures in the lipid domain were perturbed, either in the case of lipid extraction effects or in the alteration of the absorbance characteristic. Thus, the application of the oleic acid/PG system on the rat skin could reduce the resistance of the stratum corneum by reorganizing the structures of lipid domains. Such conformational alterations would bring about the possible disordering of protein structures in corneocytes.[9] Francoeur *et al.* provided evidence that the lipid phase transitions associated with the intracellular bilayers were markedly affected by treatment with oleic acid.[4] Recently, they further demonstrated[5] that oleic acid lowered the lipid phase transition temperature (T_m) of the stratum corneum lipids in conjunction with increasing the conformational freedom or flexibility of the endogenous lipid alkyl chains above the T_m. Oleic acid did not significantly change the chain disorder of the stratum corneum lipids at the temperature below T_m under those circumstances where oleic acid itself was fully disordered. Of the spectroscopic behavior of stratum corneum lipids, it has been shown that the 0.5 h treatment of human stratum corneum with oleic acid (0.5—10%) in ethanol did not affect the intensity of the 1741 cm^{-1} absorbance, which is characteristic of esterified stratum corneum lipids.[3] This result indicates that oleic acid in ethanol did not extract

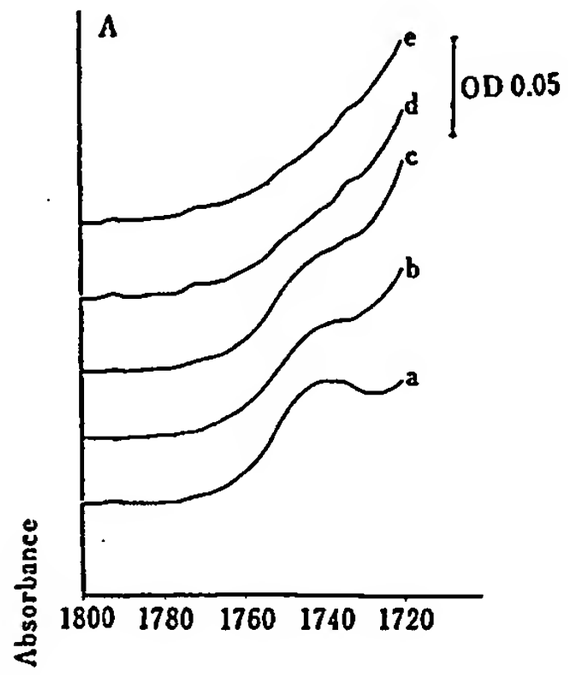

Fig. 2. Representative FT-IR/ATR Spectra of Rat Abdominal Stratum Corneum in the C=O Stretching Region Resulting from Stratum Corneum Lipids Following Treatment of the Stratum Corneum with 0.15 M Oleic Acid in PG and PG Alone

A, the skin was treated with 0.15 M oleic acid in PG either: a, without treatment; b for 5 min; c, 30 min; d, 2 h; e, 12 h. B, the skin was treated with PG Alone either: a, without treatment; b, 2 h; c, 12 h.

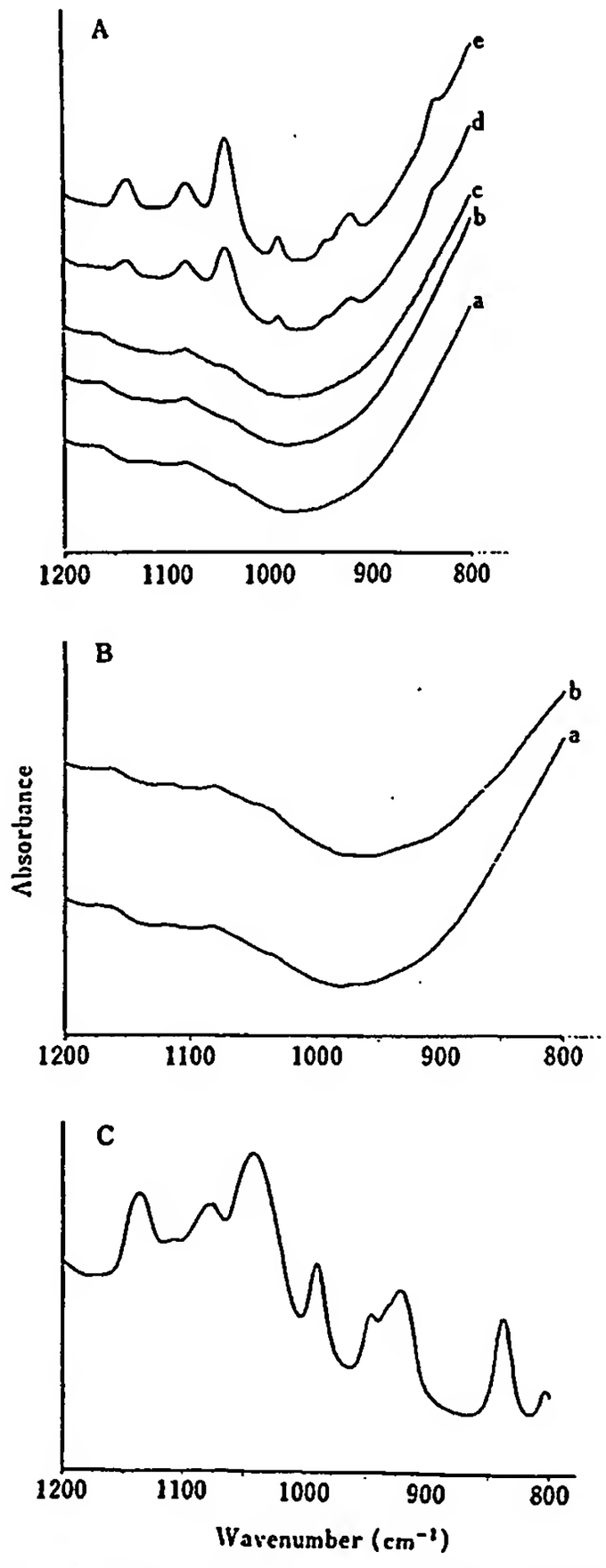

Fig. 3. Representative FT-IR/ATR Spectra of Rat Abdominal Dermal Tissues in the Region from 1200 to 800 cm^{-1} Following Treatment of the Stratum Corneum with 0.15 M Oleic Acid in PG and PG Alone

A, the skin was treated with 0.15 M oleic acid in PG either: a, without treatment; or for b, 5 min; c, 15 min; d, 30 min; e, 2 h. B, the skin was treated with PG alone either: a, without treatment; b, 2 h. C, spectrum for pure PG sample.

any lipids from the stratum corneum under this condition. By contrast, our results indicated that even 5 min treatment of the stratum corneum with 0.15 M oleic acid in PG caused a decrease in absorbance at 1740 cm^{-1}, suggesting that oleic acid in the PG system extracted the stratum corneum lipids. The difference in the action of oleic acid on the lipid extraction, thus, must be due to the difference in the system used in both experiments. It is mentioned that PG molecules may occupy some hydrophilic region between the lipid polar head groups.[8] As to the mechanism of action of oleic acid in the PG system on the stratum corneum lipids, we can speculate that oleic acid in PG may cause breakdown of the intercellular leaflet structure by solubilizing stratum corneum lipids which may then emigrate to the outside of the stratum corneum (donor compartment). Such a structural breakdown could bring about an extension of the effective volume within the stratum corneum for solutes and/or solvents which could penetrate through the inter-, and intracellular routes of dermal and epidermal tissues.

Appearance of PG in Dermal Tissues IR spectra of PG on the dermal side were measured with skin samples which have been treated with 0.15 M oleic acid in PG on the stratum corneum for either 5 min, 15 min, 30 min or 2 h, and with an untreated skin sample. The results are shown in Figs. 3A and 3B. The IR spectrum of the pure PG sample spanning the region from 1200 to 800 cm^{-1} is also shown in Fig. 3C. As indicated, the spectrum obtained following 2 h of treatment of the stratum corneum with 0.15 M oleic acid, for example, was consistent with that of the pure PG sample, and was thus identified as the spectrum resulting from PG molecules. Therefore, the peak with the highest intensity in the absorption band at 1043 cm^{-1} was selected for further study of the appearance of PG in dermal tissues. As seen in Fig. 3A, the peak resulting from PG molecules appeared following treatment with 0.15 M oleic acid in PG for 30 min, and the intensity of the peak increased further with the 2 h of treatment. However, before and following the 5 and 15 min exposure to the 0.15 M oleic acid/PG system, the spectra did not show any peak resulting from PG molecules. PG alone did not cause any change in absorbance at 1043 cm^{-1} following the 2 h of treatment as compared with the untreated sample. These results indicate that PG molecules, when used in combination with oleic acid, penetrated the dermal tissues through the epidermal tissues, and this appearance could take at least 30 min. Penetration of PG molecules through the skin has been reported in several studies which involved the use of two-compartment diffusion cells.[13-15] In these studies, however, they only described the behavior of PG molecules which appeared in the receiver compartment after the diffusion rate became constant, or they only compared the total amount of PG which penetrated the skin between systems with the penetration enhancer, but without any additives (control). Another point to be made here is that it may be possible to calculate the measurement of the steady state level, where the diffusion rate is constant, from the results of the appearance of solutes in the receiver compartment, but the time for reaching the steady state must be obtained by the plot of the amount of solutes penetrated against time. However, our results suggest that one could use FT-IR/ATR spectroscopy to directly measure the time for the steady state level to be attained by pursuing the behavior of the PG which appeared in dermal tissues.

In conclusion, FT-IR/ATR analysis of rat stratum corneum demonstrated that the oleic acid/PG system could perturb the stratum corneum lipid structures by extracting the lipids. The appearance of PG in dermal tissues following treatment of the stratum corneum with 0.15 M oleic acid in PG suggested that the reorganization of lipid domains due to the lipid extraction by the oleic acid/PG system helped PG molecules enter the dermal tissues. It was also suggested that the effective volume within the stratum corneum for solutes and/or solvents which could penetrate through the inter-, and intracellular routes could be altered in conjunction with structural changes of the lipids following treatment with the oleic acid/PG system.

References

1) G. M. Golden, J. E. Mckie, R. O. Potts, *J. Pharm. Sci.*, 76, 25 (1987).
2) V. H. W. Mak, R. O. Potts, R. H. Guy, *Pharm. Res.*, 7, 835 (1990).
3) V. H. W. Mak, R. O. Potts, R. H. Guy, *J. Control. Rel.*, 12, 67 (1990).
4) M. L. Francoeur, G. M. Golden, R. O. Potts, *Pharm. Res.*, 7, 621 (1990).
5) B. Ongpipattanakul, R. R. Burnette, R. O. Potts, M. L. Francoeur, *Pharm. Res.*, 8, 350 (1991).
6) B. W. Barry, S. L. Bennett, *J. Pharm. Pharmacol.*, 39, 535 (1987).
7) E. R. Cooper, *J. Pharm. Sci.*, 73, 1153 (1984).
8) B. W. Barry, *J. Control. Rel.*, 6, 85 (1987).
9) Y. Takeuchi, H. Yasukawa, Y. Yamaoka, Y. Morimoto, S. Nakao, Y. Fukumori, T. Fukuda, *Chem. Pharm. Bull.*, 40, 484 (1992).
10) Y. Takeuchi, H. Yasukawa, Y. Yamaoka, Y. Kato, Y. Morimoto, Y. Fukumori, T. Fukuda, *Chem. Pharm. Bull.*, 40, 1887 (1992).
11) R. Mendelsohn, R. A. Dluhy, T. Crawford, H. Mantsch, *Biochemistry*, 23, 1498 (1984).
12) P. V. Raykar, M.-C. Fung, B. D. Anderson, *Pharm. Res.*, 5, 140 (1988).
13) M. Yamada, Y. Uda, Y. Tanigawara, *Chem. Pharm. Bull.*, 35, 3399 (1987).
14) K. Sato, K. Sugibayashi, Y. Morimoto, *Int. J. Pharm.*, 43, 31 (1988).
15) B. Aungst, J. A. Blake, M. A. Hussain, *Pharm. Res.*, 7, 712 (1990).

Transdermal Oxymorphone Formulation Development and Methods for Evaluating Flux and Lag Times for Two Skin Permeation-Enhancing Vehicles

BRUCE J. AUNGST[x], JUDY A. BLAKE, NANCY J. ROGERS, AND MUNIR A. HUSSAIN

Received November 27, 1989, from *DuPont Company, Medical Products Department, P.O. Box 80400, Experimental Station, Wilmington, DE 19880-0400.* Accepted for publication January 29, 1990.

Abstract □ Oxymorphone is a candidate for transdermal delivery since it is a very potent analgesic, is not very effective orally, and has a short duration of action. In developing a transdermal delivery system, two criteria that were considered important were achieving adequate flux and minimizing the lag time. Oxymorphone skin permeation rates in vitro were very low unless skin permeation enhancers were included in the vehicle. After an initial screen of 17 formulations, two skin permeation-enhancing formulations were selected for further study. These were myristic acid:propylene glycol:oxymorphone base (A), and decylmethylsulfoxide:ethanol:water:oxymorphone · HCl (B). With either formulation and either human or hairless guinea pig skin, there was little dependence of either in vitro flux or lag time on the section of skin used (stratum corneum, epidermis, epidermis/dermis). There were significant differences between human skin and hairless guinea pig skin when comparing in vitro fluxes with the two formulations. With formulation A, fluxes through hairless guinea pig skin were three- to fivefold greater than through human skin. With B, however, fluxes through human skin were up to fivefold greater than through hairless guinea pig skin. In vitro lag times with A were generally long (≈24 h), whereas those with B were much lower (≈1 to 10 h). The species dependence of permeation enhancement and the differences in lag time between formulations could be related to differences in the mechanisms of permeation enhancement. In vivo lag times with the fatty acid:propylene glycol vehicle were estimated in hairless guinea pigs based on plasma oxymorphone concentrations. These were much lower than in vitro lag times.

The opioid analgesics are effective for alleviating moderate to severe pain. They are used primarily for postoperative and cancer pain. Many of the opioid analgesics are candidates for transdermal delivery because they are effective at low doses when administered by injection, but have low oral bioavailability. Oxymorphone (oxymorphone · HCl, Numorphan, Du Pont Pharmaceuticals) is one of these opioid analgesics. The recommended doses by injection are 1 to 1.5 mg every 4 to 6 h. No oral dosage form is available in the U.S., possibly because oral oxymorphone is much less effective than im oxymorphone.[1] A transdermal delivery system providing continuous oxymorphone delivery over a 24-h period might be preferred by patients as an alternative or supplement to injected opioid analgesics.

One criterion in developing a transdermal oxymorphone delivery system was to achieve adequate skin permeation. Preliminary experiments showed that oxymorphone diffused through human skin very slowly unless skin permeation enhancers were coadministered. In addition, a marketing concern was that a rapid onset of analgesic effect would be desirable for postsurgical use, so minimizing the lag time became a second criterion in formulation development. In this study we initially evaluated in vitro skin permeation using 17 formulations of various compositions, but generally including one of two types of skin permeation enhancers. One type of formulation contained oxymorphone base in a fatty acid:propylene glycol vehicle. In a previous study, various skin permeation enhancers were screened for their effects on naloxone skin permeability.[2] Naloxone is structurally similar to oxymorphone, but is pharmacologically an opioid antagonist. Naloxone skin penetration rates were markedly increased by propylene glycol vehicles containing fatty acids as permeation enhancers.[2] The other formulation approach was to use oxymorphone · HCl in a water:ethanol vehicle containing decylmethylsulfoxide as a skin permeation enhancer. Several studies[3–5] have shown that decylmethylsulfoxide preferentially increases skin permeability to polar solutes. Ethanol has also been proposed to increase skin permeability of polar solutes via solvent channel pathways, figuratively referred to as pores.[6] In contrast, it is thought that the fatty acid:propylene glycol vehicles increase diffusion through the intercellular lipid matrix.[7,8] An objective of this study was to compare these two types of formulations with regard to oxymorphone flux and lag time, since their mechanisms of skin permeation enhancement may differ.

Another question we addressed was whether in vitro lag times depend on the skin section used. When a drug is applied to skin in vivo, the infinite sink is provided by the blood supply, which is at the level of the epidermis/dermis junction. It was thought that in vitro lag times could overestimate the in vivo lag times if the skin used for in vitro studies included the dermal layer. We therefore compared in vitro lag times using stratum corneum, epidermis, and epidermis/dermis sections from both human and hairless guinea pig skin.

As mentioned previously, one formulation goal was to minimize the lag time in vivo. There is little information in the literature on whether in vitro skin permeation lag times correspond to in vivo lag times. This may be because lag times are usually of minor concern for other drugs or for chronic uses, because the lag time of a second dose is offset by the drug still leaching from the skin from the previously applied dose. We have compared the in vitro and in vivo lag times with one of these formulations. In vivo lag times were estimated by measuring plasma oxymorphone concentrations in a hairless guinea pig model.

Experimental Section

Materials and Formulations—Oxymorphone HCl and oxymorphone base were supplied by Du Pont Pharmaceuticals (Wilmington, DE). Myristic acid was supplied by Emery Industries, Cincinnati, OH (Emery 655). *n*-Decylmethylsulfoxide was obtained from Wateree Chemical Company (Camden, SC). Propylene glycol (PG), polyethylene glycol 400 (PEG 400), ethanol, and water were used as the solvents. Formulations were prepared by first dissolving the adjuvant (myristic acid or decylmethylsulfoxide) in the solvent. Oxymorphone base or oxymorphone · HCl was then added, either at a set concentration or until the solubility limit was reached. Complete formulation compositions are listed in the tables. These formulations were used for in vitro and in vivo skin permeation experiments.

Skin Permeation In Vitro—Diffusion rates across excised human skin and hairless guinea pig skin were measured using glass diffusion

0022-3549/90/1200-1072$01.00/0

cells. The reservoir was warmed to 37 °C with either a circulating water jacket or dry block heater and continuously stirred. Saline was used as the reservoir solution. The drug donor compartment was not stirred or heated. For most experiments, the skin surface area available for diffusion was 2.5 cm^2, the reservoir volume was 7–9 mL, and the drug donor volume was 0.5 mL. Smaller diffusion cells were used in the experiments with stratum corneum. In those cases, the skin surface area was 1.1 cm^2, and the reservoir volume was 4–5 mL, and 0.1 mL of drug donor solution was applied. The donor compartment was covered to minimize solvent evaporation.

Excised human skin specimens were obtained from an organ bank. The skin was from 21 donors having an average age of 35.4 years (SD = 13.5 years; range = 16–66 years). All donors were Caucasian and six were female. Most specimens were from thigh and calf sites, and a few specimens were from the back. Excised skin from hairless guinea pigs was also used for in vitro skin permeation studies. Male hairless guinea pigs (IAF strain, Charles River, Lakeview, NJ) weighing 400–700 g were euthanitized by ether overdose. Skin was removed from the dorsal midsection and rinsed with saline.

Human skin specimens were supplied at a thickness of ~0.4 mm, so the full epidermis and part of the dermis was intact. All excised hairless guinea pig skin specimens were cut to 0.7 mm thickness with a dermatome. The 0.4-mm human skin specimens and the 0.7-mm hairless guinea pig specimens are subsequently referred to as "epidermis/dermis" specimens. Epidermis from human and hairless guinea pig skin was isolated by immersion of the epidermis/dermis specimens in a beaker of 60 °C water for 1 min, after which the epidermis and dermis could be manually pulled apart. Stratum corneum was isolated from epidermis/dermis specimens by trypsin digestion of the underlying layers. Specimens were laid onto filter paper soaked with a solution of 0.5% trypsin (Sigma type II, 1330 BAEE U/mg activity) in 0.1 M, pH 7.4 phosphate buffer. After 2 h, the skin specimen was rinsed with saline. During the rinse, the digested portions were removed, leaving an intact stratum corneum layer.

In the diffusion studies, the entire reservoir volume was removed at the various sampling times and was replaced with drug-free saline. The amount permeating was calculated as the oxymorphone concentration multiplied by the reservoir volume. For each skin specimen, the amount permeating was plotted versus time, and the slope and intercept of the linear portion of the plot was derived by regression. Oxymorphone flux was calculated as the slope divided by the skin surface area. The intercept on the x-axis was taken as the lag time.

In Vivo Permeation Study—Hairless guinea pigs were dosed with oxymorphone transdermally, and plasma oxymorphone concentrations were determined. The dosing solution (0.25 mL) was pipetted onto the cotton swatch of a circular plastic chamber having an adhesive tape overlay (Hill Top Chamber, Hill Top Research, Cincinnati, OH). The surface area for diffusion was 2.5 cm^2. The delivery systems were applied on one side of the back of the hairless guinea pigs and were held in place by porous adhesive tape wrapped completely around the hairless guinea pig's midsection. The patch and wrap remained intact for 48 h. Blood samples (3 mL) were collected by cardiac puncture, under ether anesthesia, into heparinized tubes. Of eight animals that were dosed, four had blood samples taken at 0, 1, 4, 8, and 32 h, and four had samples taken at 0, 2, 6, 24, and 48 h. Plasma was separated and frozen until analyzed.

Analytical—All oxymorphone concentrations were determined by HPLC. For the in vitro diffusion studies, the solutions were either injected directly onto the HPLC or they were diluted and then injected. An octylsilane column (Zorbax C8, Du Pont) was used. The mobile phase contained 90% 0.2 M sodium perchlorate:0.005 M sodium citrate buffer, pH 5, and 10% acetonitrile, the flow rate was 1.4 mL/min, and detection was by UV absorbance at 280 nm.

For plasma oxymorphone determinations, 0.5-mL aliquots were transferred to glass centrifuge tubes. A 50-μL volume of a 1-μg/mL solution of nalorphine was added as an internal standard, and 0.5 mL of pH 9.3 carbonate buffer was added. Extraction was into 4 mL of anhydrous ethyl ether by vortexing. After centrifuging, the ether layer was transferred to tubes containing 200 μL of 0.02 M phosphoric acid. After vortexing and centrifuging, the ether was removed and 50 μL of the phosphoric acid phase was injected onto the HPLC. In this assay, the mobile phase contained 10% methanol, 7% acetonitrile, 0.17 g/L of disodium EDTA, and 83% 0.07 M KH_2PO_4, and the flow rate was 1 mL/min. Electrochemical detection at an applied potential of +0.90 V was employed with a glassy carbon electrode. Average retention times for oxymorphone and nalorphine were 6.5 and 12.5 min, respectively.

Results

Formulation Screening—The goal of the initial studies was to identify formulations providing high rates of oxymorphone skin permeation. Human skin epidermis/dermis specimens (0.4 mm thick) were used. The anticipated dose required for analgesia was 10 mg/24 h, or 0.4 mg/h, based on the recommended injection dosing regimen. This is approximately the same as the doses self-administered by patients recovering from cesarean delivery or orthopedic surgery using patient-controlled devices.[9] Assuming the optimum surface area of a transdermal patch would be 10–20 cm^2, the required flux would be 20–40 $\mu g/cm^2 \cdot h$. This was the targeted flux. The approaches were to use myristic acid or decylmethylsulfoxide as permeation enhancers. Formulations, their designations, and results are summarized in Table I. Myristic acid markedly enhanced the flux of oxymorphone base, using a propylene glycol vehicle (I versus II). A formulation containing 10% oxymorphone base and 10% myristic acid in propylene glycol (III) provided fluxes at the high end of the targeted range, although lag times were long (≈24 h). Flux was lower for myristic acid:PEG 400 (IV), ethanol (V), and myristic acid:ethanol (VI) vehicles containing oxymorphone base. A combination of myristic acid, ethanol, and propylene glycol (VII) was quite effective in enhancing oxymorphone base flux, but the lag times were still long.

Propylene glycol vehicles containing oxymorphone · HCl were also studied. Surprisingly, flux from the salt form was approximately equal to that from vehicles containing oxymorphone base (VIII versus I). However, the permeation-enhancing effect of myristic acid in PG was much lower for oxymorphone · HCl (sevenfold, VIII versus IX) than for oxymorphone base (85-fold, I versus II).

The second general type of permeation-enhancing vehicle employed decylmethylsulfoxide in an ethanol:water solvent. Ethanol enabled solubilization of decylmethylsulfoxide, and water was useful for dissolving oxymorphone · HCl. In the absence of decylmethylsulfoxide, oxymorphone · HCl permeated the skin relatively slowly (formulation X). Addition of 5% decylmethylsulfoxide to the vehicle (XI) increased oxymorphone flux >1000-fold. The skin permeation rates were related to the concentrations of both decylmethylsulfoxide (XI versus XII) and oxymorphone · HCl (XI versus XIII). Oxymorphone base in an ethanol:water solvent permeated skin much more rapidly than oxymorphone · HCl from ethanol:water (XIV versus X). However, 1% decylmethylsulfoxide decreased, rather than increased, oxymorphone base flux from the ethanol:water vehicle (XV). Since the solubility of oxymorphone base was <10% in both XIV and XV vehicles, one possible effect of decylmethylsulfoxide was to decrease the solubility of oxymorphone base. Oxymorphone base was less susceptible to enhancement by 1% decylmethylsulfoxide than oxymorphone HCl (XV versus XII). However, vehicles containing 2% decylmethylsulfoxide and either 2% oxymorphone base (XVI) or 2% oxymorphone · HCl (XVII) in ethanol:water gave reasonably high flux values and low lag times. Flux from the oxymorphone base formulation was again lower than from the oxymorphone · HCl formulation. That containing the HCl salt (XVII) was chosen for further study.

Isolated Skin Sections—Formulations III (oxymorphone base:myristic acid:PG) and XVII (oxymorphone · HCl:decylmethylsulfoxide:ethanol:water) were comparable in providing skin permeation rates greater than the targeted flux, but were different in lag times. Average diffusion profiles with these formulations are compared in Figure 1. The next questions were (*1*) whether the in vitro lag times depend on

Table I—In Vitro Oxymorphone Permeation through Human Epidermis/Dermis from Various Formulations

Designation	Formulation[a]	Flux, $\mu g/cm^2 \cdot h$	Lag Time, h	n[b]
I	Excess base in PG	1.1 ± 0.1	26.8 ± 2.3	6
II	Excess base in myristic acid:PG (10:90)	93.5 ± 24.4	24.3 ± 3.0	6
III	Base:myristic acid:PG (10:10:80)	40.9 ± 10.7	24.7 ± 1.8	8
IV	Excess base in myristic acid:PEG (10:90)	2.3 ± 1.3	2.2 ± 1.0	3
V	Excess base in ethanol	13.1 ± 2.7	7.4 ± 1.4	4
VI	Base[c]:myristic acid:ethanol (10:10:80)	19.1 ± 6.3	8.3 ± 3.2	4
VII	Base:myristic acid:ethanol:PG (10:10:40:40)	76.0 ± 10.2	17.4 ± 4.1	3
VIII	Excess HCl in PG	0.9 ± 0.3	2.8 ± 1.8	4
IX	HCl:myristic acid:PG (10:10:80)	6.0 ± 0.5	23.4 ± 1.6	4
X	HCl:ethanol:water (10:45:45)	0.4 ± 0.1	6.1 ± 3.8	3
XI	HCl:C_{10}MSO:ethanol:water (10:5:42.5:42.5)	583.0 ± 175.6	5.8 ± 2.4	5
XII	HCl:C_{10}MSO:ethanol:water (10:1:44.5:44.5)	119.5 ± 61.3	9.2 ± 4.0	5
XIII	HCl:C_{10}MSO:ethanol:water (1:5:47:47)	85.8 ± 8.2	4.9 ± 1.4	3
XIV	Base[c]:ethanol:water (10:45:45)	26.3 ± 4.5	0.9 ± 0.5	4
XV	Base[c]:C_{10}MSO:ethanol:water (10:1:44.5:44.5)	5.4 ± 0.8	4.8 ± 3.6	4
XVI	Base:C_{10}MSO:ethanol:water (2:2:48:48)	41.7 ± 18.1	1.4 ± 0.6	6
XVII	HCl:C_{10}MSO:ethanol:water (2:2:48:48)	114.9 ± 36.8	3.7 ± 1.5	5

[a] Abbreviations: Base, oxymorphone base; HCl, oxymorphone · HCl; PG, propylene glycol; PEG, polyethylene glycol 400; C_{10}MSO, decylmethylsulfoxide; ratios represent weights. [b] Data are mean ± SE of n number of experiments, usually using skin from n number of different donors. [c] Drug was added to 10%, but was not completely soluble at that concentration.

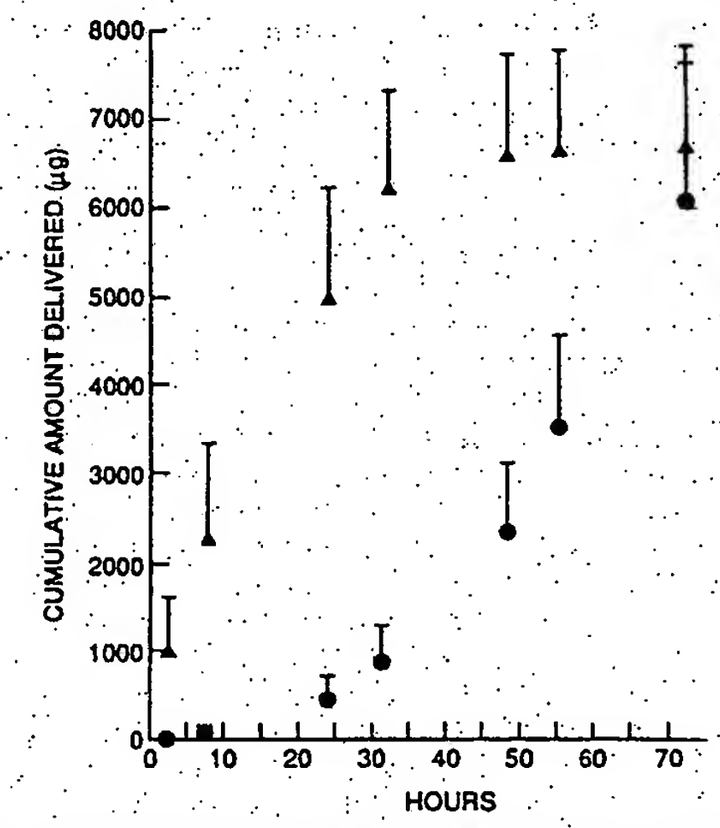

Figure 1—Averaged (+SE) permeation profiles for formulations III (●; n = 8) and XVII (▲; n = 5) using human epidermis/dermis in vitro.

the section of skin used in the study, and (2) whether in vitro lag times correspond to in vivo lag times. Oxymorphone skin permeation was characterized using isolated skin sections (epidermis and stratum corneum) for formulations III and XVII. In addition to human skin, hairless guinea pig skin and skin sections were used. These results are summarized in Table II. Although the average flux varied two- to threefold, depending on which skin sections were used, these differences were not statistically significant ($p > 0.05$, t test) for either formulation with skin from either species. An unexpected finding was that hairless guinea pig skin was more permeable than human skin for formulation III, whereas human skin was more permeable when formulation XVII was used. The lag times showed a similar, although less pronounced trend. That is, with formulation III, the lag times for human skin and skin sections were generally greater than for hairless guinea pig skin, but with formulation XVII, lag times for human skin were lower than for hairless guinea pig skin. There was just one significant difference in lag times among the full-skin specimens, epidermis, and stratum corneum within any formulation and species group. For formulation III, the lag time with epidermis was significantly lower than that for epidermis/dermis. The lag time with stratum corneum was not different from that with epidermis/dermis, so the lag times were not related to the thickness of the membrane. These data would suggest that the stratum corneum is the rate-limiting barrier to oxymorphone permeation with either formulation or species.

In Vivo Skin Permeation—Formulation III (oxymorphone base:myristic acid:PG) was applied to hairless guinea pigs and plasma oxymorphone levels were determined over a 48-h

Table II—Oxymorphone Skin Permeation Characteristics for Various Skin Sections

Section	Formulation III[a]		Formulation XVII[b]	
	Flux, $\mu g/cm^2 \cdot h$	Lag Time, h	Flux, $\mu g/cm^2 \cdot h$	Lag Time, h
Human epidermis/dermis (0.4 mm)	40.9 ± 10.7	24.7 ± 1.8	162.3 ± 51.9	3.7 ± 1.5
Human epidermis	78.4 ± 27.2	12.9 ± 3.9	105.3 ± 54.9	2.1 ± 0.9
Human stratum corneum	59.2 ± 22.9	21.7 ± 0.9	45.8 ± 1.7	0.7 ± 0.6
Hairless guinea pig epidermis/dermis (0.7 mm)	195.1 ± 43.6	17.7 ± 4.7	30.6 ± 24.3	13.1 ± 4.2
Hairless guinea pig epidermis	275.6 ± 22.6	4.5 ± 0.1	21.9 ± 3.8	3.1 ± 1.4
Hairless guinea pig stratum corneum	200.6 ± 13.7	9.4 ± 2.4	41.6 ± 18.3	5.9 ± 3.3

[a] Oxymorphone base:myristic acid:propylene glycol (10:10:80). [b] Oxymorphone · HCl:decylmethylsulfoxide:ethanol:water (2:2:48:48).

period. As shown in Figure 2, the in vivo lag time was between 2 and 4 h. No animals had detectable plasma oxymorphone concentrations at 2 h, but all had measurable levels at 4 h. In vivo there is also a pharmacokinetic lag time, as would be seen during constant iv infusion dosing, during which plasma concentrations rise from zero to some detectable level and eventually to steady state. Thus, the true diffusional lag time in vivo may be even shorter than 2–4 h. It appears, then, that in this case the in vitro lag times were not predictive of in vivo lag times, regardless of the skin section used in vitro. Plasma oxymorphone concentrations reached an apparent steady-state level and then declined, probably as the drug was depleted from the delivery system.

Discussion

Formulation of a transdermal drug delivery system requires optimizing flux while maintaining minimum skin irritation and sensitization potential. In developing a transdermal system for the opioid analgesic oxymorphone, we were also concerned with minimizing the diffusional lag time so that the onset of analgesia would not be prolonged. The goals of this work, in addition to optimizing oxymorphone flux, were (*1*) to compare lag times with different types of permeation-enhancing formulations, (*2*) to see whether in vitro lag times depend on the thickness of skin section used, and (*3*) to compare in vitro and in vivo lag times in an animal model.

Skin permeation enhancement was required for transdermal oxymorphone delivery to be feasible. In the absence of a permeation enhancer, oxymorphone flux through human skin in vitro was very low. Two types of permeation-enhancing vehicles were evaluated: myristic acid (a fatty acid) in propylene glycol, and decylmethylsulfoxide in ethanol:water. Fatty acids have been shown to enhance the skin permeation rates of various compounds, and were especially effective when the solvent was propylene glycol.[2,10] The mechanism of barrier disruption appears to involve the lipids which are tightly packed together within the intercellular spaces of the stratum corneum. Among the evidence supporting this hypothesis is the study of Golden et al.[11] in which oleic acid

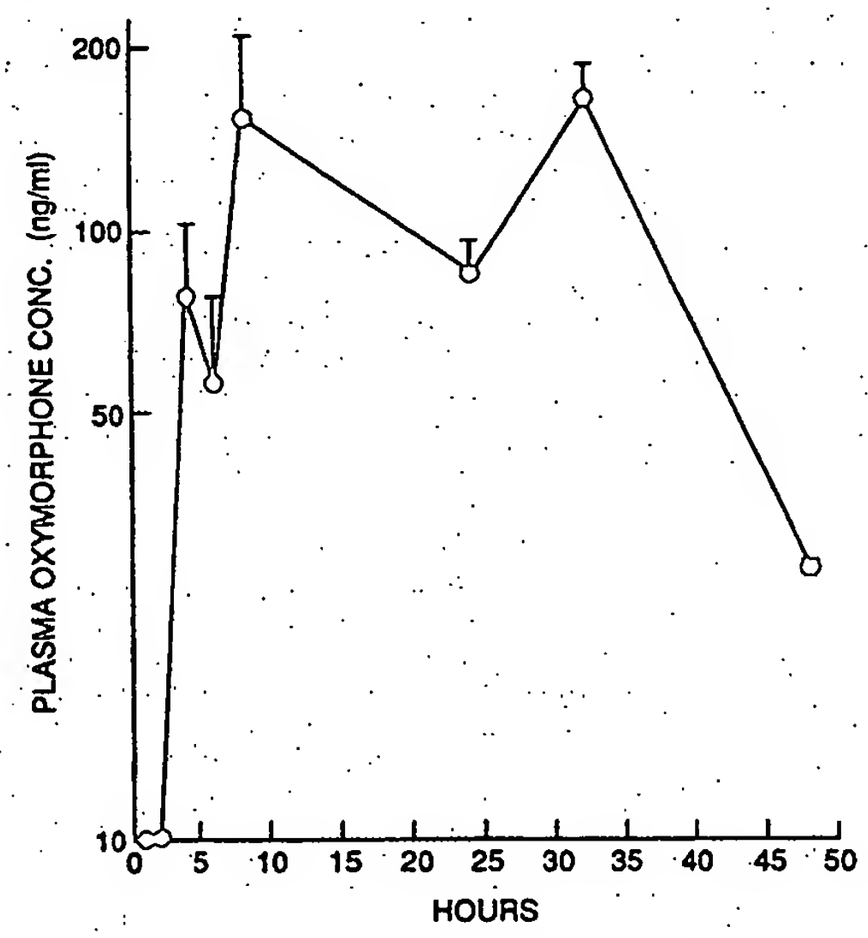

Figure 2—Plasma oxymorphone concentrations in hairless guinea pigs dosed transdermally with 0.25 mL of formulation III on a 2.5-cm² area. Each data point is the mean +SE of four animals.

treatment of stratum corneum decreased the phase transition temperature of the lipids [which was determined using differential scanning calorimetry (DSC) and infrared spectroscopy] and caused proportional changes in permeability to salicylic acid. These results are consistent with the idea that the most effective fatty acid skin permeation enhancers have hydrophobic tails, unlike those of the normal skin lipids (which are predominantly saturated alkyl groups of 16 or more carbon atoms), since they would be expected to be most disruptive of their packed structure.[12,13] Fatty acids enhanced the permeation of nonpolar solutes more than that of polar solutes.[4] In contrast, several studies have shown that decylmethylsulfoxide enhances skin permeation of polar solutes more than that of nonpolar solutes.[3,4,14] The enhancement with aqueous vehicles was much greater than with propylene glycol vehicles.[14] The mechanism of action of decylmethylsulfoxide on skin is not known, but results from DSC suggested it interacts with both proteins and lipids in the stratum corneum.[8] Various sulfoxides were shown to convert stratum corneum proteins from an alpha helix to a β-sheet conformation.[15] The mechanism of skin permeation enhancement with ethanol is also not yet clearly understood. Berner et al. showed a linear correlation between ethanol and nitroglycerin fluxes, and suggested that ethanol increased skin permeation rates by increasing the drug solubility in the skin.[16] Because aqueous:ethanol vehicles increased the flux of highly polar (mannitol) and ionic (tetraethylammonium bromide) solutes, Ghanem et al. proposed that new "pores" were formed.[6] These "pores" may be solvent-filled channels, and the mechanism of permeation enhancement may be solvent drag, wherein the solute flux is driven by the solvent flow. In such a situation, when partitioning into the lipophilic membrane is not involved, charged solutes can permeate.

Our results on enhancing oxymorphone skin permeation are consistent with the proposed mechanisms of the various enhancers. Myristic acid:PG increased the flux of oxymorphone base more than that of oxymorphone · HCl, suggesting selective enhancement of the nonpolar route. Lag times were long with these formulations, possibly because it takes time for the fatty acid to penetrate the skin and interact with the skin lipids, as suggested previously.[10] The decylmethylsulfoxide:ethanol:water vehicles also greatly increased oxymorphone flux, and the enhancement was greater for the HCl salt than for the free base. This is consistent with a mechanism involving formation of solvent channels. Lag time values were lower overall than with myristic acid:PG vehicles; this is also expected for a solvent channel mechanism.[16]

One of the applications of animal models in percutaneous absorption evaluation is for in vitro–in vivo correlations. The hairless guinea pig used in these studies is a fairly large rodent, so serial 3-mL blood samples could be taken. It was not unexpected that oxymorphone flux through human skin would differ from flux through hairless guinea pig skin. However, there was not even a rank order relationship for vehicles containing permeation enhancers. The myristic acid:PG formulation had a greater enhancing effect on hairless guinea pig skin than human skin, whereas the decylmethylsulfoxide:ethanol:water vehicles had a greater effect on human skin (Table II). Bond and Barry similarly showed that there was no consistent relationship between permeation enhancer effects on hairless mouse and human skin.[17,18] Furthermore, there was not a good correlation between the in vitro lag times using various hairless guinea pig skin sections and the apparent in vivo lag time for appearance of oxymorphone in the blood. The lag times in vivo appeared shorter than in vitro. A similar absence of correlation between in vitro lag times and in vivo drug appearance in blood was recently described for coumarin skin permeation rates using various absorption promoters in rats.[19] Therefore, the poten-

tial use of rodent animal models even for in vitro–in vivo correlations may be limited.

In vitro flux with human skin is generally believed to correlate with in vivo flux when the stratum corneum is the rate-limiting step for absorption,[20,21] so transdermal formulation development can be done using in vitro studies. Based on the in vitro fluxes with human skin, transdermal oxymorphone delivery seems feasible in that the delivery of doses equivalent to analgesic im doses can be achieved. A remaining unanswered question is whether the two types of formulations described here have different lag times in vivo. In addition, as always, the irritation and sensitization potential of any transdermal formulation has to be evaluated.

References and Notes

1. Beaver, W. T.; Wallenstein, S. L.; Houde, R. W.; Rogers, A. *J. Clin. Pharmacol.* **1977**, *17*, 186–198.
2. Aungst, B. J.; Rogers, N. J.; Shefter, E. *Int. J. Pharm.* **1986**, *33*, 225–234.
3. Cooper, E. R. In *Solution Behavior of Surfactants*, Vol. 2; Mittal, K. L.; Fendler, E. J., Eds.; Plenum: New York, 1982; pp 1505–1516.
4. Barry, B. W.; Bennett, S. L. *J. Pharm. Pharmacol.* **1987**, *39*, 535–546.
5. Touitou, E.; Fabin, B. *Int. J. Pharm.* **1988**, *43*, 17–22.
6. Ghanem, A.-H.; Mahmoud, H.; Higuchi, W. I.; Rohr, U. D.; Borsadia, S.; Liu, P.; Fox, J. L.; Good, W. R. *J. Controlled Release* **1987**, *6*, 75–83.
7. Cooper, E. R. *J. Pharm. Sci.* **1984**, *73*, 1153–1156.
8. Barry, B. W. *J. Controlled Release* **1987**, *6*, 85–97.
9. Sinatra, R. S.; Lodge, K.; Sibert, K.; Chung, K. S.; Chung, J. H.; Parker, A., Jr.; Harrison, D. M. *Anesthesiology* **1989**, *70*, 585–590.
10. Yamada, M.; Uda, Y.; Tanigawara, Y. *Chem. Pharm. Bull.* **1987**, *35*, 3399–3406.
11. Golden, G. M.; McKie, J. E.; Potts, R. O. *J. Pharm. Sci.* **1987**, *76*, 25–28.
12. Yamada, M.; Uda, Y. *Chem. Pharm. Bull.* **1987**, *35*, 3390–3398.
13. Aungst, B. J. *Pharm. Res.* **1989**, *6*, 244–247.
14. Touitou, E. *Int. J. Pharm.* **1988**, *43*, 1–7.
15. Oertel, R. P. *Biopolymers* **1977**, *16*, 2329–2345.
16. Berner, B.; Mazzenga, G. C.; Otte, J. H.; Steffens, R. J.; Juang, R.-H.; Ebert, C. D. *J. Pharm. Sci.* **1989**, *78*, 402–407.
17. Bond, J. R.; Barry, B. W. *J. Invest. Dermatol.* **1988**, *90*, 486–489.
18. Bond, J. R.; Barry, B. W. *J. Invest. Dermatol.* **1988**, *90*, 810–813.
19. Ritschel, W. A.; Barkhaus, J. K. *Arzneim.-Forsch.* **1988**, *38*, 1774–1777.
20. Barry, B. W. *Dermatological Formulations*; Marcel Dekker: New York, 1983.
21. Bronaugh, R. L.; Franz, T. J. *Brit. J. Dermatol.* **1986**, *115*, 1–11.

Physicochemical Study of Percutaneous Absorption Enhancement by Dimethyl Sulfoxide: Dimethyl Sulfoxide Mediation of Vidarabine (ara-A) Permeation of Hairless Mouse Skin

Tamie Kurihara-Bergstrom, Ph.D.,* Gordon L. Flynn, Ph.D., and William I. Higuchi, Ph.D.†
College of Pharmacy, The University of Michigan, Ann Arbor, Michigan, U.S.A.

Dimethyl sulfoxide's (DMSO) concentration-dependent influences on its own permeation rate through hairless mouse skin and on the concurrent permeation rates of water and the antiviral drug vidarabine (ara-A) have been studied at 37°C using in vitro diffusion cells. Solubilities of ara-A in DMSO-water mixtures were also determined in order to assess ara-A's relative thermodynamic activity in the binary solvent media used in the mass transfer studies. Solubilities increased exponentially with increasing percentages of DMSO. Activity coefficients decreased accordingly. When the same DMSO medium was placed in each side of diffusion cell (balanced solvent configuration) permeability coefficients for ara-A decreased exactly as ara-A's solubility increased up to a 50% DMSO concentration, indicating the observed decreases in the mass transfer coefficients have thermodynamic origins. When DMSO media were placed in either the donor or receiver side of the cell up to the same 50% concentration point and opposed by a normal saline medium on the other side (asymmetric solvent configurations), the permeability of ara-A did not decrease and at some DMSO levels was substantially increased, behavior in marked departure from thermodynamic control. The behavior disparity between the 2 configurations of the cell suggests that cross-currents of solvents play a role in permeability enhancement. Regardless of solvent configuration, permeability coefficients for ara-A at 90 and 100% DMSO strengths were exaggeratedly large, consistent with severe impairment of the stratum corneum. Similar overall permeability behavior was observed for the 2 solvents, water and DMSO. Possible underlying mechanisms for these effects and the relative importance of the various mechanisms of DMSO enhancement as a function of DMSO's concentration and configuration are discussed. *J. Invest. Dermatol. 89:274–280, 1987*

Despite the fact that vidarabine (ara-A) has been used successfully by injection in the treatment of herpes infections [1,2], the local application of ara-A to control herpes simplex manifestations of the skin has not been altogether successful. Ando and colleagues [3,4] suggested that the low efficacy of topical ara-A is due to an extremely low permeability of ara-A through skin. In this regard ara-A and its antiviral analogs have several suboptimal properties for local administration that cannot be overlooked. Vidarabine for instance, is an extremely polar, relatively large molecule, suggesting it should be very difficult to deliver through a membrane structure as compact and functionally nonpolar as the stratum corneum. Because of this difficulty, skin permeation-enhancing solvents have been tried clinically in hopes of improving the clinical effectiveness of such agents [5,6]. Since dimethyl sulfoxide (DMSO) has been the principal solvent chosen for this purpose, and since it has been shown to alter and enhance the skin permeability of other compounds [7–10], DMSO has been evaluated as a promoting agent of ara-A's permeation. Specific objectives were to determine the effect of DMSO on the permeation rate of ara-A in vitro (hairless mouse skin) and, generally, to explore the thermodynamic and kinetic limits of action of DMSO in enhancing transport of this prototypical antiviral nucleoside.

The permeability coefficient, P_{sc}, of ara-A through the skin's principal barrier layer, the stratum corneum, can be explicitly defined in terms of the effective thickness (h_{sc}), the effective diffusivity (D_{sc}), and the effective partition coefficient (K_{sc}) between the operative diffusional domain of the stratum corneum and DMSO-water solutions:

$$P_{sc} = \frac{D_{sc} \cdot K_{sc}}{h_{sc}} \qquad \text{(Eq. 1)}$$

The terms h_{sc}, D_{sc}, and K_{sc} are indicated as effective because it is not possible to separate these parameters experimentally and assign them exact values. As long as the external solvent contacting the skin does not concentrate in and alter the horny layer or does not occlude the skin and hydrate the horny layer, the thickness

Manuscript received May 12, 1986; accepted for publication February 23, 1987.
This work supported through National Institutes of Health grant NIDR DE-02731.
*Present address: Basic Pharmaceutics Research, CIBA-GEIGY Corporation, 444 Saw Mill Road, Ardsley, New York 10502.
†Present address: Department of Pharmaceutics, College of Pharmacy, The University of Utah, Salt Lake City, Utah 84112.
Reprint requests to: Gordon L. Flynn, Ph.D., College of Pharmacy, The University of Michigan, Ann Arbor, Michigan 48109-1065.
Abbreviations:
ara-A: vidarabine
DMSO: dimethyl sulfoxide

0022-202X/87/$03.50

of the stratum corneum and the permeant's diffusivity, D_{sc}, will remain unchanged, and equation 1 can be written as:

$$P_{sc} = (\text{constant})\ K_{sc} \qquad \text{(Eq. 2)}$$

The partition coefficient, K_{sc}, represents the equilibrium distribution coefficient of the permeant (ara-A in the present studies) between the phase of stratum corneum acting as the mass conducting medium (conduit phase) and the external solvent, which in these studies, is water, DMSO, or DMSO-water mixtures. Providing that the solvency of the conduit phase within the horny layer for ara-A is also unaffected by the external presence of DMSO solvent, then the partition coefficient of ara-A should strictly reflect the changing affinity of the applied phase for ara-A as the strength of DMSO is increased. Behavior regimes in which all these critical assumptions apply are evident upon comparing solubility and permeability trends. This was done previously for alkanols [11] and it was observed that the skin was unaffected by DMSO to a 50% concentration as long as the organic solvent was placed on both sides of the skin membrane.

The mole fraction solubility, X_2, of a permeant as ara-A in the applied phase is related to its activity in solution, a_2, by:

$$a_2 = \gamma_2 X_2 \qquad \text{(Eq. 3)}$$

where γ_2 is the activity coefficient. The activity, a_2, will be constant in saturated solutions, barring a change in the crystal structure, as the percentage concentrations of the solvents in a binary mixture are changed. Thus, at saturation, γ_2, the solute activity coefficient, must change oppositely and in proportion to changes in X_2 in order to maintain the product of γ_2 and X_2 constant. Since $K_{sc} = \gamma_2/\gamma_{skin}$ and providing γ_{skin} is constant, the permeability coefficient should decrease in exact proportion to the solubility increase unless diffusivity in the barrier tissues is altered. Conformity to this expectation indicates simple thermodynamic control of the permeation process. Lack of conformity indicates in a very general way that there has been structural alteration within the membrane. This critical test was applied to the data for ara-A's permeation of hairless mouse skin under various circumstances of operation of the diffusion cell.

MATERIALS AND METHODS

Materials The key materials used in these studies were ^{3}H-vidarabine (10.1 Ci/mmol) and vidarabine, gifts from Warner Lambert/Parke-Davis, Ann Arbor, Michigan; and ^{3}H-water (0.6 Ci/ml), ^{14}C-dimethyl sulfoxide (10 mCi/mmol), and a commercial liquid scintillation cocktail (Aquasol) from New England Nuclear, Boston, Massachusetts. Normal saline (Abbot Laboratories, North Chicago, Illinois) was used to make the permeation solutions and as a receiver solution component. Reagent grade dimethyl sulfoxide (Fisher Scientific Co., Fairlawn, New Jersey) was the other solvent used for preparing the donor and receiver media. It was also used to prepare the media for the solubility studies along with double-distilled water.

Diffusion Gels Small glass diffusion cells, each consisting of 2 half-cells, were used. These had half-cell compartment volumes of 1.5 ml and individually measured effective diffusional areas ranging from 0.542–0.675 cm^2. Each half-cell had a sampling port of 1 cm length and a stirring port of 3 cm length. Motors (Hurst Mfg. Co., Princeton, New Jersey) mounted above the cell and attached to stirring shafts passing through the stirring port were used to stir the media in the half-cells at 150 rpm. The stirring shafts had small teflon propellers threaded onto their ends. Skin membranes were placed between the half-cells and the unit was clamped together by a spring clamp. The cells were then immersed in a 37°C bath so that only the sampling and stirring ports broke through the liquid surface.

Membrane Preparation Male hairless mice 35–40 days of age (Skin Cancer Research Institute, Temple University Medical Center, Philadelphia, Pennsylvania) were sacrificed by spinal cord dislocation and square sections of abdominal skin, approximately 3 cm in each dimension, were immediately excised. Adhering fat and other visceral debris were removed from the skin undersurface before the skin was completely cut from the animal. After placing the skin sections between the half-cells, protruding, excess skin was trimmed off. The elapsed time from sacrifice of an animal to the beginning of a diffusion run was a few minutes.

Permeation Procedure After assembly of a cell, the donor and receiver sides were partially filled (1 ml) with the media for a given experiment. The media were either normal saline, DMSO-water mixtures (30%, 50%, 75%, or 90% DMSO) or neat DMSO. Some experiments were run with the same medium in both compartments of the cell (balanced configuration), whereas in others DMSO medium was placed in either the donor or receiver half-cell and saline was placed in the other side (asymmetric configurations). Balancing the medium eliminates net diffusive flows of the solvents. By varying the placement of the DMSO media in the asymmetric configurations, DMSO was caused to diffuse both with and against the diffusive direction of ara-A with net water diffusion opposing DMSO's in each case. The 2 asymmetric configurations allowed examination of the influence of concurrent diffusion of the solvents with or against ara-A.

The contents of a freshly filled cell were mixed for 5 min to temperature equilibration. Then 200 μl samples from each cell side were counted to make certain there was no residual radioactivity remaining from previous runs. This was strictly precautionary, because between runs, the cells were washed, rinsed liberally, soaked in permanganate cleaning solution overnight, and then cleaned again. The radioisotope free donor compartment was charged with 200 μl containing from 1–5 μCi of radiolabeled permeant(s) and 200 μl of appropriate solvent were added to the receiver. In studies in which solvent flows themselves were measured, the radiolabeled charge was sometimes placed in the half-cell contacting the dermis and diffusion was followed from receiver to donor.

Initial concentrations of the radiolabeled material were based on samples withdrawn from the half-cells 2 min after adding the radiochemical charge. At every 1000 s thereafter for a total of 7000 s (usual case) or longer, 100 μl samples were drawn from the half-cell opposing that containing the radioactive permeant. Fresh solvent of the appropriate composition was added to replace the solvent removed in sampling and corrections in sample concentrations were made to account for the attending dilution involved.

Samples were directly transferred to vials containing 10 ml of scintillation cocktail. These were assayed on a liquid scintillation counter (Beckman LS 9000 Scintillation Counter, Beckman Instruments, Fullerton, California). Each sample was counted for 10 min.

Data Analysis The concentration of radiolabel in the receiver half-cell was plotted as a function of time after correction was made for the dilution of sampling. The steady state region was identified graphically and the slope through the data in this region was estimated using least squares analysis. The permeability coefficient for a run was then calculated from:

$$P = \frac{V_r \cdot \frac{dc}{dt}}{A \cdot \Delta C} \qquad \text{(Eq. 4)}$$

where:

P = permeability coefficient (cm/h),

V_r = receiver volume (1.4 cm^3),

$\frac{dc}{dt}$ = rate of change of concentration (flux rate) in the receiver compartment in the steady state (counts/100 μl sample/10 min counting time),

ΔC = initial radiochemical concentration in the donor chamber (counts/100 μl sample/10 min counting time), and

A = diffusional area (cm^2).

Solubility Determinations Large excesses of crystalline ara-A were equilibrated with the pure solvents and binary solvent mixtures in well stirred jacketed flasks set up on a magnetic stirrer. Samples from the ara-A slurries were withdrawn periodically by syringe and, after coupling on a filter holder, were filtered through fluoropore filters (Millipore Corp., Bedford, Massachusetts) having a 0.5 μm pore size. This effectively removed all particulate matter. The samples were appropriately diluted with water and assayed. Sampling was continued until a solubility plateau was obtained (Fig 1).

High-performance liquid chromatography (Waters Chromatography Division, Millipore Corp., Milford, Massachusetts) was used to assay for solubility. The mobile phase was methanol: water, 20:80, and the column was a μ-Bondapak C-18 reverse-phase type. Solvent was passed through the system at 2.0 ml/min and at this flow rate the retention time was 4 min. Standard solutions of ara-A were prepared in 10% DMSO for calibration of the integrated area at 254 nm. The injection volume for standard and unknown solutions was 20 μl. The sensitivity range of the chromatographic system was determined to be 0.1 μg/ml and excellent linearity was observed over the range of concentrations used for assay. Areas from standard solutions were routinely determined prior to quantification of unknown samples.

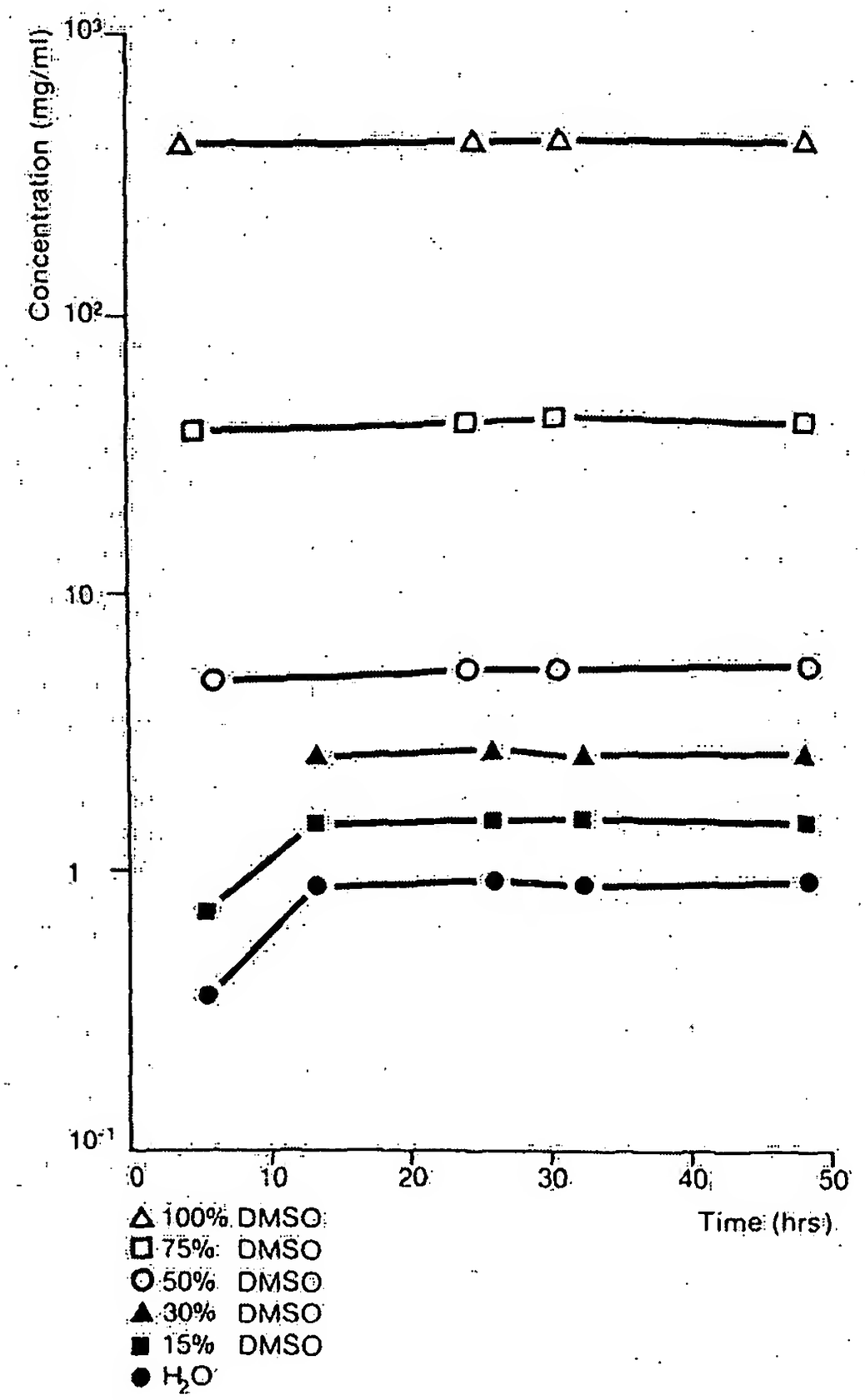

Figure 1. Solution profiles for ara-A in varying DMSO concentrations at 37°C as a function of time.

Table I. Comparison of Permeability Coefficients of Vidarabine Administered to Hairless Mouse Skin in Dimethyl Sulfoxide-Water Media

System (donor-receiver)	P × 10^3* (cm/h)	Ratio (A)/(B)
(A) Saline–saline	(3.16 ± 0.34) × 10^{-3}	1.1
(B) Saline–saline	(3.10 ± 0.58) × 10^{-2}	
(A) 30% $(CH_3)_2SO_4$–saline	(1.33 ± 0.56) × 10^{-2}	1.8
(B) 30% $(CH_3)_2SO_4$–30% $(CH_3)_2SO_4$	(7.96 ± 3.80) × 10^{-3}	
(A) 50% $(CH_3)_2SO_4$–saline	(8.81 ± 1.80) × 10^{-2}	14.4
(B) 50% $(CH_3)_2SO_4$–50% $(CH_3)_2SO_4$	(6.19 ± 1.64) × 10^{-3}	
(A) 75% $(CH_3)_2SO_4$–saline	(5.15 ± 1.95) × 10^{-1}	59.8
(B) 75% $(CH_3)_2SO_4$–75% $(CH_3)_2SO_4$	(1.09 ± 0.81) × 10^{-2}	
(A) 90% $(CH_3)_2SO_4$–saline	(5.19 ± 2.46) × 10^{-1}	0.94
(B) 90% $(CH_3)_2SO_4$–90% $(CH_3)_2SO_4$	(5.57 ± 1.17) × 10^{-1}	
(A) 100% $(CH_3)_2SO_4$–saline	1.29 ± 0.23	0.07
(B) 100% $(CH_3)_2SO_4$–100% $(CH_3)_2SO_4$	18.9 ± 1.64	

In set A the dimethyl sulfoxide was placed in the donor compartment only (one of the two possible asymmetric cell configurations). In set B identical dimethyl sulfoxide solutions were placed on both sides of the skin (balanced configuration).

*Average of three results and standard deviation.

RESULTS

Permeability coefficients obtained for ara-A in both the balanced and the asymmetric solvent configurations of the cells are given in Table I. The DMSO media were placed in contact with the external (stratum corneum) surface of the skin in the asymmetric mode in these experiments. The ratios of the permeability coefficients in the 2 modes of operation are given in the *right-hand column*. Data for the 2 different asymmetric configurations of the cell are given in Table II. Ratios of the data for the 2 configurations are provided in the *right-hand column*. With the exception of the saline-to-saline control experiment, data for the asymmetric configuration with the organic solvent phase in contact with the stratum corneum represent separate experiments. This was because matched samples of skin were taken from the animals and compared as sets. The agreement in the results of common experiments in the first and second data sets is reasonable.

Data for the concurrent permeation of DMSO, water, and ara-A are given in Table III. These experiments also involved the gathering of totally independent ara-A data. It can be seen that

Table II. Comparison of Permeability Coefficients of Vidarabine Administered to Hairless Mouse Skin in Dimethyl Sulfoxide-Water Media

System (donor-receiver)	P × 10^3* (cm/h)	Ratio (A)/(C)
(A) Saline–saline	(3.16 ± 0.34) × 10^{-2}	1.1
(C) Saline–saline	(3.10 ± 0.58) × 10^{-2}	
(A) 30% $(CH_3)_2SO_4$–saline	(2.11 ± 1.17) × 10^{-2}	0.5
(C) Saline–30% $(CH_3)_2SO_4$	(4.89 ± 3.11) × 10^{-2}	
(A) 50% $(CH_3)_2SO_4$–saline	(4.91 ± 2.44) × 10^{-2}	0.4
(C) Saline–50% $(CH_3)_2SO_4$	(1.32 ± 0.60) × 10^{-1}	
(A) 75% $(CH_3)_2SO_4$–saline	(4.68 ± 1.48) × 10^{-1}	4.06
(C) Saline–75% $(CH_3)_2SO_4$	(1.53 ± 1.20) × 10^{-1}	
(A) 100% $(CH_3)_2SO_4$–saline	(8.12 ± 1.91) × 10^{-1}	0.9
(B) Saline–100% $(CH_3)_2SO_4$	(9.27 ± 1.78) × 10^{-1}	

In these cases the solvents are configured in the asymmetric modalities. In set A the dimethyl sulfoxide media were in contact with the stratum corneum, whereas in set B the dimethyl sulfoxide media were placed against the dermal side of the skin membranes.

*Average of three results and standard deviation.

Table III. Concurrent Permeation Rate of Vidarabine, Dimethyl Sulfoxide, and Water Through Hairless Mouse Skin

% Dimethyl Sulfoxide	Permeability Coefficient × 10^3 (cm/h)[a]			
	P vidarabine[b]	P dimethyl sulfoxide[b]	P H_2O[b,d]	P H_2O[c]
0	(3.37 ± 1.19) × 10^{-2}		1.30 ± 0.18	1.90 ± 0.22
15	(2.45 ± 0.20) × 10^{-2}	(6.02 ± 0.72) × 10^{-2}		
30	(3.90 ± 1.52) × 10^{-2}	(6.93 ± 3.00) × 10^{-2}	1.82 ± 0.32	1.77 ± 0.42
50	(4.69 ± 1.70) × 10^{-1}	(9.98 ± 3.52) × 10^{-1}	1.48 ± 0.58	2.72 ± 0.55
75	(7.74 ± 1.22) × 10^{-1}	4.16 ± 1.11	21.4 ± 10.3	65.5 ± 16.1
100	1.09 ± 0.10	4.13 ± 0.05		150 ± 20.0

[a] Average of four results and standard deviation.
[b] Donor → receiver.
[c] Receiver → donor.
[d] Permeability coefficients of individual species identified by subscripts.

these asymmetric data agree well with like data from the first 2 sets.

Solubility data are shown in Fig 1. It is notable that the solubility equilibrium was achieved in a day's time in all instances. The plateaus (and plateau standard deviations) were 0.972 ± 0.016, 1.72 ± 0.02, 2.71 ± 0.07, 5.72 ± 0.08, 44.5 ± 0.87, and 433 ± 21 mg/ml for water, 15%, 30%, 50%, 75%, and neat DMSO respectively.

DISCUSSION

Kligman [12] may have been the first to document the marked concentration dependency of DMSO's ability to enhance skin permeation when he noted that fluorescein's permeation of excised human skin membranes was nil until the concentration of DMSO in the medium used to apply fluorescein exceeded 50%. From there fluorescein's permeability increased systematically and dramatically to a DMSO strength of 90%. Substantial back diffusion of water was also noted by Kligman [12] and was given as the reason the penetration rate dropped back between 90 and 100% DMSO. Subsequently, Sweeney and colleagues [13] showed it took DMSO concentrations above 60% to accelerate tritiated water's permeation of skin. Elfbaum and Laden demonstrated much the same to be true for DMSO mediation of picric acid permeation of skin [14] and, in related experiments, saw the same kind of concentration dependency for the swelling of hair fibers [15]. Whealing reactions of intact skin share this general concentration dependency [16]. More recently, work by Kurihara-Bergstrom and associates [11] has shown that the permeation behaviors of simple alkanols as methanol, butanol, and octanol through hairless mouse skin are similarly dependent on DMSO's solution strength. The present experiments performed on hairless mouse skin further support the idea that it takes a highly enriched DMSO media to produce pronounced enhancements of permeability. Being more detailed and systematic than most past works, subtleties of behavior not previously apparent are also revealed. For example, although the data for the balanced and asymmetric configurations, plotted in Fig 2, follow patterns that fit expectations drawn from the literature, these data also show that the manner of configuration of the solvent phases external to the mouse skin has a remarkable effect on permeation.

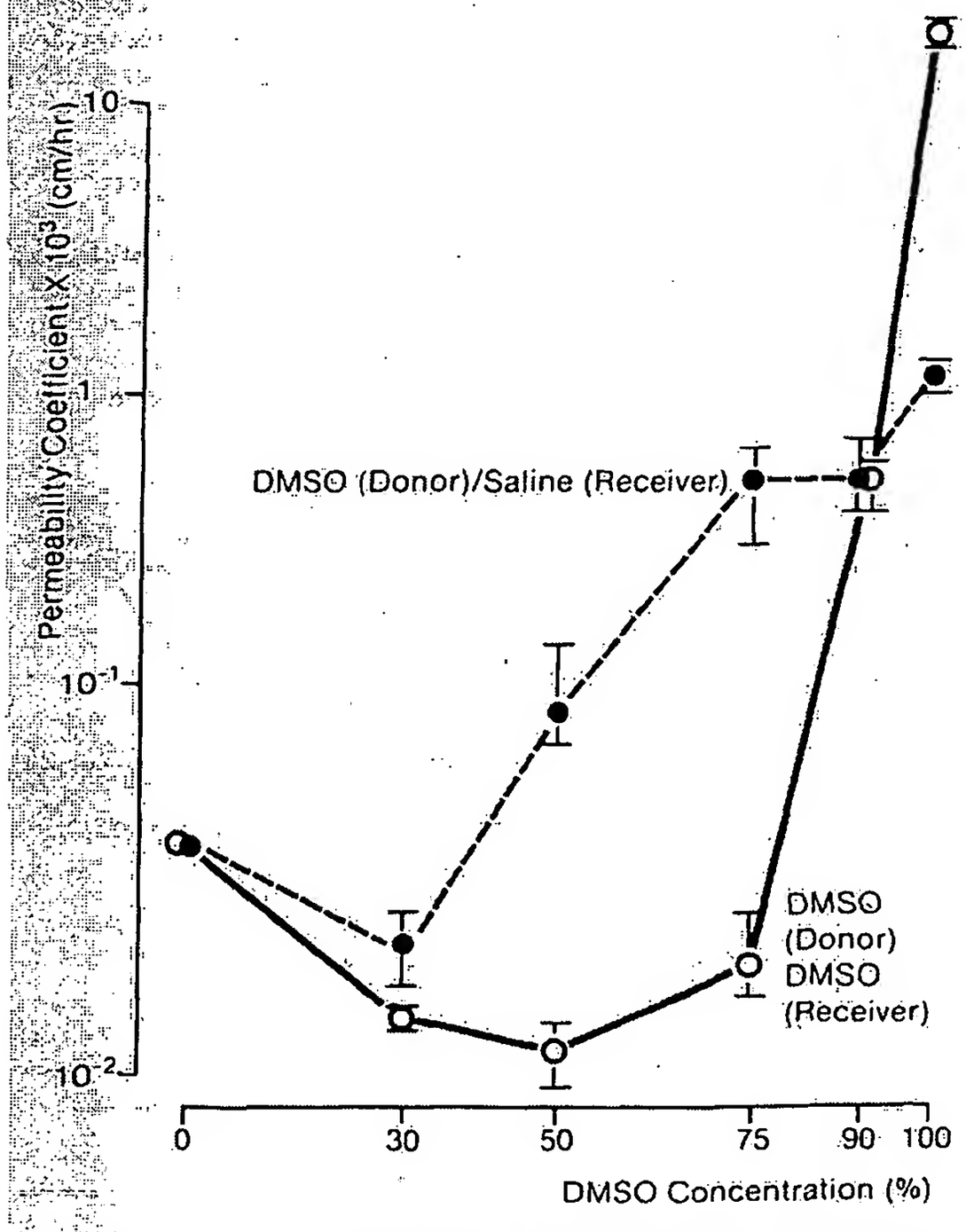

Figure 2. Comparison of permeability coefficients of ara-A through hairless mouse skin in DMSO-water media (DMSO-saline). *Closed circles*, DMSO media were in contact with the stratum corneum only; *open circles*, DMSO media were placed on both sides of the skin.

In the balanced configuration, the permeability coefficient of ara-A systematically declines to 50% DMSO and remains smaller than the permeability coefficient from saline even to a 75% DMSO concentration. Extraordinarily large increases in permeability are noted, however, when DMSO's strength is increased first to 90% and then to 100%. In the normal asymmetric configuration with DMSO in contact with the stratum corneum, the permeability coefficient drops slightly from the value found in saline to that in 30% DMSO (not significant) and then increases sharply at the 50% DMSO strength. In 50% DMSO it is over twice the magnitude of the reference saline value ($p < 0.01$) and over 14 times the value found for balanced configuration at 50% DMSO ($p < 0.05$). An eight-fold further increase is seen at 75% DMSO where the asymmetric value is now about 60 times higher than the value in the comparable balanced configuration, a highly statistically significant difference ($p < 0.01$). No further increase is noted in permeability when the DMSO strength is raised to 90%, a concentration at which the curves for the asymmetric and balanced configurations intersect. In neat DMSO the permeability coefficient in the asymmetric configuration is at its highest at 1.3 × 10^{-3} cm/h. This is now a highly significant ($p < 0.001$) 14.6 times smaller than found in the balanced mode, however.

The decline in permeability in the balanced configuration to the 50% DMSO concentration is due to an increasing ability of the increasingly concentrated DMSO media to solvate ara-A. This ability is directly and relatively reflected accurately in solubility patterns. At any predetermined concentration of ara-A, the in-

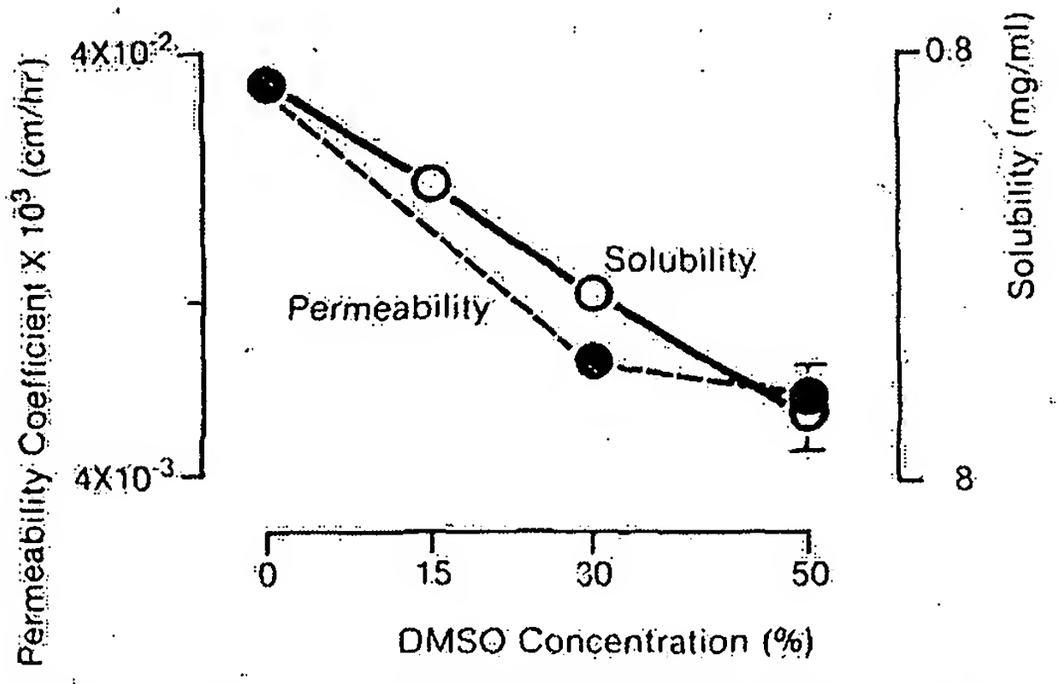

Figure 3. Comparison of permeability coefficient and solubility of ara-A between water and 50% DMSO-water media. *Closed circles*, permeability coefficients; *open circles*, solubility.

creasing ability of DMSO enriched media to solvate the compound directly translates to decreased stratum corneum-water partitioning, and everything else equal, proportionally decreased flux. This is reflected directly in the permeability coefficient, which is a concentration normalized parameter. Since the six-fold decrease in permeability from saline to 50% DMSO is matched by a six-fold increase in solubility over the same range of DMSO concentration (Fig 3), it appears that to the 50% DMSO strength in the balanced configuration DMSO's influence is strictly thermodynamic, a conclusion in keeping with results of experiments with select alkanols [11]. The permeability coefficients of ara-A applied in 75, 90, and 100% DMSO in the balanced configuration take a dramatic upwards turn, a marked qualitative departure from the thermodynamic (partitioning) trend. This unequivocally indicates DMSO has in some way altered the properties of the stratum corneum at these higher levels.

In contrast, unmistakable stratum corneum impairment by DMSO is seen at the 50% strength when this solvent medium is placed in only the donor compartment. This appears to be somewhat true for the 30% medium as well. Thus, the way the solvents are configured around the skin membrane itself has a marked influence on permeability. The data compiled in Table III indicate there are large net cross-currents of water and DMSO in the asymmetric circumstances, the major difference between the balanced and asymmetric modes. The inference is strong that the diffusive exchange of solvents causes disruption of the horny layer's structure. This idea is in keeping with the proposed enhancement mechanism of Chandrasekaran and coworkers [10], who were the first to note that, when configured asymmetrically, DMSO and water produce a separation of stratum corneum cell layers, presumably through osmotically derived stresses. Given the behaviors seen in the balanced configuration, it would appear the solvent cross-flows are of singular importance to DMSO permeability enhancement in the asymmetric modality at the intermediate DMSO concentrations. At concentrations above 50% other factors of enhancement must necessarily come into play given that marked enhancement of permeability is seen in the balanced configuration. It was previously demonstrated [11] that under the conditions of these experiments, substantial amounts of soluble organic substances are eluted from the skin, presumably mostly lipids, above the 50% DMSO strength, with the amounts extracted increasing sharply as DMSO is further enriched. By eluting soluble substances, the solvent induces a porosity on the skin and diffusion can proceed through solvent-filled channels in the stratum corneum matrix.

Concentrated DMSO is also capable of directly denaturing the keratin protein of the horny layer and disrupting ordered lipid structures, additional factors that may be involved when DMSO is applied in essentially an undiluted state. It is notable that there is crossover of the 2 profiles at the 90% DMSO strength and a strikingly higher permeability of ara-A from the balance configuration when the medium of application is neat DMSO. We suspect that DMSO is more effective in eluting substance from the skin and also as a denaturant when it is placed in both compartments of the cell. In this mode there would be no dilution of the DMSO solvent at the skin's surface as the result of the diffusion of water through the skin. There are other plausible bases for this disparity between the balanced and asymmetric modes. For instance, the tendency for ara-A to partition into the cellular epidermis beneath the stratum corneum is diminished when the dermal surface is bathed in saline. Vidarabine's diffusive current across the epidermal and dermal strata might thereby be reduced to a fraction of what it is when all cellular water is exchanged for DMSO. Disruption and collapse of cell membrane structures is yet another possible contributing factor to the high permeability of ara-A when it is diffusing from neat DMSO into neat DMSO.

In their work with pilocarpine hydrochloride, Chandrasekaran and coworkers [10] showed that the side of placement of DMSO in the asymmetric configuration has an effect on permeability. It can be seen in Fig 4 that this also makes a difference for ara-A. Each way of asymmetric configuration can produce the higher permeability depending on the specific DMSO concentration, a factor not noted previously. The total picture suggests that disruptive stresses are experienced within the horny structure irrespective of which side the DMSO media are placed. At 30 and 50% DMSO, mass transfer is favored when the DMSO phase is in the receiver chamber. If the degree of damage is independent of placement, which seems a reasonable possibility, then the higher permeability at low-to-moderate DMSO concentrations seen when the ara-A is placed in a saline donor and is diffusing into a DMSO receiver reflects that the permeability change resulting from damage to the horny layer is neutralized to a degree by decreased solvation of ara-A and increased thermodynamic activity in the donor phase. Not only does the thermodynamic activity remain higher when the donor is saline, but ara-A also finds the receiver a better sink as it permeates the tissue.

The situation appears to be different when DMSO strength is greater than 50%. Here we suspect that elution of soluble matter from the stratum corneum is favored when the DMSO is in direct contact with the horny layer. This would explain the change in the order of permeability at the 75% DMSO strength. Curiously,

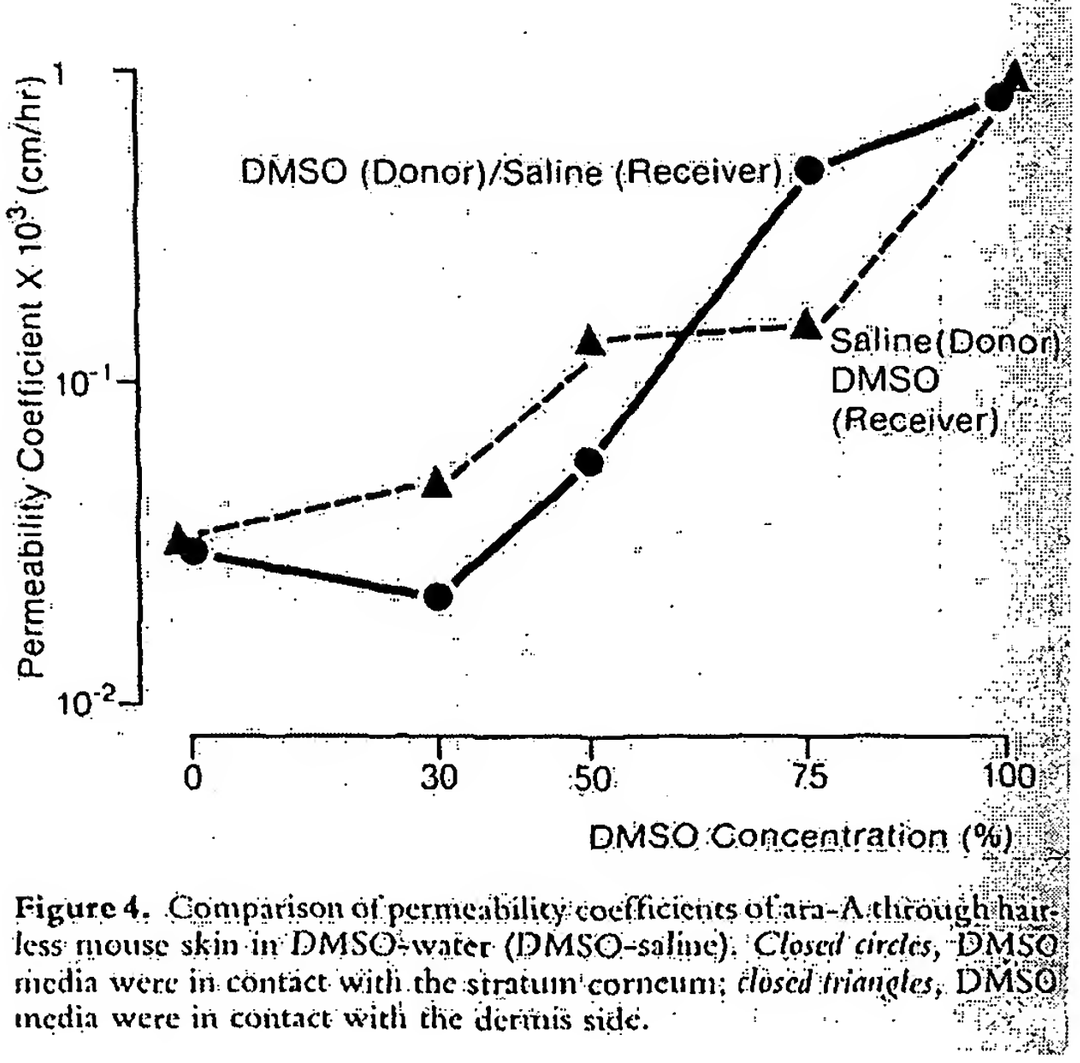

Figure 4. Comparison of permeability coefficients of ara-A through hairless mouse skin in DMSO-water (DMSO-saline). *Closed circles*, DMSO media were in contact with the stratum corneum; *closed triangles*, DMSO media were in contact with the dermis side.

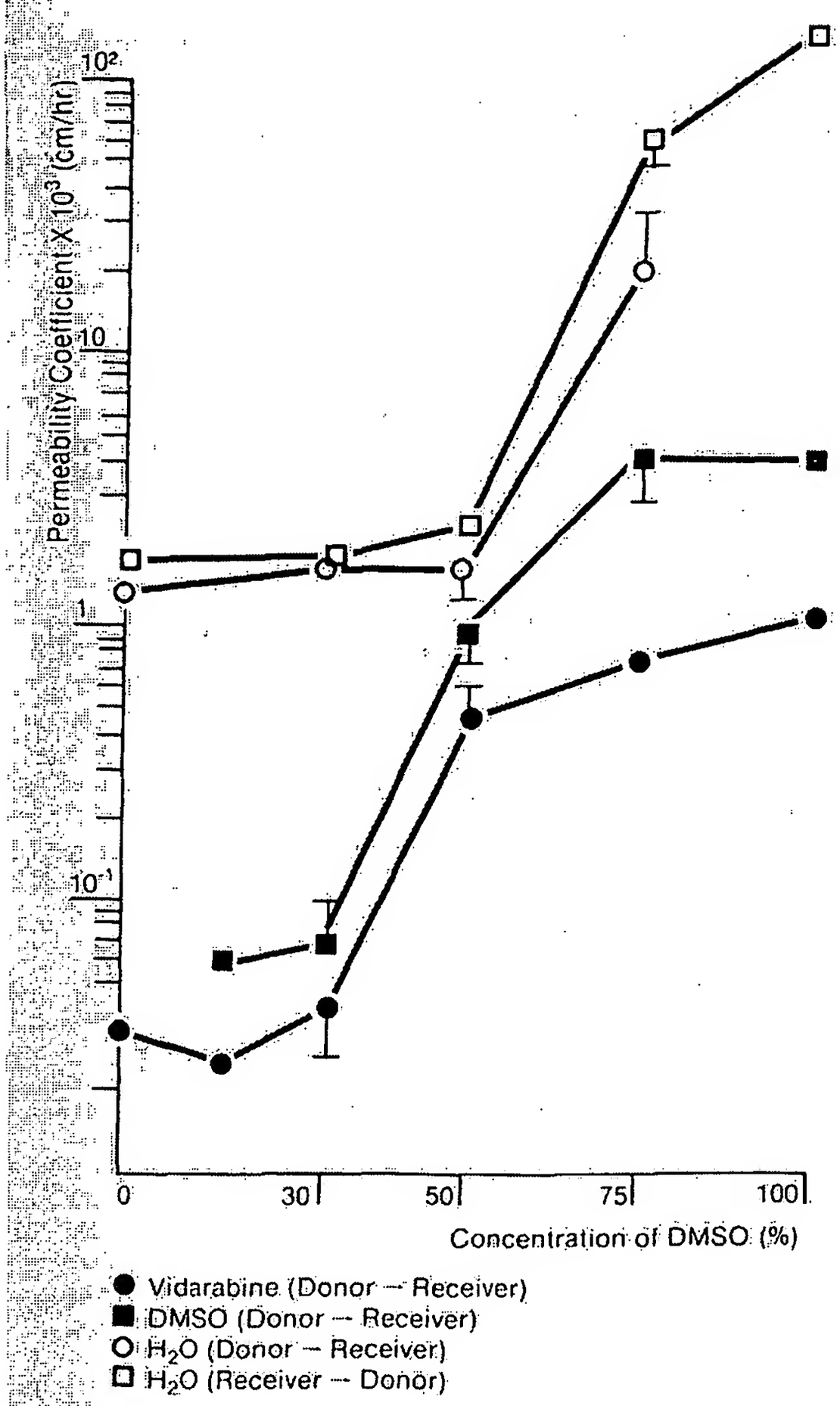

Figure 5. Concurrently determined permeability coefficients of ara-A, DMSO, and water through hairless mouse skin as a function of DMSO concentration.

the two asymmetric configuration curves come together again when the DMSO is in a neat state. Either the various contributions to barrier impairment catch up to each other at this point or there are opposing effects, which by pure chance, exactly offset each other. The latter explanation seems more plausible as it appears to us that the permeability retarding thermodynamic influence of DMSO when it is in the donor chamber is sufficient to offset the presumed differential in impairment of the horny layer in the same solvent configuration.

In either asymmetric configuration solvent cross-flows have been indicated as important to the mechanism of penetration enhancement. Additional support for this premise is given in Fig 5 for the specific asymmetric configuration with the DMSO media in contact with the stratum corneum side of the skin. Permeability coefficients of tritiated water into and out of the skin are displayed. Once concentration is taken into account, as it is in the calculation of such concentration normalized mass transfer coefficients, there appears to be little directionality to the permeability of this species. The permeability coefficients displayed for DMSO are for a net flux concurrent with and in the same direction as ara-A's.

Notably, no matter the DMSO concentration, there is, in every instance, a manifold greater backflow of water out of the skin than the diffusive flow of DMSO into it. If there were a "carrier effect," it would work against ara-A's permeation. In other words, ara-A molecules are not being drawn through the skin on a stream of solvent, the implication of the phase "carrier effect," but rather the chemical species are independently diffusing through the skin field variously altered by DMSO-water interactions with the tissue. Moreover, although the permeabilities of all 3 species, water, DMSO, and ara-A, fit well with the broader expectations of permeability as a function of DMSO concentration, it appears water's quantitative sensitivities to DMSO are unique. It will be noted that there is a large increase in the permeability coefficient at 50% DMSO for both DMSO and ara-A. Water's permeability coefficient on the other hand seems unaffected by DMSO until much higher DMSO concentrations are reached. This lack of DMSO sensitivity for water at intermediate DMSO strengths seems to have also been seen by Sweeney et al [13]. This strongly suggests that the delamination of the stratum corneum thought responsible for the increased permeability of ara-A does not of itself favor the diffusion of water. Thus, it appears that different mechanisms control the rates of diffusion of these very different molecular species within the horny structure.

Overall, it is shown that the manner in which DMSO produces permeability-enhancing effects on skin is influenced by the manner of application of DMSO and the concentration of DMSO. Partitioning factors are one determinant of permeability and in the simplest instances these alone control permeation rates. There is also clear evidence that several types of stratum corneum impairment are involved. All of these factors together lead to very complex DMSO concentration dependencies for its skin permeability enhancing effects, as revealed in standard diffusion cell experiments.

REFERENCES

1. Schwartz PM, Shipman C Jr, Drach JC: Antiviral activity of arabinosyladinine and arabinosylhypoxanthine in herpes simplex virus-infected KB cells: selective inhibition of viral deoxyribonucleic acid synthesis in the presence of an adenosine deaminase inhibitor. Antimicrob Agents Chemother 10:64–74, 1976
2. Whitley RJ, Soong S, Dolin R, Galasso GJ, Chien LT, Alford CA: Adenine arabinoside therapy of biopsy-proved herpes simplex encephalitis. N Engl J Med 297:289–294, 1977
3. Ando HY, Ho NFH, Higuchi WI: Skin as an active metabolizing barrier. I. Theoretical analysis of topical bioavailability. J Pharm Sci 66:1525–1527, 1977
4. Ando HY, Higuchi WI: In vitro estimates of topical bioavailability. J Pharm Sci 66:755–757, 1977
5. Allenby AC, Creasey NH, Edginton JAG, Fletcher JA, Schock C: Mechanism of action of accelerants on skin permeation. Br J Dermatol 81(suppl 4):47–55, 1969
6. Stoughton RB: Dimethyl sulfoxide induction of a steroid reservoir in human skin. Arch Dermatol 91:657–660, 1965
7. Stoughton RB, Fritsche W: Influence of dimethyl sulfoxide on human percutaneous absorption. Arch Dermatol 90:512–517, 1964
8. Ritschel WA: Sorption promoters in biopharmaceutics. Angew Chem Int Ed Eng 8:99–703, 1969
9. Durrheim HH, Flynn GL, Higuchi WI, Behl CR: Permeation of hairless mouse skin. I. Experimental methods and comparison with human epidermal permeation by alkanols. J Pharm Sci 69: 781–786, 1980
10. Chandrasekaran SK, Campbell PS, Michaels AS: Effect of dimethyl sulfoxide on drug permeation through human skin. American Institute of Chemical Engineers Journal 23:810–816, 1977
11. Kurihara-Bergstrom T, Flynn GL, Higuchi WI: Physicochemical study of percutaneous absorption enhancement by dimethyl sulfoxide: kinetic and thermodynamic determinants of dimethyl sulfoxide mediated mass transfer of alkanols. J Pharm Sci 75:479–486, 1986
12. Kligman AM: Topical pharmacology and toxicology of dimethyl sulfoxide—part 1. JAMA 193:796–804, 1965

13. Sweeney TM, Downes AM, Matoltsy AG: The effect of dimethyl sulfoxide on the epidermal water barrier. J Invest Dermatol 46:300–302, 1966

14. Elfbaum SG, Laden K: The effect of dimethyl sulfoxide on percutaneous absorption: a mechanistic study, part I. J Soc Cosmet Chemists 19:119–127, 1968

15. Elfbaum SG, Laden K: The effect of dimethyl sulfoxide on percutaneous absorption: a mechanistic study, part II. J Soc Cosmet Chemists 19:163–172, 1968

16. Sulzberger MB, Cortese TA Jr, Fishman L, Wiley HS, Peyakovich PS: Some effects of dimethyl sulfoxide on human skin in vivo. Ann NY Acad Sci 141:437–450, 1967

Increased Skin Permeability for Lipophilic Molecules

EUGENE R. COOPER

Received July 30, 1982, from *The Procter & Gamble Co., Miami Valley Laboratories, Cincinnati, OH 45247.* Accepted for publication August 25, 1983. Present address: Alcon Laboratories, Fort Worth, TX 76134.

Abstract □ Treatment of the epidermis with surfactants can markedly increase the transport of polar molecules but only marginally increases the transport of nonpolar (lipophilic) molecules. Thus, other vehicle systems are needed to increase the transport of lipophilic molecules. One method to accomplish this increased transport is to add small quantities of polar lipids to a base vehicle containing propylene glycol. The transport of nonpolar materials such as salicylic acid can be increased by an order of magnitude by the addition of small amounts of fatty acids or alcohols to a formulation. The effect of this mixed system is much greater than the effect of any of the agents alone.

Keyphrases □ Transport systems—increased skin permeability, lipophilic molecules □ Lipophilic molecules—transport systems, increased skin permeability

The stratum corneum, which is the main barrier to cutaneous transport (1), is structurally a complex membrane, and thus, transport probably takes place through a variety of pathways. It has been suggested in a study of the effect of temperature on the penetration of alcohols (2) that there are at least two pathways for transport across the skin: a polar pathway and a nonpolar pathway. The polar pathway is associated with the protein component of the stratum corneum and might be envisioned as aqueous channels in the protein; the nonpolar pathway is associated with the lipid component.

In recent studies (3), the attempt has been made to clarify and support the hypothesis that there are at least two parallel pathways for transport by using surfactant treatment, which greatly increases the transport of polar molecules but only slightly increases the transport of nonpolar molecules. For example, it has been found that treatment of the human epidermis with decylmethyl sulfoxide greatly increases the transport of salicylic acid at pH 9.9 (ionized or polar form) but only slightly increases salicylic acid transport at pH 2.65 (un-ionized or nonpolar form). Other studies have shown that the transport of 1-propanol is greater than that of propylene glycol or glycerol. That is, even though propylene glycol has a much higher oil–water partition coefficient than glycerol (4), its cutaneous flux from aqueous solution is only slightly greater than that of glycerol but much less than that of 1-propanol. Thus, as the polarity of a molecule is increased, *i.e.*, its oil–water partition coefficient decreases, a polarity exists for which the oil–water partition coefficient is not related to transport. These results differ noticeably from those obtained previously (2), in which even 1-pentanol is claimed to transport *via* a polar pathway.

The existence of multiple transport pathways in skin points to the possibility for design of vehicles to alter the permeability of the skin *via* the different pathways, as the surfactants seem to uniquely alter the polar pathway. Certain two-component systems have been found which alter transport differently from the way the components behave individually. The purpose of this report is to describe the effects of these vehicle systems on the transport of nonpolar molecules across skin. Salicylic acid was used as a prototype nonpolar compound, but similar results were obtained on many other nonpolar compounds. A model is proposed to interpret these findings, but the mechanism by which these vehicles alter transport is still unknown.

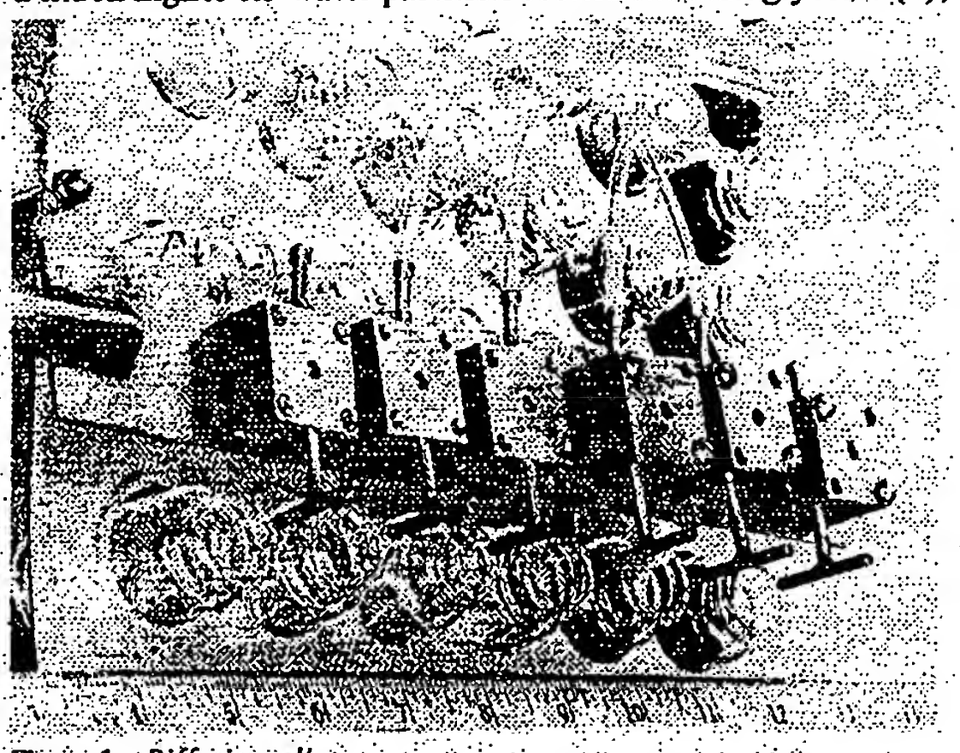

Figure 1—*Diffusion cell.*

EXPERIMENTAL SECTION

Materials—Salicylic acid[1], [^{14}C-carboxylate]salicylic acid[2], the fatty acids and alcohols[3], propylene glycol[4], diethylene glycol[5], and the polyethylene glycols[6] were obtained commercially. The sulfoxides (purity >95%) were synthesized[7], and the dimethyl polysiloxane[8] rubber membranes were cast on a large stainless steel plate. All other chemicals used were of reagent grade.

Diffusion Studies—*Epidermis Preparation*—Full-thickness human ab-

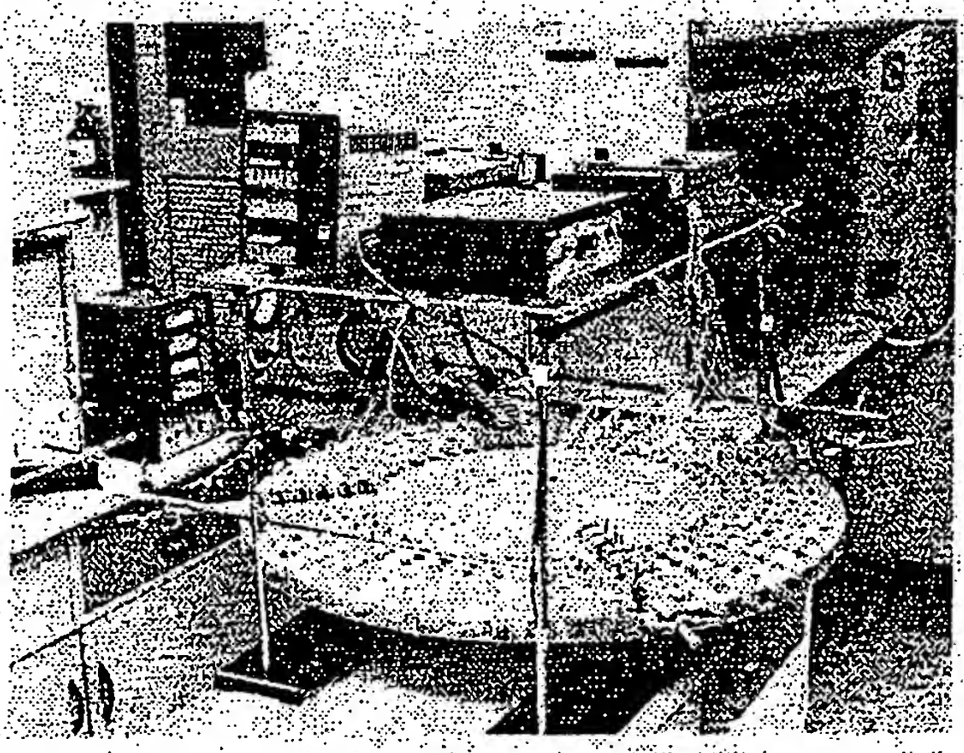

Figure 2—*Diffusion Apparatus.*

[1] Fisher Scientific Co., Cincinnati, Ohio.
[2] ICN Chemicals, Radioisotope Division, Irvine, Calif.
[3] Nu-Chek Prep, Inc., Elysian, Minn.
[4] J. T. Baker Chemical Co., Phillipsburg, N.J.
[5] Aldrich Chemical Co., Inc., Metuchen, N.J.
[6] Ventron Corp., Danvers, Mass.
[7] Miami Valley Laboratories.
[8] MDX-4-4210 elastomer and MDX-4-4210 curing agent; Dow Corning, Midland, Mich.

0022-3549/84/0800-1153$01.00/0

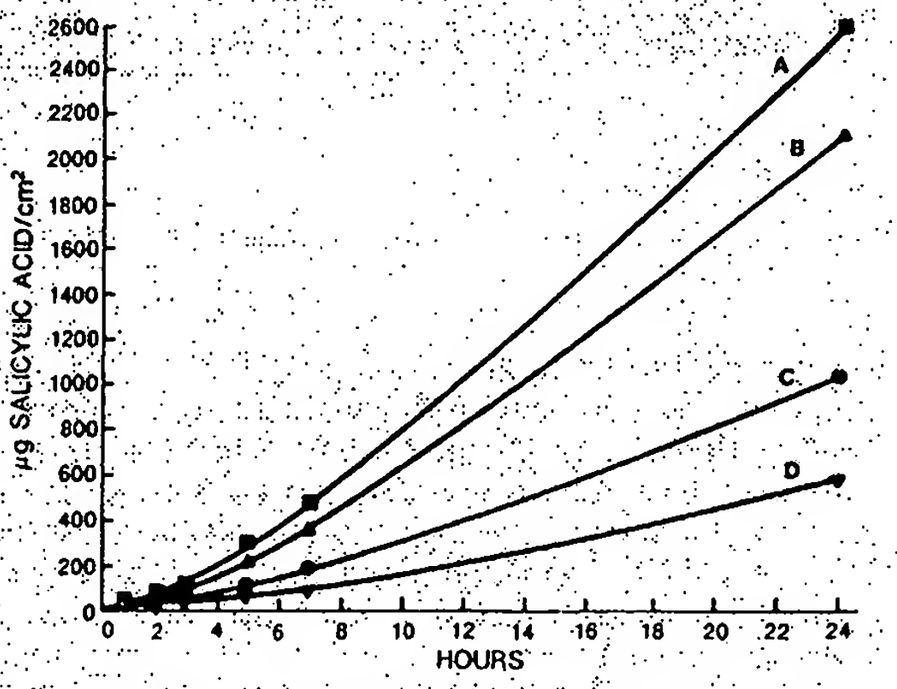

Figure 3—*Effect of polar solvents on salicylic acid transport across human epidermis. Key: (A) 24% salicylic acid in diethylene glycol; (B) 19% salicylic acid in propylene glycol; (C) 30% salicylic acid in tetraethylene glycol; (D) 27% salicylic acid in pentaethylene glycol.*

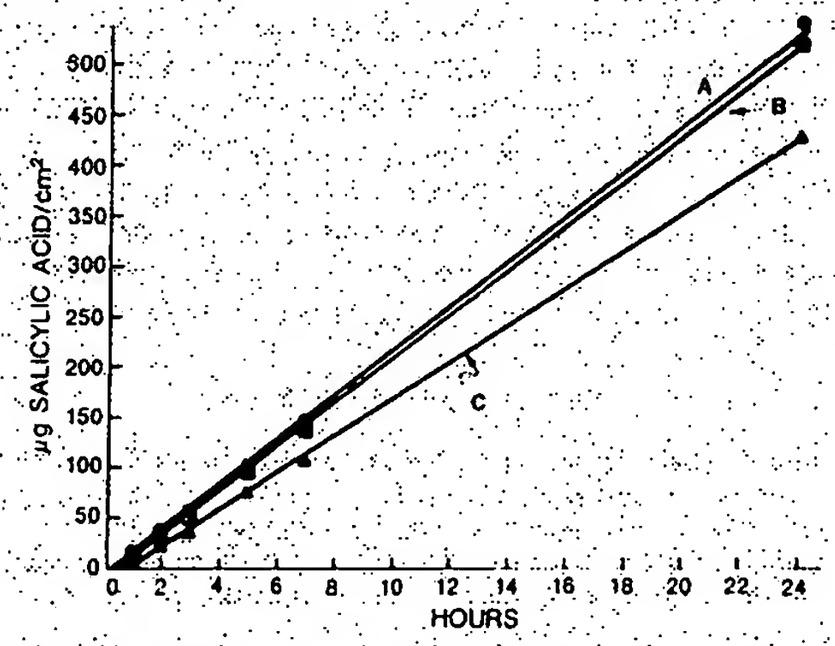

Figure 4—*Effect of polar solvents on salicylic acid transport across silicone rubber. Key: (A) 30% salicylic acid in tetraethylene glycol; (B) 19% salicylic acid in propylene glycol and 24% salicylic acid in diethylene glycol; (C) 27% salicylic acid in pentaethylene glycol.*

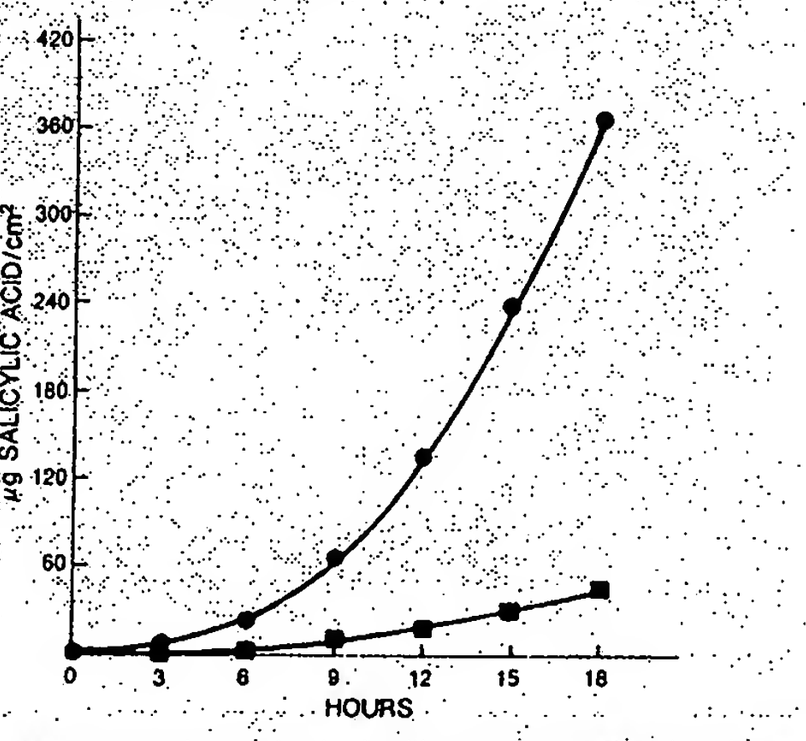

Figure 5—*Penetration of 1% salicylic acid across human epidermis. Key: (●) 0.1 M oleic acid in propylene glycol; (■) propylene glycol.*

dominal skin was obtained at autopsy and frozen until ready for use. The subcutaneous fat was removed with a scalpel, and the skin was placed in water at 60°C for 80 s. The epidermis was carefully removed and mounted (outer surface up) on aluminum foil before rinsing in 0°C hexane for 10 s to remove

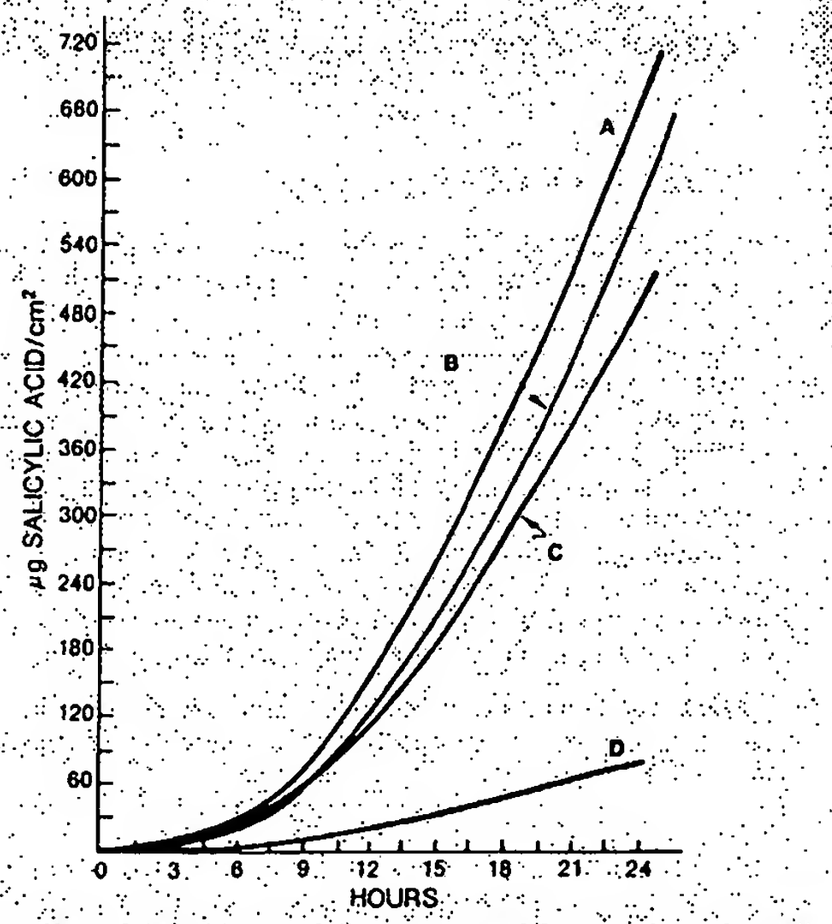

Figure 6—*Effect of the addition of cis-unsaturated fatty acids on the penetration of 1% salicylic acid in propylene glycol across human epidermis. Key: (A) 0.1 M myristoleic acid; 0.1 M palmitoleic acid; (C) 0.1 M oleic acid; (D) propylene glycol.*

any fat contamination. The epidermis was either used immediately or wrapped in a plastic sheet[9] and frozen.

Experimental Apparatus—The epidermis was mounted in diffusion cells as pictured in Fig. 1. The flat surfaces of the cell provide a pressure seal after the epidermis is placed between the two compartments, which are bolted together. Up to 100 µL of solution can be placed in the chamber above the skin. The area for transport is 0.122 cm². Water was pumped *via* a multichannel peristaltic pump through the lower compartment at 3.5 mL/h and collected in scintillation vials placed in a programmable rotating fraction collector. Figure 2 shows the entire assembly. The volume of water in the chamber beneath the skin is ~5 µL, so the volume beneath the skin is replaced ~100 times/h. The temperature of the experiments was that of the laboratory, 22 ± 1°C.

Assay for Penetration—Approximately 1 µCi of radioactive tracer was used for each diffusion cell. The quantity of radioactive tracer transported

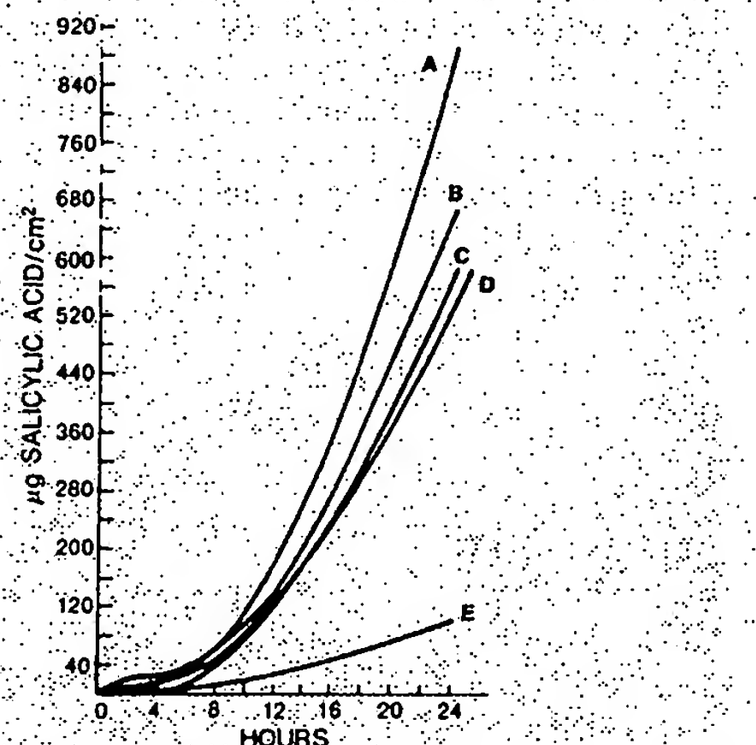

Figure 7—*Effect of the addition of cis-unsaturated fatty acids on the penetration of 1% salicylic acid in propylene glycol across human epidermis. Key: (A) 0.1 M vaccenic acid; (B) 0.1 M 10-heptadecannoic acid; (C) 0.1 M petroselenic acid; (D) 0.1 M eicosenoic acid; (E) propylene glycol.*

[9] Saran Wrap.

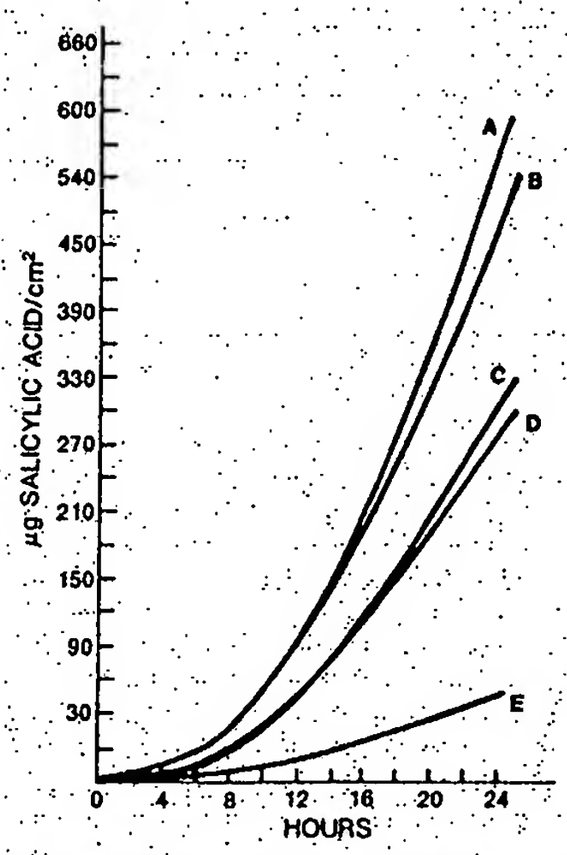

Figure 8—*Effect of the addition of polyunsaturated fatty acids on the penetration of 1% salicylic acid in propylene glycol across human epidermis. Key: (A) 0.1 M linolenic acid; (B) 0.1 M linoleic acid; (C) 0.1 M vaccenic acid; (D) 0.1 M linoelaidic acid; (E) propylene glycol.*

across the skin and collected in the scintillation vials was determined by liquid scintillation counting. The scintillation counting solution (10 mL), added to each 7-mL sample, consisted of cocktail stock solution. The latter consisted of 2,5-diphenyloxazole (8 g) and 1,4-bis(4-methyl-5-phenyloxazol-2-yl) benzene (0.16 g) per liter of toluene.

Variation in Data—The epidermal transport from each vehicle was determined in quadruplicate, and the variation in the data was ±25%. Data on each graph represent separate experiments run on different days with different epidermal samples.

RESULTS AND DISCUSSION

The vehicles described in this paper are two-component systems consisting of a polar solvent, such as propylene glycol, and a lipid, such as oleic acid. The choice of polar solvent is important, since there is a wide range in the effects of polar solvents. For example, it can be seen in Fig. 3 that propylene glycol and diethylene glycol support a high rate of transport of salicylic acid but that the flux drops off some as the number of ethylene oxide groups is increased. (Note that comparisons are made among saturated solutions to ensure equal thermodynamic activity.) Transport of salicylic acid across a dimethyl polysiloxane membrane (Fig. 4) was essentially the same from each of these

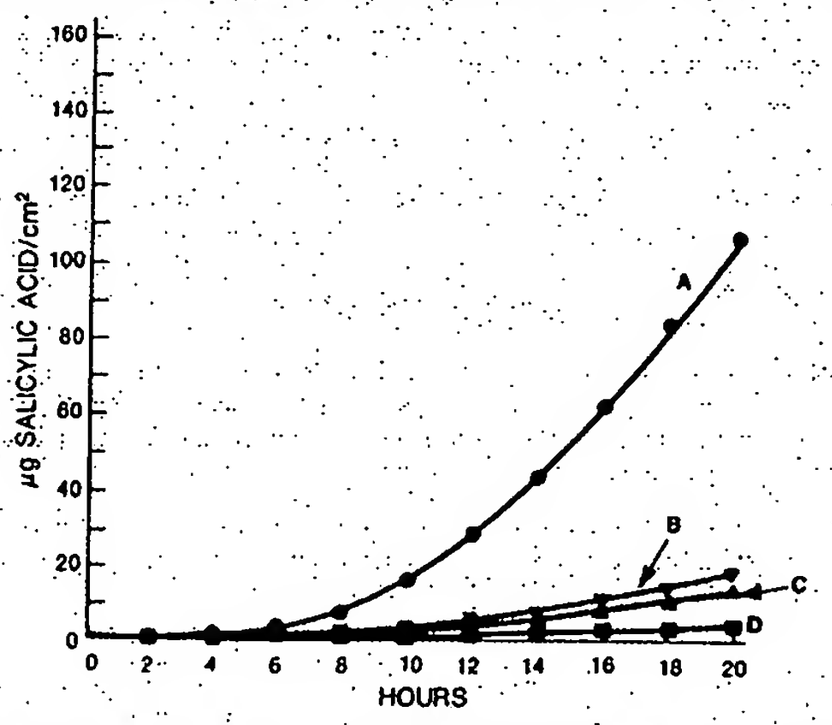

Figure 9—*Effect of the addition of fatty acids on the penetration of 1% salicylic acid in propylene glycol across human epidermis. Key: (A) 0.1 M oleic acid in propylene glycol; (B) 0.1 M lauric acid in propylene glycol; (C) 0.1 M decanoic acid in propylene glycol; (D) propylene glycol (control).*

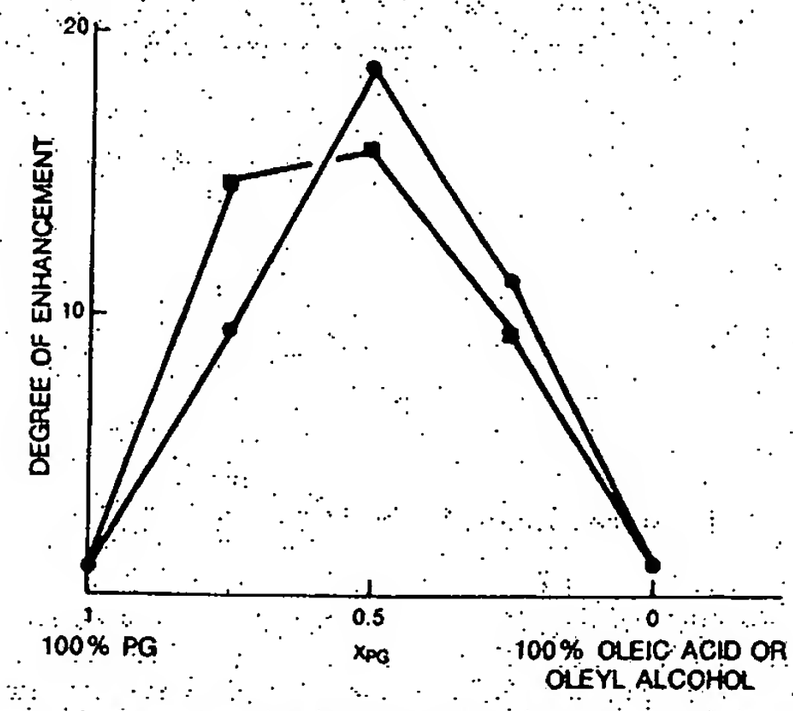

Figure 10—*Degree of enhancement of salicylic acid steady-state flux as a function of propylene glycol mole fraction ($X_{propylene\ glycol}$) from saturated solutions. Key: (■) oleyl alcohol; (●) oleic acid.*

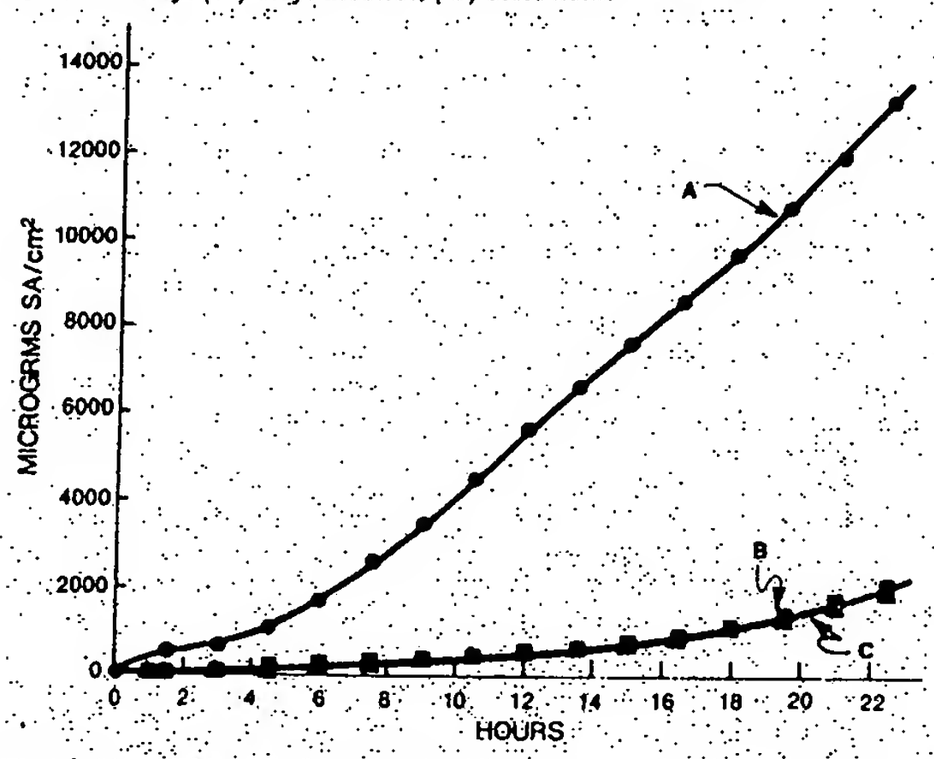

Figure 11—*Effect of sulfoxides on salicylic acid transport across human epidermis. Key: (A) 24% salicylic acid in propylene glycol plus 0.1 M oleyl methyl sulfoxide; (B) 21% salicylic acid in propylene glycol; (C) 22% salicylic acid in propylene glycol plus 1 M decyl methyl sulfoxide.*

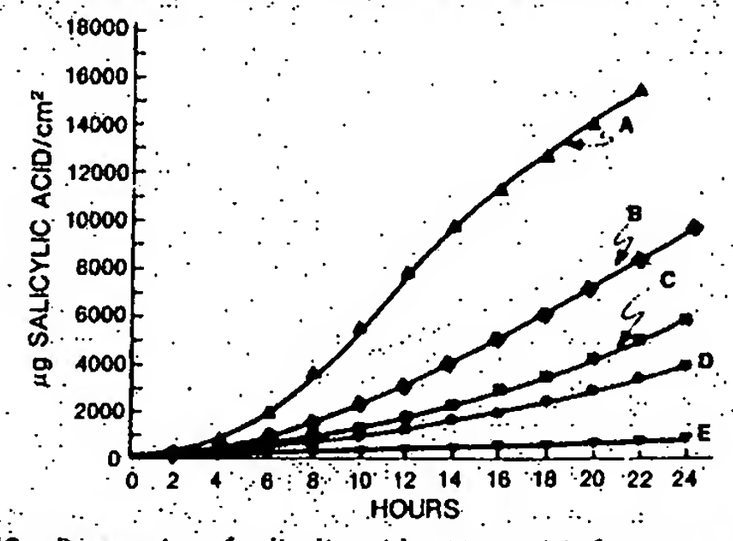

Figure 12—*Penetration of salicylic acid at saturation from propylene glycol–alcohol vehicles across human epidermis. Key: (A) 21% salicylic acid in 0.25 mole fraction decanol–propylene glycol; (B) 22% salicylic acid in 0.25 mole fraction hexanol–propylene glycol; (C) 22% salicylic acid in 0.25 mole fraction octanol–propylene glycol; (D) 22% salicylic acid in 0.25 mole fraction butanol–propylene glycol; (E) 20% salicylic acid in propylene glycol.*

solvents. This result indicates that polar solvents interact differently with skin and that the variations in transport are not due to solution phenomena.

The addition of a small amount of oleic acid to propylene glycol provides for a rather large increase in salicylic acid transport (Fig. 5). (Similar increases

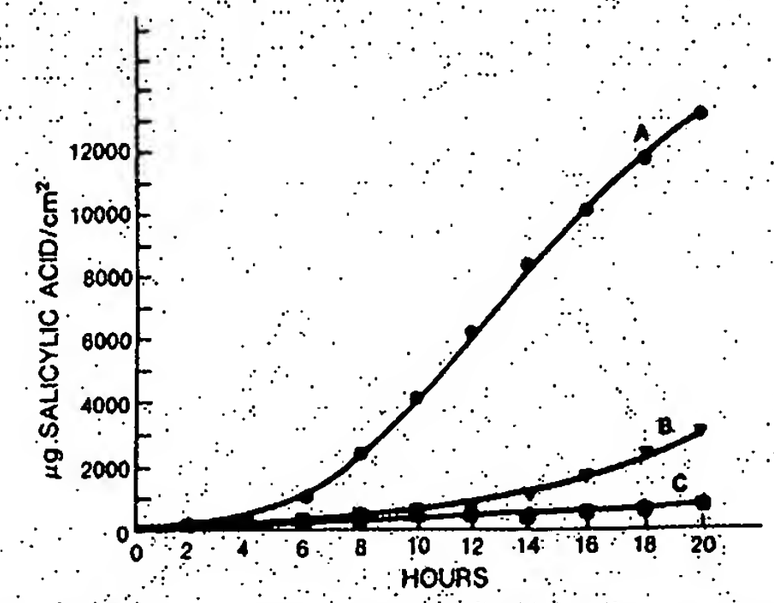

Figure 13—*Penetration of salicylic acid at saturation from oleic acid–propylene glycol or 1,2-butanediol vehicles across human epidermis. Key: (A) 15% salicylic acid in 0.25 mole fraction oleic acid–propylene glycol; (B) 15% salicylic acid in 0.25 mole fraction oleic acid–1,2-butanediol; (C) 23% salicylic acid in propylene glycol or 1,2-butanediol.*

in transport were also observed for the other polar solvents, but only the results for propylene glycol are presented.) Other unsaturated fatty acids give a similar result. Figures 6–8 show the effects of chain length and number and type of double bonds. The effect is reduced for saturated fatty acids (Fig. 9). Long-chain saturated fatty acids are too insoluble in propylene glycol for any effect on transport to be observed.

As the concentration of oleic acid (or oleyl alcohol) is increased, the transport of salicylic acid is also increased, up to a point. As the concentration of lipid is further increased, the flux of salicylic acid decreases (Fig. 10). Here, as mentioned above, transport from saturated solutions is compared to ensure equal driving force (chemical potential). The transport of salicylic acid from saturated solutions of propylene glycol (~22%) and oleic acid (~4%) [or water (0.2%)] are the same. However, use of a mixture of the two materials gives a ~20-fold increase in the transport rate.

The hydrocarbon chain seems to be the important factor as to whether a lipid will increase transport. For example, it can be seen (Fig. 11) that only the unsaturated methyl sulfoxide increases transport. Stearyl methyl sulfoxide also had no effect on transport. However, for alcohols, even the saturated chains can increase transport (Fig. 12). Here, the longer chains are more effective at increasing transport until the length of the chain exceeds 14. At this point, solubility of the alcohol becomes too small for an effect on transport to be observed. Other diols also exhibit this synergism with lipids, but the effect is less pronounced as the chain length is increased (Figs. 13 and 14).

The mechanism by which the epidermal barrier properties are altered is

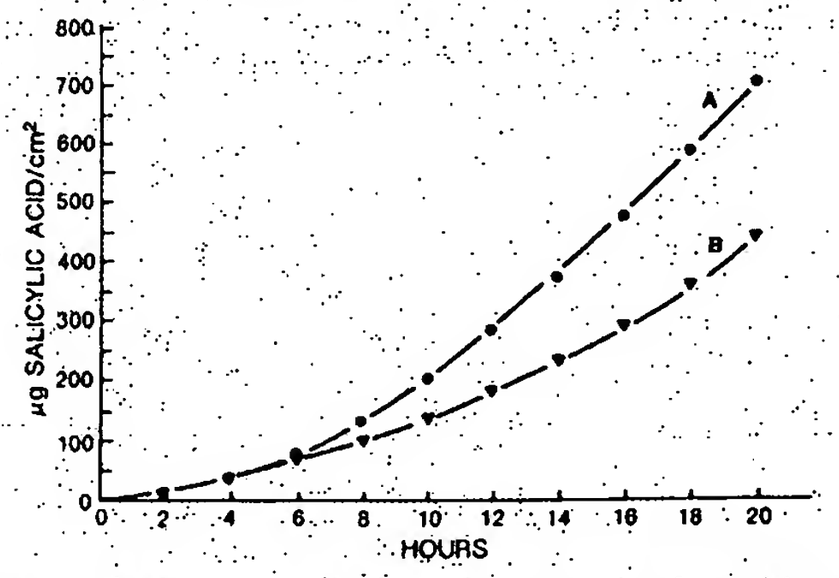

Figure 14—*Penetration of salicylic acid at saturation from oleic acid–1,2-hexanediol vehicles across human epidermis. Key: (A) 24% salicylic acid in 0.25 mole fraction oleic acid–1,2-hexanediol; (B) 14% salicylic acid in 1,2-hexanediol.*

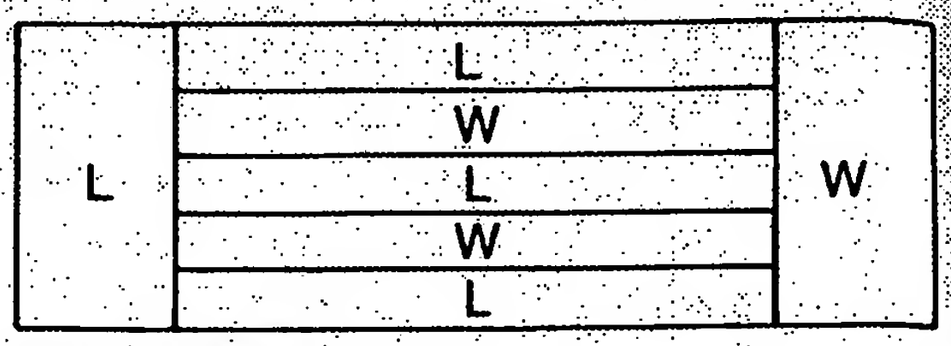

Figure 15—*Model for skin transport.*

not known, but differential scanning calorimetry studies of the stratum corneum[10] indicate that the two-component systems result in an increased fluidization of the stratum corneum lipids. This effect could then result in more rapid diffusion of the molecules across skin. The use of two different solvents to increase solute solubility has been known for some time as "cosolvency" and "blending" (5), and there might be a connection between cosolvency and the effects observed in this study on skin transport.

Regardless of the detailed mechanism by which these vehicles act, the results presented here open the door to the investigation of multicomponent systems to alter the barrier properties of skin. The penetration-aid guidelines obtained from this study and an earlier report (3) indicate that, for polar molecules, the head groups dominate (ionic > zwitterionic > nonionic) and for nonpolar molecules (polar solvent plus lipid), the hydrocarbon chains dominate. It was predicted that branched-chain lipids would be as effective as unsaturated lipids; this was, indeed, the case for isostearic acid.

A general way to categorize the pathways for transport in skin is depicted in Fig. 15, in which no attempt was made to assign a pathway to a particular morphological structure. J_s, the flux at steady state, can be written as:

$$J_s = a_w J_w + a_{Lw} J_{Lw} + (1 - a_w - a_{Lw}) J_L$$

where a_w is the area fraction of the aqueous pathway, a_{Lw} is the area function of the lipid–water pathway, J_w is the flux across the aqueous pathway, J_{Lw} is the flux across the lipid–water pathway, and J_L is the flux across the lipid pathway. It seems clear that there exists a continuous polar pathway, because the flux (at constant concentration) levels off with a decreasing oil–water partition coefficient and because surfactants act primarily to increase the transport of polar molecules. The pathway with the largest area fraction is probably the lipid–water pathway because molecules that have high solubility in both oil and water have the greatest transport. The lipid continuous pathway is included to account for the transport of very lipophilic molecules (such as benzyl salicylate), for which water becomes a major barrier to transport. The two-component systems described in this report act primarily on the lipid barriers, but they may have some effect on the polar pathway.

REFERENCES

(1) R. J. Scheuplein and I. H. Blank, *Physiol. Rev.*, **51**, 702 (1971).

(2) I. H. Blank, R. J. Scheuplein, and D. J. MacFarlane, *J. Invest. Derm.*, **49**, 582 (1967).

(3) E. R. Cooper, in "Solution Behavior of Surfactants: Theoretical and Applied Aspects," K. L. Mittal and E. J. Fendler, Eds., Plenum, New York, N.Y., 1982.

(4) E. M. Wright and J. R. Diamond, *Proc. R. Soc. B.*, **172**, 227 (1969).

(5) K. Shinoda, "Principles of Solution and Solubility," Dekker, New York, N.Y., 1978, chap. 10.

ACKNOWLEDGMENTS

The author would like to acknowledge Patricia Sprong and Gregory Albright for conducting many of the experiments presented in this paper and Bret Berner for pointing out the similarity between cosolvency and blending and the results observed for skin transport.

[10] Experiments were performed in collaboration with Randy Wickett at the Miami Valley Laboratories.

THE JOURNAL OF INVESTIGATIVE DERMATOLOGY
Vol. 46, No. 3

Printed in U.S.A.

Preliminary and Short Report

THE EFFECT OF DIMETHYL SULFOXIDE ON THE EPIDERMAL WATER BARRIER*

THOMAS M. SWEENEY, M.D., ALAN M. DOWNES, M.S.† AND A. GEDEON MATOLTSY, M.D.

Recently dimethyl sulfoxide (DMSO) has been reported to have several properties suggesting a wide range of possible medical uses (1–4). Its apparent ability to enhance the percutaneous absorption of dissolved substances was especially interesting to us (5, 6). As part of a study *in vitro* of the epidermal water barrier, we treated the epidermis of the hairless mouse with DMSO and determined its effect on the rate of passage of tritiated water through the skin. In view of the current interest in DMSO, the results of this study are presented here.

Full thickness skin from hairless mice (strain HRS/J; obtained from The Jackson Laboratory, Bar Harbor, Maine) 8–16 weeks of age was used. This species was chosen because the absence of eccrine sweat glands and the small size of the hair follicles minimize these routes as significant pathways of penetration. Preliminary studies with the technic described below showed that although the flow rate of tritiated water varied from specimen to specimen in the range 0.18–1.08 mg/cm/hr (based on 80 determinations), water passed through a particular piece of skin at a constant rate so that measurements were reproducible for 24 hours after the mouse was killed. Hence, valid conclusions on the effect of DMSO on the epidermal water barrier could be drawn only with difficulty by comparing average flow rates. Therefore, the effect of DMSO was studied by first measuring the actual rate of flow of tritiated water for each piece of excised skin. Subsequent measurements, made after DMSO application, can then be related to the initially obtained values. Thus, the following technic was used to study the effect of DMSO.

Immediately after dissection, the skin was cut into six pieces, each of which was clamped between two glass cells which enabled the rate of flow of water through an area of 0.71 cm^2 to be measured. Each cell had three outlets, one to drain the water, the other two attached to a reservoir with an air-lift to circulate the liquid. Isotonic saline (5 ml; pH 6.4) was added to each side of the apparatus, and tritiated water (0.05 ml; 400 μc/ml) was then added to the epidermal side. The experiments were done at 25–26° C. Three samples (0.5 ml) were taken from the dermal side at 30 minute intervals beginning one hour after the addition of the tritiated water; the volume was restored by adding 0.5 ml saline after each sampling. The results of preliminary experiments indicate that a steady rate of penetration of tritium is reached within one hour. Each sample was placed in a counting tube and 12.5 ml of a solution of a scintillator (a mixture of 4 gm diphenyloxazole, 25 mg p-bis[2-(5-phenyloxazolyl)]-benzene, and 50 gm naphthalene dissolved in dioxane to a total volume of one liter) was added. The radioactivity of these samples and appropriate standards was measured in a Nuclear Chicago Liquid Scintillation Counter, model #701. The flow rate was then calculated in mg/cm^2/hr. After the rate of passage of tritiated water had been determined for each piece of skin, the chambers were emptied and rinsed with saline. DMSO in varying concentrations was then added to the epidermal side and left in contact with the epidermis for 30 minutes. The chambers were again emptied and thoroughly washed by circulating several changes of saline over a 30-minute period. The rate of passage of tritiated water was then measured again as described above.

The effect of DMSO on the epidermal water barrier was evaluated by dividing the final flow rate of tritiated water by the initial one and plotting the ratio as a function of concentration of DMSO. The results (Fig. 1) indicate that there was no significant change in the rate of passage of water through the skin when the epidermis was treated for 30 minutes with aqueous DMSO in concentrations up to 50%. There was an increase, approximately 50%, however, when 60% DMSO was used, and a much larger increase, about 10-fold, when 75% DMSO was applied. With 90% DMSO or with undiluted DMSO, the rate of passage increased about 90-fold. The increased flow rates were constant, and there was no evidence of a trend towards recovery of the barrier to the passage of water.

The following experiments were then done to see if there was an additional effect due to presence of DMSO in contact with the epidermis during diffusion. After completion of sampling to define the initial rate of flow of water, DMSO was added directly to the solution on the epidermal side to

Received for publication October 30, 1965.
* From the Department of Dermatology, Boston University School of Medicine, and Evans Memorial Department of Clinical Research, University Hospital, Boston University Medical Center, Boston, Massachusetts.
This investigation was supported in part by research grant AM 05924 and graduate training grant T1-AM 5295, National Institute of Arthritis and Metabolic Diseases, and general research support grant FR 05380, National Institutes of Health, United States Public Health Service.
† Present address: C.S.I.R.O., Division of Animal Physiology, Parramatta, N. S. W., Australia.

produce concentrations ranging from 20 to 50%. Sampling from the dermal side was continued for a period of four hours. Under these conditions the rate of passage of tritiated water was unchanged, as shown in Fig. 2. The effect of time of exposure to DMSO was also studied. The results (Table I) show that the rate of flow of tritiated water increased with longer treatment periods; the increases, however, were small compared with those due to increasing the concentration of DMSO.

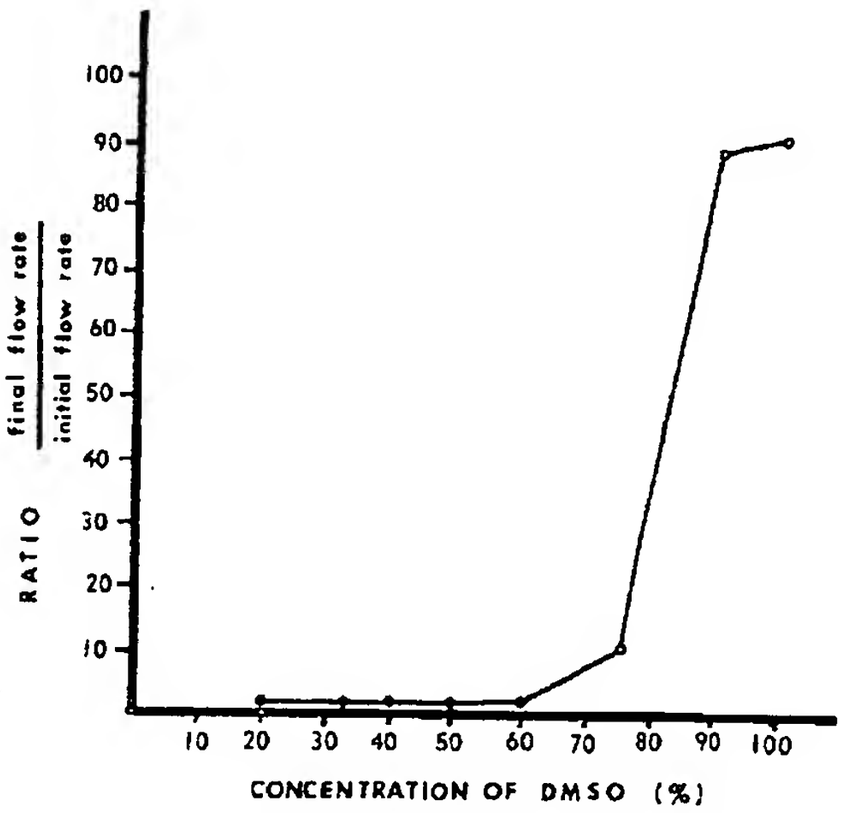

FIG. 1. Change in the flow rate of tritiated water through hairless mouse skin after treatment of the epidermis with various concentrations of DMSO *in vitro* for 30 minutes.

These results suggest three significant conclusions. Firstly, they show that the concentration of DMSO is far more important than the time of exposure in determining the effect on the water barrier. Secondly, the increases in the rate of passage of water due to exposure to concentrated aqueous solutions of DMSO are apparently permanent *in vitro*. And finally, DMSO does not appear to have any special ability to promote the passage

TABLE I

Rate of passage of tritiated water through the skin of the hairless mouse in vitro *after treatment with DMSO for various periods of time*

Concentration of DMSO (%)	Treatment period (minutes)	Rate of flow of water (mg/cm²/hr)		Ratio $\frac{\text{Final rate of flow}}{\text{Initial rate of flow}}$
		Initial	Final	
50	30	.52	.58	1.1
	60	.28	.46	1.5
	120	.30	.67	2.1
75	10	.66	4.3	6.4
	20	.39	2.6	6.7
	30	.44	4.2	9.6

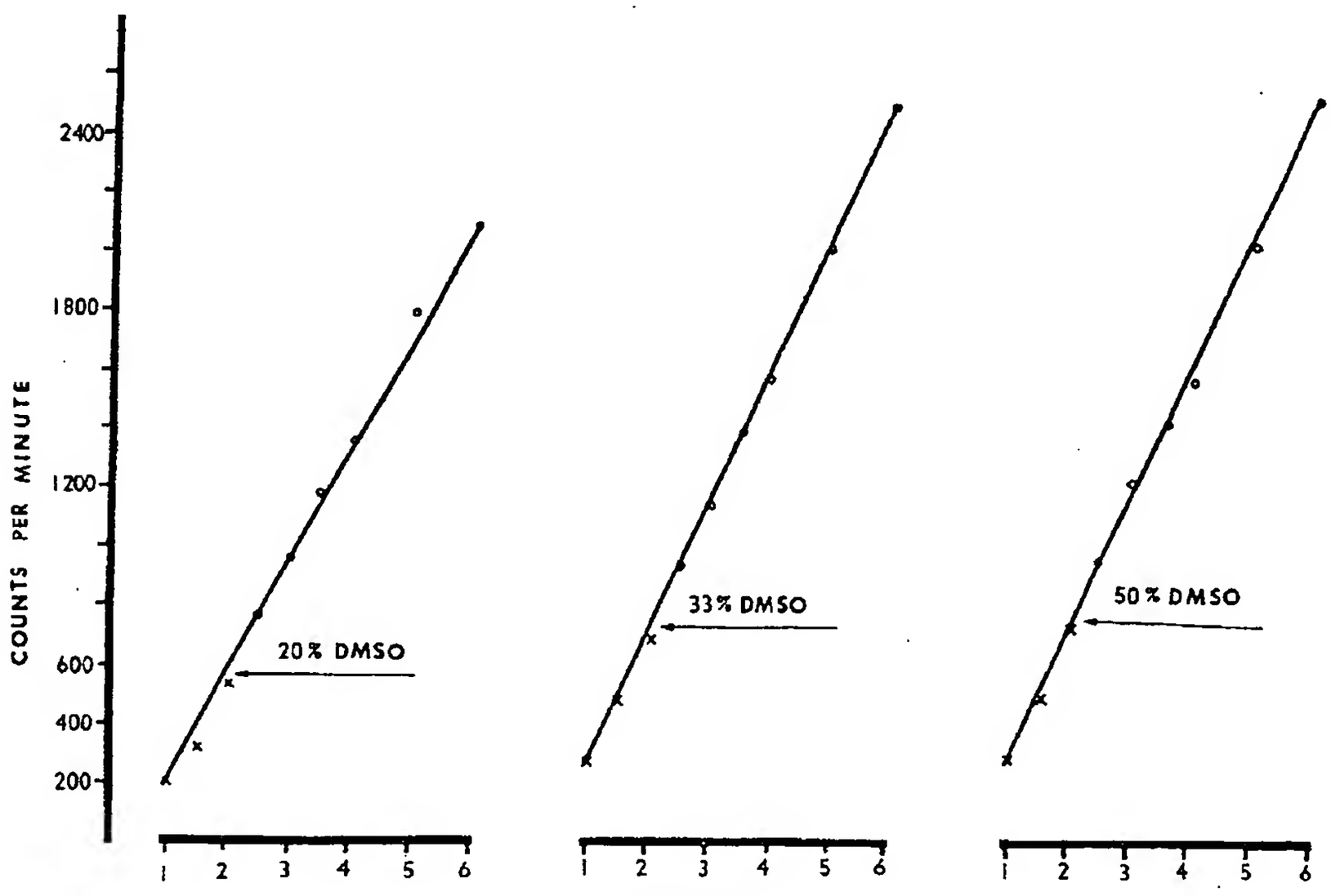

FIG. 2. Flow rate of tritiated water through hairless mouse skin *in vitro* before and after addition of DMSO in varying concentrations to the epidermal side of the chamber.

of water through the skin by its mere presence, at least in this experimental situation.

It is interesting to note that the higher concentrations of DMSO which we found necessary to produce permanent effects on the water barrier (Fig. 1), are in the same range found by Kligman (6) to be necessary to enhance the penetration of substances such as tetrachlorosalicylanilide, Declomycin, and sodium fluorescein through human skin *in vitro*. However, Kligman found that pretreatment of discs of human horny layer, obtained from autopsy material, with 50% or 90% aqueous DMSO or with undiluted DMSO for 24 hours produced only minor changes in the rate of passage of water. Further studies will be necessary to resolve this apparent difference from our results.

SUMMARY

Excised skin of hairless mice was clamped between two glass cells filled with saline and after the addition of tritiated water to the epidermal side, the rate of passage of tritiated water for each piece of skin was determined. Then, DMSO in varying concentrations was either added directly to the solution on the epidermal side or was applied to the epidermal side for varying periods of time. Subsequently, the new rate of passage of tritiated water was determined and compared with the initial value. The results showed that:

(1) DMSO does not appear to have any special ability to promote the passage of water through the skin by its mere presence,

(2) permanent changes are produced in the rate of passage of water through the skin by application of concentrated solutions of DMSO (60–100%), and

(3) the concentration of DMSO is far more significant than the time of exposure in determining the effect on the water barrier.

REFERENCES

1. Jacob, S. W., Bischel, M. and Herschler, R. J.: Dimethyl sulfoxide (DMSO): a new concept in pharmacotherapy. Curr. Ther. Res., *6:* 134, 1964.
2. Jacob, S. W., Bischel, M. and Herschler, R. J.: Dimethyl sulfoxide: effect on the permeability of biologic membranes (preliminary report). Curr. Ther. Res., *6:* 193, 1964.
3. Rosenbaum, E. E., Herschler, R. J. and Jacob, S. W.: Dimethyl sulfoxide in musculoskeletal disorders. J.A.M.A., *192:* 309, 1965.
4. Stoughton, R. B.: Dimethylsulfoxide (DMSO) induction of a steriod reservoir in human skin. Arch. Derm. (Chicago), *91:* 657, 1965.
5. Stoughton, R. B. and Fritsch, W.: Influence of Dimethylsulfoxide (DMSO) on human percutaneous absorption. Arch. Derm. (Chicago), *90:* 512, 1964.
6. Kligman, A. M.: Topical pharmacology and toxicology of Dimethyl sulfoxide Part I. J.A.M.A., *193:* 796, 1965.

J. Soc. Cosmetic Chemists, 19, 119–127 (Feb. 5, 1968)

The Effect of Dimethyl Sulfoxide on Percutaneous Absorption: A Mechanistic Study, Part I

STANLEY G. ELFBAUM, Ph.D., and KARL LADEN, Ph.D.*

Presented before the Mid-Atlantic Chapter, February 14, 1967

Synopsis—An *in vitro* skin penetration system has been described in which intact abdominal guinea pig skin has been utilized as the membrane. The passage of picrate ion through this membrane in the presence of dimethyl sulfoxide (DMSO) is a passive diffusion process which shows adherence to Fick's First Law of Diffusion. In order to produce substantial enhancement effects, relatively large concentrations of DMSO were required. Effective concentrations of DMSO caused the skin membranes to acquire a more turgid and wrinkled appearance. It has been shown by diffusion and isotope techniques that the absolute rate constant for the penetration of DMSO is approximately 100 times greater than that for the picrate ion. Thus, the two substances transferred independently of each other through the skin.

Introduction

In recent years, dimethylsulfoxide (DMSO) has been reported as a solvent which, in addition to having a host of claimed therapeutic properties, has the ability of rapidly penetrating human skin and enhancing the percutaneous absorption of materials dissolved therein (1–7). While there have been numerous reports concerning the utility of DMSO in promoting percutaneous absorption both *in vivo* and *in vitro*, few studies have appeared concerning its mechanism of action upon the barrier to absorption through the skin (7).

Recently, disclosure of potential medical hazards associated with the use of DMSO has precluded its widespread use in humans (6). How-

* Gillette Research Institute, 6220 Kansas Avenue, N. E., Washington, D. C. 20011.

ever, an understanding of its mode of action could lead to the discovery of other methods to enhance percutaneous absorption. To achieve this goal, the *in vitro* percutaneous passage of picrate ion in the presence of dimethyl sulfoxide has been examined in detail.

Materials and Methods

White male guinea pigs ranging in size from 600–1200 g were obtained from Dublin Laboratory Animals, Inc., Dublin, Va. Reagent grade picric acid was purchased from Allied Chemical and Dye Corp., New York, N. Y., "certified" reagent grade dimethyl sulfoxide from Fisher Scientific Company, Fairlawn, N. J., ethylene glycol monomethyl ether from Mallinckrodt Chem. Works, New York, N. Y.; dimethyl-C^{14} sulfoxide and Liquifluor (25× concentrate liquid scintillator) were obtained from New England Nuclear Corporation, Boston, Mass. All other chemicals were obtained as pure as possible.

Intact abdominal guinea pig skin was utilized as a membrane between a set of glass diffusion chambers. Hair was removed from the skin either by wax epilation several days prior to sacrificing the animal or with an electric clipper. Animals were usually sacrificed by a lethal injection of $MgSO_4$, and the skin was rapidly excised and frozen. Attempts were made to utilize the skin within 48 hours after procurement. Ainsworth has reported that the chemical permeability of excised skin is almost unchanged for at least two days if bacterial decomposition is prevented by cold storage (8).

Since large variations in skin permeability were often seen from animal to animal and have even been reported from different skin sites of a single animal (9, 10), any one series of experiments whose results are reported here in a single figure or graph was performed using skin from a relatively small area of the abdomen of a single guinea pig.

It has also been observed in this laboratory that differences in the preparation of the animals could result in large variations in permeability characteristics from animal to animal. Skin from wax epilated animals often showed greater permeability characteristics than skin from animals which had not been so treated. This was probably due to an incomplete recovery of the barrier layer. On occasion, erratic results within a given series from the same animal were obtained which were attributed to inherent or mechanically induced variations.

Prior to beginning an experiment, portions of the frozen skin were cut and positioned as the membranes between L-shaped glass diffusion chambers. A pinch clamp which locked and sealed the chamber-membrane-chamber assembly in place was then applied. Any overlapping

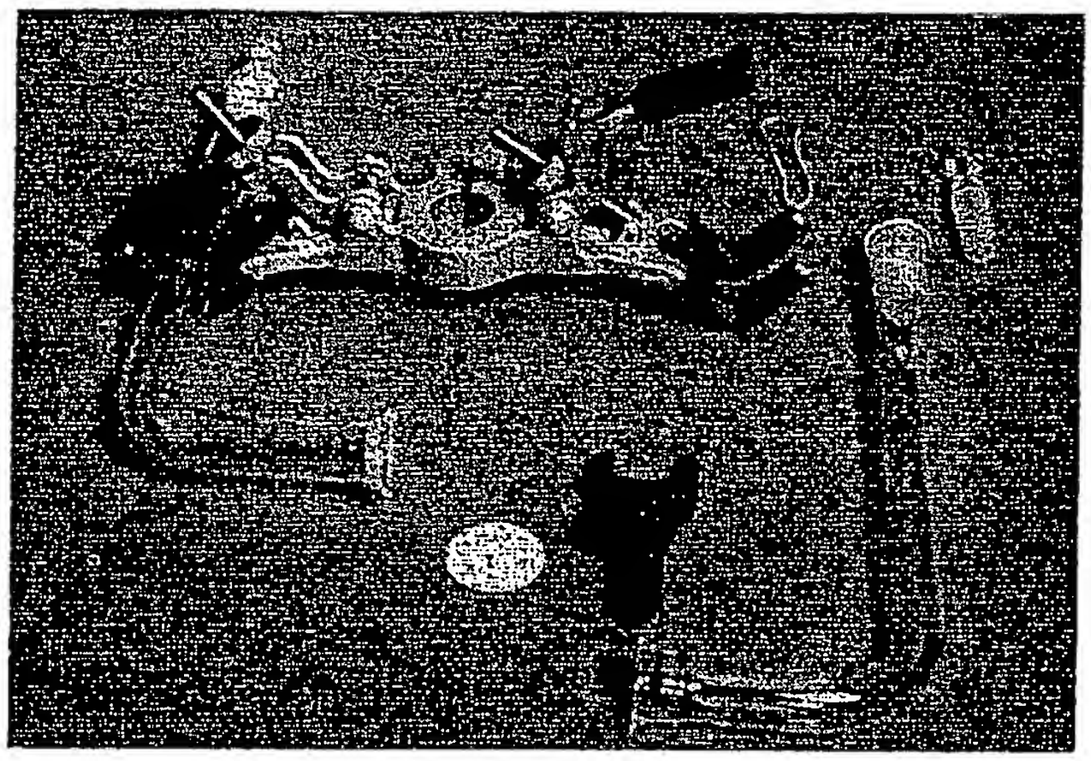

Figure 1. Unassembled diffusion chambers

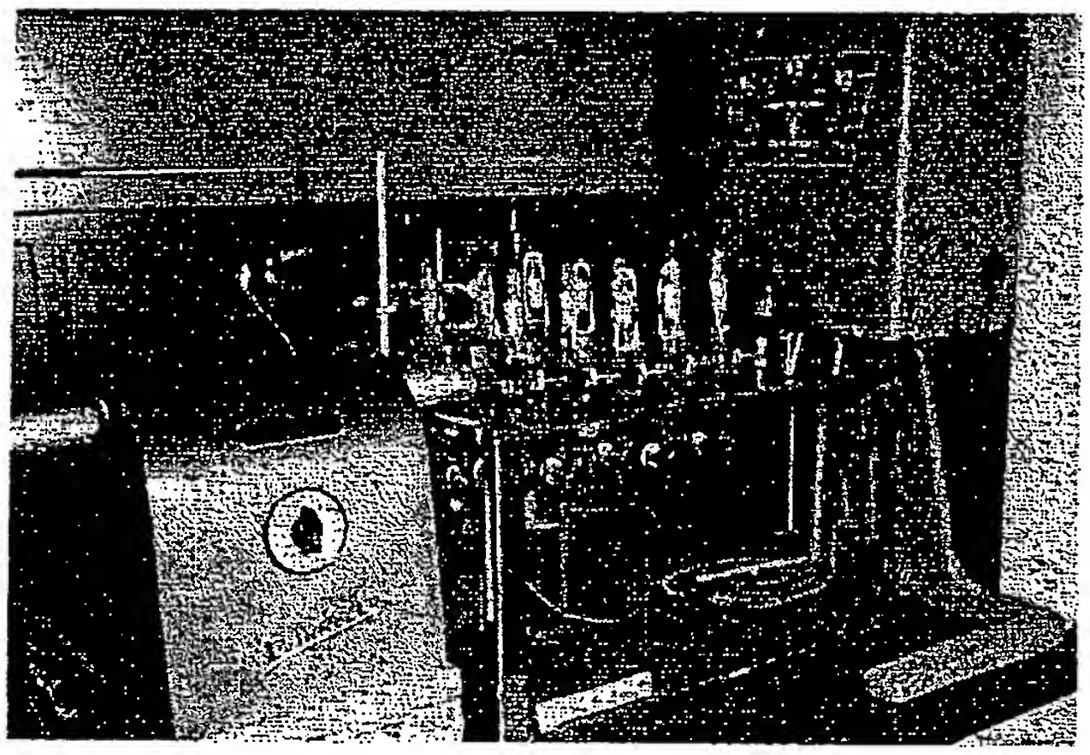

Figure 2. Assembled diffusion chambers mounted in thermostated water bath

skin was cut away leaving a circular membrane area of approximately 3 cm^2. The entire assembly was then mounted on a Burrell wrist-action shaker which positioned the diffusion assembly in a thermostated water bath (Figs. 1 and 2).

In a typical diffusion experiment, picric acid was dissolved in an 80% (v/v) DMSO/pH 7.0 buffer solution (monopotassium phosphate-sodium hydroxide 0.025 *M*). Fifteen milliliters of this solution was then placed in the epidermal chamber and 15 ml. of pH 7.0 buffer was placed in the dermal chamber. Glass beads were added to ensure proper mixing and a gentle shaking motion was then initiated. All diffusion experiments reported in this paper were performed at pH 7.0 and 30° ± 0.05°C.

The passage of picrate ion from the epidermal chamber to the dermal chamber was followed spectrophotometrically using a Beckman DU Spectrophotometer equipped with a Gilford Model 220 absorbance Indicator. Samples were withdrawn at various times from the dermal chamber. Prior to withdrawing the first sample, a small piece of glass wool was submerged in the dermal chamber. Thus, by placing the tip of the sampling pipet onto the wad of glass wool, any small particles resulting from the use of intact skin could be filtered. The optical density reading at 362 mμ was immediately obtained and the sample was placed back in the dermal chamber. In practice, this operation can be carried out in several minutes. Concentrations of picrate were calculated by using a value of 14700 M^{-1} cm^{-1} for the molar extinction coefficient at 362 mμ.

Initial studies indicated that, after a lag period, the picrate ion concentration in the dermal chamber increased in a linear manner with respect to time. The data have been treated in accordance with Fick's First Diffusion Law in the following manner:

$$\frac{dc}{dt} = k_p A (C_e - C_d) \tag{1}$$

where:

C_i = initial concentration of picrate in epidermal chamber
C_e = concentration of picrate at time t in epidermal chamber
C_d = concentration of picrate at time t in dermal chamber
A = area of membrane
k_p = absolute rate constant

If $C_d \ll C_e$, equation 1 reduces to

$$\frac{dc}{dt} = k_p A C_e \tag{2}$$

At early times during the diffusion process, C_e is approximately equal to C_i and equation 2 becomes

$$\frac{dc}{dt} = k_p A C_i \tag{3}$$

dc/dt can be obtained from the linear portion of the progression curve of concentration versus time. A and C_i are experimentally measurable. Thus, the absolute rate constant for a given experiment can be calculated.

In experiments in which dimethyl-C^{14} sulfoxide was utilized, the diffusion rate of DMSO was determined by sampling 0.1 ml aliquots of

the dermal chamber at various times, adding this to 15 ml of counting fluid (6 parts of ethylene glycol monomethyl ether to 10 parts of 1:25 Liquiflor scintillation fluid) and determining the amount of dimethyl-C^{14} sulfoxide using a Packard Tri-Carb Liquid Scintillation Spectrometer.

Results and Discussion

While the *in vitro* skin penetration of several ions and covalent molecules has been shown to obey Fick's First Diffusion Law (11), it was necessary to show that the penetration of picrate ion in the presence of DMSO is also a passive diffusion process.

The results of a study demonstrating the applicability of Fick's Law are presented in Table I. The DMSO concentration was maintained at 80% (v/v) while the picrate concentration was changed over a 13 fold range. With the exception of one experiment, the data do exhibit adherence to equation 2. Thus, the system approximates a passive diffusion process.

In order to get some estimate as to the reproducibility of the data obtainable with this system, five identical experiments were set up with skin membranes obtained from a small abdominal area of a single guinea pig. The results are shown in Table II.

With evidence thus available on the kinetics of the diffusion process and on the reproducibility of the system, experiments were designed to study in detail the effect of DMSO on this system.

The penetration rates of picrate ion as a function of dimethyl sulfoxide concentration were studied, and the results are presented in Fig. 3.

Table I

Fick's Law Study[a]

% DMSO (v/v)	Initial Concentration of Picrate Ion (M)	Absolute Rate Constant (cm hr^{-1})
80	1.56×10^{-2}	13.7×10^{-4}
80	4.14×10^{-2}	14.2×10^{-4}
80	6.68×10^{-2}	30.7×10^{-4}
80	9.75×10^{-2}	17.5×10^{-4}
80	19.8×10^{-2}	13.8×10^{-4}

[a] (A young male guinea pig was sacrificed by a lethal injection of $MgSO_4$. The abdominal hair was clipped and the abdominal skin was immediately excised and frozen. The length of time between procurement and utilization of the skin was approximately 24 hours. The skin had been kept frozen until use.)

It can be concluded from these results, in agreement with others (3, 7), that large concentrations of DMSO are required before appreciable enhancement of penetration can occur. Although Stoughton (1) has reported enhanced penetration with relatively low concentrations of DMSO, it is perhaps possible that his experimental procedures allowed for evaporation of water from the treatment solutions thus effectively changing the DMSO concentrations.

It was also observed in these experiments that those skin membranes which had been in contact with the greater concentrations of dimethyl sulfoxide appeared more wrinkled and stretched and swollen, yet much less pliable than those skin membranes which had been in contact with buffer or lower concentrations of DMSO. A literature search revealed

Table II

Reproducibility Study[a]

% DMSO (v/v)	Initial Concentration of Picrate Ion (M)	Absolute Rate Constant (cm hr^{-1})
70	3.75×10^{-2}	14.7×10^{-4}
70	3.75×10^{-2}	15.5×10^{-4}
70	3.75×10^{-2}	15.5×10^{-4}
70	3.75×10^{-2}	12.1×10^{-4}
70	3.75×10^{-2}	17.6×10^{-4}
Average and standard deviation = $15.1 \times 10^{-4} \pm 2.0 \times 10^{-4}$		

[a] (The abdomen of a male guinea pig was wax epilated, and the animal was sacrificed 3 days later by a lethal injection of $MgSO_4$. The abdominal skin was immediately excised and frozen. The length of time between procurement and utilization of the skin was 24–48 hours. The skin was kept frozen until use.)

Table III

Effect of DMSO Concentration on Percutaneous Absorption of Picrate Ion[a]

% DMSO (v/v)	Initial Conc. of Picrate (M)	Approximate Lag Time (hr)
0	4.81×10^{-2}	5.2
20	3.24×10^{-2}	5.2
40	5.61×10^{-2}	4.9
60	5.15×10^{-2}	5.0
72	3.73×10^{-2}	4.0
80	6.70×10^{-2}	<2
92	3.53×10^{-2}	<2

[a] (The abdomen of a male guinea pig was wax epilated, and the animal was sacrificed 3 days later with a lethal injection of $MgSO_4$. The abdominal skin was immediately excised and frozen. The length of time between procurement and utilization of the skin was about 3 days. The skin was kept frozen until use.)

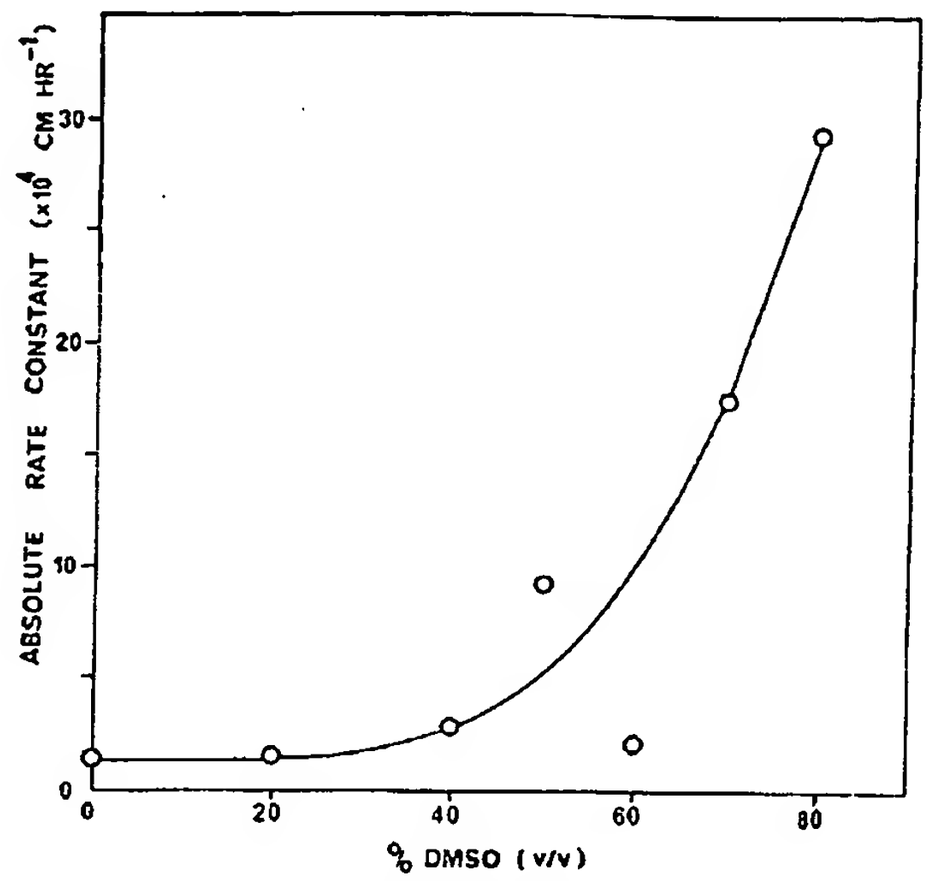

Figure 3. Effect of DMSO concentration on percutaneous absorption of picrate ion (pH 7.0, 30° ± 0.05°C)

that this observation had been made by others (2, 3). This observation will be treated in greater detail in Part II of this paper.

In other experiments, an additional observation was made concerning the lag times which are the times necessary for the picrate ion concentrations in the dermal chambers to increase in a linear manner with time. With increasing concentrations of DMSO, the lag times generally decreased. While these lag times do not enter into the calculation of the absolute rate constant, they could be indicative of the rate of some alteration in the diffusion process brought about by DMSO. These results are shown in Table III.

Since the experiments described above involved establishing a large concentration gradient for DMSO across the skin membrane, it was decided to study whether this concentration gradient was important for the enhanced percutaneous penetration of picrate ion.

Experiments were set up in which the penetration of picrate was studied in the absence of DMSO; with DMSO on the epidermal side of the skin membrane and buffer on the dermal side; and with DMSO on both sides of the skin membrane. The results shown in Table IV demonstrate that the enhanced penetration of picrate is not altered by eliminating the concentration gradient for DMSO across the skin.

In order to establish conclusively that DMSO does not "carry" picrate through the skin, experiments were performed in which the rates

Table IV

Mechanistic Studies of DMSO as a Percutaneous Carrier[a]

Expt.	Epidermal Chamber Contents	Dermal Chamber Contents	Absolute Rate Constant (cm hr^{-1})
1	Buffer[b] and picrate (5.93×10^{-2} M)	Buffer[b]	6.89×10^{-4}
2	80% DMSO in buffer[b] and picrate (7.55×10^{-2} M)	Buffer[b]	14.6×10^{-4}
3	80% DMSO in buffer[b] and picrate (7.55×10^{-2} M)	80% DMSO in buffer[b]	16.2×10^{-4}

[a] (The abdomen of a young male guinea pig was wax epilated. The animal was allowed to recover for five days and then sacrificed by a lethal injection of $MgSO_4$. The abdominal skin was immediately excised and frozen. The time between procurement and utilization of the skin was within 24 to 48 hours. The skin was kept frozen until use.)

[b] 3×10^{-2} M.

Table V

Picric Acid–Dimethyl-C^{14} Sulfoxide Penetration Studies[a]

Initial Concentration of Picric Acid (M)	% C^{14}-DMSO (v/v)	Absolute Rate Constant (cm hr^{-1})
5.17×10^{-2}	0	3.29×10^{-4}
8.51×10^{-2}	80	a. Picrate 13.1×10^{-4}
		b. C^{14}-DMSO 12.7×10^{-2}

[a] (A male guinea pig was sacrificed by a lethal injection of $MgSO_4$. The abdominal skin was clipped and the abdominal skin was immediately excised and frozen. The length of time between procurement and utilization of the skin was approximately 24 hours. The skin was kept frozen until use.)

of penetration of picrate and DMSO were studied. The results of this isotope experiment (Table V) show that the absolute rate constant for the *in vitro* diffusion of dimethyl sulfoxide through the skin membrane was approximately 100 times greater than that of the picrate ion, thus clearly demonstrating their independent transfer through the skin.

ACKNOWLEDGMENTS

The authors wish to thank Mr. Brian Rogers for his initial work in the procurement of the skin membranes.

(Received June 13, 1967)

Part II will be published in Volume XIX, No. 3, March, 1968.

References

(1) Stoughton, R. B., and Fritsch, W., Influence of dimethylsulfoxide (DMSO) on human percutaneous absorption, *Arch. Dermatol.*, **90**, 512 (1964).
(2) Rosenbaum, E. E., *et al.*, Dimethyl sulfoxide in musculoskeletal disorders, *J. Am. Med. Assoc.*, **192**, 109 (1965).
(3) Kligman, A. M., Topical pharmacology and toxicology of dimethyl sulfoxide—Part 1, *ibid.*, **193**, 796 (1965).
(4) Kligman, A. M., Dimethyl sulfoxide—Part 2, *Ibid.*, **193**, 923 (1965).
(5) Stone, O. J., Thiabendazole in dimethyl sulfoxide for Tinea Nigra Palmaris, *Arch. Dermatol.*, **93**, 241 (1966).
(6) Leake, C. D., Dimethyl sulfoxide, *Science*, **152**, 1646 (1966).
(7) Sweeney, T. M., *et al.*, The effect of dimethyl sulfoxide on the epidermal water barrier, *J. Invest. Dermatol.*, **46**, 300 (1966).
(8) Ainsworth, M., Methods for measuring percutaneous absorption, *J. Soc. Cosmetic Chemists*, **11**, 69 (1960).
(9) Kligman, A. M., The biology of the stratum corneum, in Montagna, W. and Lobitz, W. C., Jr., *The Epidermis*, Academic Press, N. Y., 1964, pp. 387–433.
(10) Vinson, L. J., *et al.*, The nature of the epidermal barrier and some factors influencing skin permeability, *Toxicol. Appl. Pharmacol.*, **7**, 7 (1965).
(11) Tregear, R. T., The permeability of mammalian skin to ions, *J. Invest. Dermatol.*, **46**, 16 (1966).

Influence of Dimethylsulfoxide (DMSO)

On Human Percutaneous Absorption

R. B. STOUGHTON, MD

AND

WILLIAM FRITSCH, MD

CLEVELAND

In vitro and in vivo quantitative measurements indicate that dimethylsulfoxide (DMSO) enhances human percutaneous absorption of certain chemical agents.

Dimethylsulfoxide (DMSO) is a colorless liquid which is an excellent solvent. It has recently been suggested that this agent is beneficial in a number of diseases of man.[1] It has also been shown that DMSO enhances penetration of chemical agents through the urinary bladder of animals [1] and that it enhances viability of tissues when frozen.[2-4]

This report concerns in vivo and in vitro quantitative studies of the influence of DSMO on percutaneous absorption in human skin. In vivo studies were made of hexopyrronium bromide (quaternary),* naphazoline hydrochloride (Privine Hydrochloride),† and fluocinolone acetonide.‡ In vitro studies were made of C^{14}-hexopyrronium chloride (tertiary),* and 4-C^{14}-hydrocortisone.§

Supported by a grant from the Armed Forces Epidemiology Board.

Director of Dermatology (Dr. Stoughton) and Resident in Dermatology (Dr. Fritsch), Western Reserve University.

Methods

A. *In Vivo.*—Healthy, young, adult male and female subjects were used. Techniques for this type of assay have been previously reported by Cronin and Stoughton,[5] Clendenning and Stoughton,[6] and McKenzie and Stoughton.[7] The volar surfaces of the forearms were used. The DMSO || containing fluid was compared with the non-DMSO containing fluid by placing each on equivalent areas of the forearms. The presence or absence of the physiologic reaction (inhibition of sweating, vasoconstriction and/or pilomotion) was determined after a designated interval of time. If the reaction was present, it was recorded as a positive response (see Tables 1, 2, and 3).

1. Hexopyrronium bromide (a quaternary anticholinergic agent) [8] (see Fig 1*a*) was dissolved in

* Supplied by A. H. Robins Company, Richmond, Va.

† Supplied by Ciba Company, Summit, NJ.

‡ Supplied by Syntex Company, Palo Alto, Calif.

§ Purchased from New England Nuclear Corporation, Boston.

|| Supplied by Crown Zellerbach Company, Camas, Wash.

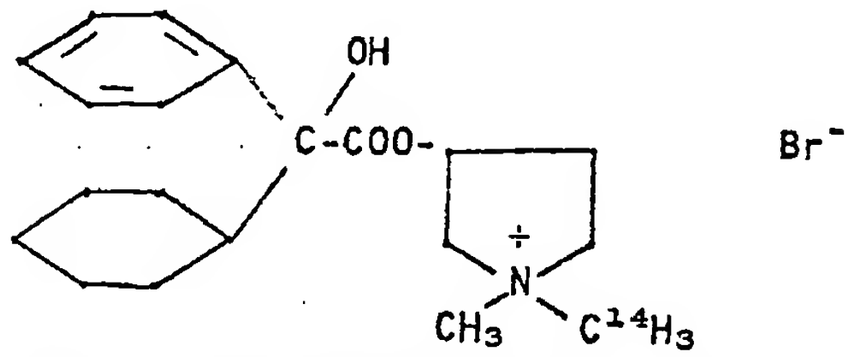

Fig 1A.—Hexopyrronium bromide (quaternary), 1-methyl-3-pyrrolidyl-1-C^{14} α-phenylcyclohexane-glycolate methobromide. The unlabeled form of hexopyrronium bromide was used for the in vivo studies.

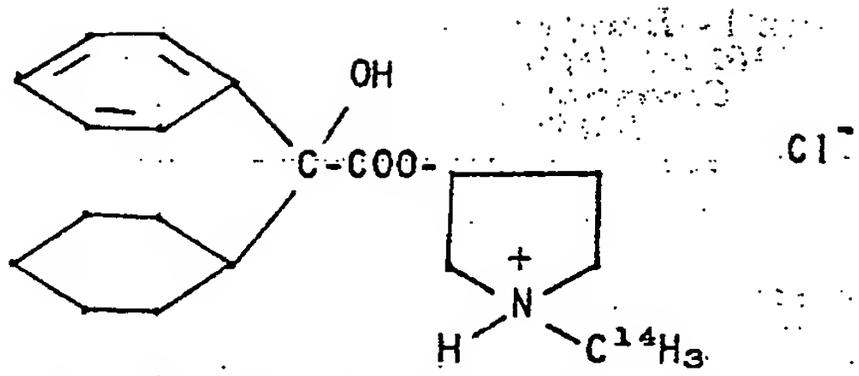

Fig 1B.—Hexopyrronium chloride (tertiary), 1-methyl-3-pyrrolidyl-1-C^{14} α-phenylcyclohexane-glycolate hydrochloride. This form of labeled hexopyrronium was used for the in vitro study.

95% alcohol. DMSO was added to the appropriate concentration. An equivalent amount of water was added to the control without DMSO. Then 0.01 cc of each concentration of hexopyrronium bromide with 20% DMSO was applied to the forearm. The same was done without DMSO to the opposite forearm along with a control of only 20% DMSO in 95% alcohol. In most subjects there was erythema at the site of 20% DMSO, but this subsided completely in all subjects by six hours. All subjects washed their forearms with soap and water 30 minutes after topical applications. Determinations of sweat inhibition were made 20 hours later. The subjects were exposed to an environment of 86 F-94 F and 50%-60% humidity for 30 minutes. Sweating and inhibition of sweating in focal areas was determined with the conventional starch-iodine technique. Concentrations of hexopyrronium bromide used were 1.0%, 0.2%, 0.04%, 0.008%, and 0.0016%.

2. Napthazoline hydrochloride was dissolved in 95% alcohol. DMSO was added to the appropriate concentration. An equivalent amount of water was added to the controls without DMSO. Applications to the forearms were as described above for hexopyrronium bromide. Vasoconstriction and pilomotion was determined 30-60 minutes after initial application. Maximal response is in this period of time. Concentrations of naphthazoline used were 5%, 1%, 0.2%, 0.04%, and 0.008%.

3. Fluocinolone acetonide, with and without DMSO, was prepared and applied as above. DMSO in 25% and 10% preparations was tested with fluocinolone acetonide in various concentrations. When tested under a perforated metal guard,[7] concentrations of fluocinolone acetonide were 0.05%, 0.01%, 0.002%, and 0.0008%. When tested under Saran Wrap, concentrations were 0.001%, 0.0002%, 0.00004%, and 0.000008%.

Both the guard and Saran Wrap were left in place about eight hours, and vasoconstriction was determined 9-20 hours after initial application.

B. *In Vitro.*—The methods used are described in detail in a previous publication.[9] Skin of grossly normal appearance removed from surgically amputated legs or breasts was frozen and stored for use in these experiments (see Table 4). The specimens of skin were trimmed and mounted on special glass chambers (see Fig 2). Glass wells were glued to the skin defining an area of 1.76 cm^2. The amount

Fig 2.—Special glass chambers used for in vitro studies with human skin.

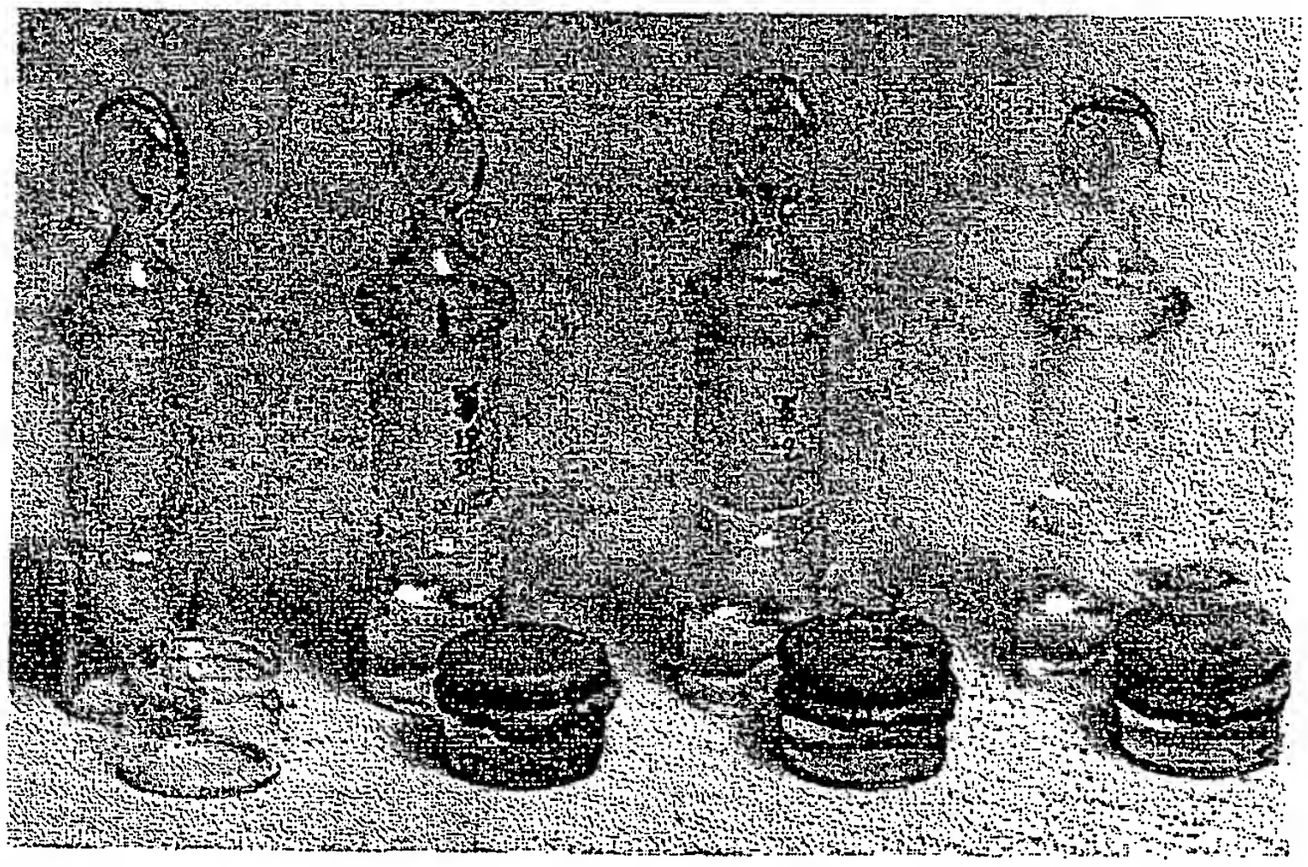

Stoughton—Fritsch

TABLE 1.—*Hexopyrronium Bromide (Quaternary) (0.01 cc) Applied to Forearms in Different Concentrations With and Without DMSO in Ten Subjects* *

	1%	0.2%	0.04%	0.008%	0.0016%
With 20% DMSO	9/10	9/10	7/10	3/10	0/10
Without DMSO	6/10	2/10	0/10	0/10	0/10

* Positive responses listed under each concentration of hexopyrronium bromide (eg, 9/10 indicates nine positive responses in ten subjects tested).

of 10 ml of saline was placed in each chamber. An aliquot of a solution of a C^{14}-labeled compound [hydrocortisone-4-C^{14} or hexopyrronium chloride (tertiary, methyl-C^{14}) (see Fig 1*b* and 3) in absolute ethanol (see Table 5)] was placed in each well. Aliquots were also placed directly into liquid scintillation counting vials for determination of the total number of counts applied. For each of the two substances tested the skin was treated in one of two different ways: (1) continuous contact with a solvent (DMSO or H_2O) or (2) transient contact with a solvent.

In the former treatment, the solvent was either DMSO (0.3 ml) or water (0.3 ml) and was applied over the C^{14}-labeled compound after the ethanol had evaporated. The well was then sealed from above with a coverslip. The chambers were incubated for 24 hours at 37 C. Aliquots of saline were removed and placed in scintillation counting vials. Most of the water was evaporated in a gentle stream of air, and drying was completed in a desiccator under a partial vacuum. The amounts of 1.0 ml of distilled water and then 15 ml of scintillation fluid were added

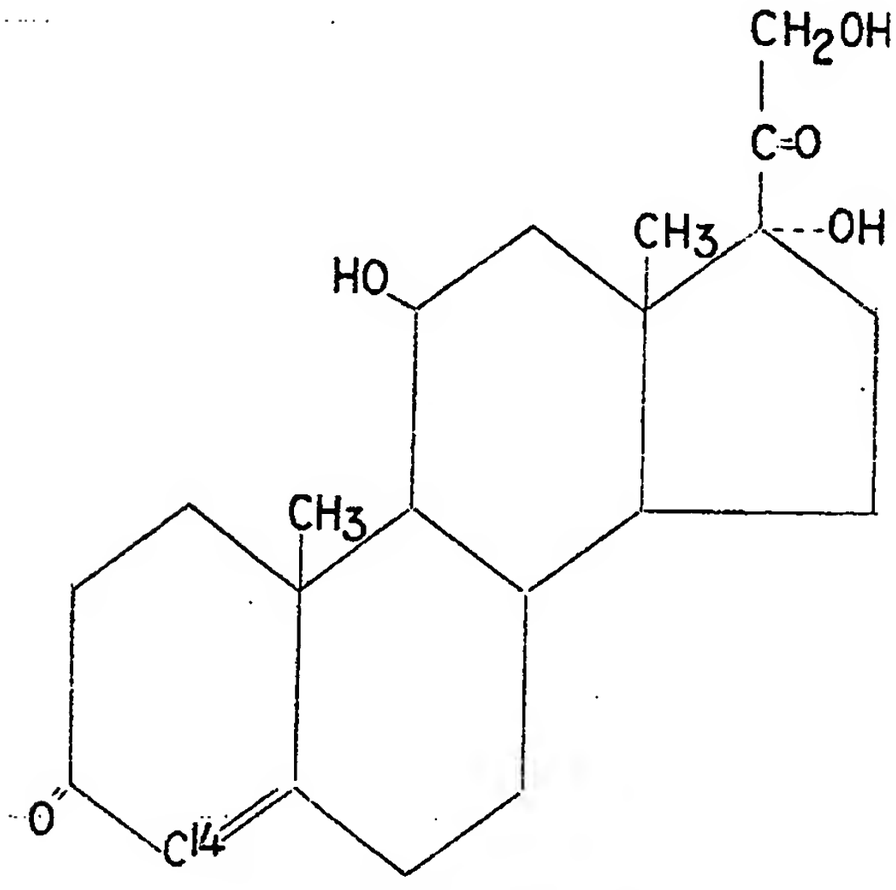

Fig 3.—4-C^{14} hydrocortisone.

TABLE 2.—*Naphazoline (0.01 cc) Applied Topically to Forearms to Compare Effect of Different Concentrations of DMSO on Absorption* †*

	5%	1%	0.2%	0.04%	0.008%
With 50% DMSO	14/14	14/14	14/14	10/14	4/14
With 25% DMSO	22/24	22/24	20/24	8/24	0/24
With 10% DMSO	14/14	10/14	8/14	4/14	0/14
Without DMSO	12/16	8/16	2/16	0/16	0/16

* Positive responses (vasoconstriction and pilomotion) listed under each concentration of naphazoline (eg, 14/14 indicates 14 positive responses in 14 subjects tested).

† Concentrations of DMSO from 50%-10% without naphazoline did not result in vasoconstriction or pilomotion.

to each vial, and counting was done on a Nuclear-Chicago liquid scintillation spectrometer.

In the case of transient exposure to the solvent, 0.05-ml of a 25% solution of the solvent (DMSO or H_2O) in absolute ethanol was applied inside the well. Immediately thereafter, a given quantity (see Table 5) of the C^{14}-labeled compound in ethanol was applied, and the liquid in the well was thoroughly mixed by rotary agitation. The skin surface was then blown dry with a gentle stream of air at room temperature. The total duration or exposure to the solvent (about 25 minutes) was held fairly constant. Incubation was carried out for 24 hours at 37 C with the wells open at a relative humidity of 88% in a Blue M FR-251-C environmental cabinet. Sampling and counting were done as above.

TABLE 3.—*Fluocinolone Acetonide (0.01 cc) Applied Topically to Forearms in Different Concentrations With and Without DMSO, With Areas of Application Either Covered by a Perforated Metal Guard or Occluded With Saran Wrap for Eight Hours* †*

A. Protected With Perforated Metal Guard

	0.05%	0.01%	0.002%	0.0004%	0.00008%
With 25% DMSO	10/10	9/10	7/10	3/10	0/10
With 10% DMSO	10/10	8/10	6/10	2/10	0/10
Without DMSO	9/10	6/10	3/10	0/10	

B. Occluded With Saran Wrap

	0.001%	0.002%	0.00004%	0.000008%
With 25% DMSO	12/12	8/12	3/12	0/12
Without DMSO	12/12	7/12	3/12	0/12

* Positive responses indicated by vasoconstriction (eg, 7/10 indicates seven positive responses in ten subjects).

† 25% DMSO alone did not give vasoconstriction in any of the subjects.

TABLE 4.—*Data on the Human Skin Used in the in Vitro Experiments*

	Designation	Age of Donor	Sex of Donor	Race of Donor	Diagnosis	Region
	L-7	46	Male	Caucasian	Gangrene	Leg
	L-9	61	"	Negro	"	"
S-7	BH	—	Female	Caucasian	Carcinoma	Breast
S-7	BJ	—	"	Negro	"	"
S-7	BL	—	"		"	"
S-7	BR	48	"	Caucasian	"	"
S-7	BS	48	"	"	"	"
S-6	BA	64	Female	Caucasian	Carcinoma	Breast
S-6	BE	—	"	Negro	"	"
S-6	BU	—	"	Caucasian	"	"
S-6	BW	70	"	"	"	"
S-6	BY	—	"	"	"	"

Knowing the number of counts applied and the number of counts recovered for each specimen, the per cent penetration per 24 hours was calculated. The efficiency of counting was the same for all samples counted. The scintillation fluid used consisted of 4.0 gm of PPO (2,5-diphenyloxazole) and 0.100 gm of POPOP [1,4-his-2(phenyloxazolyl)-benzene] diluted to 1.0 liter with toluene. The counting temperature was ambient.

TABLE 5.—*Supplementary Data, Methods*

References to Tables 6-9	Mg Applied	Counts Applied	Volume of Ethanol (Ml)	Average Temperature, C	Temperature Range	Average % Relative Humidity	Maximum % Counting Error One Standard Deviation
1	0.02	6.00×10^5	0.02	37.5	36.5-38.0	—	±0.64
2	0.10	7.58×10^4	0.10	37.0	36.0-37.9	87	±2.8
3A	8.0	4.72×10^5	0.40	37.1	37.0-37.5	—	±5.4
3B	1.27	8.65×10^4	0.10	37.4	36.9-37.9	—	±0.82
4	1.27	8.65×10^4	0.10	37.1	36.0-38.0	87	±2.0

Results

A. *In Vivo.*—1. DMSO enhances percutaneous absorption of hexopyrronium bromide (quaternary) by at least a factor of 25 as measured by this system (Table 1). The control site with 20% DMSO alone showed inhibition of sweating at 2 hours but no inhibition after 20 hours.

2. Naphazoline percutaneous absorption is enhanced by DMSO concentrations of 50%, 25%, and 10%. The maximum influence seemed to be induced by the highest concentration of DMSO. The increase in penetration with 50% DMSO as compared to no DMSO was in the order of 25-fold (Table 2).

3. Percutaneous absorption of fluocinolone acetonide seems to be enhanced by DMSO when applied under the perforated guard. This increase seems to be definite but not as great as it is with hexopyrronium bromide or naphazoline. The increase is in the order of five-fold or less and is present with 10% and 25% DMSO (Table 3).

There was no significant increase in penetration when DMSO was compared under Saran Wrap occlusive dressing (Table 3).

B. *In Vitro.*—DMSO was superior to water in respect to enhancing the penetration of C^{14}-hexopyrronium chloride (tertiary) (Tables 8 and 9). The increase was by a factor of at least two for continuous exposure and by about four for transient exposure.

TABLE 6.—*Hydrocortisone-4-C^{14}, Continuous Contact With Solvent*

Reference to Table 2	Skin Specimen	Number of Trials	Solvent	Average % Penetration per 24 Hours	Range	Factor Increase DMSO/H_2O
1	L-7	5	DMSO	0.35	0.06-0.80	.248
	L-9	3				
	L-7	4	H_2O	1.41	0.31-3.15	
	L-9	3				

TABLE 7.—*Hydrocortisone-4-C¹⁴, Transient Contact With Solvent*

Reference to Table 2	Skin Specimen	Number of Trials	Solvent	Average % Penetration per 24 Hours	Range	Factor Increase DMSO/H₂O
2	S-7 (Breast)	9	DMSO	15.1	2.28-26.2	6.71
		8	H₂O	2.25	0.56-6.35	

In the case of continuous exposure to the solvent, H_2O was superior to DMSO in promoting the penetration of hydrocortisone (Table 6). However, in the case of transient exposure DMSO was superior to water (Table 7) in promoting penetration of hydrocortisone by a factor of about seven.

It is interesting that DMSO is apparently in some cases more effective than water in producing increased premeability of the skin, particularly considering the marked effect of the latter. The greater effect of DMSO on transient exposure may be due to the facilitation of a very rapid initial penetration of the stratum corneum.

Comment

The mechanism by which DMSO increases penetration of these agents is unknown to us. It has been previously stated that the vehicle has little effect on the penetration of the incorporated agent.[10] We do know that changes in environment will greatly influence penetration [9-11] as will removal or severe damage to the horny layer.[12,13] The authors are unaware of any agent other than water which will influence percutaneous absorption to the extent of DMSO and not cause any obvious or prolonged damage to the skin other than transient erythema. However, this is a broad and difficult subject which is beyond the scope of this paper to review. Those interested in details of this problem are urged to consult previous reviews.[10,13,14]

Generic and Trade Names of Drugs

Naphazoline hydrochloride—Privine Hydrochloride.

TABLE 8.—*Hexopyrronium-Methyl-C¹⁴ (Tertiary), Continuous Contact With Solvent*

Reference to Table 2	Skin Specimen	Number of Trials	Solvent	Average % Penetration per 24 Hours	Range	Factor Increase DMSO/H₂O
3A	L-6 (Leg)	3	DMSO	1.37	0.84-2.20	27.4
		3	H₂O	0.05	0.03-0.07	
3B	S-6 (Breast)	4	DMSO	14.8	7.3-19.9	2.48
		4	H₂O	5.96	2.2-11.2	

Dr. A. L. Lorincz of the University of Chicago suggested that DMSO be investigated in regard to its ability to influence percutaneous absorption.

Richard B. Stoughton, MD, 2065 Adelbert Rd, Cleveland, Ohio.

REFERENCES

1. Jacobs, S. W.; Bischel, M.; and Herschler, R. J.: Dimethylsulfoxide (DMSO): New Concept in Pharmacotherapy, Curr Ther Res 6:134-135, 1964.

2. Smith, A. U.; Ashwood-Smith, J. J.; and Young, M. R.: In Vitro Studies on Rabbit Corneal Tissue, Exp Eye Res 2:71, 1963.

TABLE 9.—*Hexopyrronium-Methyl-C¹⁴ (Tertiary), Transient Contact With Solvent*

Reference to Table 2	Skin Specimen	Number of Trials	Solvent	Average % Penetration per 24 Hours	Range	Factor Increase DMSO/H₂O
4	S-6 (Breast)	10	DMSO	21.6	5.30-50.1	4.4
		10	H₂O	4.90	2.02-8.86	

3. Block, J.: Preservative Solutions for Freezing of Whole Organs In Vitro, Fed Amer Soc Exp Biol, 1963; Fed Proc 22:170, 1963.

4. Huggins, C. E.: Reversible Agglomeration Used to Remove Dimethylsulfoxide From Large Volumes of Frozen Blood, Science 139:504, 1963.

5. Cronin, E., and Stoughton, R. B.: Percutaneous Absorption of Nicotinic Acid and Ethyl Nicotiniate in Human Skin, Nature (London) 195:1103, 1962.

6. Clendenning, W. E., and Stoughton, R. B.: Importance of Aqueous/Lipid Partition Coefficient for Percutaneous Absorption of Weak Electrolytes, J Invest Derm 30:47-49, 1962.

7. McKenzie, A. W., and Stoughton, R. B.: Method for Comparing Percutaneous Absorption of Steroids, Arch Derm 86:608-610, 1962.

8. Stoughton, R. B.; Chiu, F.; Fritsch, W.; and Nurse, D.: Topical Suppression of Eccrine Sweat Delivery With New Anticholinergic Agent, J Invest Derm 42:151-155, 1964.

9. Fritsch, W., and Stoughton, R. B.: Effect of Temperature and Humidity on Penetration of C^{14} Acetyl Salicylic Acid in Excised Human Skin, J Invest Derm 41:307-310, 1963.

10. Rothman, S.: Physiology and Biochemistry of the Skin, Chicago: University of Chicago Press, 1954.

11. Brown, E., and Scott, W.: Absorption of Methyl Salicylate by Human Skin, J Pharmacol Exp Ther 50:32, 1934.

12. Blank, I. H.; Griesemer, R. D.; and Gould, E.: Penetration of an Anticholinesterose Agent (Sarin) Into Skin: I. Rate of Penetration Into Excised Human Skin, J Invest Derm 29:299, 1957.

13. Malkinson, F., and Rothman, S.: "Percutaneous Absorption," in Handbuch der Haut- und Geschlechtskrankheiten, Berlin: Springer-Verlag, 1963.

14. Guillot, M., and Valette, Q.: Physicochemical Conditions of Cutaneous Absorption, J Physiol (Paris) 46:31-98, 1954.

Pharmaceutical Research, Vol. 7, No. 7, 1990

Research Article

Contributions of Drug Solubilization, Partitioning, Barrier Disruption, and Solvent Permeation to the Enhancement of Skin Permeation of Various Compounds with Fatty Acids and Amines

Bruce J. Aungst,[1,2] Judy A. Blake,[1] and Munir A. Hussain[1]

Received February 7, 1989; accepted February 10, 1990

The contributions of several proposed mechanisms by which fatty acids and amines might increase skin permeation rates were assessed. Permeation rates of model diffusants with diverse physicochemical properties (naloxone, testosterone, benzoic acid, indomethacin, fluorouracil, and methotrexate) through human skin were measured *in vitro*. The enhancers evaluated were capric acid, lauric acid, neodecanoic acid, and dodecylamine. Increased drug solubility in the vehicle, propylene glycol (PG), in some cases accounted for the increases in flux in the presence of adjuvants, since permeability coefficients were unchanged. Partition coefficients of some drugs into isopropyl myristate or toluene were increased by the adjuvants, but this did not occur for combinations of an acid with a base (adjuvant-drug or drug-adjuvant). Increases in flux not accounted for by increases in drug solubility or partitioning were assumed to involve disruption of the barrier function of skin (increased skin diffusivity). All fatty acids increased skin diffusivity of naloxone, testosterone, indomethacin, and fluorouracil but not of methotrexate or benzoic acid. Dodecylamine increased skin diffusivity only for fluorouracil. Capric acid and dodecylamine, but not lauric acid or neodecanoic acid, increased the skin permeation rate of PG, suggesting that enhanced solvent penetration could also be involved as a mechanism for increased skin permeation of the drug. However, the increase in PG flux due to dodecylamine was nullified when methotrexate was added to the vehicle, possibly because of a dodecylamine/methotrexate interaction. These studies demonstrate that drug solubilization in the vehicle, increased partitioning, increased solvent penetration, and barrier disruption each can contribute to increased skin permeation rates in the presence of fatty acids and amines. The relative contributions of the mechanisms vary with the drug, the adjuvant, and the vehicle.

KEY WORDS: skin permeation; enhancer; fatty acid; membrane; transport; ion pairing; solvent drag.

INTRODUCTION

Numerous adjuvants have been used to increase skin permeation rates. These compounds have potential application for improving the skin penetration of poorly absorbed, systemically or topically active drugs. Their effects vary from drug to drug. Rational selection of a skin permeation enhancer and optimization of a skin permeation enhancing effect require an understanding of how drugs are affected by certain enhancers and how that varies from drug to drug. This depends at least partly on the mechanisms of permeation enhancement.

Fatty acids comprise one class of skin permeation enhancers for salicylic acid (1), acyclovir (2), naloxone (3), and several other drugs. The goals of this study were to compare the effects of fatty acids on the skin permeation rates of several drugs and to determine the contributions of various proposed mechanisms by which fatty acids might increase skin permeation rates.

One likely mechanism involved is reduction of skin resistance as a permeability barrier by disruption of the tightly packed lipid regions of the stratum corneum, which increases penetration through the intercellular lipid matrix (4). Differential scanning calorimetry and infrared spectroscopy indeed showed that skin permeability changes were proportional to physical changes in the stratum corneum lipids (5).

Another possible mechanism is increased skin/vehicle partitioning of the drug. A fatty acid adjuvant and an amine drug may form a lipophilic ion pair, thereby increasing drug partitioning into skin. Green and Hadgraft suggested this mechanism for the increased diffusion of β-blockers by fatty acids across an artificial isopropyl myristate membrane (6). They further showed that oleic acid and lauric acid each increased the isopropyl myristate/buffer partition coefficient of naphazoline, a base, providing evidence for an ion pairing role in skin penetration enhancement (7).

A third mechanism of skin permeation enhancement by adjuvants invokes increased solvent transport into or across

[1] DuPont Medical Products, P.O. Box 80400, Wilmington, Delaware 19880-0400.

[2] To whom correspondence should be addressed.

0724-8741/90/0700-0712$06.00/0

the skin. If the adjuvant increases the penetration rate of the solvent, drug solubility in the skin and skin penetration of the drug would also increase if the drug has a high affinity for the solvent. In the case of oleic acid enhancement of molsidomine skin penetration, Yamada *et al.* demonstrated a correlation between the penetration rates of molsidomine and the polyhydric alcohol vehicle, and they proposed a solvent drag mechanism for permeation enhancement (8).

The skin permeation enhancing effects of fatty acids and a fatty amine were studied using six compounds as model diffusants. These compounds were naloxone base, testosterone, a nonionizable drug, and four acids, benzoic acid, indomethacin, fluorouracil, and methotrexate. The structures of these compounds are shown in Fig. 1. We have examined how the flux, solubility, partitioning, and skin diffusivity of each of these compounds are affected by adjuvants. The fatty acids studied as adjuvants were capric acid (C_{10}), lauric acid (C_{12}), and neodecanoic acid, a branched-chain C_{10} fatty acid. Capric acid and lauric acid were previously shown to be the most effective enhancers within a series of saturated, straight-chain fatty acids, using naloxone as the diffusant (3). In another study neodecanoic acid was as effective as capric acid and lauric acid in increasing naloxone skin penetration rates, but it appeared to have a lower skin irritation potential (10). Dodecylamine was examined to see whether a basic adjuvant had effects on acidic drugs similar to the effects of fatty acid adjuvants on basic drugs. We also evaluated the effects of adjuvants on the skin permeation of the vehicle. The solvent used as the vehicle was propylene glycol. Previous studies have shown that the skin permeability enhancing effects of fatty acids are greatest with propylene glycol vehicles (3,8).

MATERIALS AND METHODS

Materials. Capric acid, lauric acid, testosterone, indomethacin, 5-fluorouracil, and methotrexate [(+)-amethopterin trihydrate] were purchased from Sigma. Naloxone base was from DuPont Pharmaceuticals. Propylene glycol U.S.P. and benzoic acid were supplied by Fisher. Isopropyl myristate was obtained from Kodak. Dodecylamine and stearylamine were obtained from Fluka. Phenylethylamine base was from Aldrich. Triethylamine was from EM Science. Akzo Chemie America generously provided bis-(2-hydroxyethyl)oleylamine (Ethomeen O/12) and polyoxyethylene(5)oleylamine (Ethomeen O/15), which are referred to as PEG-2 oleamine and PEG-5 oleamine, respectively. Neodecanoic acid is a mixture of highly branched fatty acid isomers of the general formula R_3CCOOH, in which the average number of carbon atoms is 10. It was supplied by Exxon Chemicals. [^{14}C]Propylene glycol (1,2-propanediol, [1-^{14}C]; sp act, 40 mCi/mmol) was obtained from ICN Biomedicals. Human skin specimens, dermatomed to an approximate thickness of 0.4 mm, were obtained from an organ bank. The skin donor population consisted of 22 people, of which 2 were nonwhite and 7 were female. The donor age averaged 37 ± 15 years. The majority of specimens were from the thighs and the calves.

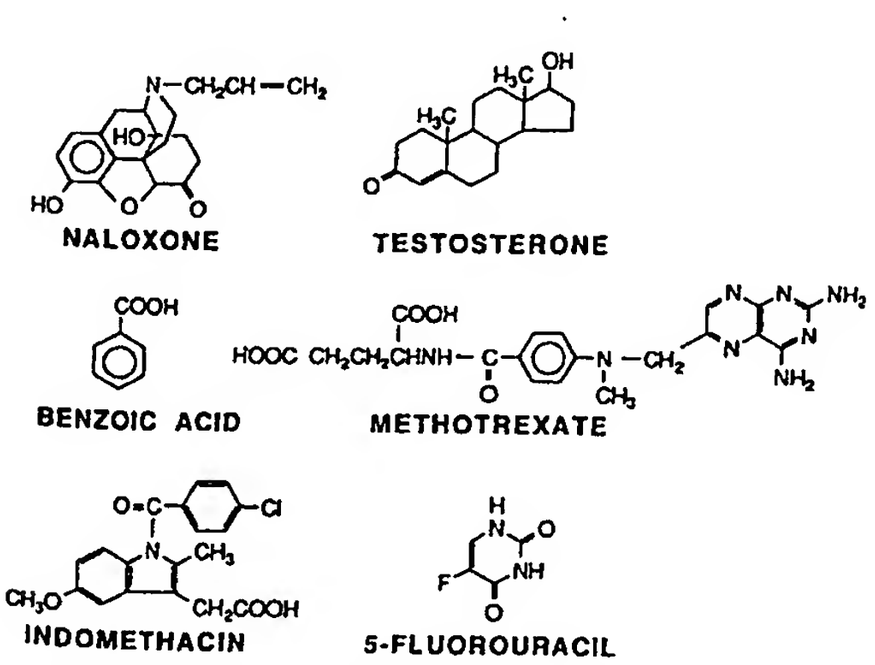

Fig. 1. Structures of the drugs used as model diffusants.

Skin Permeation. In vitro skin permeation rates were measured using glass diffusion cells in which human cadaver skin was clamped into a position separating donor and reservoir compartments. The reservoir was maintained at 37°C using a circulating water jacket or a dry block heater and was constantly stirred. The reservoir solution was selected to optimize drug solubility so that sink conditions were maintained. For indomethacin, fluorouracil, and methotrexate the reservoir was 0.1 *M* phosphate buffer at pH 7.4; saline was used for naloxone, benzoic acid, and propylene glycol; for testosterone the reservoir was 2% bovine serum albumin in saline. The entire reservoir volume (7–9 ml) was removed at the sampling times and replaced with drug-free solution. The donor vehicle volume was 0.5 ml. The donor chamber was sealed from the atmosphere with parafilm. The diffusional surface area was 1.8 cm^2. Each drug was evaluated using skin from at least three separate donors, and in most cases where direct comparisons of vehicles were made, the same skin donors were used to evaluate all vehicles.

The vehicles were propylene glycol or 0.5 *M* adjuvant in propylene glycol. The fatty acid or dodecylamine/propylene glycol mixtures were warmed to melt and dissolve the adjuvant. Clear solutions were obtained, unless indicated otherwise. The various drugs were then added to these vehicles in excess in saturated solubility. These suspensions were used for skin permeation experiments. Drug solubilities in the vehicles were determined after filtration and dilution or extraction. In some experiments, the drug was added to the vehicles in concentrations below saturation. The vehicles for measuring propylene glycol skin permeation had 2 μCi [^{14}C]propylene glycol/ml, and 0.5 ml was applied to the skin.

Partition Coefficients. Partition coefficients of the test drugs from propylene glycol vehicles, and the effects of fatty acids and dodecylamine, were examined using toluene and isopropyl myristate as the lipophilic phases. Octanol, which has a polarity similar to that of the lipids of skin (9), was not used because it was miscible with the propylene glycol vehicles. The saturated solutions used as vehicles in the skin permeation studies were filtered and diluted 10-fold with drug-free vehicle to give solutions with concentrations 1/10th of the drug solubility. These were equilibrated with equal volumes of isopropyl myristate or toluene by end-to-end mixing at room temperature (≈22°C) for at least 16 hr. The phases were then separated and diluted with methanol or extracted with 0.1 *N* NaOH (in the cases of fluorouracil and methotrexate), and the drug concentrations in both phases

were determined by HPLC. The solubility and partition coefficient data represent one to three determinations.

Analyses. Concentrations of naloxone, testosterone, benzoic acid, indomethacin, fluorouracil, and methotrexate in skin permeation samples and for partition coefficients were determined by HPLC. The assay conditions are outlined in Table I. The albumin in the samples from the testosterone skin permeation experiment was precipitated with 2 vol of methanol and was removed by filtration prior to HPLC analysis. [^{14}C]Propylene glycol concentrations were determined by counting 0.5-ml aliquots of the reservoir samples after the addition of 5-ml volumes of scintillation cocktail.

Data Analysis. The amount of drug permeating through skin during a sampling interval was calculated based on the measured reservoir concentration and volume. Plots of amount permeating vs time were made for each experiment. Flux was calculated as the slope of the linear portion of the plot and was normalized to 1-cm^2 surface area. [^{14}C]-Propylene glycol flux was expressed as the percentage of the applied amount delivered per hour and was not corrected for surface area. All flux data are reported as the mean ± SE of at least three determinations.

RESULTS

One goal of this study was to evaluate separately the effects permeation enhancing adjuvants have on drug solubility in the vehicle, partition coefficient, and skin diffusivity. The effects on solubility were measured directly. The permeability coefficient, P, was calculated as the flux, J, divided by the drug concentration in the saturated solution, C^s. P is a composite variable which includes drug partitioning into skin and the diffusion coefficient or diffusivity of the drug in the stratum corneum. Skin permeation rates are dependent on the stratum corneum/vehicle partition coefficients. These values are difficult to determine accurately. It was judged that the contribution of any mechanism that increases partitioning, such as ion pairing, would be evident in organic solvent/vehicle partition coefficients (K). The organic solvents were isopropyl myristate and toluene. Increases in P not accounted for by increases in K were assumed to involve increased skin diffusivity, indicative of barrier disruption.

Solubility, skin permeation, and partitioning data for the model compounds, and the effects of fatty acids and dodecylamine, are summarized in Table II.

Naloxone. The fatty acids increased naloxone solubility approximately 2- to 3-fold but increased naloxone flux 30- to 40-fold; P values increased at least 10-fold. In previous work naloxone solubility in lauric acid/propylene glycol solvent mixtures increased linearly with increasing lauric acid concentrations (3). This could be indicative of complexation or ion pair formation, but the effects of fatty acids on naloxone partitioning into isopropyl myristate or toluene were not indicative of formation of lipophilic ion pairs. Each fatty acid slightly increased $K^{toluene/PG}$, but there were no consistent effects on $K^{IM/PG}$. Furthermore, dodecylamine increased the partitioning of naloxone base into both isopropyl myristate and toluene. Considering the relative effects of dodecylamine on P (31-fold increase relative to control) and $K^{IM/PG}$ (72-fold increase) and $K^{toluene/PG}$ (19-fold increase), the effect of dodecylamine appears to be primarily on partitioning.

Testosterone. The effects of the fatty acid adjuvants on testosterone were to increase slightly C^s, $K^{IM/PG}$, and $K^{toluene/PG}$. Because the increases in P were consistently greater than the increases in K, some barrier disruption was evidenced. Dodecylamine decreased solubility in the vehicle, increased P (6-fold), and increased $K^{IM/PG}$ (14-fold) and $K^{toluene/PG}$ (22-fold). Since the increases in K were greater than the increase in P, there was no suggestion of dodecylamine increasing skin diffusivity.

Benzoic Acid. Benzoic acid represents a solute with high solubility in PG and high intrinsic skin permeability. None of the acid or amine adjuvants had a very great effect on any parameter determined.

Indomethacin. In the absence of an enhancer, the average flux for indomethacin was approximately 1000-fold lower than that of benzoic acid. However, permeability coefficients of indomethacin and benzoic acid were similar for vehicles containing capric acid or lauric acid. Neodecanoic acid was less effective in increasing indomethacin P. Each fatty acid had very little effect on indomethacin solubility. The increases in P were much greater than the increases in K, so increased skin diffusivity is likely. In the presence of dodecylamine, indomethacin solubility and flux increased to the same extent, so that there was no net change in P. Changes in K with dodecylamine were not consistent. The effect of dodecylamine on indomethacin skin permeation provides an example of an adjuvant apparently increasing flux solely by solubilizing the drug in the vehicle.

Table I. Chromatographic Methods Employed for Drug Analyses

Drug	Column	Mobile phase	Flow rate (ml/min)	Detection (nm)
Naloxone	C_8	Acetonitrile/THF/0.05 *M* phosphate buffer, pH 3 (10/0.8/89.2)[a]	1.4	284
Testosterone	C_8	Acetonitrile/0.1 *M* acetate buffer, pH 4 (50/50)	2.0	242
Benzoic acid	C_8	Acetonitrile/0.2 *M* acetate buffer, pH 3.5 (25/75)	1.4	230
Indomethacin	C_8	Acetonitrile/0.04 *M* phosphoric acid (55/45)	1.2	260
Fluorouracil	C_8	0.01 *M* acetate buffer/0.05% triethylamine, pH 4	1.2	266
Methotrexate	C_8	Methanol/THF/citrate phosphate buffer, pH 3.2 (15/4/81)	2.0	303

[a] All ratios are volume ratios.

Table II. Solubility (C^s), Flux (J), Permeability Coefficient (P), and Partition Coefficients (K) for Various Model Drugs Using Propylene Glycol Vehicles and Fatty Acid or Amine Adjuvants

	C^s (mg/ml)	J ($\mu g/cm^2$ hr)[a]	P (cm/hr)	$K^{IM/PG}$	$K^{toluene/PG}$
Naloxone					
PG	28.3	3.6 ± 1.2	1.3×10^{-4}	0.09	0.45
Capric acid/PG	70.0	111.4 ± 37.3	1.6×10^{-3}	0.04	0.74
Lauric acid/PG	62.0	136.1 ± 42.6	2.2×10^{-3}	0.13	0.75
Neodecanoic acid/PG	48.7	145.7 ± 63.1	3.0×10^{-3}	0.08	0.78
Dodecylamine/PG	6.2	25.1 ± 0.9	4.0×10^{-3} (31)[b]	6.47 (72)	8.52 (19)
Testosterone					
PG	67.8	4.0 ± 0.9	5.9×10^{-5}	0.18	0.18
Capric acid/PG	89.7	14.2 ± 3.4	1.6×10^{-4}	0.29	0.48
Lauric acid/PG	91.3	21.9 ± 4.3	2.4×10^{-4}	0.32	0.67
Neodecanoic acid/PG	74.0	21.4 ± 3.3	2.9×10^{-4}	0.25	0.39
Dodecylamine/PG	28.0	10.4 ± 0.8	3.7×10^{-4} (6)	2.49 (14)	4.04 (22)
Benzoic acid					
PG	250	557 ± 71	2.2×10^{-3}	0.20	0.20
Capric acid/PG	229	815 ± 82	3.6×10^{-3}	0.28	0.24
Lauric acid/PG	259	726 ± 89	2.8×10^{-3}	0.25	0.32
Neodecanoic acid/PG	271	648 ± 74	2.4×10^{-3}	0.27	0.32
Dodecylamine/PG	231	902 ± 166	3.9×10^{-3}	0.04	0.19
Indomethacin					
PG	7.6	0.5 ± 0.05	6.6×10^{-5}	0.30	0.17
Capric acid/PG	9.9	23.3 ± 3.4	2.4×10^{-3}	0.49	0.89
Lauric acid/PG	11.6	51.2 ± 16.7	4.4×10^{-3}	0.60	1.05
Neodecanoic acid/PG	8.8	5.8 ± 2.2	6.6×10^{-4}	0.48	0.85
Dodecylamine/PG	136.5	7.7 ± 1.2	5.6×10^{-5}	0.14	0.71
Fluorouracil					
PG	12.4	1.4 ± 0.4	1.1×10^{-4}	0.002	4×10^{-4}
Capric acid/PG	8.1	92.0 ± 3.5	1.1×10^{-2}	0.01	0.02
Lauric acid/PG	7.0	81.9 ± 4.9	1.2×10^{-2}	0.01	0.04
Neodecanoic acid/PG	8.6	45.6 ± 2.7	5.3×10^{-3}	0.01	0.01
Dodecylamine/PG	63.3	527.6 ± 30.0	8.3×10^{-3}	0.01	0.06
Methotrexate					
PG	2.7	7.0 ± 5.9	2.6×10^{-3}	—[c]	—
Capric acid/PG	2.4	8.8 ± 6.5	3.7×10^{-3}	—	—
Lauric acid/PG	3.5	10.1 ± 6.6	2.9×10^{-3}	—	—
Neodecanoic acid/PG	3.0	16.0 ± 4.7	5.3×10^{-3}	—	—
Dodecylamine/PG	54.1	131.8 ± 56.3	2.4×10^{-3}	—	—

[a] Mean ± SE.
[b] Numbers in parentheses are relative to the PG control.
[c] Partition coefficients were too low to measure.

Fluorouracil. Dodecylamine also solubilized (fivefold) fluorouracil, another drug with acidic functionality. However, unlike indomethacin, fluorouracil P was also increased (75-fold) by dodecylamine. Fluorouracil K values were very low, and increased in the presence of each fatty acid or amine adjuvant, to account at least partly for the increases in P. The fatty acids also greatly increased fluorouracil flux and P, and part of the increase in P may have been due to increases in K.

Methotrexate. For methotrexate, neither flux, C^s, nor P was markedly increased in the presence of fatty acids. The effects of dodecylamine on methotrexate were similar to those with indomethacin: increased solubility, proportional increase in flux, and no change in P. Partitioning of methotrexate into either isopropyl myristate or toluene was negligible using control or adjuvant vehicles.

Dodecylamine increased flux of methotrexate and indomethacin by solubilization without affecting P, but increased fluorouracil P, as well as C^s. This indicates that this adjuvant has apparently different mechanisms of promoting skin permeation, depending on the drug. To illustrate this further, the effects of dodecylamine were also studied at fixed concentrations of methotrexate (1 mg/ml) or fluorouracil (5 mg/ml) in the vehicle. Results are shown in Fig. 2. Dodecylamine did not increase methotrexate flux significantly, but fluorouracil flux increased 78-fold. These results are consistent with those using drug-saturated vehicles.

Other Bases as Permeation Enhancers. The effects of some other adjuvants with basic functionality were studied using indomethacin and fluorouracil as diffusants. Results are given in Table III, together with the previously presented results for control and dodecylamine vehicles. Because

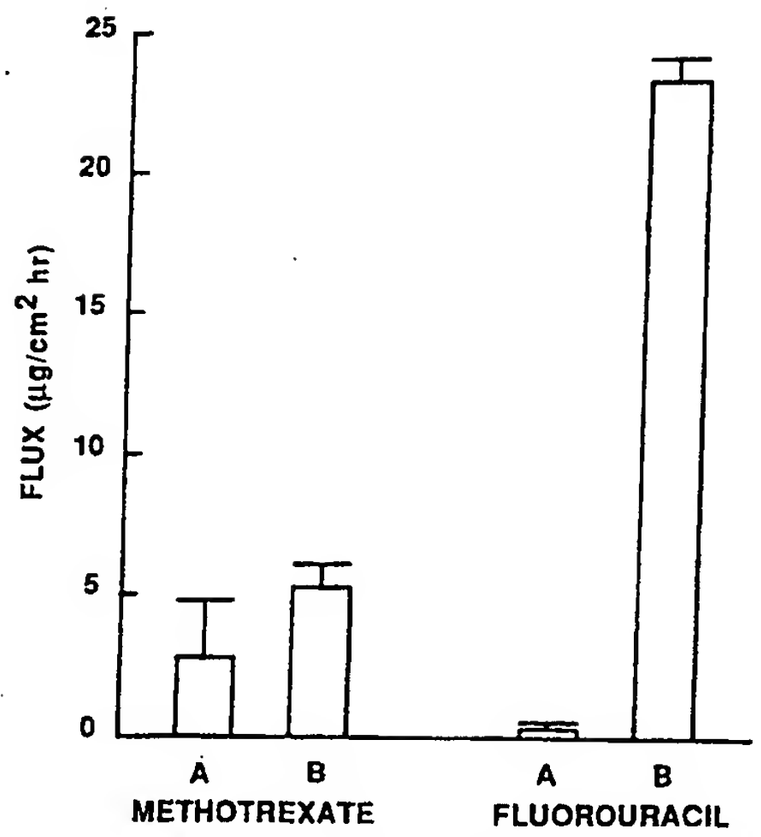

Fig. 2. Flux of methotrexate or fluorouracil from propylene glycol (A) or propylene glycol containing 0.5 *M* dodecylamine (B). Vehicles contained 1 mg/ml methotrexate or 5 mg/ml fluorouracil.

some of the vehicles were semisolid, solubility of the drug could not be measured. However, for those indomethacin vehicles for which solubility was determined, it was increased by each adjuvant. Indomethacin permeability coefficients, on the other hand, were increased only by NaOH (twofold) and triethylamine (fivefold). Indomethacin flux in the presence of phenylethylamine or stearylamine was the same as control. These adjuvants affected indomethacin and fluorouracil differently. Triethylamine and phenylethylamine both increased fluorouracil solubility and flux, but since these increases were proportional to each other, *P* was not affected. In contrast, PEG-2 oleamine and PEG-5 oleamine both increased *P* but did not affect fluorouracil solubility. Sodium hydroxide and stearylamine increased flux, but the vehicles were semisolid and C^s could not be measured. These results confirm that adjuvants affect different drugs in different ways.

Propylene Glycol Skin Permeation. The rate of skin penetration of the solvent can influence the permeation rate of dissolved solutes because the resistance of the barrier could change as it absorbs solvent and because drug partitioning into a solvent-soaked membrane may be different than into a dry or hydrated membrane. Propylene glycol skin permeation was characterized using fatty acid/PG or dodecylamine/PG vehicles. Results are given in Table IV. Each fatty acid increased the PG skin permeation rate, but only the effect of capric acid was statistically significant. Dodecylamine produced an even greater increase in PG skin permeation. However, in a vehicle saturated with methotrexate, the enhancing effect of dodecylamine was negated, as shown in Fig. 3. Presumably the adjuvants must penetrate into skin to exert their effects on the barrier properties of skin. Inhibition by methotrexate of the enhancing effect of dodecylamine on PG flux suggests that an interaction of dodecylamine and methotrexate occurs in the vehicle to inhibit dodecylamine skin penetration. Perhaps this is why dodecylamine did not affect methotrexate *P*, as shown in Table II.

DISCUSSION

Various mechanisms have been proposed to account for the effects of fatty acids on skin permeation. These include increased drug solubility in the vehicle, increased partitioning into the skin, increased solvent penetration, and barrier disruption. The dependence of flux on each of these variables can be illustrated with a diffusion equation in which drug flux through a membrane at steady state, from a saturated solution into a sink, is represented as

$$J = C^s K_m D/h$$

Table III. Effects of Various Basic Adjuvants on Solubility (C^s), Flux, and Permeability Coefficient of Indomethacin and Fluorouracil

	C^s (mg/ml)	Flux (μg/cm² hr)	*P* (cm/hr)
Indomethacin			
PG	7.6	0.5 ± 0.05	6.6×10^{-5}
Dodecylamine/PG	136.5	7.7 ± 1.2	5.6×10^{-5}
Triethylamine/PG	132.8	40.7 ± 21.8	3.1×10^{-4}
Phenylethylamine/PG	ND[a]	0.4 ± 0.2	ND
PEG-2 oleamine/PG	115.7	3.9 ± 0.9	3.4×10^{-5}
PEG-5 oleamine[b]/PG	125.8	1.2 ± 0.6	9.5×10^{-6}
NaOH/PG	88.7	12.6 ± 5.8	1.4×10^{-4}
Stearylamine/PG	ND	0.7 ± 0.06	ND
Fluorouracil			
PG	12.4	1.9 ± 0.5	1.5×10^{-4}
Dodecylamine/PG	63.3	527.6 ± 30	8.3×10^{-3}
Triethylamine/PG	47.7	10.4 ± 1.2	2.2×10^{-4}
Phenylethylamine/PG	59.1	9.7 ± 2.2	1.6×10^{-4}
PEG-2 oleamine/PG	16.0	272.7 ± 59.4	1.7×10^{-2}
PEG-5 oleamine[b]/PG	14.8	26.6 ± 4.4	1.8×10^{-3}
NaOH/PG	ND	12.5 ± 6.9	ND
Stearylamine/PG	ND	21.7 ± 11.0	ND

[a] Not determined.
[b] Adjuvant was not completely soluble at 0.05 *M*.

Table IV. Effects of Fatty Acid Adjuvants and Dodecylamine on Propylene Glycol Skin Penetration

	Propylene glycol	
Adjuvant (0.5 *M*)	Flux (%/hr)	Lag time (hr)
None	0.8 ± 0.4	3.5 ± 1.7
Capric acid	7.5 ± 1.6	3.0 ± 1.1
Lauric acid	1.4 ± 0.2	1.0 ± 0.5
Neodecanoic acid	1.6 ± 0.2	2.2 ± 1.8
Dodecylamine	15.7 ± 1.9	2.2 ± 0.7

J is the flux per unit area of membrane, K_m is the membrane/vehicle partition coefficient, C^s is the drug concentration in the vehicle at the solubility limit, D is the diffusion coefficient, and h is the membrane thickness. K_mD/h is the permeability coefficient (P). Increased drug diffusion rates in the presence of adjuvants could be due to changes in any of the variables K_m, C^s, D or h. D reflects, among other things, the structural properties of the skin. We evaluated the relative contributions of the proposed mechanisms of fatty acid skin permeation enhancers by examining their effects on drug solubility, partitioning, and permeability coefficient of diverse acidic, basic, and neutral permeants. We also examined the effects of amine and other basic adjuvants on these diverse model compounds.

Our results indicate that each of the proposed mechanisms (i.e., increased drug solubility in the vehicle, increased partition coefficient, barrier disruption, and increased solvent permeation) may be associated with the increased flux in the presence of fatty acid adjuvants and dodecylamine. The relative contributions of these mechanisms varied from drug to drug, however. Table V lists examples of the drugs for which these mechanisms appeared to contribute to increased flux. The most consistent effects were for acidic adjuvants to increase the solubility of the basic drug in the vehicle and for basic adjuvants to increase the solubilities of acidic drugs. For some drug/adjuvant combinations (e.g., indomethacin/dodecylamine) this effect completely accounts for the increase in flux, since the permeability coefficient was unchanged. However, it may be difficult to predict *a priori* which adjuvants will have only a solubilizing effect. For example, triethylamine and phenylethylamine increased fluorouracil flux by increasing only its solubility in the vehicle (P was unchanged). However, both of these adjuvants increased P for indomethacin (Table III).

Skin permeation could also be increased by increasing the partitioning of the drug into the skin. Ion pairing has been proposed in several publications as a possible mechanism of increasing partitioning. Lee and Kim (11) demonstrated that ion pairing could substantially increase the penetration of ionic drugs through synthetic hydrophobic membranes using nonaqueous vehicles with a low dielectric constant. An ion pairing mechanism was proposed for the enhancement of penetration of β-blockers across an isopropyl myristate membrane in the presence of fatty acids (6). Synthetic ion pairs of trospium, wherein the counterions were alkyl sulfates, had greater skin permeation rates than trospium chloride (12). The bioavailability of dermally applied diltiazem hydrochloride was increased by the inclusion of lipophilic, anionic counterions (13). Sodium salicylate increased the skin penetration and partition coefficient (octanol/pH 7.4 buffer) of isopropamide iodide, presumably by formation of a lipophilic ion pair (14). Oleic acid and lauric acid increased both the isopropyl myristate/buffer partition coefficient and the skin permeation rate of naphazoline, a base, but the partition coefficients of caffeine and methyl nicotinate were not affected by the fatty acids (7). We evaluated the possibility of increased partitioning into skin, by measuring partitioning into isopropyl myristate and toluene. There were several adjuvant/drug combinations which resulted in increased partitioning of the drug. We found no evidence of adjuvant and drug counterions forming more lipophilic ion pairs, however. On the contrary, the fatty acids increased the partition co-

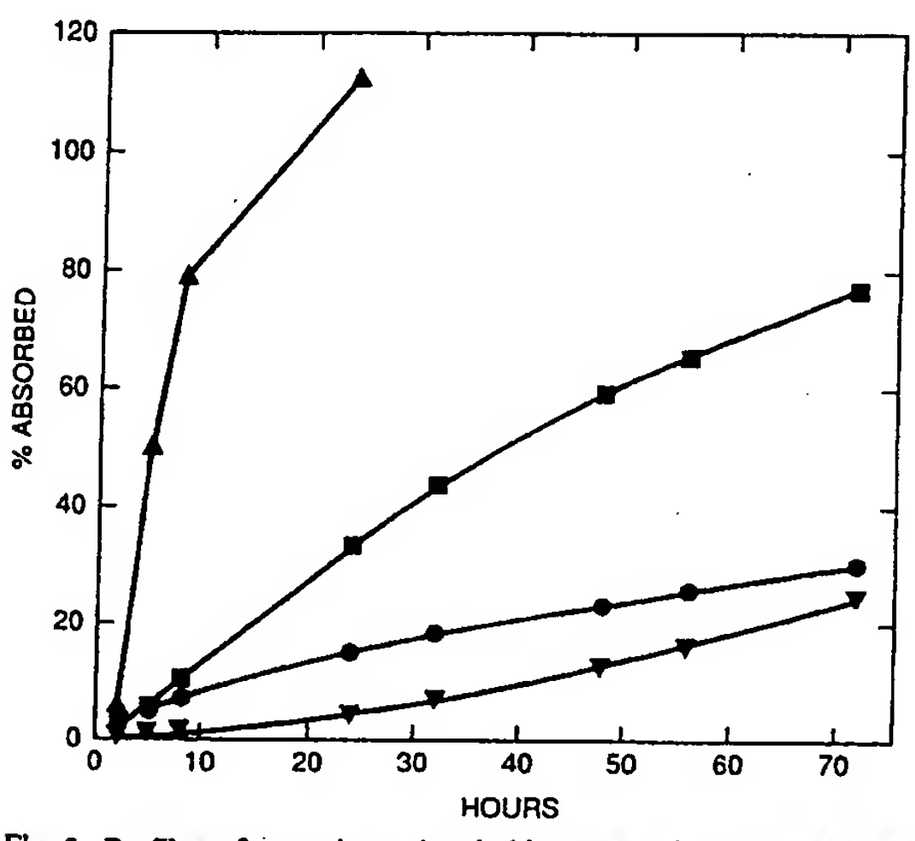

Fig. 3. Profiles of propylene glycol skin penetration from vehicles containing no adjuvant (●), 0.5 *M* lauric acid (■), 0.5 *M* dodecylamine (▲), or 0.5 *M* dodecylamine and saturated with methotrexate (▼).

Table V. Mechanisms Involved in the Skin Penetration Enhancing Effects of Fatty Acids and Dodecylamine and Those Drugs Affected via the Specified Mechanism

	Adjuvant	
Mechanism	Fatty acids	Dodecylamine
Increased drug solubility in vehicle	Naloxone	Indomethacin Fluorouracil Methotrexate
Increased partition coefficient	Indomethacin Fluorouracil	Naloxone Testosterone
Disrupted barrier function of skin	Naloxone Testosterone Indomethacin Fluorouracil	Fluorouracil
Increased skin penetration of solvent	Yes	Yes

efficients of the acidic drugs indomethacin and fluorouracil, and dodecylamine increased the partition coefficients of naloxone base. One difference in methodology between our work and those studies cited above (6,7,12–14) is that the donor vehicles used were entirely or predominantly aqueous. We did not evaluate the apparent pH of the vehicles and do not know if the drug or adjuvant were ionized, a requirement for ion pairing. Thus, although we show no evidence for ion pairing, we cannot state that it cannot contribute to enhanced skin permeation under other conditions.

The permeation rate of the solvent can also be an important factor influencing the permeation rate of the drug. A correlation between metronidazole and PG skin permeation rates from PG vehicles was described (15). Similar relationships were described for indomethacin (16), molsidomine (8), and narcotic analgesics (17) from fatty acid/PG vehicles and for nicorandil penetration from fatty acid ester/PG vehicles (18). The results of increased solvent penetration into the skin may include increased drug solubility in the skin and increased barrier disruption if the solvent itself is a penetration enhancer. Kadir *et al.* have shown that propionic acid vehicles enhanced the skin permeation of theophylline (19) and adenosine (20) because of rapid propionic acid skin penetration and solubilization of the drug in the skin–propionic acid medium. We did not measure PG skin permeation rates with all drug/adjuvant/vehicle combinations, but our data show that the permeation rate of the vehicle can be influenced by the presence of adjuvant or drug. Drug solubility in the membrane should be most influenced by the PG skin penetration rate for those drugs with a high affinity for PG, as evidenced by low partition coefficients. Some adjuvants can have the dual synergistic effects of increasing drug solubility in the vehicle and increasing the skin penetration rate of the vehicle.

The remaining proposed mechanism is disruption of the barrier function of the skin. Fatty acids can change the physical chemical characteristics of skin, as shown using differential scanning calorimetry and infrared spectroscopy for oleic acid-treated stratum corneum (5). Specifically, fatty acids seem to disrupt the packed structure of the intercellular lipids of the stratum corneum (4). We have not measured barrier disruption directly but have attributed any increase in P, not accompanied by a proportional increase in K, to increased diffusivity. The fatty acids were shown to increase skin diffusivity and permeation rates of naloxone, indomethacin, and fluorouracil. However, the effects of fatty acids were inconsistent; P values for benzoic acid and methotrexate were unaffected. To examine the relationship between compound structure and permeability enhancement, we calculated the increase in P in the presence of lauric acid ($P^{lauric}/P^{control}$) for each diffusant. The $P^{lauric}/P^{control}$ values were independent of whether the compounds had basic, neutral, or acidic functional groups (Table VI). There was also no relationship to their octanol/water partition coefficients or molecular weights. The effects of dodecylamine on barrier disruption also varied from drug to drug, and a significant disruption effect was indicated only for fluorouracil. One reason for the inconsistent effects on skin diffusivity from drug to drug is that the drug, adjuvant, and vehicle interact to each influence the penetration of the others. Susceptibility to permeation enhancement may also depend on the routes of drug permeation through skin, which may vary from drug to drug.

Table VI. Comparison of the Increase in Permeability Coefficient with Lauric Acid ($P^{lauric}/P^{control}$) for the Various Model Drugs and Some of Their Physical Chemical Properties

Diffusant	$P^{lauric}/P^{control}$	Log K (octanol/water)[a]	Molecular weight
Naloxone	16.92	1.53	327
Testosterone	4.07	3.32	288
Benzoic acid	1.27	1.95	122
Indomethacin	66.67	3.08	358
Fluorouracil	109.09	−0.92	130
Methotrexate	1.12	−1.85	454

[a] Values are from Ref. 21.

We conclude from these studies that fatty acid and amine adjuvants can increase skin permeation by a combination of several mechanisms. The relative contributions of those mechanisms vary depending on the drug and adjuvant. We are not yet able to predict which mechanism will predominate for any one drug/adjuvant/vehicle combination.

REFERENCES

1. E. R. Cooper. *J. Pharm. Sci.* 73:1153–1156 (1984).
2. E. R. Cooper, E. W. Merritt, and R. L. Smith. *J. Pharm. Sci.* 74:688–689 (1985).
3. B. J. Aungst, N. J. Rogers, and E. Shefter. *Int. J. Pharm.* 33:225–234 (1986).
4. B. W. Barry. *J. Contr. Res.* 6:85–97 (1987).
5. G. M. Golden, J. E. McKie, and R. O. Potts. *J. Pharm. Sci.* 76:25–28 (1987).
6. P. G. Green and J. Hadgraft. *Int. J. Pharm.* 37:251–255 (1987).
7. P. G. Green, R. H. Guy, and J. Hadgraft. *Int. J. Pharm.* 48:103–111 (1988).
8. M. Yamada, Y. Uda, and Y. Tanigawara. *Chem. Pharm. Bull.* 35:3399–3406 (1987).
9. P. V. Raykar, M.-C. Fung, and B. D. Anderson. *Pharm. Res.* 5:140–150 (1988).
10. B. J. Aungst. *Pharm. Res.* 6:244–247 (1989).
11. S. J. Lee and S. W. Kim. *J. Contr. Rel.* 6:3–13 (1987).
12. P. Langguth and E. Mutschler. *Arzneim. Forsch.* 37:1362–1366 (1987).
13. T. Ishikura, T. Nagai, Y. Sakai, T. Shishikura, H. Ebisawa, and Y. Machida. *Drug Design Deliv.* 1:285–295 (1987).
14. C.-S. Young, C.-K. Shim, M.-H. Lee, and S.-K. Kim. *Int. J. Pharm.* 45:59–64 (1988).
15. B. Mollgaard and A. Hoelgaard. *Acta Pharm. Suec.* 20:443–450 (1983).
16. F. Kaiho, H. Nomura, E. Makabe, and Y. Kato. *Chem. Pharm. Bull.* 35:2928–2934 (1987).
17. M. Mahjour, B. E. Mauser, and M. B. Fawzi. *Int. J. Pharm.* 56:1–11 (1989).
18. K. Sato, K. Sugibayashi, and Y. Morimoto. *Int. J. Pharm.* 43:31–40 (1988).
19. R. Kadir, D. Stempler, Z. Liron, and S. Cohen. *J. Pharm. Sci.* 76:774–779 (1987).
20. R. Kadir, D. Stempler, Z. Liron, and S. Cohen. *J. Pharm. Sci.* 77:409–413 (1988).
21. C. Hansch and A. Leo. *Subtituent Constants for Correlation Analysis in Chemistry and Biology*, John Wiley & Sons, New York, 1979.